

1968

Structural analysis and design of cast iron soil pipes and fittings

Ma'an Hamid Jawad
Iowa State University

Follow this and additional works at: <https://lib.dr.iastate.edu/rtd>

 Part of the [Civil Engineering Commons](#)

Recommended Citation

Jawad, Ma'an Hamid, "Structural analysis and design of cast iron soil pipes and fittings" (1968). *Retrospective Theses and Dissertations*. 3246.
<https://lib.dr.iastate.edu/rtd/3246>

This Dissertation is brought to you for free and open access by the Iowa State University Capstones, Theses and Dissertations at Iowa State University Digital Repository. It has been accepted for inclusion in Retrospective Theses and Dissertations by an authorized administrator of Iowa State University Digital Repository. For more information, please contact digirep@iastate.edu.

This dissertation has been
microfilmed exactly as received

68-10,466

JAWAD, Ma'an Hamid, 1943-
STRUCTURAL ANALYSIS AND DESIGN OF CAST
IRON SOIL PIPES AND FITTINGS.

Iowa State University, Ph. D., 1968
Engineering, civil

University Microfilms, Inc., Ann Arbor, Michigan

STRUCTURAL ANALYSIS AND DESIGN OF CAST IRON
SOIL PIPES AND FITTINGS

by

Ma'an Hamid Jawad

A Dissertation Submitted to the
Graduate Faculty in Partial Fulfillment of
The Requirements for the Degree of
DOCTOR OF PHILOSOPHY

Major Subject: Structural Engineering

Approved:

Signature was redacted for privacy.

In Charge of Major Work

Signature was redacted for privacy.

Head of Major Department

Signature was redacted for privacy.

Dean of Graduate College

Iowa State University
Ames, Iowa

1968

TABLE OF CONTENTS

	Page
NOTATIONS	xiv
1. INTRODUCTION	1
1.1 Foreword	1
1.2 Object	3
1.3 Scope	3
1.4 Literature Survey	6
1.5 Survey of Inspectors, Contractors and Wholesalers	7
2. RESIDUAL STRESSES	10
2.1 Introduction	10
2.2 Magnitude of Residual Stresses	11
2.3 Effect of Residual Stresses	18
3. STRENGTH OF BURIED PIPES	23
3.1 Introduction	23
3.2 Variables Affecting the Barrel Thickness	24
3.3 Earth Fill Loading	31
3.4 Load Increase on Pipe due to Live Loading	34
3.5 Conversion of Pipe Load to 3-Edge Bearing Load	37
3.6 Summary	39
4. EXPERIMENTAL YARNING AND THERMAL STRAINS IN 4-INCH PIPES	40
4.1 Temperature Distribution in the Hubs and Spigots	40
4.2 Yarning Strain Distribution in Hubs and Spigots	46

	Page
4.3 Thermal Strain Distribution in Hubs and Spigots	50
4.4 Concluding Statement	57
5. CAULKING STRAINS	58
5.1 Introduction	58
5.2 Experimental Strain Distribution in the Hub and Spigot of 4-inch Pipes	58
5.3 Theoretical Strain Distribution in Hubs	69
5.4 Theoretical Strain Distribution in Spigots	80
5.5 Strain Variation Around a Caulked Joint	86
5.6 Effect of Lead Depth on the Maximum Strains	88
5.7 Relaxation Test	89
5.8 Caulking at Low Temperatures	91
5.9 Summary of Strain Due to the Joining Operation	93
6. ELASTOMERIC GASKET JOINTS	95
6.1 Introduction	95
6.2 Strains in the Hubs and Spigots	95
7. EFFECTS OF BUILDING MOVEMENTS AND SOIL SETTLEMENTS ON STRENGTH REQUIREMENTS FOR PIPE SYSTEM	98
7.1 Introduction	98
7.2 Behavior of Individual Pipes and Lead- Oakum Joints Subjected to Bending	98
7.3 Ultimate Strength of Lead-Oakum Joints Subjected to Bending	108
7.4 Leakage Tests for Elastomeric and Lead- Oakum Joints	108

	Page
7.5 Conclusion	113
8. DESIGN RECOMMENDATIONS FOR THE HUBS	115
8.1 Preliminary Design Charts	115
8.2 Evaluation of the Caulking Pressure P	117
8.3 Design Charts	122
8.4 Observations on Presently Manufactured Hubs	123
9. DESIGN RECOMMENDATIONS FOR THE SPIGOTS	129
9.1 Design Chart	129
9.2 Determination of the Stress σ_l and the Caulking Force P_1	129
10. DESIGN RECOMMENDATIONS FOR THE BARRELS	135
10.1 Design Chart	135
11a. SUMMARY	140a
11b. ACKNOWLEDGMENT	140e
12. LITERATURE CITED	141
13. APPENDIX A.	145
A.1 Literature Survey	145
A.2 Survey of Performance of Cast Iron Soil Pipe and Fittings	156
14. APPENDIX B. MAIN DIMENSIONS OF THE PIPES USED AND HUB CONFIGURATIONS OF VARIOUS BRANDS	185
15. APPENDIX C.	191
C.1 Comparison Between Strains Obtained by means of Oscilloscopes and Brush Amplifiers	191
C.2 Caulking Strains	193

	Page
16. APPENDIX D. COMPUTER PROGRAM FOR THE DETERMINATION OF DESIGN CHARTS; DESIGN CHARTS FOR THE VARIOUS PIPE DIAMETERS USED; AND COMPUTER PROGRAM DETERMINING THE FORCE P FOR SPECIFIC DIMENSIONS	196
17. APPENDIX E. DESIGN CHARTS FOR EARTH AND SURFACE LIVE LOADING ON PIPES	221

LIST OF FIGURES

Figure	Page
2.1. Location of strain gages in 4-inch pipe and bends	12
2.2. Location of strain gages and rosetts in 4-inch T and Y branches	13
3.1. Range of variables in buried pipe study	25
3.2. Effect of trench width on trench load due to earth loads	29
4.1. Location of thermocouples in hub of pipe 4D11 and spigot of 4D12	41
4.2. Temperature distribution in hub of pipe 4D11 due to pouring lead at 1,000° F	43
4.3. Temperature distribution in spigot of pipe 4D12 due to pouring lead at 1,000° F	45
4.4. Strain gage location in hubs and spigots of 4D pipes	48
4.5. Thermal strains in longitudinal gages of hub 4D11	51
4.6. Characteristic curves for FA gages (top) and FAB gages (bottom)	53
4.7. Thermal strain envelope in hubs of pipe brands 4D11 and 4D2 due to pouring lead at 1,000° F	54a
4.8. Thermal strain envelope in spigots of pipe brands 4D12 and 4D3 due to pouring lead at 1,000° F	56
5.1. Maximum caulking strain envelope in hubs of 4-inch pipes	63
5.2. Maximum caulking strain envelope in spigots of 4-inch D brand pipes	68
5.3. Idealized cross section of hubs	70

Figure	Page
5.4. Cross section of the spigot	81
5.5. Strain variation in a hub during caulking	87
5.6. Strain relaxation of gage No. 3 of spigot 4A7 and gage No. 9 of hub 4F11	92
7.1. Setup for single pipe test	99
7.2. Moment curvature relations for single pipe tests	100
7.3. Setup for two-pipe test	102
7.4. Moment rotation relations for two-pipe tests	103
7.5. Stress distribution in the spigot of a test joint	104
7.6. Load deflection relations for a two-pipe continuous beam compared with idealized cases	106
8.1. Relationship between hub dimensions F, R, and S for 2-inch pipes	124
8.2. Relationship between hub dimensions F, R, and S for 3-inch pipes	124
8.3. Relationship between hub dimensions F, R, and S for 4-inch pipes	125
8.4. Relationship between hub dimensions F, R, and S for 5-inch pipes	125
8.5. (top) Relationship between hub dimensions F, R, and S for 6-inch pipes	126a
8.6. (bottom) Relationship between hub dimensions F, R, and S for 8-inch pipes	126a
8.7. (top) Relationship between hub dimensions F, R, and S for 10-inch pipes	127a
8.8. (bottom) Relationship between hub dimensions F, R, and S for 12-inch pipes	127a
8.9. Relationship between hub dimensions F, R, and S for 15-inch pipes	128

Figure	Page
9.1. Relationship between ratio of modulus of rupture to caulking force and spigot thickness	130
10.1. Relationship between three-edge bearing load and pipe wall thickness for various pipe diameters	139
A.1. Questionnaire	157
A.2. Percent observing breakage	162
A.3. Percent observing frequent breakage	164
A.4. Ordinary yarning iron	182
A.5. Small yarning iron	183
A.6. Long yarning iron	183
A.7. Ordinary caulking iron	184
A.8. Heavy caulking iron	184
B.1. Main dimensions of pipes	186
B.2. Hub configurations of 4-inch pipes	188
B.3. Hub configurations of 8-inch pipes	189
B.4. Hub configurations of 12-inch pipes	190
C.1. Yarning strains in the hub as recorded by oscilloscopes	192
C.2. Yarning strains in the hub as recorded by Brush amplifiers	192
C.3. Fast sweep trace of a caulking strain wave (single blow)	194
C.4. Slow sweep trace of caulking strain waves (several blows)	194
D.1. Computer program used in preparing Figs. D-2 - D.37	197

Figure	Page
D.2. Design parameters for 2-inch hubs with hub wall thickness of 0.10 inch	200
D.3. Design parameters for 2-inch hubs with hub wall thickness of 0.12 inch	200
D.4. Design parameters for 2-inch hubs with hub wall thickness of 0.14 inch	201
D.5. Design parameters for 2-inch hubs with hub wall thickness of 0.16 inch	201
D.6. Design parameters for 3-inch hubs with hub wall thickness of 0.12 inch	202
D.7. Design parameters for 3-inch hubs with hub wall thickness of 0.16 inch	202
D.8. Design parameters for 3-inch hubs with hub wall thickness of 0.20 inch	203
D.9. Design parameters for 3-inch hubs with hub wall thickness of 0.24 inch	203
D.10. Design parameters for 4-inch hubs with hub wall thickness of 0.12 inch	204
D.11. Design parameters for 4-inch hubs with hub wall thickness of 0.16 inch	204
D.12. Design parameters for 4-inch hubs with hub wall thickness of 0.20 inch	205
D.13. Design parameters for 4-inch hubs with hub wall thickness of 0.24 inch	205
D.14. Design parameters for 5-inch hubs with hub wall thickness of 0.12 inch	206
D.15. Design parameters for 5-inch hubs with hub wall thickness of 0.16 inch	206
D.16. Design parameters for 5-inch hubs with hub wall thickness of 0.20 inch	207
D.17. Design parameters for 5-inch hubs with hub wall thickness of 0.24 inch	207

Figure	Page
D.18. Design parameters for 6-inch hubs with hub wall thickness of 0.16 inch	208
D.19. Design parameters for 6-inch hubs with hub wall thickness of 0.20 inch	208
D.20. Design parameters for 6-inch hubs with hub wall thickness of 0.24 inch	209
D.21. Design parameters for 6-inch hubs with hub wall thickness of 0.28 inch	209
D.22. Design parameters for 8-inch hubs with hub wall thickness of 0.24 inch	210
D.23. Design parameters for 8-inch hubs with hub wall thickness of 0.28 inch	210
D.24. Design parameters for 8-inch hubs with hub wall thickness of 0.34 inch	211
D.25. Design parameters for 8-inch hubs with hub wall thickness of 0.40 inch	211
D.26. Design parameters for 10-inch hubs with hub wall thickness of 0.28 inch	212
D.27. Design parameters for 10-inch hubs with hub wall thickness of 0.32 inch	212
D.28. Design parameters for 10-inch hubs with hub wall thickness of 0.36 inch	213
D.29. Design parameters for 10-inch hubs with hub wall thickness of 0.40 inch	213
D.30. Design parameters for 12-inch hubs with hub wall thickness of 0.32 inch	214
D.31. Design parameters for 12-inch hubs with hub wall thickness of 0.36 inch	214
D.32. Design parameters for 12-inch hubs with hub wall thickness of 0.42 inch	215
D.33. Design parameters for 12-inch hubs with hub wall thickness of 0.48 inch	215

Figure	Page
D.34. Design parameters for 15-inch hubs with hub wall thickness of 0.34 inch	216
D.35. Design parameters for 15-inch hubs with hub wall thickness of 0.38 inch	216
D.36. Design parameters for 15-inch hubs with hub wall thickness of 0.42 inch	217
D.37. Design parameters for 15-inch hubs with hub wall thickness of 0.48 inch	217
D.38. Computer program used in determining appropriate factors of safety of various pipe hubs tested	218
E.1. (top) Curves for transition-width ratio	222
E.2. (bottom) Surface load factors for two passing trucks	222
E.3. Diagram for coefficient C_d for ditch conduits	224
E.4. Relationship between pipe diameters and ratio of trench load to equivalent 3-edge bearing load	225

LIST OF TABLES

Table	Page
2.1. Residual stresses in pipe and bends	15
2.2. Residual stresses in T and Y branches	16
2.3. Modulus of rupture of as-received and stress relieved pipe sections	20
3.1. Earth loading on 8-inch pipes	33
3.2. Load on 8-inch pipe due to earth and surface live loading	36
3.3. Total equivalent 3-edge bearing load for 8-inch diameter pipes	38
4.1. Maximum strains (μ in./in.) in hubs and spigots of 4D pipes due to yawing	49
5.1. Longitudinal caulking strain distribution in hubs of 4-inch pipes	61
5.2. Circumferential caulking strain distribution in hubs of 4-inch pipes	62
5.3. Longitudinal caulking strain distribution in spigots of 4-inch pipes	65
5.4. Circumferential caulking strain distribution in spigots of 4-inch pipes	66
5.5. Ratio of m/J for various pipe diameters	84
5.6. Relaxation of strain (μ in./in.) in caulked joints	90
6.1. Strains in elastomeric gasket joints	96
7.1. Summary of ultimate strength and leakage test results	109
8.1. Values of A for various pipe diameters	116
8.2. Strains and forces in pipe hubs	118a

Table	Page
8.3. Equivalent caulking forces, lbs./in.	121
8.4. Equivalent caulking forces with a safety factor of 2	122
9.1. Caulking forces in pipe spigots	131
9.2. Caulking forces in various pipe diameters	133
9.3. Recommended spigot thicknesses	133
10.1. Equivalent 3-edge bearing loads ^a for various pipe installations	136
A.1. Areas in which frequent breakage was observed by more than 10%	165
A.2. Comparison of observations made by inspectors, contractors and wholesalers	166
B.1. Main dimensions of test specimens, inches	187
E.1. Percentage of trench load on pipes	226

NOTATIONS

- A = Inside diameter of pipe hub, inches.
- a = Radius of bead from the central axis to the neutral axis, inches.
- a_1 = Radius of hub from the central axis to the neutral axis, inches.
- $B^4 = \frac{3(1 - \nu^2)}{\rho^2 \delta^2}$, inch⁻⁴.
- B_c = Outside width of conduit, feet.
- B_d = Horizontal width of ditch at top of conduit, feet.
- CISP = Cast iron soil pipe.
- cm. = Centimeters.
- C_c = Load coefficient for positive projecting conduits.
- C_d = Load coefficient for ditch conduits.
- C_n = Load coefficient for negative projecting conduits.
- $D = \frac{E\delta^3}{12(1 - \nu^2)}$ = flexural rigidity, lbs.-in.
- d = Inside diameter of pipe, inches.
- E = Modulus of elasticity, psi.
- F = Length of hub bead, inches.
- FA = Foil type strain gages with 1/4 inch length, 120 ohm resistance, and a coefficient of thermal expansion of 6×10^{-6} in./in./°F.
- S = Thickness of hub wall, inches.

- FAB = Bakelite type strain gages with 1/4 inch length, 120 ohm resistance, and a coefficient of thermal expansion of 6×10^{-6} in./in./°F.
- FAE = Epoxy type strain gages with 1/4 inch length, 120 ohm resistance, and a coefficient of thermal expansion of 6×10^{-6} in./in./°F.
- FAR = Foil type rosettes with 1/4 inch length, 120 ohm resistance, and a coefficient of thermal expansion of 6×10^{-6} in./in./°F.
- °F = Temperature, degrees Fahrenheit.
- H = Height of earth fill, feet.
- J = Outside diameter of pipe spigot, inches.
- K = Rankine's lateral pressure ratio.
- lbs./in. = Force, pounds per inch.
- M = Moment at various sections of pipes.
- M_R = Modulus of rupture, psi.
- m = Distance of application of load from end of spigot.
- mm/sec. = Velocity, millimeter per second.
- P = Applied radial load, lbs./in.
- p = Projection ratio.
- psi = Pressure, pounds per square inch.
- R = Thickness of hub bead, inches.
- R_n = Net thickness of the cross section of the hub bead, inches.
- r_{sd} = Settlement ratio for a negative projecting conduit.
- r = Radius of spigot from central axis to the neutral axis, inches.

SV	= Service weight pipe or fitting.
t	= Wall thickness of pipe or fittings, inches.
u	= Coefficient of internal friction of fill material.
u'	= Coefficient of friction between fill material and sides of ditch
v	= Poisson's ratio.
W	= Maximum load applied on pipes, lbs./ft.
W _c	= Earth loading on pipes, lbs./ft.
w	= Deflection, inches.
XH	= Extra heavy weight pipe or fitting.
α	= Coefficient of thermal expansion, in./in. ^o F.
γ	= Unit weight of earth, pounds per cubic foot.
$\epsilon_l, \epsilon_\phi$	= Longitudinal and circumferential strains, respectively, μ in./in.
μ in./in.	= Strain, micro-inches per inch.
σ_l, σ_ϕ	= Longitudinal and circumferential stresses, respectively, psi.
ρ	= Radius of shell measured from the neutral axis to the centroidal axis, inches.
δ	= Thickness of shell, inches.

Specimen Identification: The letter refers to the brand used. Six brands of pipes and fittings were tested. These were marked brands A to F.

The number to the left of this letter gives the diameter of the specimen used. The number to the right of the

letter refers to the weight of pipe: 1-6 are XH weight pipes and fittings and 7-16 are SV weight pipes and fittings. The number following the dash refers to the test sequence. For example, 4A10-3 is a 4-inch pipe or fitting of brand A and is a SV weight. This specimen was used in the third test of a sequence of tests.

1. INTRODUCTION

1.1 Foreword

Cast iron soil pipes and fittings must withstand certain forces during their life span. The thicknesses of the barrel, spigot, hub wall, and hub bead must be sufficient to resist these applied forces. The dimensions of pipe presently manufactured have been determined from experience and not through a theoretical or experimental study. As a result, the thicknesses of the various parts of a given size pipe might be more or less than actually needed to resist the forces. Design by structural analysis may result in a better proportioned pipe.

Since the structural dimensions of presently manufactured pipes of various diameters are based on experience rather than engineering principles, different factors of safety against failure may result in the various sizes of pipes as well as in various parts of a given size. However, in a piping system, failure of one pipe causes the whole system to cease functioning. Thus, pipes of various diameters having various factors of safety are not the most economical or realistic. A better scientific evaluation of the required thicknesses for each size of pipe and fitting is needed. It then may be economically feasible for the cast iron soil pipe producers to manufacture only one weight of pipe for each diameter

instead of two weights (service and extra heavy) as presently done.

During the last fifteen years there has been a considerable mechanical revolution in the cast iron soil pipe industry. Most of the foundries are using the new centrifugal casting for pipes instead of the old static casting; hence, more control and improvement of the process and quality of the product.

In fittings, static casting is still being used. However, the quality of these fittings has been improved through better control of dimensional tolerances and manufacturing processes. Even though the quality of pipes and fittings have been improved, the actual forces acting on them are still unknown and the stresses undetermined. This uncertainty in the magnitude of the forces is probably reflected by the requirements of various codes around the country. Some codes specify extra heavy weight pipes and fittings for some installations, while others specify service weight pipes and fittings for the same types of installations. This inconsistency may be due to the lack of information on the magnitude of forces and stresses in pipes. With this lack of information, specification writers tend to require the same pipes they have been using in the past. This may result in an uneconomical use of the pipes. Thus, scientific analysis of the hub bead, hub wall, spigot end, and barrel section is needed to determine the thicknesses required for

each critical load condition on the piping system.

1.2 Object

The dimensions for a single weight pipe of each size were to be determined which would give satisfactory performance during installation and through the intended service life of the plumbing system. In particular, it was desired to determine barrel, spigot, and hub thicknesses, and the dimensions of the hub bead necessary to withstand the forces acting on the pipe with a sufficient factor of safety.

1.3 Scope

In order to determine the required thicknesses of the pipe components, it was necessary first to consider the types of forces acting on pipe and fitting systems. In general, these factors can be categorized according to the following stages of the pipe life:

1. Manufacturing
2. Transportation
3. Installation
4. Service life.

In the manufacturing process, forces or stresses are induced by the differential cooling of the pipe after casting. These stresses are called residual stresses. The magnitude of these stresses and their effect on the ultimate strength of the cast iron soil pipe is discussed in Chapter 2.

The stresses during the transportation stage are caused mainly by the impact forces that occur during loading, hauling, and unloading. These forces were not considered in

this research since a product such as cast iron soil pipe should be handled with the degree of care necessary to insure delivery on the job in a good condition.

In Chapter 3, the procedure to determine the earth loads acting on buried pipe and pipe that is loaded with fill is given. Concentrated surface loads from vehicles are also considered. In addition, a method is given in which the required thickness of the barrel is related to a three-edge bearing load which in turn is related to the earth load on the pipe.

Stresses created during the installation of a pipe system resulted from the joining of pipes together. The two kinds of joints that were of concern in this study were the lead-oakum joint and the gasket type joint. Construction of the lead-oakum joint consists of the following three operations: (1) packing oakum into the joint, (2) pouring molten lead into the joint over the oakum, and (3) ramming the lead into the joint with a caulking tool. Strains and stresses are developed in the hubs and spigots of pipes and fittings during each of these operations. Chapter 4 covers the experimental determination of yawning and thermal strains. Chapter 5 covers the experimental strains due to caulking as well as the development of theoretical equations necessary to relate the joint construction forces to hub and spigot dimensions. The reduction in the stresses due to creep of the lead is

also discussed in this chapter.

Stresses in the hub and spigot of a gasket type joint are caused by forcing the spigot into the hub which has been fitted with an elastomeric gasket. The gasket is compressed and exerts forces on the hub and spigot. The experimental determination of these strains are presented in Chapter 6.

The effect of building movements and soil settlements on pipe systems is discussed in Chapter 7. These building movements and soil settlements were simulated by laboratory tests.

In Chapters 8, 9, and 10, recommendations for structural dimensions of the hub bead, hub wall, spigot and barrel are presented in the form of design charts and tables.

Prior to specific research on cast iron soil pipe, a literature survey was made in order to not duplicate previous research that could be directly applied to this study. In addition, a survey of city inspectors, plumbing contractors, and wholesalers concerning performance of cast iron soil pipe was made.

In summary, the research effort consisted of both experimental and theoretical studies with the work divided into the following phases:

1. Literature survey
2. Survey of city inspectors, plumbing contractors, and wholesalers concerning performance of cast iron soil pipe.
3. Determination of the effect of residual stresses

4. Strains and stresses in joints during construction
5. Forces on, and strength of buried pipes
6. Effect of building movements and earth settlements on pipe systems
7. Preparation of design charts and tables for the thickness of hub wall, hub bead, spigot, and barrel.

1.4 Literature Survey

A summary of this survey is given in Section A.1 of Appendix A. The survey revealed work in the following areas:

1. Material properties of cast iron
2. Stresses in pipes due to internal pressure
3. Thermal stresses in individual pipes
4. Earth loading on buried pipes
5. Bending and torsional stresses
6. Stresses in fittings and joints
7. Structural analysis of pipe systems
8. Thickness requirements, residual stresses, and pipe supports.

Extensive work had been conducted at Iowa State University on loads and design requirements for buried pipe over a period of more than two decades. The studies were both experimental and theoretical. The calculation of earth loads and barrel thickness requirements presented in later chapters of this report are all based upon this previous work. No discussion of this work is given here since it will be

presented in the appropriate chapters and the pertinent references given there.

In all the other areas of this research, little information was available that could be directly applied to cast iron soil pipe. However, information that is used is referenced where used.

1.5 Survey of Inspectors, Contractors and Wholesalers

The survey served a two-fold purpose:

1. To obtain information from inspectors, contractors and wholesalers as to their observance of the behavior of both service weight and extra heavy weight cast iron soilpipes and fittings.
2. To acquaint those involved in the use of cast iron soil pipe and fittings with the research being conducted at Iowa State University and by the Cast Iron Soil Pipe Institute.

A questionnaire was mailed to 250 plumbing inspectors, 600 plumbing contractors, and 200 plumbing wholesalers. A 29 percent response was received. A copy of the letter of transmittal and questionnaire is shown in Appendix A (Fig. A.1). The questions concerned location (hub, spigot, barrel) and frequency of breakage for both SV and XH weight pipe. Information was obtained on the conditions during handling, construction and service life in which breakage was observed.

Only general conclusions of the survey are given below since the complete analysis and discussion of the survey is given in Section A.2 of Appendix A.

"Frequent" breakage was observed by more than 10 percent of those answering the questionnaire during only the handling and construction phases of the life of the pipe (Fig. A.3). Since the consideration for handling the pipe and fittings were eliminated from this study for reasons previously mentioned, it appears that the pipe failures have occurred mainly during the construction of the joint. In this case, 29 percent observed frequent breakage during the caulking operation. This implies that 71 percent did not observe appreciable breakage. Also, the fact that the most failures observed were in the caulking operation is reasonable since any undetected breakage from handling would show up during the caulking operation.

It should be pointed out here that it is unreasonable to expect a product to be designed with a factor of safety so high that practically no failure will ever exist. A design of this nature would be highly uneconomical.

In the questionnaire, failures were observed in buried pipe due to improper bedding, laying or backfilling. It was unfortunate, however, that no questions were asked on failures of buried pipe properly installed. However, in the comment section of the questionnaire not one comment out of 149 reported failures of buried pipe (A.2.1.1, A.2.1.2, A.2.1.3). Therefore, it seems reasonable to assume that if

the bedding and backfilling is properly done, that the present cast iron soil pipe gives satisfactory service in the buried condition.

In general, the survey indicated that both SV and XH weight pipe gave satisfactory performance.

2. RESIDUAL STRESSES

2.1 Introduction

Residual stresses are formed in the pipes and fittings as a result of plastic deformation. This plastic deformation results from the differential cooling of the various parts of the pipes or fittings. The purpose of this study was, first, to obtain an indication of the approximate magnitude of the residual stresses in cast iron soil pipe and fittings, but, more importantly, to determine if residual stresses affected significantly their ultimate strength.

Residual strains were measured by means of electric resistance strain gages bonded at various sections. Initial readings of these strain gages were taken, then the sections were sawed apart and final readings taken. The difference between the initial readings and the final readings of the gages at the sections indicated the residual strains. These strains were then converted to stresses by using a modulus of elasticity (E) of 16×10^6 psi and a Poisson's ratio (ν) of 0.25 and an indication of this magnitude was obtained.

The effect of residual stresses on ultimate strength was determined by the use of a number of three-edge bearing tests. Several lengths of pipe which were sand cast and of pipe which were cast in permanent molds were cut at

mid length. Half of the sections were stress-relieved to remove the residual stresses. A comparison of the three-edge bearing loads of the sections of the as-received pipe and the stress-relieved sections were used to determine the effect of the residual stresses.

2.2 Magnitude of Residual Stresses

A straight length of pipe and 45° bend, 90° bend, T branch, and a Y branch fittings, of brand D were used in investigating the magnitude of residual stresses. FA gages were bonded at various locations along the pipe and fittings. The location of the strain gages is shown in Figs. 2.1 and 2.2. The 45° bend had essentially the same gage locations as the 90° bend shown in Fig. 2.1. Most of the gages were placed at critical points, where the effects of differential cooling would probably cause maximum residual strains, such as changes in configuration and thickness. The rest of the gages were placed to give an indication of the strain distribution.

In barrels of straight long pipes, maximum residual strains are primarily in the longitudinal or circumferential direction due to symmetry. Hence, at any desired point along the pipe, only two orthogonal gages were required. In bends and in the hub areas of pipes, maximum strains were also measured in the longitudinal and circumferential directions as a rough estimation of strains. Maximum strains might, however, have been in some other direction

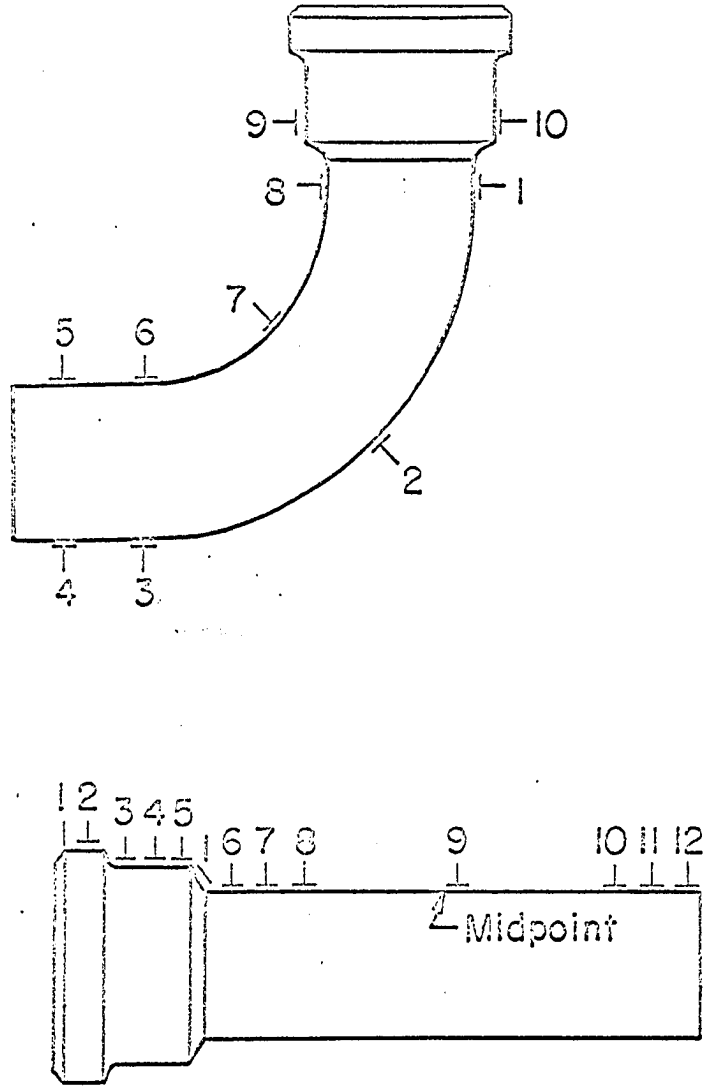


Fig. 2.1. Location of strain gages in 4-inch pipe and bends

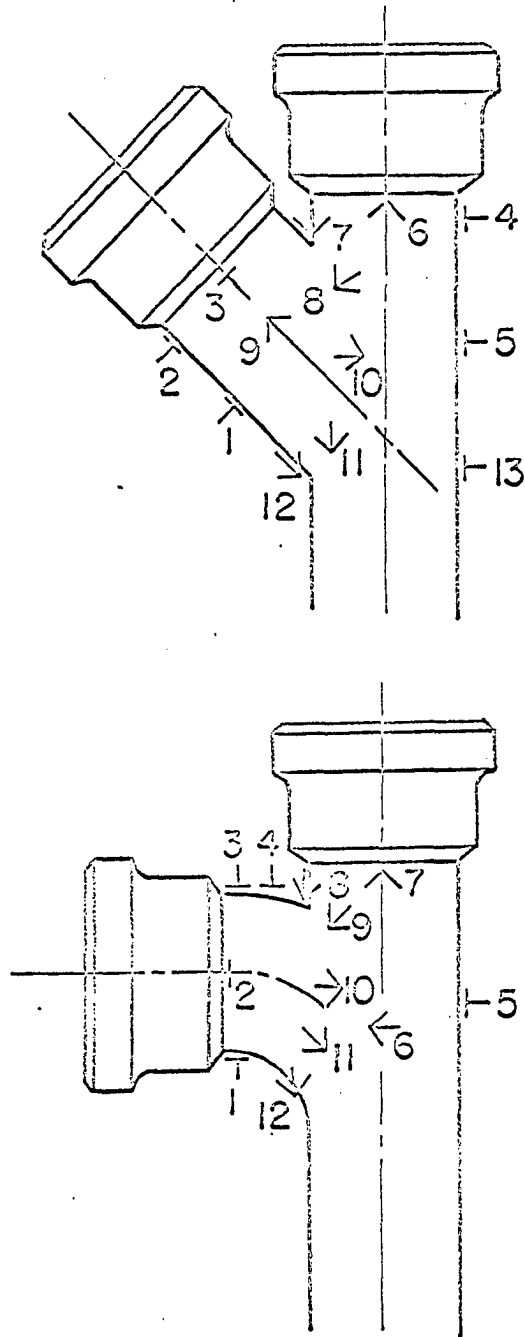


Fig. 2.2. Location of strain gages and rosettes in 4-inch T and Y branches

although the magnitude of the measured strains approached the maximums. In T and Y branches, the principal strain distribution is not known. Thus, rosettes were used to find these principal strains.

The strain values obtained from the above gages were converted to stresses by using E as 16×10^6 psi and ν as 0.25. The stress values for the straight pipe, 45° bend, and 90° bend are shown in Table 2.1. The maximum circumferential stresses occurred in the 90° bend and were 8,150 psi in compression and 4,650 psi in tension. The maximum longitudinal compressive stress, which is perpendicular to the circumferential stress at the point measured, was 5,550 psi and occurred in the 90° bend. The maximum longitudinal tensile stress occurred in the straight pipe and was 1,700 psi.

Residual strains were all compressive in the pipe barrel. This is to be expected since all the strain measurements were taken on the outside surface of the pipe which cools first in a newly cast specimen. However, values shown in Table 2.1 and 2.2 were only intended as an approximate indication of the general magnitude desired at the selected points.

The maximum stresses and their orientation in T and Y branches are shown in Table 2.2. The orientation angles shown in the table were measured from the circumferential axis at that particular point. All measurements were taken as positive clockwise. The maximum stresses occurred in the Y branch and were 9,250 psi in compression and 3,200 psi in

Table 2.1. Residual stresses in pipe and bends

Gage No.	45° FITTING		90° FITTING		STRAIGHT PIPE	
	Strain μ in./in.	Stress Psi	Strain μ in./in.	Stress Psi	Strain μ in./in.	Stress Psi
1C	-173 ^a	-4100	-50	-1150	+9	+100
2C	-168	-3600	-	0	+24	0
3C	-208	-4500	-123	-2500	-137	-3300
4C	-	0	-105	-1800	-164	-3600
5C	-295	-6000	-422	-8150	+154	+1450
6C	-262	-5100	+86	+900	-101	-2700
7C	-156	-2950	+269	+4650	-248	-4750
8C	-116	-1800	+115	+1700	-182	-3500
9C	-	-	-199	-3850	-176	-4050
10C	-	-	-56	-2050	-78	-1700
11C	-	-	-	-	-74	-700
12C	-	-	-	-	-	-
1L	-236	-4850	-33	-800	-210	0
2L	-171	-3750	+3	0	-95	-1450
3L	-208	-4500	-78	-1900	-213	-4300
4L	0	0	-10	-700	-139	-3950
5L	-202	-4800	-211	-5550	-260	-3750
6L	-124	-3300	-131	-1800	-216	-4200
7L	-71	-1900	+5	+1350	-115	-3050
8L	-	-	-56	-450	-97	-2500
9L	-	-	-99	-2600	-228	-4650
10L	-	-	-222	-4050	-90	-1900
11L	-	-	-	-	+117	+1700
12L	-	-	-	-	-72	-1150

^a Minus sign indicates compression.

Table 2.2. Residual stresses in T and Y branches

Gage No.	T-BRANCH		Gage No.	Y-BRANCH	
	Stress psi	Orientation ^a		Stress psi	Orientation ^a
1C	-3300 ^b	0°	1C	-4300	0°
1L	-4350	90°	1L	+3200	90°
2C	-3050	0°	2C	+1900	0°
2L	-4050	90°	2L	+2600	90°
3C	-6350	0°	3C	-3850	0°
3L	-3750	90°	3L	-5100	90°
4C	-3150	0°	4C	+ 700	90°
4L	-6450	90°	4L	+1450	0°
5C	-4200	90°	5L	+1250	0°
5L	-2050	0°	5C	-	-
6A	-2500	19°	6A	-7800	135°
6B	-4850	109°	6B	-3050	225°
7A	-5300	94°	7A	+1900	0°

^a With respect to the circumferential axis at the point measured.

^b Minus sign indicates compression.

Table 2.2. (Continued)

Gage No.	T-BRANCH		Gage No	Y-BRANCH	
	Stress psi	Orientation ^a		Stress psi	Orientation ^a
7B	-8250	134°	7B	- 100	90°
8A	-1350	94°	8A	-5400	0°
8B	-4750	4°	8B	-9250	90°
9A	-4200	15°	9A	-4650	133°
9B	-6800	105°	9B	-6650	48°
10A	+2150	0°	10A	-	-
10B	-3400	90°	10B	-	-
11A	-2500	292°	11A	- 250	141°
11B	-4100	22°	11B	-9250	231°
12A	+ 700	-122°	12L	0	0°
12B	+ 350	- 22°	12C	-4200	90°

tension. Assuming the ultimate compressive stress of cast iron to be about 90,000 psi, the maximum residual stress measured was about 10%. With an ultimate tensile stress of 21,000 psi, the maximum residual stress was 15%.

2.3 Effect of Residual Stresses

The effect of the above residual stresses on the ultimate strength of the pipes was next investigated. Sections of pipes brand A (sand cast) and brand C (permanent metal mold cast) were used as test specimens. Eight pipes of each brand were cut into two equal parts making a total of about 32 pieces. Half of those were stress relieved by heating to about 1,050° F for two hours and then furnace cooled to a temperature of about 600° F before they were removed. The sections were taken from both the spigot half and the hub half of the pipes. All the pieces were then tested in a three-edge bearing test to determine the modulus of rupture. This three-edge bearing test is a standardized procedure in which two closely spaced longitudinal non-deflecting supports are placed at the bottom of the pipe section with the third bearing placed at the top. Load is then applied through these supports. The load was applied by a Baldwin-Southwark Hydraulic Testing Machine with a maximum capacity of 400,000 lbs.

The modulus of rupture was then defined by the following equation:

$$M_R = \frac{W(0.0795)(d + t)}{t^2} \quad (2.1)$$

where,

M_R = modulus of rupture, psi

W = maximum load applied, lbs./ft.

d = inside diameter of pipe, inches

t = wall thickness, inches.

Half of the specimens tested above had hubs. The crushing load, though, was applied to the barrel while the hubs were load-free. In calculating the modulus of rupture, the effect of these hubs on the strength of pipes was neglected. Although the modulus computed in this manner only gives an approximate value, it is sufficient since the purpose of these tests is to determine if stress relief (removal of residual stresses) changes the ultimate strength. Thus, if the same criteria is used to compute the modulus of rupture for the as-received and stress-relieved specimens, a comparison can readily be made. The results of the above tests are shown in Table 2.3. The first column in this table shows the test number and indicates the type of specimen. The second column indicates whether the pipe is stress relieved or not.

The total crushing load, in pounds, applied on the pipe is given in column 6. This load is converted to lbs./ft. of pipe in column 7. The last column lists the relative modulus of rupture of the test specimen as calculated from Eq. 2.1.

Table 2.3. Modulus of rupture of as-received and stress relieved pipe sections

Code No. Col. (1)	Stress Relieved (2)	Length inches (3)	Inside Diam. inches (4)	Thickness inches (5)	Crushing Load lbs. (6)	lbs./ft. (7)	M _R psi (8)
4A7S*-1	YES	30.000	3.905	0.182	12800	5100	50000
4A8S-2	YES	29.878	3.905	0.175	14800	5960	63100
4A9S-3	NO	29.878	3.812	0.180	12800	5150	50400
4A10S-4	NO	29.812	3.875	0.210	17300	6980	51400
4A7H-5	YES	32.878	3.905	0.175	13000	5400	60160
4A8H-6	YES	32.688	3.905	0.170	13300	5500	63180
4A9H-7	NO	32.810	3.878	0.180	13300	5500	56360
4A10H-8	NO	32.125	3.878	0.210	17700	7320	55100
4A1S-9	YES	30.000	4.062	0.252	25300	10100	54500
4A2S-10	YES	29.940	4.062	0.255	22900	9200	48700
4A3S-11	NO	29.878	4.000	0.260	27200	10900	54800
4A4S-12	NO	29.940	4.062	0.250	24400	9800	54200
4A1H-13	YES	32.439	4.062	0.250	23000	9500	51400

*The letter before the dash refers to the section of pipe used.
S is spigot and H is hub.

Table 2.3. (Continued)

Code No. Col. (1)	Stress Relieved (2)	Length inches (3)	Inside Diam. inches (4)	Thickness inches (5)	Crushing Load lbs. (6)	lbs./ft. (7)	M _R psi (8)
4A2H-14	YES	32.439	4.031	0.255	24300	10000	51900
4A3H-15	NO	32.625	4.062	0.250	26300	10860	58700
4A4H-16	NO	32.500	4.188	0.260	25000	10350	51750
4C7S-17	YES	29.940	3.875	0.195	14100	5680	48500
4C8S-18	YES	32.878	3.878	0.195	14420	5290	45000
4C9S-19	NO	29.812	3.970	0.197	14000	5620	47000
4C10S-20	NO	30.125	3.970	0.182	11900	4740	47500
4C7H-21	YES	33.125	3.940	0.200	14600	6050	50200
4C9H-22	NO	33.125	3.970	0.190	12500	5190	47700
4C10H-23	NO	32.878	3.935	0.178	12400	5120	53600
4C1S-24	YES	30.000	4.062	0.245	23500	9400	54000
4C2S-25	YES	29.810	4.031	0.268	30300	12200	58000
4C3S-26	NO	29.940	3.935	0.270	27700	11100	50800
4C4S-27	NO	30.000	3.940	0.275	34000	13600	60000
4C1H-28	YES	33.188	4.094	0.245	25600	10600	59600
4C2H-29	YES	33.062	4.031	0.245	29400	12200	60600
4C3H-30	NO	33.125	3.970	0.270	32500	13420	62200
4C4H-31	NO	33.000	3.935	0.265	32300	13400	64500

For brand A, the average M_R was 54,200 psi for as-received sections and 55,400 psi for relieved sections. For brand C, the average was 54,200 psi for as-received sections and 54,800 psi for relieved sections. The moduli of rupture calculated for the stress relieved sections were not significantly different from those of the as-received sections. Therefore, it can be concluded that the residual stresses have no significant effect upon the ultimate strength of pipes. Thus, residual stresses will be disregarded in any further discussion since they did not affect the ultimate strength of the cast iron.

The modulus of rupture was 56,500 psi for specimens with hubs and 52,400 psi for specimens without hubs. Thus, specimens with hubs had an 8% increase in strength compared with those without hubs. This difference can be expected because of the neglect of the effect of the hub in the calculations.

3. STRENGTH OF BURIED PIPES

3.1 Introduction

The determination of wall thicknesses for buried cast iron soil pipes depends upon the loads on the pipes from earthfill and superimposed live loads. An estimation of these loads is obtained by formulas developed from theory and experiments discussed in Section A.1 of Appendix A. These loads are basically a function of the type, depth, and width of the trench; the magnitude and location of live loads; and the diameter of the pipe.

For each bedding condition, the maximum trench load, causing failure of pipe, was divided by a factor to give it the same magnitude as the ultimate 3-edge bearing load needed to fail the same pipe. This factor is called the 3-edge bearing ratio. This ratio is also used to convert any trench load for a given bedding condition to a corresponding 3-edge bearing load.

The 3-edge bearing load required for crushing of the pipe is related to the required thickness by Eq. 2.1:

$$M_R = \frac{W(0.0795)(d + t)}{t^2} \quad (2.1)$$

where,

M_R = modulus of rupture, psi

W = maximum load applied, lbs./ft.

d = inside diameter of pipe, inches

t = wall thickness, inches

Thus, for a given strength of cast iron and pipe diameter, the wall thickness required for any field installation can be obtained by: 1) obtaining the earth and surface live loads, 2) relating these loads to the 3-edge bearing load, and 3) relating the 3-edge bearing load to the thickness by Eq. 2.1.

A more detailed explanation of the procedures and factors considered in this study are presented in Reference 1. In addition, numerous results for non-critical installations are given. However, a summary of these areas are presented in this chapter and Appendix A.

3.2 Variables Affecting the Barrel Thickness

The main variables affecting the barrel thickness considered in this research are:

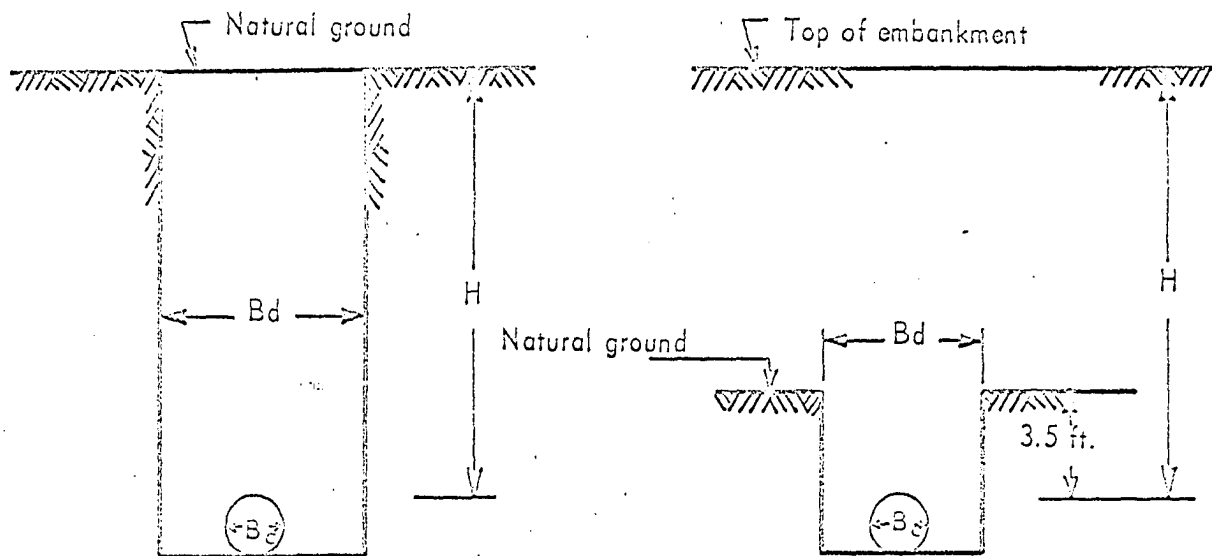
1. Bedding condition
2. Trench and backfill conditions
3. Size of movable surface loads
4. Pipe diameter
5. Wall thickness.

The range of these variables is shown in Fig. 3.1.

The number of types of backfills and bedding conditions are numerous (2)*. However, commonly used conditions in addition to conditions giving maximum stresses were considered. These conditions can be classified into the following categories:

*Numbers in parentheses refer to Section 12 (Literature Cited).

Soil unit weight: 120 pcf



Case 1: Ditch conduit condition.

Case 2: Negative projecting conduit condition

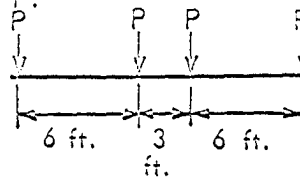
Pipe diameter - B_c (inside)
 2 in., 3 in., 4 in., 5 in., 6 in., 8 in.,
 10 in., 12 in., and 15 in.

Height of fill - H
 2 ft. to 20 ft.

Width of ditch - B_d
 24 in. or more

B_c = external pipe diameter
 (estimated at $d + 1/2$ in.)

Bedding and backfill
 conditions - A, B, C,
 D, E, and F.



$P \approx 9000$ lbs

Surface load

Fig. 3.1. Range of variables in buried pipe study

- A. Flat-bottom trench, backfilling not tamped
- B. Flat-bottom trench, backfilling tamped
- C. Pipe supported on blocks, backfilling not tamped, average block spacing is 5 feet
- D. Pipe supported on blocks, backfilling tamped, average block spacing is 5 feet
- E. Bottom of trench shaped to fit bottom of pipe for about 90 degrees (unevennesses filled in by sand as required), backfilling not tamped
- F. Bottom of trench shaped to fit bottom of pipe for about 90 degrees (unevennesses filled in by sand as required), backfilling tamped.

In each case (except conditions C and D), it was assumed that holes have been dug for the hubs. In conditions C and D, it was assumed that barrels were resting on the blocks at the bottom of the trench.

In soil pipe installations, the pipes are normally laid in trenches dug with mechanical backhoes. However, it is possible that additional embankment may also be placed over the top of a shallow trench or that other excavating equipment, such as shovels and drag lines, are used. Thus in this study, two cases of buried conduits, as shown in Fig. 3.1 were considered:

Case 1: Ditch conduit

Case 2: Negative projecting conduit

with the width of the trench varying from a minimum of 24 inches to any width in Case 1 and from 24 to 36 inches for Case 2, and the depth of fill varying from 2 feet to 20 feet in both cases. In these cases the load on the pipe generally increases with both trench width and pipe depth.

In the case of the ditch conduit, however, if the trench width becomes large enough at a given depth, the effects of the trench sides become negligible and the load is constant for any further increase in width. The width at which the ditch conduit load becomes constant is called the "transition width" and the load is equal to that on a pipe placed on original soil and under a fill on any width. It should be noted that in trenches for smaller pipes (up to 8 inches) and shallow trenches (up to about 12 feet), where a mechanical backhoe is normally used, this transition width is about 30 inches or less. This is normally exceeded in the trenching operation. However, for larger pipe of deeper installations, where the transition width increases, the trench width will also increase due to the equipment required for excavating the trench. Therefore, assuming a trench width equal to the transition width is a realistic conservative assumption. The design for any specific trench width or depth, however, can be obtained from using Eqs. A.4 to A.6 of Appendix A.

An indication of the effect of trench width can be seen in Fig. 3.2. In this figure, the trench load on the

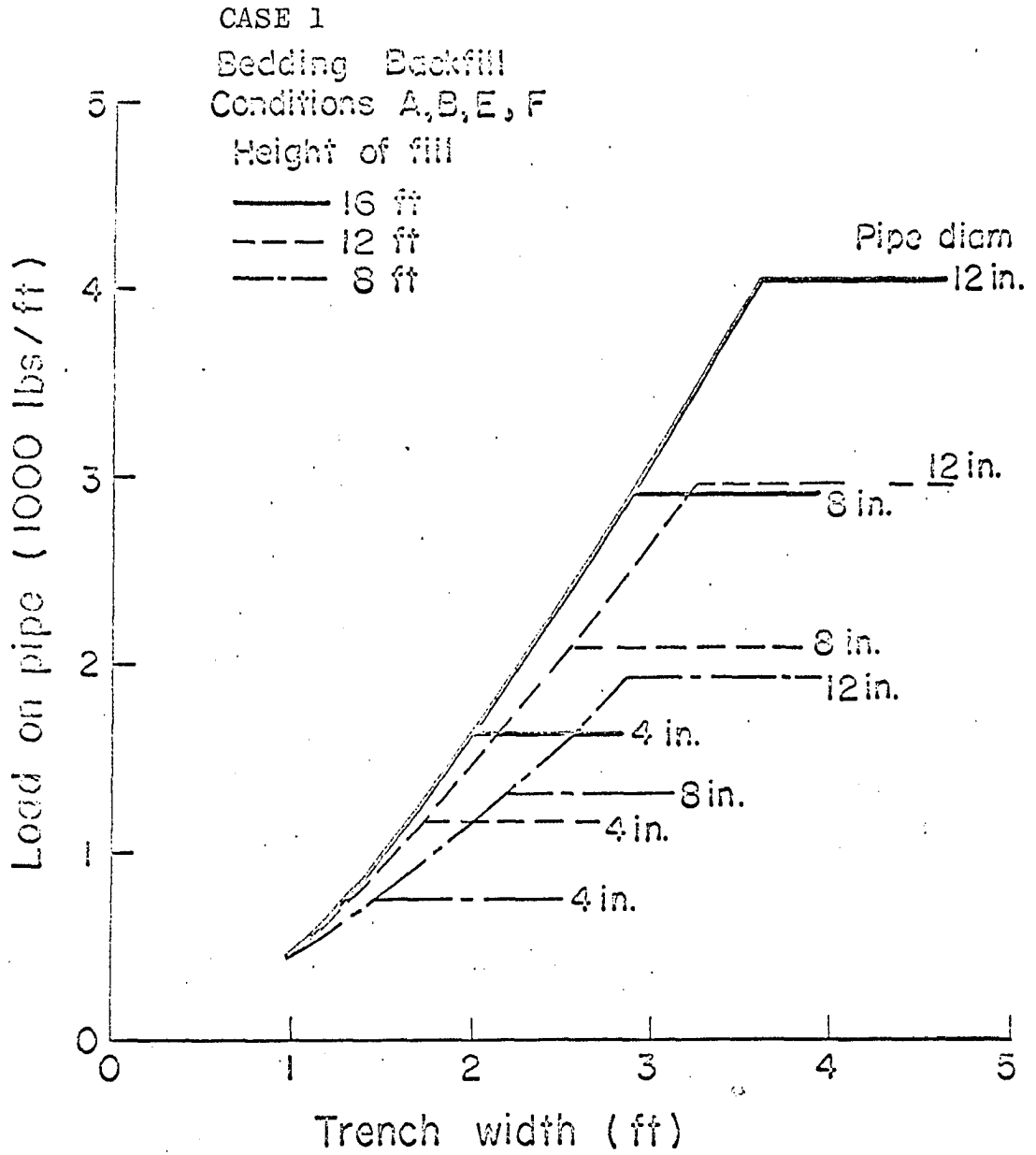


Fig. 3.2. Effect of trench width on trench load due to earth loads

pipe due to earth loads is shown as a function of the trench width. The transition width is the trench width at which the curve becomes horizontal. It can be seen that the transition width is a function of the pipe diameter and depth of fill. If, as mentioned, for a given pipe and depth, the trench width (at the top of the pipe) is less than the transition width, a reduction in load (and an increase in the factor of safety) can be obtained. For example, if a 12-inch pipe is buried at 12 feet, the load with a trench width at top of pipe of 39 inches or more (transition width) is 2,950 lbs./ft.; whereas, at a trench width at top of pipe of 30 inches, the load is only 2,040 lbs./ft. Again, however, it should be noted that only for larger diameter pipe and deep trenches is a reduction of this type generally possible. In most instances, the transition width is exceeded.

For the negative projecting conduit (Fig. 3.1), the width of trench is usually very narrow as it is generally constructed by digging a shallow trench with a backhoe. Then the ground level is raised to grade using fill. The trench loads obtained for this condition will fall between that for a ditch conduit with a trench width equal to that of the narrow ditch and that for a positive conduit (or a ditch conduit at transition width). The procedure for the determination of trench loads for Case 2

installations and computations for a number of critical installations are presented in Reference 1.

Frequently, a rather wide ditch is used down to near the level at which the pipe is to be placed. Then a narrow trench (width less than transition width) is used to the level of the pipe. The load in this case, would be reduced from that at the transition width because of the effect of the narrower trench. Case 2 shown in Fig. 3.1 is typical of the installation of this type. The width of the soil acting on the pipe is taken as that of the narrow trench. The width is then used in Eq. A.4 or A.5 to calculate the load on the pipes.

3.3 Earth Fill Loading

It was mentioned in the previous section that the maximum loading on pipe occurs when the width of the ditch exceeds a specified width called the transition width. For trench widths up to and including this critical width, the loads on pipes can be obtained from Eq. A.4:

$$W_c = C_d \gamma B_d^2 \quad (A.4)$$

where,

W_c = earth load on pipes, lbs./ft.

γ = unit weight of earth, pounds per cubic foot

B_d = horizontal width of ditch at top of conduit, feet

C_d = load coefficient for ditch conduits. This coefficient can be evaluated from Fig. 24-3 of Reference 2.

The unit weight of earth was taken as 120 pcf. Although this may be heavier than much of the fill used, it is considered as a realistic conservative assumption for all installations. If the actual weight of the fill is known, then the external loads due to the fill can be proportionately increased or decreased.

For illustrative purposes, the critical values for C_d and B_d at the transition width for an 8-inch diameter pipe are obtained as shown in Table 3.1 for various fill heights. The ratio of the fill height to the outside diameter of the pipe is computed in the second column of this table. Knowing this ratio, the value of B_d/B_c at the transition width can be determined from charts (2) prepared for this purpose (Fig. E.1 of Appendix E*). This chart was obtained by equating the ditch condition equation (Case 1, Fig. 3.1) to the positive projecting conduit condition (a pipe resting on virgin or firm soil and covered by fill). In this chart, K_u and K_u' (where K is Rankine's lateral pressure ratio, u is the coefficient of internal friction of fill material, and u' is the coefficient of friction between fill material and sides of ditch) have been each set equal to 0.165 to obtain a realistic maximum and to have the same soil in each case. From this graph, the values

*The chart shown here does not cover all H/B_c ratios. Charts shown in Reference 3 cover all ratios shown in Table 3.1.

Table 3.1. Earth loading on 8-inch^a pipes

A. Bedding Conditions A, B, E, and F							
H ft.	H/B_c	B_d/B_c ^b	B_d feet	H/B_d	C_d	B_d^2 (feet) ²	W lbs./ft.
(1)	(2)	(3)	(4)	(5)	(6)	(7)	(8)
8	11.46	3.08	2.15	3.72	2.37	4.62	1315
12	17.18	3.62	2.53	4.74	2.72	6.40	2090
16	22.91	4.14	2.89	5.54	2.90	8.35	2905
20	28.64	4.58	3.20	6.25	3.05	10.24	3750

B. Bedding Condition D							
H ft.	H/B_c	B_d/B_c ^c	B_d feet	H/B_d	C_d	B_d^2 (feet) ²	W lbs./ft.
8	11.46	2.72	1.96	4.08	2.50	3.85	1155
12	17.18	3.25	2.27	5.29	2.87	5.15	1775
16	22.91	3.68	2.57	6.22	3.10	6.60	2455
20	28.64	4.03	2.81	7.12	3.25	7.90	3080

^a The outside diameter of this pipe, B_c , was taken as $d + 2t = 0.698$ ft.

^b In selecting these values from Fig. E.1, a value of r_{sd} was taken as 0.75 (this value was recommended by the American Water Works Association and is listed in Reference 3).

^c In selecting these values from Fig. E.1, a value of r_{sd} was taken as 0.30 (this value was recommended by the American Water Works Association and is listed in Reference 3).

of B_d/B_c are obtained (col. 3 of Table 3.1). The values of B_d can then easily be determined by multiplying the ratio of B_d/B_c by B_c . Having B_d , the value of C_d is determined from Fig. E.3 of Appendix E and is shown in column 6 of Table 3.1. Figure E.3 was obtained from the definition of C_d (4). In using Fig. E.3, a value of Ku' for clay of 0.130 was used to give a more realistic upper bound and to maximize the conditions.

However, instead of using the equations for ditch condition, the equations and factors for a positive projecting conduit could have been employed as a trench of transition width. In this case, the critical value of Ku is 0.1924 and should be used to obtain an upper bound. This can be verified by studying Figs. 24-10 to 24-13 of Reference 2.

Knowing the values of w , C_d , and B_d , the maximum trench load from earth fill can be evaluated from Eq. A.4. The last column of Table 3.1 shows W . To these values of W , any load from surface live loading should be added.

3.4 Load Increase on Pipe due to Live Loading

Although most of the load on the pipe is due to the earth backfill, the effects of a surface live load may be significant near the surface. Since it is possible for a soil pipe to be placed under driveways, load areas, or other locations where surface live loads are possible, a simulated live load has been considered. This live load consists of two passing trucks with both of the rear axles

over the pipe at the same time. The adjacent wheels of the two trucks are 3 feet apart, center to center, and the load on each rear wheel is 9,000 lbs. The wheels are 6 feet apart on the axles. To this load has been added a 50% impact factor for consideration of a rough surface. Figure E.2 of Appendix E gives load curves for various diameters for this type of loading.

Using an 8-inch pipe as an example, the calculations for the loading on this pipe due to live load is given in Table 3.2. The first column gives the same height of fill as used in Table 3.1. The second column lists the load factors, as obtained from Fig. E.2, for the various depths of earth fill. This factor is multiplied by the load of one truck wheel (9,000 lbs.) and also by a 50% impact factor. The result is shown in the third column of this table. The effect of this total load on the pipe is a function of its bedding condition. Table E.1 shows the percentage of load to be used for each bedding condition. Using this table, column four of Table 3.2 was obtained. Multiplying the values of column three by those of column four, the live loads on the pipe for various depths are determined. These loads are then added to the earth loads that are listed in Table 3.1. The final total load is shown in the last column of Table 3.2.

Table 3.2. Load on 8-inch pipe due to earth and surface live loading

A. Bedding Conditions, A, B, E, and F						
H ft.	Load Factor	Factor x 1.5 x 9000	% of Load to be used	Truck Load lbs./ft.	W lbs./ft.	Total Trench Load Truck Load + W lbs./ft.
8	0.010	135	1.00	135	1315	1450
12	0.005	65	1.00	65	2090	2155
16	0.004	55	1.00	55	2905	2960
20	0.003	40	1.00	40	3750	3790

B. Bedding Condition D						
H ft.	Load Factor	Factor x 1.5 x 9000	% of Load to be used	Truck Load lbs./ft.	W lbs./ft.	Total Trench load Truck Load + W lbs./ft.
8	0.010	135	0.90	120	1155	1275
12	0.005	65	0.95	65	1775	1840
16	0.004	55	0.95	50	2455	2505
20	0.003	40	0.95	40	3080	3120

3.5 Conversion of Pipe Load to 3-Edge Bearing Load

The actual stress in the pipe that is induced by these loads is a function of the pipe size (thickness and diameter) and the bedding and backfill conditions. From studies conducted at Iowa State University, the relationship between the trench load acting on the top of the pipe previously computed and the standardized 3-edge bearing load has been determined for various bedding and backfill conditions (3-edge bearing ratio). These relationships for the six field conditions considered in this study are shown in Fig. E.4 of Appendix E.

This figure shows that Type C installation results in very large pipe stresses and, thus, it is not recommended for any type of installation. Therefore, this installation has not been considered in any previous calculations. This installation was also eliminated from consideration in developing the design charts given in Chapter 10.

Figure E.4 of Appendix E shows the 3-edge bearing ratio for various pipe diameters and bedding conditions. The total load W should be divided by this ratio to obtain the equivalent 3-edge bearing load. This ratio is listed in Table 3.3 for the 8-inch pipe for various bedding conditions. The load W , obtained in Table 3.2, is then divided by this ratio to obtain the 3-edge bearing load shown in Table 3.3. Knowing this bearing load for various

installations, the thicknesses that correspond to that particular installation condition can be computed from Eq. 2.1.

Table 3.3 Total equivalent 3-edge bearing load for 8-inch diameter pipes

Bedding and Backfill Condition						
H Ft.	3-edge bearing factor	A 1.15	B 1.34	D 0.84	E 1.50	F 1.80
8		1260	1080	1520	965	805
12		1875	1610	2190	1435	1200
16		2575	2210	2980	1975	1645
20		3295	2830	3715	2525	2105

However, before the thickness can be determined from Eq. 2.1, an indication of the strength of the pipe must be obtained. The modulus of rupture which was used in the subsequent determination of minimum wall thicknesses was determined on the basis of:

- a. a comparison with the minimum tensile strength value of 21,000 psi as specified in ASTM Specification A74 - 64.
- b. the results of 24 3-edge bearing tests of pipes furnished for this study. Several tests were conducted on pipe of each brand and all resulting strengths exceeded the minimum value selected. Knowing the

diameter of pipe and the wall thickness, the crushing load in the tests could be used to compute M_R from Eq. 2.1. A detailed outline of the tests is presented in Reference 1.

Based on the results of a and b above, a minimum value of modulus of rupture of 45,000 psi was specified. This value was confirmed by the results of the residual stress tests of the spigot halves of the pipes tested in the as-received condition (Table 2.3).

3.6 Summary

In the last three sections, a procedure was given to obtain loads on cast iron soil pipes. These loads were then converted to 3-edge bearing loads from which the thicknesses were obtained by Eq. 2.1.

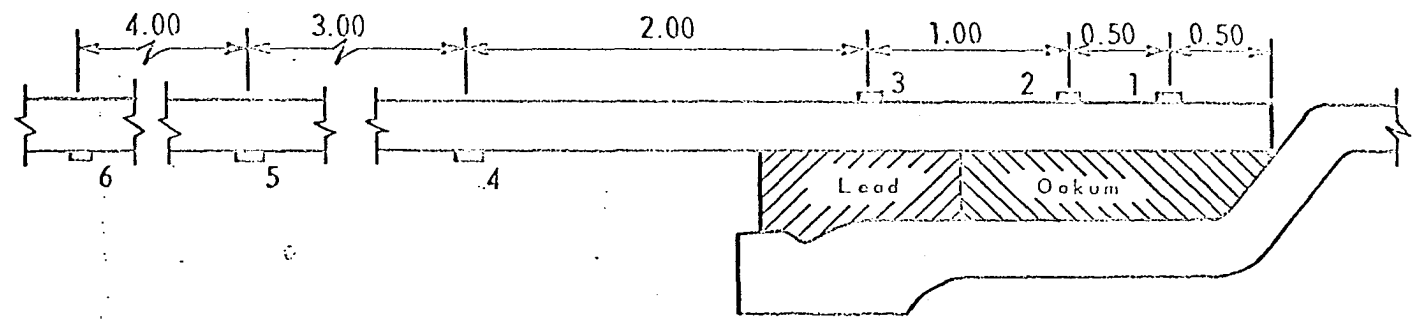
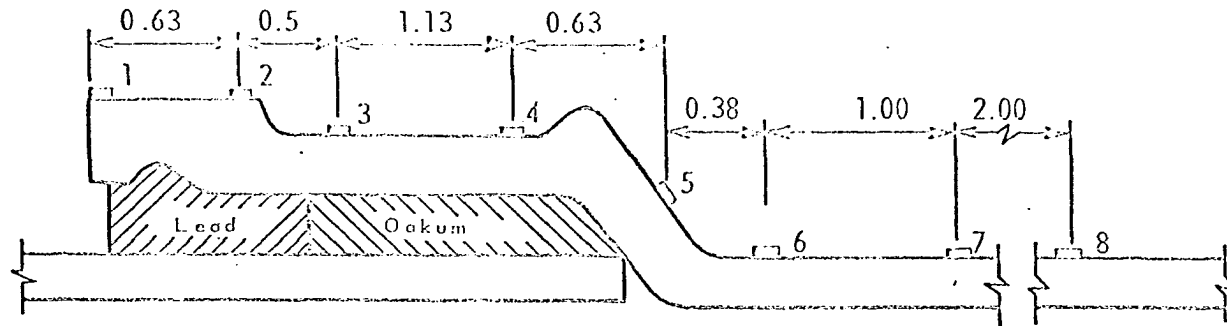
All of the previous example calculations were made for an 8-inch pipe. However, the same procedure can be followed to obtain the 3-edge bearing loads for various bedding installations of various pipe diameters.

4. EXPERIMENTAL YARNING AND THERMAL STRAINS IN 4-INCH PIPES

4.1 Temperature Distribution in the Hubs and Spigots

Measurements of the temperature variation along the hub and spigot of a typical pipe due to pouring lead were taken for two purposes: 1) to select the proper type of strain gages to be used, and 2) to correct for apparent strain in the gages due to temperature increase. This correction improves the strain obtained only slightly since the strain gages used were temperature compensating. A large variation or inaccuracy in the value of this correction will not effect the actual strain more than one or two percent because the strain correction values are small for temperature compensated gages. Thus no need of high accuracy was needed in the graphs. In fact, corrections could have been neglected with only a slight decrease of the accuracy in the obtained strains. However, it was decided to use corrections for more accurate results.

Iron-constantine thermocouples were used to measure the temperature distribution along the hub and spigot. The thermocouple wires were soldered at one end to the pipe and the other ends connected to pyrometers. Figure 4.1 shows the location of the points where temperature measurements were taken. The thermocouples were attached to the hub and spigot at the vicinity of the lead area and at points of abrupt



Note: All dimensions in inches

Fig. 4.1. Location of thermocouples in hub of pipe 4D11 and spigot of 4D12

changes in the hub configuration. Thermocouples were also placed along the hub and spigot a sufficient distance so that the location could be determined in the pipe where the temperature rise due to pouring lead is negligible.

The temperature of the lead poured in the joints was about 1,000° F. This is the approximate temperature at which the oxide which has formed on the surface of the molten lead begins to change in color from yellow to red ($Pb_2O_3 - Pb_3O_4$). Also, this is approximately the kindling temperature of paper. Most plumbers use one of these tests as the lower limit of temperature of the molten lead.

Pipe brand D was used for the temperature measurement. The reason for using this brand was to compare thermal and caulking strains to residual strains already determined for this brand of pipe. The temperature distribution measurements for hub 4D11 are shown in Fig. 4.2. In this figure, the curve numbers refer to the corresponding thermocouple locations shown in Fig. 4.1. Figure 4.2 shows that locations 1 and 2 at the lip of the hub reached the maximum temperature of about 200° F. The other locations reached temperatures between 100° F and 175° F.

FAB gages were used to measure strains in the lip of the hub. These gages were temperature compensated up to 400° F; well above the maximum 200° F recorded in the lip area. FA gages were used in the rest of the hub area

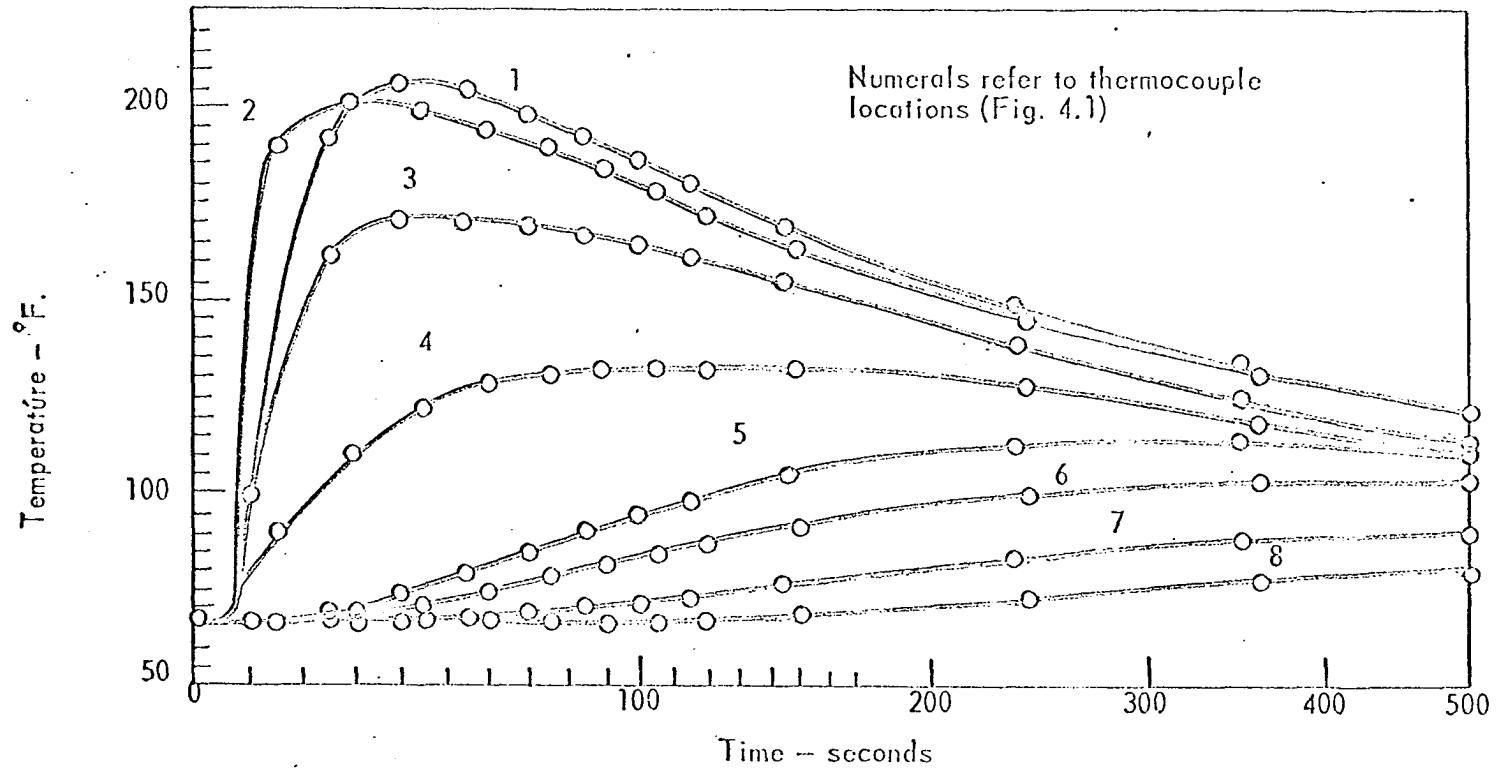


Fig. 4.2. Temperature distribution in hub of pipe 4D11 due to pouring lead at 1,000° F

where the temperature did not exceed 150° F. These gages were temperature compensated up to 150° F.

The maximum temperature in the spigot of pipe 4D12 was 250° F. This temperature occurred about one inch from the center of the lead area (point 2, Figs. 4.1 and 4.3). From Fig. 4.3, it can be seen that points 1, 2, and 3 had temperatures higher than 150° F while the temperature at locations 4, 5, and 6 was lower than 150° F. Hence, FAB gages were used in locations 1, 2, and 3 while FA gages were used in 4, 5, and 6.

The maximum temperature in the XH spigot of pipe 4D3 was about 200° F. This temperature was about 60° F less than that obtained in the SV weight spigot whose thickness was one-half that of the XH spigot. The temperature of the hubs and spigots of both the XH and SV weights reached the maximum at about the same time.

It should be pointed out that the SV hub of brand D had about the same dimensions as the XH hub. Hence, temperature shown in Fig. 4.2 might not have been a maximum for a SV hub. However, the maximum temperature in an ordinary SV weight hub of other brands should not be appreciably larger than that shown in Fig. 4.2. This follows from the spigot tests discussed in the previous paragraph. Using an XH spigot rather than an SV resulted in a 60° F decrease in the temperature for a 100% increase in thickness. The decrease in thickness of the SV hub compared to the XH

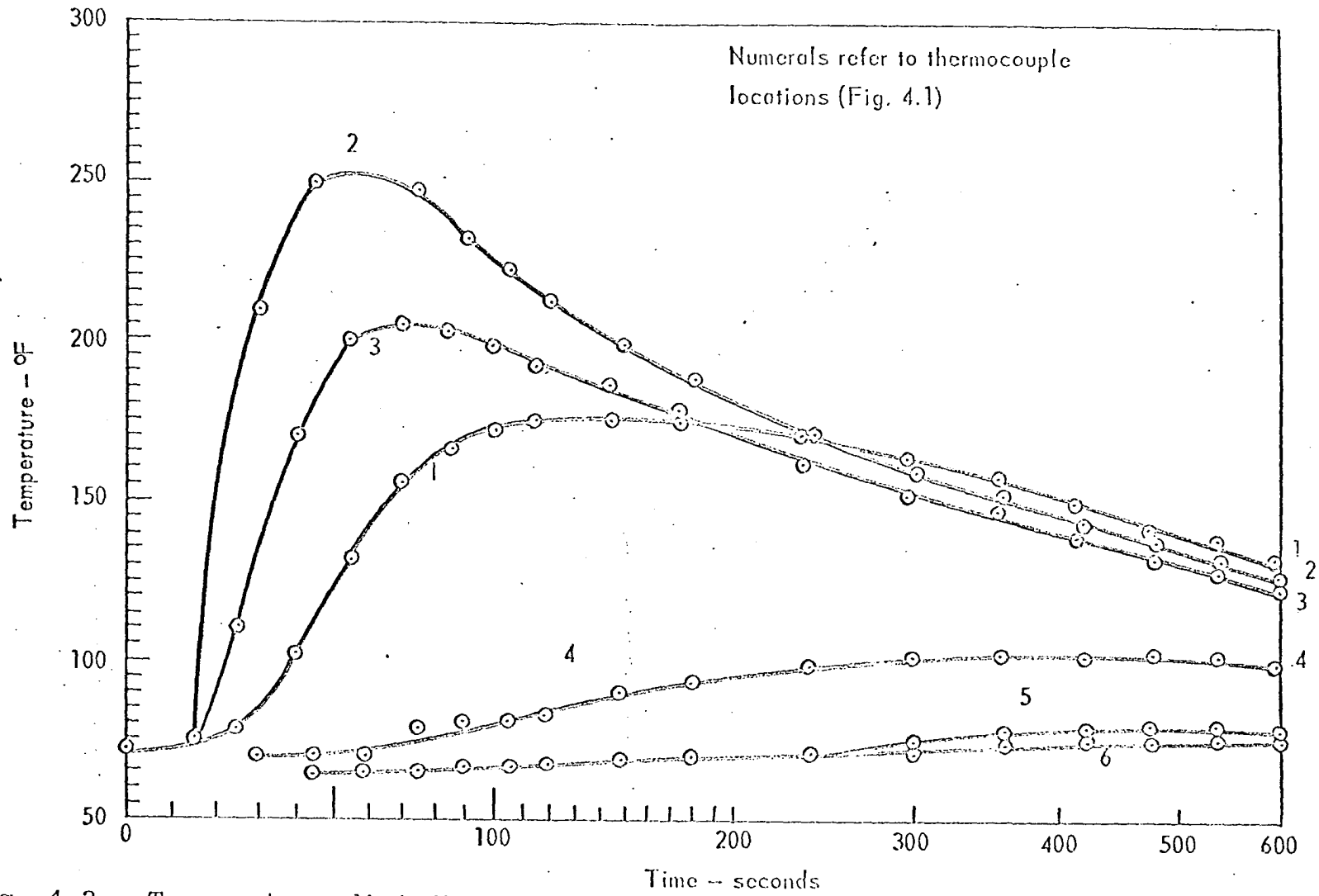


Fig. 4.3. Temperature distribution in spigot of pipe 4D12 due to pouring lead at 1,000° F

hub is only about 30%. Thus, the temperature increase in an SV hub should not be more than 60° F. The determination of the temperature within 60° F is within the accuracy desired in this research.

The curves in Figs. 4.2 and 4.3 were used in the temperature correction of apparent strain in the gages due to increased temperature (Section 4.3). These curves were plotted for an SV spigot and an XH hub. However, these curves were used for all SV and XH weights of all brands. This procedure is justified since the temperature correction was done on an already temperature compensated gage. Thus, this correction is secondary in nature. Even a 50% error in estimating the actual temperature in a spigot or hub will result in a correction error of 2% of the ultimate strain based on a cast iron strength of 21,000 psi.

4.2 Yarning Strain Distribution in Hubs and Spigots

After placing the spigot into the hub, and before thermal stresses are induced, the yarning operation is done. It consists mainly of inserting rings of oakum around the joint. The ends of the rings are overlapped in a staggered form to prevent leakage when the pipe system is in use. These rings are forced-in, one at a time, by using a hammer and a yarning tool. Some yarning tools used are shown in Appendix A.

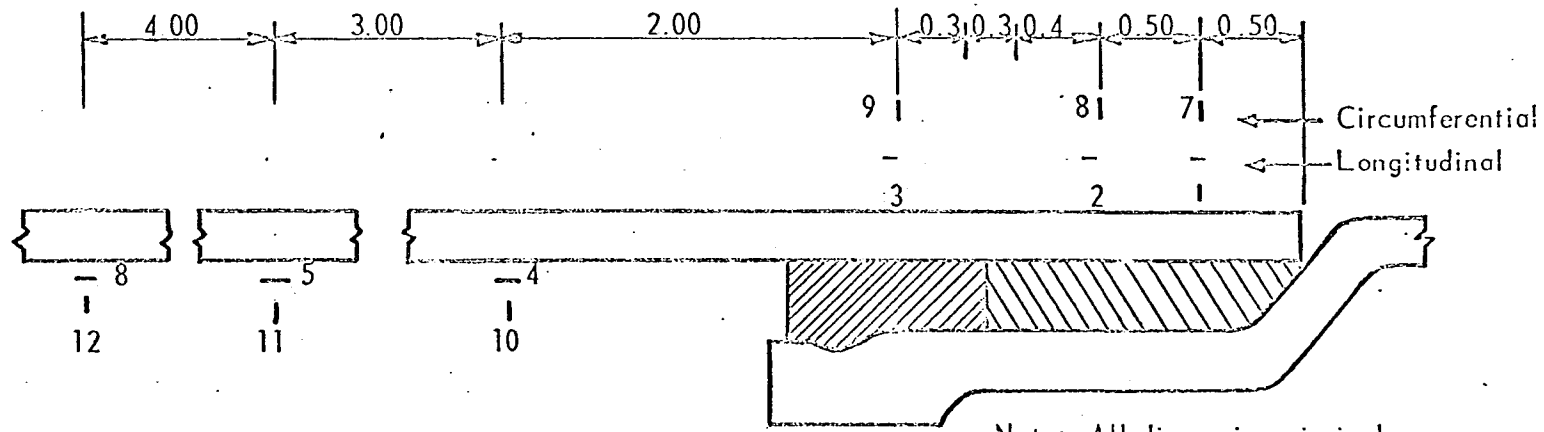
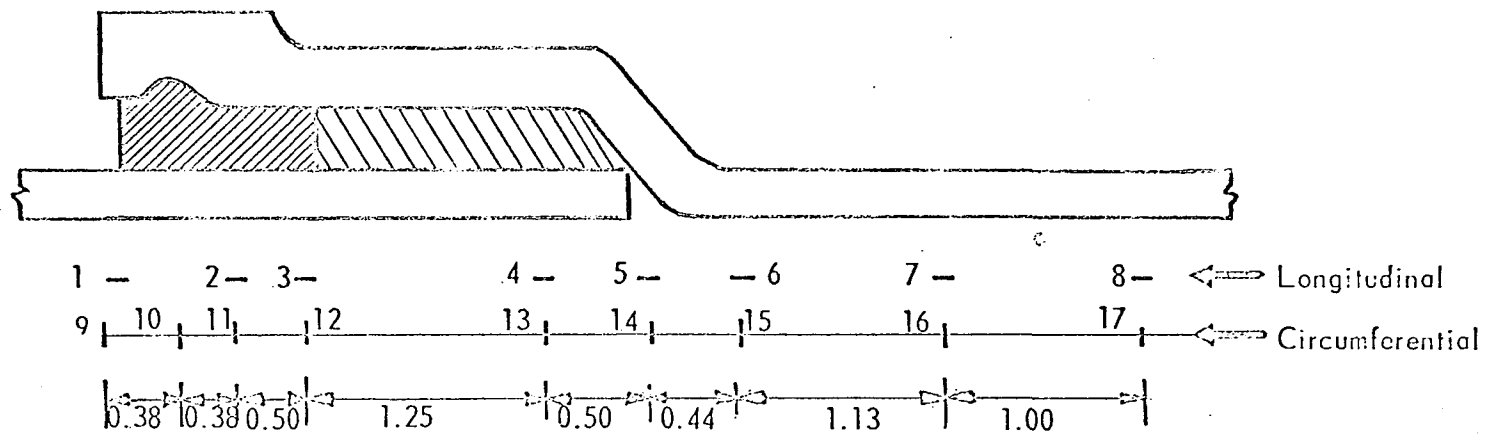
Hubs of pipes 4D2 and 4D12 plus spigots of pipes 4D3 and 4D11 were employed for the yarning strain distribution.

These hubs and spigots were the same ones used for the temperature investigation. This was done in order to compare yawning strains with thermal strains. Strain gages were bonded on the hubs and spigots at the locations shown in Fig. 4.4*. Since these gages were also used for thermal measurements, FAB gages were used in locations where the temperature exceeded 150° F. In the hubs, gages 1, 2, and 10 were FAB. In the spigots, gages 1, 2, 4, 9, 10, and 13 were FAB. All other gages were ordinary FA type.

Strains were measured continuously during yawning by Brush Recording Amplifiers, Model BL-520. The use of the amplifiers was justified due to the slow time-rise of the stress wave. The dynamic and static components of the strain were too small to require the use of the oscilloscope. This is verified in Appendix C.

The maximum approximate strains obtained from yawning are shown in Table 4.1. Gages not listed had zero strains. The maximum strain in the hub was 100 μ in./in. in tension and practically zero in compression. In the spigot, the maximum strain was 29 μ in./in. in compression and 275 μ in./in. in tension. The above strains were all

*With the exception of gages 9 and 11 in the hub, these gages were used in caulking as explained later.



Note: All dimensions in inches

Fig. 4.4. Strain gage location in hubs and spigots of 4D pipes

Table 4.1. Maximum strains (μ in/in) in hubs and spigots of 4D pipes due to yawning

HUB						
Gage Number	SV	Max. Comp.	Final + -	XH	Max. Comp.	Final + -
	Max. Tension			Max. Tension		
1	20	0	+20	0	0	0
10	100	15	0	25	0	0
12	20	10	0	0	0	0
13	30	0	0	0	0	0

SPIGOT ^a			
Gage Number	SV	Max. Comp.	Final + -
	Max. Tension		
1	40	80	0
2	40	20	+40
3	40	30	0
4	35	20	0
7	290	275	+30
8	270	245	-20
9	235	140	+20
10	70	115	-20

^a No measurements were taken for the XH Spigot since the strains were practically zero.

circumferential. All final strains were practically zero. Thus, no yarning strains were added to the strain of the second joining operation, pouring the lead. However, strains from other joining operations will be compared to the yarning strains in order to obtain location and magnitudes of the maximum strains. Knowing the locations and magnitude of the maximum strains for each operation will allow further tests with considerably less instrumentation.

4.3 Thermal Strain Distribution in Hubs and Spigots

Oakum is packed tightly during the yarning process to about one inch from the edge of the hub. This one inch is then filled with molten lead*. Hubs and spigots of the previous section were used for determining the thermal strain distribution. This setup allowed for comparison of strains during the yarning operation in construction of the joint.

Samples of strain distribution in hubs and spigots are shown in Fig. 4.5. All other gages had similar patterns. Since the strain gages were heated with the pipe, slight apparent strain was also reported in the temperature compensated gages. This apparent strain was eliminated according

*Most codes specify a minimum depth of the lead surface from the edge of the hub as one inch.

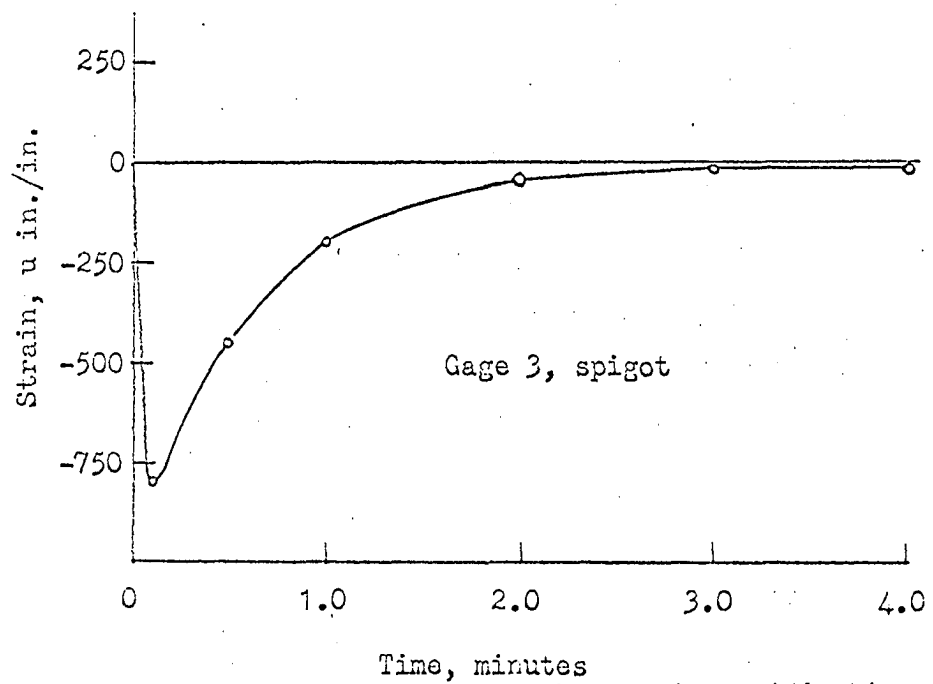
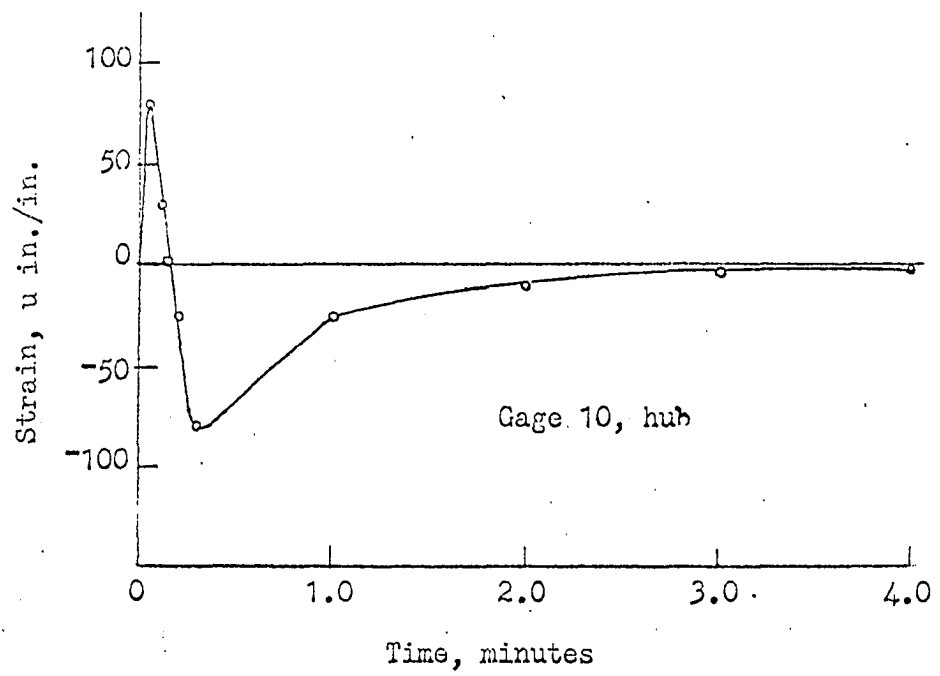


Fig. 4.5. Typical variations of thermal strains with time

to the correction curves shown in Fig. 4.6. These curves were furnished by the manufacturer of the gages (Baldwin-Lima-Hamilton). The time was noted at which the strain was desired. At this time, the temperature was found from either Fig. 4.2 or Fig. 4.3. With this temperature, the apparent strain was obtained from Fig. 4.5 and a corresponding correction was made to obtain the true strain.

Figure 4.7 shows the maximum thermal strains for hubs 4D2 and 4D11. The maximum measured strains were 155μ in./in. in compression and 95μ in./in. in tension. The maximum tensile strain occurred near the lip area while the maximum compressive strain occurred at the end of the hub. Thus, the maximum tensile strain shown above was about half the maximum compressive strain in the hub. But, since the strength of cast iron in tension is about one-fourth that of compression, tensile strains govern in the hub and the lip area is the critical section of the hub. All strains after the joint cooled down were zero.

The difference of the strain pattern shown in Fig. 4.7 is partly due to the variation in lead temperature, location

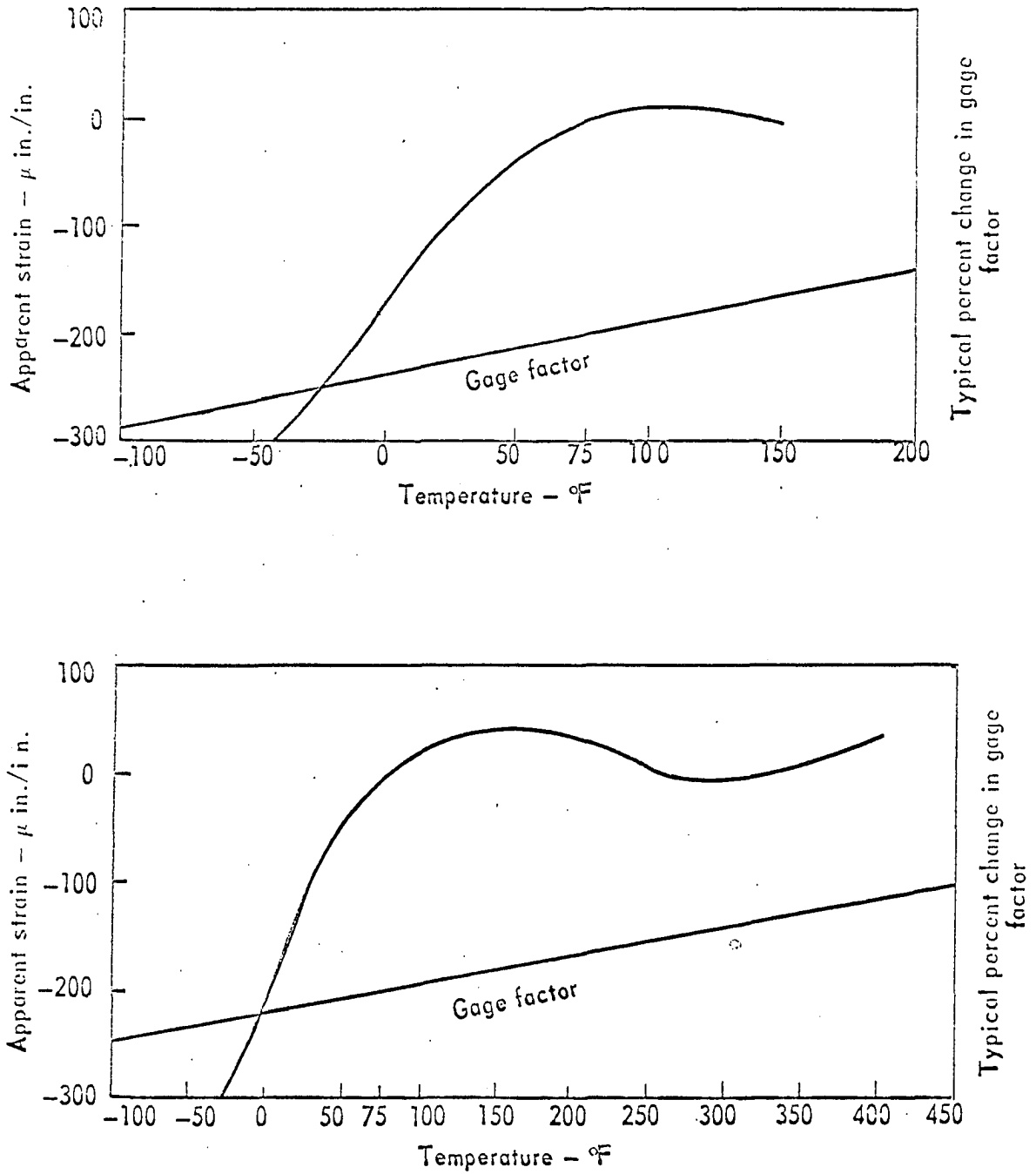
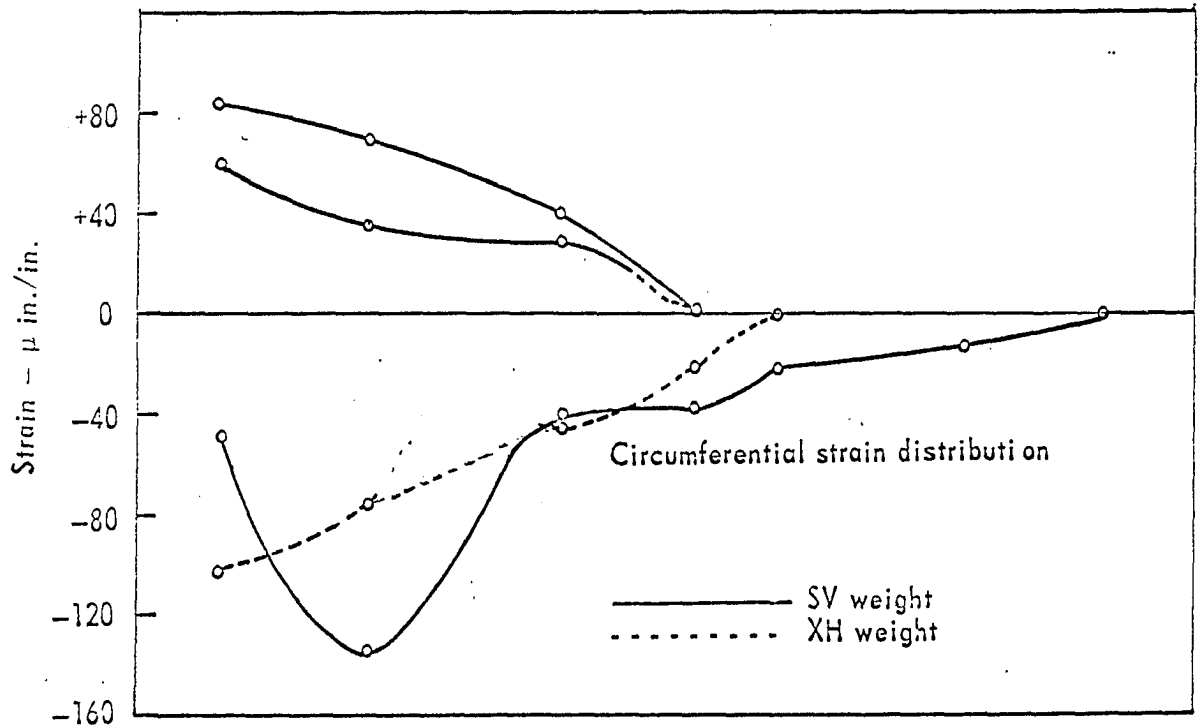
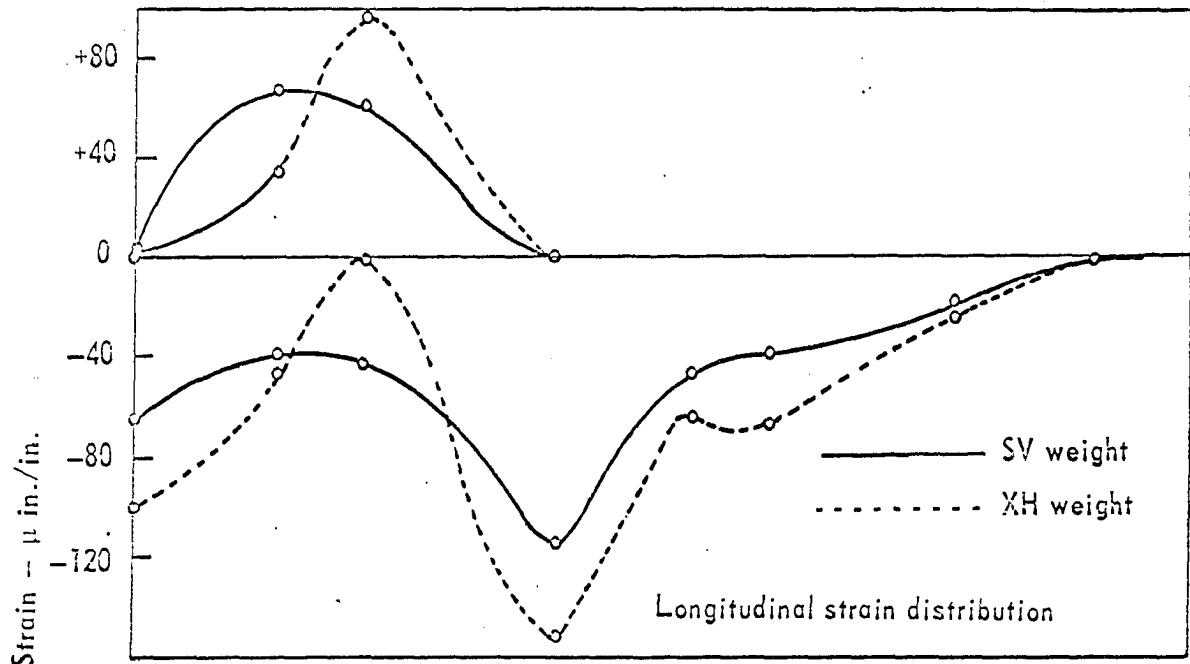
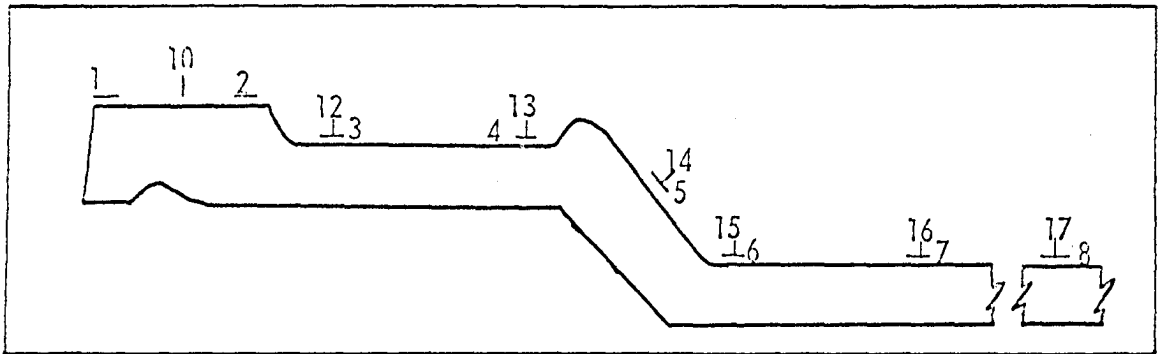


Fig. 4.6. Characteristic curves for FA gages (top) and FAB gages (bottom)

Fig. 4.7. Thermal strain envelope in hubs of pipe brands 4D11 and 4D2 due to pouring lead at 1,000° F



from which lead was poured, and the quantity of lead used in the joint. In both weights, there were no strains 4 inches away from the hub area.

The strain distribution in the spigots of pipes 4D3 and 4D12 is shown in Fig. 4.8. The strains were obtained in a similar manner as those of the hub. The figure indicates that the maximum strains were in the SV weight spigot. The maximum longitudinal strains were 310μ in./in. in tension and 800μ in./in. in compression. The maximum circumferential strains were 150μ in./in. in tension and 550μ in./in. in compression. Therefore, the circumferential strains govern the strength requirements for the spigot. The figure also indicates that the maximum strains are in the vicinity of the lead ring. Furthermore, there were no strains seven inches from the spigot end.

Figures 4.7 and 4.8 discussed above, show the envelope of maximum thermal strain obtained from the time lead was poured till the time the joint was at room temperature again. Thus, the variation of the strains with time at each point could not be studied from the plots shown. Also, the plots do not show the fact that maximum temperatures at different points were reached at various times. The plots only indicate an envelope of strains at the measured points. In between measured points, an approximate curve was fitted.

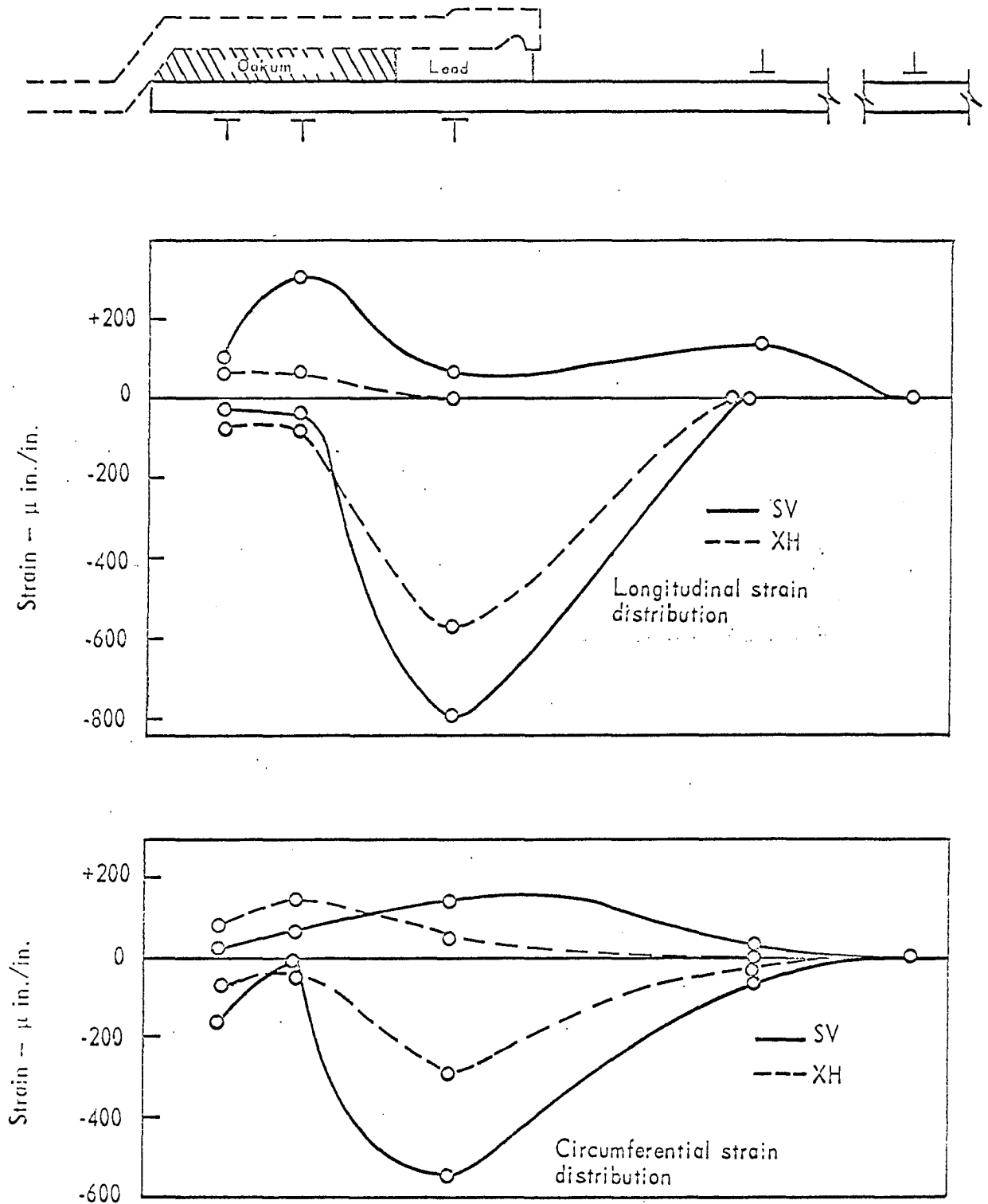


Fig. 4.8. Thermal strain envelope in spigots of pipe brands 4D12 and 4D3 due to pouring lead at $1,000^{\circ}$ F

4.4 Concluding Statement

The maximum yarning tensile strain was 100μ in./in. in the hub and 275μ in./in. in the spigot. These yarning strains were lower than the caulking strains discussed later (Chapters 5, 8, and 9). Also, since strains after completing the yarning operation were zero, they will not be superimposed on other strains in the joining operation. In fact, yarning strains will not be considered in any further discussion since their maximum value was too small compared to the maximum caulking strains.

The maximum tensile thermal strains were 95μ in./in. in the hub and 310μ in./in. in the spigot. These strains reached their maximum value within one minute after pouring lead in the joint, then dissipated to practically zero when the joint cooled down (Fig. 4.5). The maximum values obtained, however, were smaller than the caulking strains discussed in Chapters 5, 8, and 9. These caulking strains varied from 260 to 900μ in./in. in the hub and 300 to 500μ in./in. in the spigot. Hence, thermal strains will not be considered in any further discussion since caulking strains will control the design of the hubs and spigots.

The design criteria for cast iron is based on its stress. However, in the above discussion, only strains were considered. This is appropriate since the magnitude of the result of the combination of these strains to give maximum stress is practically the same as the magnitude of the separate strains compared.

5. CAULKING STRAINS

5.1 Introduction

Caulking of the joint is performed shortly after pouring lead in the joint. It consists of forcing the lead ring to about 1/8 inch below the edge of the hub with a caulking iron and a hammer. A normal caulking operation consists of caulking around the inside then the outside of the solidified lead ring, or vice versa. Caulking irons vary in shape and size. Types of caulking irons used in this research are shown in Appendix A. Unless otherwise indicated, all caulking of the 4-inch pipes used in this research was done once around the outside and once around the inside.

Caulking strains were measured by means of Tektronix, Type 502A, cathode ray oscilloscopes (CRO). Permanent records of the strains were recorded by polaroid pictures taken with cameras mounted on the screens of the oscilloscopes.

5.2 Experimental Strain Distribution in the Hub and Spigot of 4-inch Pipes

Caulking strain distribution in the hub and spigot was needed for two reasons: 1) to find the location of maximum strains, and 2) to determine how far caulking strains extended along the hub and spigot.

Hubs of pipes 4D11 and 4D2 were used for determining the caulking strain distribution. These are the same hubs that were

used in the thermal strain investigation. Hence, a direct comparison can be made between thermal and caulking strains. The gage locations for both the longitudinal and circumferential strain measurements are shown in Fig. 4.4*. During the caulking process, only the strains of four gages could be simultaneously measured with the available facilities. Also, both circumferential and longitudinal strains were measured in any one test. After caulking a joint and measuring four strains, the lead was melted and a new joint was made. For most tests, this new joint was caulked and the strains from three other gages and one from the previous test were measured and so on. Thus, the common gage between any two joint tests served to indicate the consistency or variation in caulking the joints.

The dynamic component of the caulking strains was small compared to the static component as discussed in C.2 of Appendix C. This is partly due to the high damping quality of cast iron and the soft nature of lead. The maximum dynamic component of the strain was about 200μ in./in. with an average of 100μ in./in. However, the strains given in this report are the maximum which include static and dynamic. No effort was made to separate the total strain into its static and dynamic components. Longitudinal strains are

*With the exception of gages 9 and 11. These gages were bonded on a brand B pipe hub. The use of this hub is discussed later in this section.

shown in Table 5.1 and circumferential strains in Table 5.2.

Caulking strains were obtained for hubs 4D11 and 4D2. Both of these hubs were used in the thermal strain investigation with gages bonded as shown in Fig. 4.4*. The 4D2 hub, although XH, had similar dimensions as hub 4D11. Hence, the strains for hub 4D11 (rows 1 to 6, Tables 5.1 and 5.2) were averaged with those of hub 4D2 (rows 7 to 10, Tables 5.1 and 5.2).

The average strain for each gage location for both hub tests were plotted as a solid line in Fig. 5.1. This line indicates that the maximum tensile strain due to caulking is in the hub bead. The maximum tensile strain was $265 \mu \text{ in./in.}$ circumferentially and $70 \mu \text{ in./in.}$ longitudinally. Gage # 10, which indicated the maximum strain was at the middle of the hub bead. Thus, the exact distribution of the strain along the hub bead was not yet known. To determine this distribution, and to determine the maximum strain in an SV hub, hub of pipe 4B14 was used with gages at locations 9, 10, 11, and 12. Three tests were run. The strains are shown in rows 11 to 13 of Table 5.1 and 5.2. The average of these strains is shown in Fig. 5.1 as a dotted line. This line indicates that the maximum tensile strain is approximately uniform along the hub bead and diminishes rapidly beyond that. The

*With the exception of gages 9 and 11. These gages were bonded on a brand B pipe hub. The use of this hub is discussed later in this section.

Table 5.1. Longitudinal caulking strain distribution^a in hubs of 4-inch pipes

Test #	Gage #							
	1	2	3	4	5	6	7	8
	+ ^b -	+ -	+ -	+ -	+ -	+ -	+ -	+ -
4D11-1	50 70	50 60	-	-	-	-	-	-
4D11-2	-	-	0 150	30 60	-	65 100	-	-
4D11-3	-	-	-	40 35	-	-	30 75	40 70
4D11-4	-	-	-	-	-	-	-	-
4D11-5	-	-	-	15 65	55 40	50 100	-	-
4D11-6	-	-	0 140	-	-	-	-	-
4D2-7	40 130	40 70	30 160	-	-	-	-	-
4D2-8	-	-	-	-	-	90 100	50 70	-
4D2-9	-	-	-	140 100	30 100	-	-	-
4D2-10	-	-	-	-	-	-	-	50 30
4B14-11	-	-	-	-	-	-	-	-
4B14-12	-	-	-	-	-	-	-	-
4B14-13	-	-	-	-	-	-	-	-

^a Values of strain are given in μ in/in.

^b Positive indicates tension and negative indicates compression.

Table 5.2. Circumferential caulking strain distribution^a in hubs of 4-inch pipe

Test #	9		10		11		12		13		14		15		16		17	
	+ ^b	-	+	-	+	-	+	-	+	-	+	-	+	-	+	-	+	-
4D11-1	-	-	-	-	-	-	-	-	-	-	50	65	-	-	80	20	-	-
4D11-2	-	-	-	-	-	-	-	-	-	-	50	65	-	-	-	-	-	-
4D11-3	-	-	-	-	-	-	-	-	-	-	-	-	-	-	-	-	40	40
4D11-4	-	-	-	-	-	-	-	-	-	-	-	-	20	40	-	-	-	-
4D11-5	-	-	-	-	-	-	-	-	-	-	-	-	-	-	-	-	-	-
4D11-6	-	-	-	-	-	130	60	35	30	-	-	-	-	-	-	-	-	-
4D2-7	-	-	330	100	-	-	-	-	-	-	-	-	-	-	-	-	-	-
4D2-8	-	-	-	-	-	-	-	-	-	-	-	-	80	30	60	30	0	-
4D2-9	-	-	-	-	-	60	80	60	40	-	-	-	-	-	-	-	-	-
4D2-10	-	-	200	150	-	-	-	-	-	-	30	30	-	-	-	-	100	100
4B14-11	100	65	150	50	-	0	0	-	-	-	-	-	-	-	-	-	-	-
4B14-12	350	0	250	0	300	0	25	0	-	-	-	-	-	-	-	-	-	-
4B14-13	225	100	-	-	150	0	75	0	-	-	-	-	-	-	-	-	-	-

^a Values of strain are given in μ in/in.

^b Positive indicates tension and negative indicates compression.

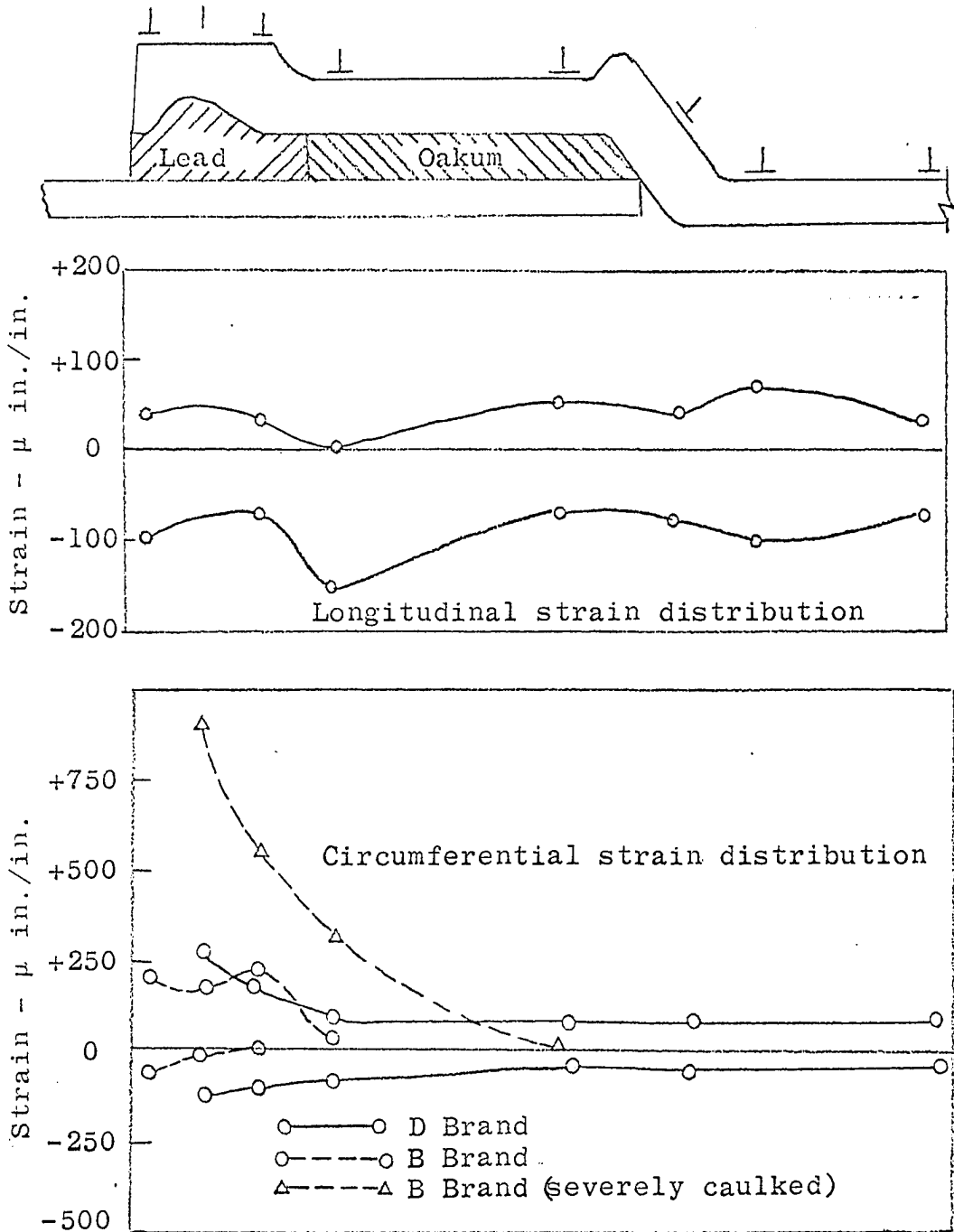


Fig. 5.1. Maximum caulking strain envelope in hubs of 4-inch pipes

maximum tensile strain was 225μ in./in. circumferentially. It can be concluded then that the critical section in the hub is the hub bead, as shown in the figure, and that strains decrease rapidly beyond that causing no appreciable strain in the hub wall and barrel area.

To measure the maximum strain that can occur in the hub due to caulking, hub 4B14 was severely caulked. The maximum strain measured was 900μ in./in. in tension and was at the bead. The strain distribution due to this severe caulking is shown in the lower part of Fig. 5.1.

It should be pointed out that the strains shown above were obtained from joints that were caulked by laboratory technicians with no previous experience. Thus, these joints were not expected to be caulked as sound as those caulked by professional plumbers. As a consequence, the magnitude of the measured strains (Tables 5.1 and 5.2) might have been lower than that obtained from normal caulking performed by a plumber. The strains obtained here, however, were only intended to indicate the location of the maximum strain area. Their actual maximum value was not of primary importance at this point. With the location of the maximum strain region known, the amount of instrumentation would be cut at a minimum. This results in a more efficient use of time and materials.

Table 5.3. Longitudinal caulking strain distribution^a
in spigots of 4-inch pipes

Test #	1		2		3		4		5		6	
	+ ^b	-	+	-	+	-	+	-	+	-	+	-
4D3-1	-		-		175	75	50	100	-		-	
4D3-2	50	50	50	90	-		-		-		-	
4D3-3	-		-		-		-		30	70	0	80
4D3-4	-		-		-		-		-		-	
4D12-5	-		-		-		90	20	120	30	-	
4D12-6	40	100	40	90	-		-		-		-	
4D12-7	-		-		500	0	-		-		100	100
4D12-8	-		-		500	0	-		-		-	

^a Values of strain are given in μ in/in.

^b Positive indicates tension and negative indicates compression.

The same spigots used in the investigation of thermal strains were used to determine the caulking strain distribution. Strain gages were bonded as shown in Fig. 4.4. The strains for spigot 4D3, an XH weight, are shown in the first four rows of Tables 5.3 and 5.4. The maximum tensile strain was 175 μ in./in. longitudinally and the maximum compressive strain was 260 μ in./in. circumferentially.

Table 5.4. Circumferential caulking strain distributio^a
in spigots of 4-inch pipes

Test #	9		10		13		16		17		18			
	^b		+	+	-	-	+	+	-	-	+	+	-	-
4D3-1	-			-				-			-		-	
4D3-2	-			-	150	260	110	90			-		-	
4D3-3	130	120	120	180			-				-		-	
4D3-4	-			-			-		100	30	120	30		
4D12-5	-			-			-	80	170	120	70		-	
4D12-6	280	210	340	270			-				-		-	
4D12-7	-			-	400	675		-			-		50	75
<u>4D12-8</u>	-			-			-				-		50	80

^a Values of strain are given in μ in/in.

^b Positive indicates tension and negative indicates compression.

To compare the above results with those of the SV weight, spigot of pipe 4D12 was tested. Strains obtained are shown in rows 5 to 8 in Tables 5.3 and 5.4. The maximum tensile strain was 500μ in./in. longitudinally and the maximum compressive strain was 675μ in./in. circumferentially. Thus, assuming approximately the same austerinity of caulking in all tests run, the strain in the SV weight was about 2.5 times that of the XH weight.

Strain distribution of the SV weight spigot is shown by the solid line in Fig. 5.2. The dotted line is for the strain distribution of the XH weight spigot. The maximum strain in both cases is in the vicinity of the lead zone. Since only one gage was bonded in the area where maximum strain was measured, the true maximum might not have yet been indicated. However, the strains obtained here were only intended to indicate the location of the maximum strain area. Their actual maximum value was not of primary importance at this point. Figure 5.2 also indicates that these strains diminish rapidly away from the lead zone and are practically zero at seven inches from the end of the spigot.

After establishing the fact that the critical section in the hub is the bead and the critical section in the spigot is around the lead zone, a theoretical solution was formulated to predict strain distribution in other pipe sizes, and to establish design equations. The theoretical strain distribution is discussed in the next two sections.

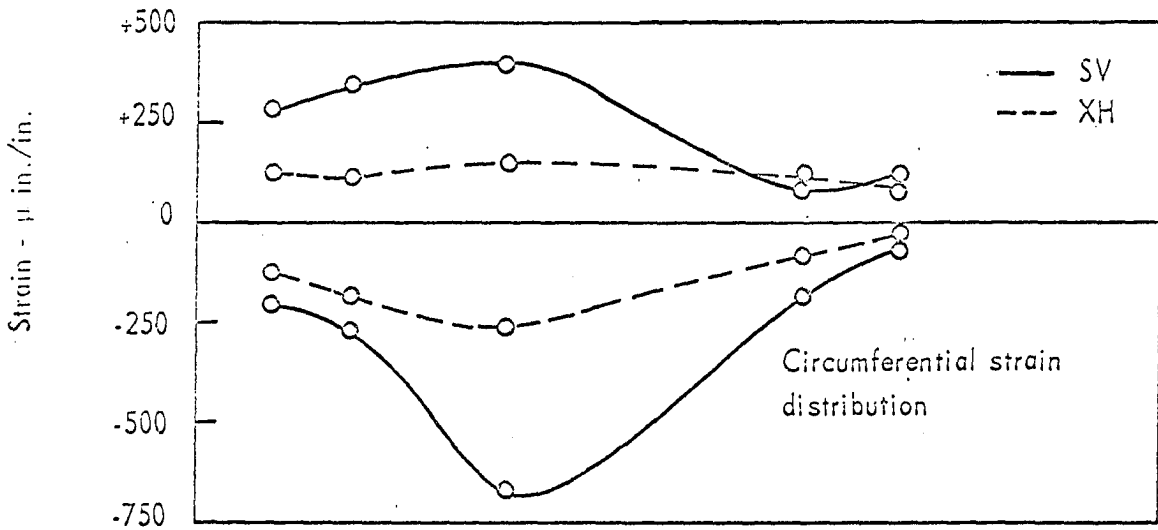
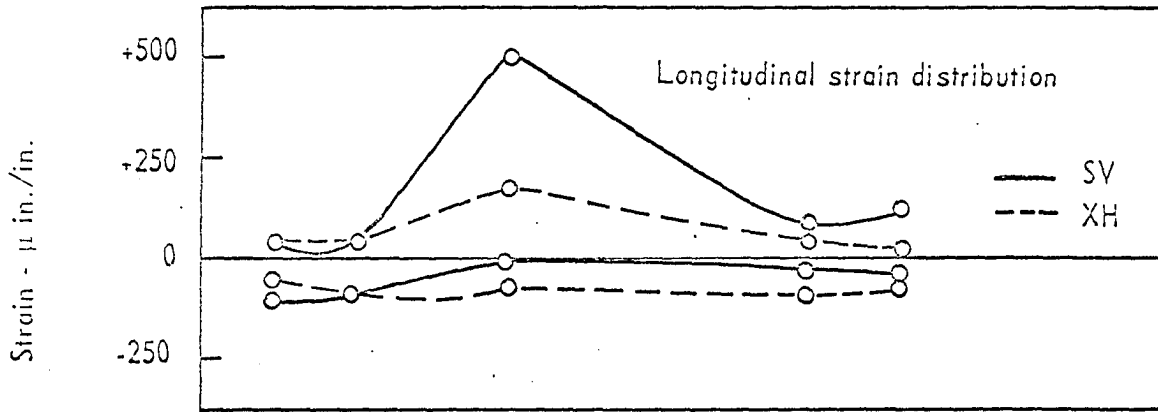
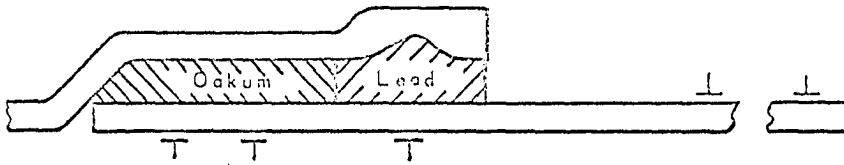


Fig. 5.2. Maximum caulking strain envelope in spigots of 4-inch D brand pipes

5.3 Theoretical Strain Distribution in Hubs

For the strain analysis of the hub due to caulking, the cross section is idealized as shown in Fig. 5.3b. The caulking force applied to the hub is assumed to be a radial line load located at the end of the hub. The hub is separated into two parts at the point of discontinuity of the thickness (Fig. 5.3b). Each part is analyzed as a thin cylindrical shell. The hub bead is considered as a short shell and hence end conditions influence the strain values. Forces acting on the bead are the caulking force P , shear Q , and moment M . The rest of the hub is considered as an infinitely long shell acted upon by the moment M and shear Q . Notice that P , Q , and M are all uniformly distributed along the circumference. The sign convention used in the following analysis is shown in Fig. 5.3c.

Equations for the hub bead will be first established. The general solution of a cylindrical shell that is symmetrical around the longitudinal axis and is not subjected to axial forces is given by Timoshenko (5) as:

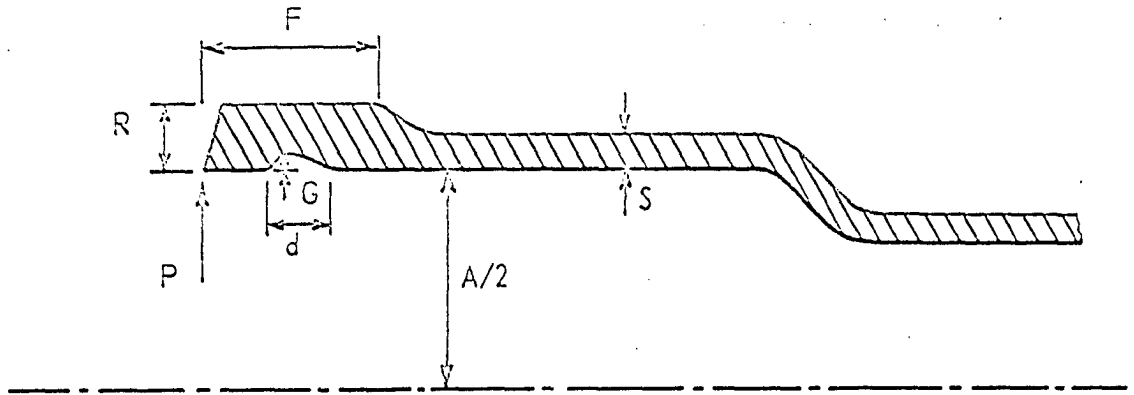
$$w = c_1 \sin Bx \sinh Bx + c_2 \sin Bx \cosh Bx + c_3 \cos Bx \sinh Bx + c_4 \cos Bx \cosh Bx \quad (5.1)$$

where,

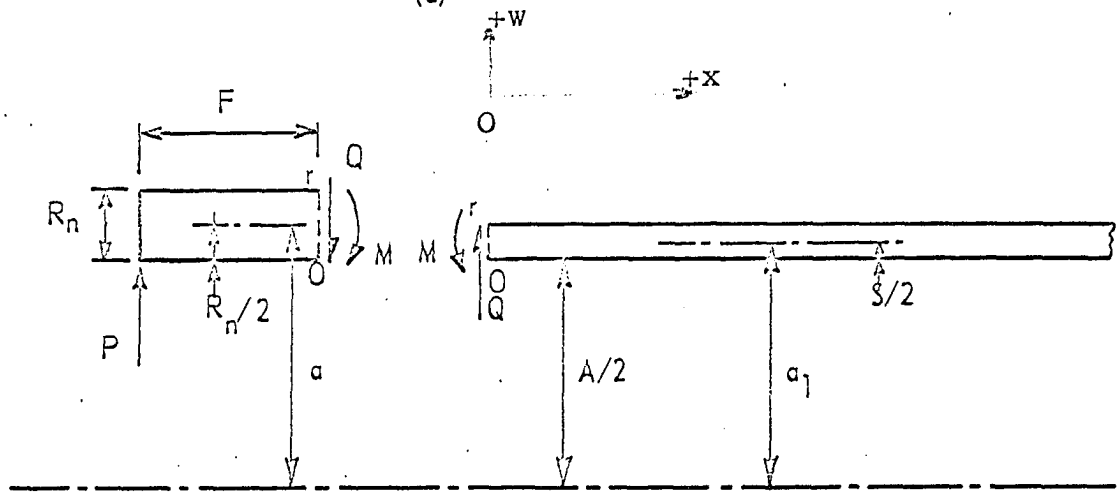
w = deflection of the neutral axis, inches

c_1, c_2, c_3, c_4 = constants depending on the boundary conditions

$$B^4 = \frac{3(1 - \nu^2)}{a^2 R_n^2}, \text{ inch}^{-4}$$



(a)



(b)

Deflection = $\uparrow +$

Shear = $\rightarrow +$

(c)

Fig. 5.3. Idealized cross section of hubs

v = Poisson's ratio

$R_n = \frac{RxF - 0.667Gd}{F}$ = net thickness of the hub bead, inches

$a = \frac{A}{2} + R_n/2$ = radius of the hub bead measured from the central axis to the neutral axis.

A = inside diameter of the pipe hub, inches

x = horizontal coordinate taken positive to the right and negative to the left of point 0 that is shown in Fig. 5.3b.

Dimensions R , F , G , and d are shown in Fig. 5.3a.

Neglecting the force P for the time being, the values of c_1 to c_4 can be obtained using the following boundary conditions:

at $x = 0$,

$$-D \left(\frac{d^2 w}{dx^2} \right) = M \quad \text{and} \quad D \left(\frac{d^3 w}{dx^3} \right) = Q$$

at $x = -F$

$$\frac{d^2 w}{dx^2} = 0 \quad \text{and} \quad \frac{d^3 w}{dx^3} = 0$$

where,

$$D = \frac{ER_n^3}{12(1 - \nu^2)} = \text{flexural rigidity, lbs-in.}$$

E = modulus of elasticity, psi.

Substituting Eq. 5.1 into the first two boundary conditions results in:

$$c_1 = \frac{-M}{2DB^2} \tag{5.2}$$

$$c_2 - c_3 = \frac{Q}{2DB^3} \quad (5.3)$$

Substituting Eqs. 5.1, 5.2, and 5.3 into the third boundary condition gives:

$$c_3 (\sin BF \cosh BF - \cos BF \sinh BF) - c_4 \sin BF \sinh BF = k_1 \quad (5.4)$$

where:

$$k_1 = \frac{M}{2DB^2} \cos BF \cosh BF + \frac{Q}{2DB^3} \cos BF \sinh BF \quad (5.5)$$

Again, substituting Eqs. 5.1, 5.2, and 5.3 into the last boundary condition results in:

$$c_3 (-2 \sin BF \sinh BF) + c_4 (\sin BF \cosh BF + \cos BF \sinh BF) = k_2 \quad (5.6)$$

where:

$$k_2 = \frac{M}{2DB^2} (\sin BF \cosh BF - \cos BF \sinh BF) - \frac{Q}{2DB^3} (\cos BF \cosh BF - \sin BF \sinh BF) \quad (5.7)$$

Solving Eqs. 5.4 and 5.6 simultaneously for c_3 and c_4 , and substituting for k_1 and k_2 the values given by Eqs. 5.5 and 5.7, the following is obtained:

$$c_3 = \frac{BM(\sin BF \cos BF + \sinh BF \cosh BF) + Q \sinh^2 BF}{2DB^3 (\sin^2 BF - \sinh^2 BF)} \quad (5.8)$$

$$c_4 = \frac{BM(\sin^2 BF \cosh^2 BF + \cos^2 BF \sinh^2 BF)}{2DB^3 (\sin^2 BF - \sinh^2 BF)} + \frac{Q(\sinh BF \cosh BF - \sin BF \cos BF)}{2DB^3 (\sin^2 BF - \sinh^2 BF)} \quad (5.9)$$

Substituting the value of c_3 back into Eq. 5.3, c_2 is obtained:

$$c_2 = \frac{BM(\sin BF \cos BF + \sinh BF \cosh BF) + Q\sin^2 BF}{2DB^3(\sin^2 BF - \sinh^2 BF)} \quad (5.10)$$

Next, the constants c_1 to c_4 are evaluated for force P.

With this force acting alone, the boundary conditions are:

at $x = 0$

$$\frac{d^2 w}{dx^2} = 0$$

$$\frac{d^3 w}{dx^3} = 0$$

at $x = -F$

$$\frac{d^2 w}{dx^2} = 0$$

$$D \left(\frac{d^3 w}{dx^3} \right) = P$$

Substituting Eq. 5.1 into the first two boundary conditions given above result in:

$$c_1 = 0 \quad (5.11)$$

$$c_2 = c_3 \quad (5.12)$$

Substituting Eqs. 5.1, 5.11 and 5.12 in the third boundary condition gives:

$$c_3(\cos BF \sinh BF - \sin BF \cosh BF) + c_4 \sin BF \sinh BF = 0 \quad (5.13)$$

while substituting Eqs. 5.1, 5.11, and 5.12 in the last boundary condition results in:

$$c_3(-2 \sin BF \sinh BF) + c_4(\sin BF \cosh BF + \cos BF \sinh BF) = \frac{P}{2B^3 D} \quad (5.14)$$

Solving Eqs. 5.13 and 5.14 simultaneously for c_3 and c_4 yields:

$$c_3 = \frac{P \sin BF \sinh BF}{2DB^3(\sin^2 BF - \sinh^2 BF)} \quad (5.15)$$

$$c_4 = \frac{-P(\cos BF \sinh BF - \sin BF \cosh BF)}{2DB^3(\sin^2 BF - \sinh^2 BF)} \quad (5.16)$$

Adding the constants c_1 , c_2 , c_3 , c_4 given by Eqs. 5.11, 5.12, 5.15, 5.16 to the constants given by Eqs. 5.2, 5.8, 5.9, 5.10, the final solution for the deflection of the short shell due to P , Q , and M is given by Eq. 5.1 with the following constants:

$$c_1 = \frac{-M}{2DB^2} \quad (5.2)$$

$$c_2 = \frac{BM(\sin BF \cos BF + \sinh BF \cosh BF)}{2DB^3(\sin^2 BF - \sinh^2 BF)} + \frac{Q \sin^2 BF + P \sin BF \sinh BF}{2DB^3(\sin^2 BF - \sinh^2 BF)} \quad (5.17)$$

$$c_3 = \frac{BM(\sin BF \cos BF + \sinh BF \cosh BF)}{2DB^3(\sin^2 BF - \sinh^2 BF)} + \frac{Q \sinh^2 BF + P \sin BF \sinh BF}{2DB^3(\sin^2 BF - \sinh^2 BF)} \quad (5.18)$$

$$c_4 = \frac{BM(\sin^2 BF \cosh^2 BF + \cos^2 BF \sinh^2 BF) + Q(\sinh BF \cosh BF - \sin BF \cos BF)}{2DB^3(\sin^2 BF - \sinh^2 BF)}$$

$$+ \frac{-P (\cos BF \sinh BF - \sin BF \cosh BF)}{2DB^3 (\sin^2 BF - \sinh^2 BF)} \quad (5.19)$$

Knowing the values of c_1 , c_2 , c_3 , and c_4 given by the above four equations, the deflection at any point in the hub bead, considered as a short cylindrical shell, can be determined from Eq. 5.1. The deflection from this equation is to the left of point 0 in Fig. 5.3 and is in terms of the known equivalent caulking force P and the unknowns M and Q .

As mentioned previously, the deflection of the hub wall extending to the right of point 0 (Fig. 5.3) can be assumed to be that of an infinitely long shell. The deflection equation for this case is given by Timoshenko (5) as:

$$w = \frac{-B_1 x}{2B_1^3 D_1} B_1 M (\sin B_1 x - \cos B_1 x) + Q \cos B_1 x \quad (5.20)$$

where:

$$B_1^4 = \frac{3(1 - \nu^2)}{a_1^2 S^2}$$

$$D_1 = \frac{ES^3}{12(1 - \nu^2)} \quad (5.21)$$

S = thickness of hub wall, inches

a_1 = $A/2 + S/2$ = radius of the hub wall measured from the central axis to the neutral axis.

At $x = 0$, the deflection and slope are given by:

$$w = \frac{-B_1 M + Q}{2B_1^3 D_1} \quad (5.22)$$

$$\theta = \frac{dw}{dx} = \frac{2B_1 M - Q}{2B_1^2 D_1} \quad (5.23)$$

Equations 5.1 and 5.20 express the deflection along the hub bead (to the left of point 0, Fig. 5.3b) and the hub wall (to the right of point 0, Fig. 5.3b), respectively. These deflections are in terms of the known force P and the unknown quantities M and Q. These quantities can be evaluated by matching the continuity conditions along the discontinuity line r0 (Fig. 5.3b). The deflection and slope at point 0 obtained from Eq. 5.1 are equated to the deflection and slope at the same point obtained from Eq. 5.20. This results in two simultaneous equations from which the unknown quantities M and Q can be obtained.

To simplify terms, the deflections and slopes at point 0 due to P, Q, and M can be evaluated separately. The following notations are used:

w_R = deflection at point 0 of the hub wall

w_L = deflection at point 0 of the hub bead

θ_R = slope at point 0 of the hub wall

θ_L = slope at point 0 of the hub bead.

Case I: Due to load P.

From Eqs. 5.1 and 5.19,

$$w_L = \frac{-P(\cos BF \sinh BF - \sin BF \cosh BF)}{2DB^3 (\sin^2 BF - \sinh^2 BF)} \quad (5.24)$$

From Eqs. 5.1, 5.17, and 5.18,

$$\left(\frac{dw}{dx}\right)_L = \theta_L = \frac{2BP \sin BF \sinh BF}{2DB^3 (\sin^2 BF - \sinh^2 BF)} \quad (5.25)$$

$$w_R = 0 \quad (5.26)$$

$$\theta_R = 0 \quad (5.27)$$

Case II: Due to force Q.

Using the same procedure as above,

$$w_L = \frac{Q(\sinh BF \cosh BF - \sin BF \cos BF)}{2DB^3 (\sin^2 BF - \sinh^2 BF)} \quad (5.28)$$

$$w_R = \frac{Q}{2B_1^3 D_1} \quad (5.29)$$

$$\theta_L = \frac{BQ(\sin^2 BF + \sinh^2 BF)}{2DB^3 (\sin^2 BF - \sinh^2 BF)} \quad (5.30)$$

$$\theta_R = \frac{-Q}{2B_1^2 D_1} \quad (5.31)$$

Case III: Due to moment M.

$$w_L = \frac{BM(\sin^2 BF \cosh^2 BF + \cos^2 BF \sinh^2 BF)}{2DB^3 (\sin^2 BF - \sinh^2 BF)} \quad (5.32)$$

$$w_R = \frac{-B_1 M}{2B_1^3 D_1} \quad (5.33)$$

$$\theta_L = \frac{2B^2 M (\sin BF \cos BF + \sinh BF \cosh BF)}{2DB^3 (\sin^2 BF - \sinh^2 BF)} \quad (5.34)$$

$$\theta_R = \frac{M}{B_1 D_1} \quad (5.35)$$

Since the sections to the left of point 0 and to the right of point 0 are actually continuous at their junction r_0 , the following conditions exist:

1. deflections w_R are equal to deflections w_L at point 0. i.e.,

sum of the deflections given by Eqs. 5.26, 5.29, and 5.33 are

equal to the sum of the deflections given by Eqs. 5.24, 5.28 and 5.32. (5.36)

2. rotations Θ_R are equal to rotations Θ_L at point 0, i.e., sum of the rotations given by Eqs. 5.27, 5.31, and 5.35 are equal to the sum of the rotations given by Eqs. 5.25, 5.30, and 5.34. (5.37)

For any given P, the solution of conditions 5.36 and 5.37 results in the values of M and Q which exist between the two pipes due to continuity. Once M and Q are known, the deflection in the hub bead can be calculated by Eq. 5.1 and in the hub wall by Eq. 5.20.

The circumferential strain at any point in the hub bead is then given by:

$$\epsilon_{\phi} = w/a \quad (5.38)$$

where,

ϵ_{ϕ} = circumferential strain, in./in., with tensile strain considered as positive.

5.3.1 Circumferential strain distribution in the hub of pipe 4D11 The dimensions of this pipe are shown in Table

B.1. From this table and Fig. 5.3, the following results:

$$R_n = 0.5067 \quad S = 0.35 \quad a_1 = 2.753$$

$$a = 2.675 \quad B = 1.0940 \quad BF = 0.96$$

$$D = 18.513 \times 10^4 \quad D_1 = 6.102 \times 10^4 \quad B_1 = 1.3200$$

Condition 5.36 becomes

$$356.00 Q - 470.27 M = - 212.13 P - 433.08 Q - 755.93 M \quad (5.36)$$

while condition 5.37 becomes

$$-470.27 Q + 1241.53 M = - 721.51 P - 755.97 Q - 1849.09 M \quad (5.37)$$

Solving the above two equations results in:

$$M = - 0.216 P \quad \text{and} \quad Q = - 0.191 P.$$

Substituting the values of M and Q into Eqs. 5.2, 5.17, 5.18, and 5.19 gives:

$$c_1 = \frac{48.74 P}{10^8} \qquad c_2 = \frac{-101.15 P}{10^8}$$

$$c_3 = \frac{-61.78 P}{10^8} \qquad c_4 = \frac{33.70 P}{10^8}$$

With these constants, Eq. 5.1 can be used for the determination of the deflection at any point along the bead, and Eq. 5.20 for any point along the hub wall.

Knowing w , ϵ_{ϕ} is obtained by Eq. 5.38. For example:

At the end of the bead, $\epsilon_{\phi} = 0.86 P \mu \text{ in./in.}$

At the middle of the bead, $\epsilon_{\phi} = 0.45 P \mu \text{ in./in.}$

At the point of discontinuity of thickness, ϵ_{ϕ}
 $= 0.12 P \mu \text{ in./in.}$

5.3.2 Comparison between experimental and theoretical strain distribution The above calculation shows that the maximum strain in the 4D11 hub occurs at the end of the bead area. This agrees with the experimental results shown in Fig. 5.1. Thus, knowing the strain at the edge of the hub bead experimentally, a theoretical value of P can be determined from the theoretical strain expression. Note, however, that this P is not the true one but rather a

theoretical equivalent one. This is so since the exact distribution is not known. However, the exact distribution is not what is sought after here. Only an equivalent force P is required that will result in the same maximum strain indicated by the gages during caulking. By knowing the values of the equivalent P for maximum strains obtained from caulking of different pipes, design charts can be prepared as discussed in Chapter 8.

5.4 Theoretical Strain Distribution in Spigots

Figure 4.1 shows that the centroid of the lead ring is about 2 inches from the end of the spigot. Since the strains vanish very rapidly along shells subjected to partial loading, it is assumed that the resultant caulking force acts at a large distance from the end of the spigot. The validity of this assumption is verified in Section 5.4.1. As in the hub, the caulking force applied is assumed as a concentrated radial line loading as shown in Fig. 5.4. This assumption is actually an upper bound for the design equations and is probably as accurate as any other assumed distribution. For line loading far from the ends, Timoshenko (5) gives:

$$w = \frac{-P_1 e^{-Bx}}{8B^3 D} (\sin Bx + \cos Bx) \quad (5.39)$$

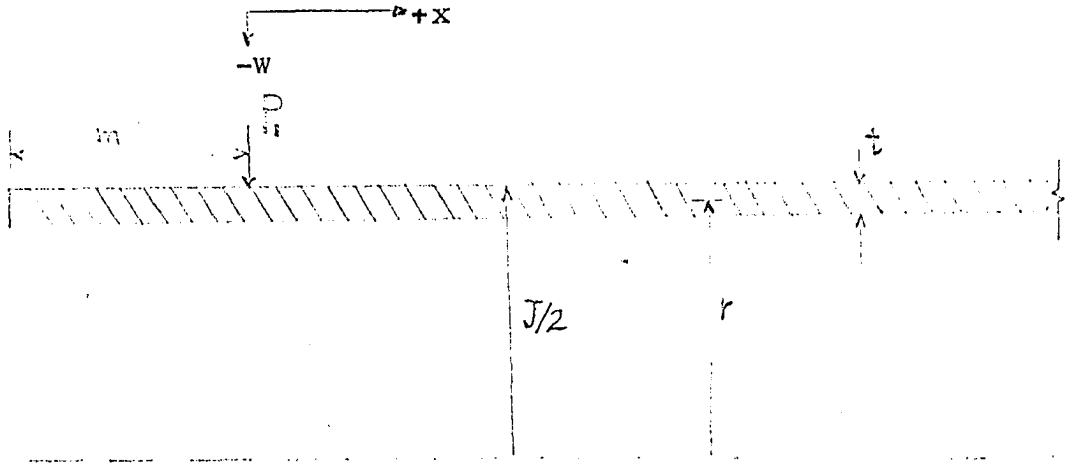


Fig. 5.4. Cross section of the spigot

where,

P_1 = line load on the spigot,

$$B^4 = \frac{3(1 - \nu^2)}{r^2 t^2}, \quad D = \frac{Et^3}{12(1 - \nu^2)}$$

The maximum moment is given by:

$$M_{\ell} = D \left(\frac{d^2 w}{dx^2} \right)_{x=0} = \frac{P_1}{4B} \quad (5.40)$$

and for cylindrical shells with no axial force:

$$M_{\Phi} = \nu M_{\ell} = \frac{\nu P_1}{4B} \quad (5.41)$$

where:

M_{ℓ} = longitudinal moment at $x = 0$.

M_{Φ} = circumferential moment at $x = 0$.

The stresses at $x = 0$ are given by

$$\sigma_{\ell} = \pm \frac{6M_{\ell}}{t^2} = \pm \frac{3P_1}{2Bt^2} \quad (5.42)$$

$$\sigma_{\Phi} = \pm \frac{6M_{\Phi}}{t^2} + \frac{N_{\Phi}}{t} = \pm \frac{3 v P_1}{2 B t^2} + \frac{Ew}{r} \quad (5.43)$$

where:

σ_{ℓ} , σ_{Φ} = longitudinal and circumferential stresses,
respectively, at $x = 0$

N_{Φ} = circumferential force which is equal to
 Etw/r .

The maximum longitudinal tensile strain used in the design is given by

$$\epsilon_{\ell} = \frac{1}{E} (\sigma_{\ell} - v\sigma_{\Phi}) \quad (5.44)$$

where

ϵ_{ℓ} = longitudinal strain.

For P_1 applied as shown in Fig. 5.4, σ_{ℓ} is tensile on the inside surface of the pipe. The first term of the σ_{Φ} expression is also tensile on the inside surface while the second term is compressive. Substituting Eqs. 5.42 and 5.43, with the appropriate signs, into Eq. 5.44 results in:

$$\epsilon_{\ell} = \frac{1}{E} \left[\frac{6(1-v^2) P_1}{4 t^2 B} + \frac{v E P_1}{8rB^3D} \right], \text{ on the inside surface} \quad (5.45)$$

Substituting the actual values of v , B , and D in this equation results,

$$\epsilon_{\ell} = \frac{1.25 P_1 r^{0.5}}{E t^{1.5}} \quad (5.46)$$

The stresses are given by

$$\sigma_{\ell} = \frac{E}{1 - \nu^2} (\epsilon_{\ell} + \nu \epsilon_{\phi}) \quad (5.47)$$

$$\sigma_{\phi} = \frac{E}{1 - \nu^2} (\epsilon_{\phi} + \nu \epsilon_{\ell}) \quad (5.48)$$

The maximum tensile stresses occur on the inside surface of the pipe. In the above two equations, ϵ_{ϕ} is given by Eq. 5.38 with a negative sign, and ϵ_{ℓ} is given by Eq. 5.45. Substituting these expressions into Eqs. 5.47 and 5.48 results in:

$$\sigma_{\ell} = \frac{1.16 r^{0.5} P_1}{t^{1.5}} \quad (5.49)$$

$$\sigma_{\phi} = \frac{0.93 r^{0.5} P_1}{t^{1.5}} \quad (5.50)$$

Thus knowing the experimental maximum caulking strain ϵ_{ℓ} , the equivalent caulking force P_1 can be obtained from Eq. 5.46. Knowing P_1 , the stresses can be computed from Eqs. 5.49 and 5.50. For any radius r , Eq. 5.49 gives a higher value of stress compared to Eq. 5.50 and hence will result in a larger required t when it is used as a design formula. Equation 5.49 will be used in developing the design charts discussed in Chapter 9.

5.4.1 Applicable range of Eq. 5.39 In the derivation of Eq. 5.39, the load is assumed to be at an infinite distance from the end of the pipe. The equation is used for the analysis of spigots where the load is at a finite distance

from the end. The error involved in such an application will now be evaluated. The error will be the largest when the ratio of m/J is the smallest, where J is the outside pipe diameter and m is the distance of the load from the spigot end as shown in Fig. 5.4.

The exact distance m for each size of pipe is not known. However, Fig. 5.2 indicates that the maximum strain occurs near the centroid of the lead area. If the force P_1 is assumed to act at that point, then the distance m is given by the equation

$$m = Y - 0.5 \text{ inch}$$

where, Y is the telescoping length of the spigot inside the hub, and 0.5 corresponds to one-half the lead depth in the joint. Using this equation and the pipe dimensions given in Reference 6, values of m/J for all sizes of pipe are calculated as shown in Table 5.5.

Table 5.5 Ratio of m/J for various pipe diameters

Pipe size inch	m inch	J inch	m/J
2	2.00	2.30	0.870
3	2.25	3.30	0.682
4	2.50	4.30	0.581
5	2.50	5.30	0.472
6	2.50	6.30	0.397
8	3.00	8.38	0.358
10	3.00	10.50	0.286
12	3.75	12.50	0.300
15	3.75	15.62	0.241

From this table, it is seen that the value of m/J is the smallest for the 15-inch pipe. From Reference 6, the dimensions of the 15-inch pipes are given by:

$$t = 0.25 \text{ inches} \quad J = 15.62 \text{ inches} \quad m = 3.75 \text{ inches}$$

Corresponding to these dimensions,

$$B = 0.993 \quad \text{and} \quad Bm = 3.50 \text{ in./in.}$$

The moment at the location of P_1 with m finite will now be determined by superposition of 1) solution assuming m infinite, and 2) a correction solution. The correction solution is obtained as follows. First Eq. 5.39 is used to find the shear and moment at $Bm = 3.50 \text{ in./in.}$ from the point of application of the load in an infinitely long shell. These are:

$$M = 0.0104 P_1 \quad \text{and} \quad Q = -0.0141 P_1.$$

In the actual pipe used here (15-inch), the moment and shear must be zero at a distance of $Bm = 3.50 \text{ in./in.}$ since this corresponds to the free end of the pipe. Thus as a correction, equal and opposite moment and shear must be applied at the pipe end to counterbalance the above. The moment at the location of P_1 assuming m infinite is given by Eq. 5.40:

$$M = P_1/4B = 0.2680 P_1.$$

The moment from the correction solution can be calculated from a deflection equation similar to Eq. 5.20:

$$M = D \frac{d^2 w}{dx^2} = \frac{1}{2B} [2B M e^{-Bx} (\cos Bx + \sin Bx) + 2Q e^{-Bx} \sin Bx]$$

and at $x = m$

$$M = -0.0006 P_1$$

Therefore, the error is equal to $0.0006 P_1 / 0.2680 P_1$ or approximately 0.2 %/o. Thus, Eq. 5.39 is considered valid for all pipe sizes.

5.5 Strain Variation Around a Caulked Joint

Caulking strains were measured by strain gages bonded at a spot on the hub or spigot. Since caulking is not uniform around the joint, the gages might not have indicated the real maximum strains around the circumference. To investigate this possibility, four gages were bonded around the hub bead at a 90° interval. The variation of the resulting strains due to caulking is shown in Fig. 5.5. In this test, the hub broke at the vicinity of gage #4 170 seconds after caulking started. The maximum strains in the gages were about the same. Gages 1, 2, 3, and 4 registered a maximum of 700, 600, 700, and 700 μ in./in., respectively. Hence, a gage bonded at one spot should give a good indication of the maximum strains due to caulking. However, after the joint is caulked, variation is to be expected. Thus, if caulking had stopped at 110 seconds, gages 1 to 4 would have registered 600, 400, 280, and 300 μ in./in., respectively.

The caulking force P used in the theoretical analysis of hubs and spigots was assumed as a static uniform force around the joint. The magnitude of this force will cause the maximum strain that is indicated by the above gages. This assumption is on the safe side since, 1) the force is assumed to act as maximum all the way around the joint, and

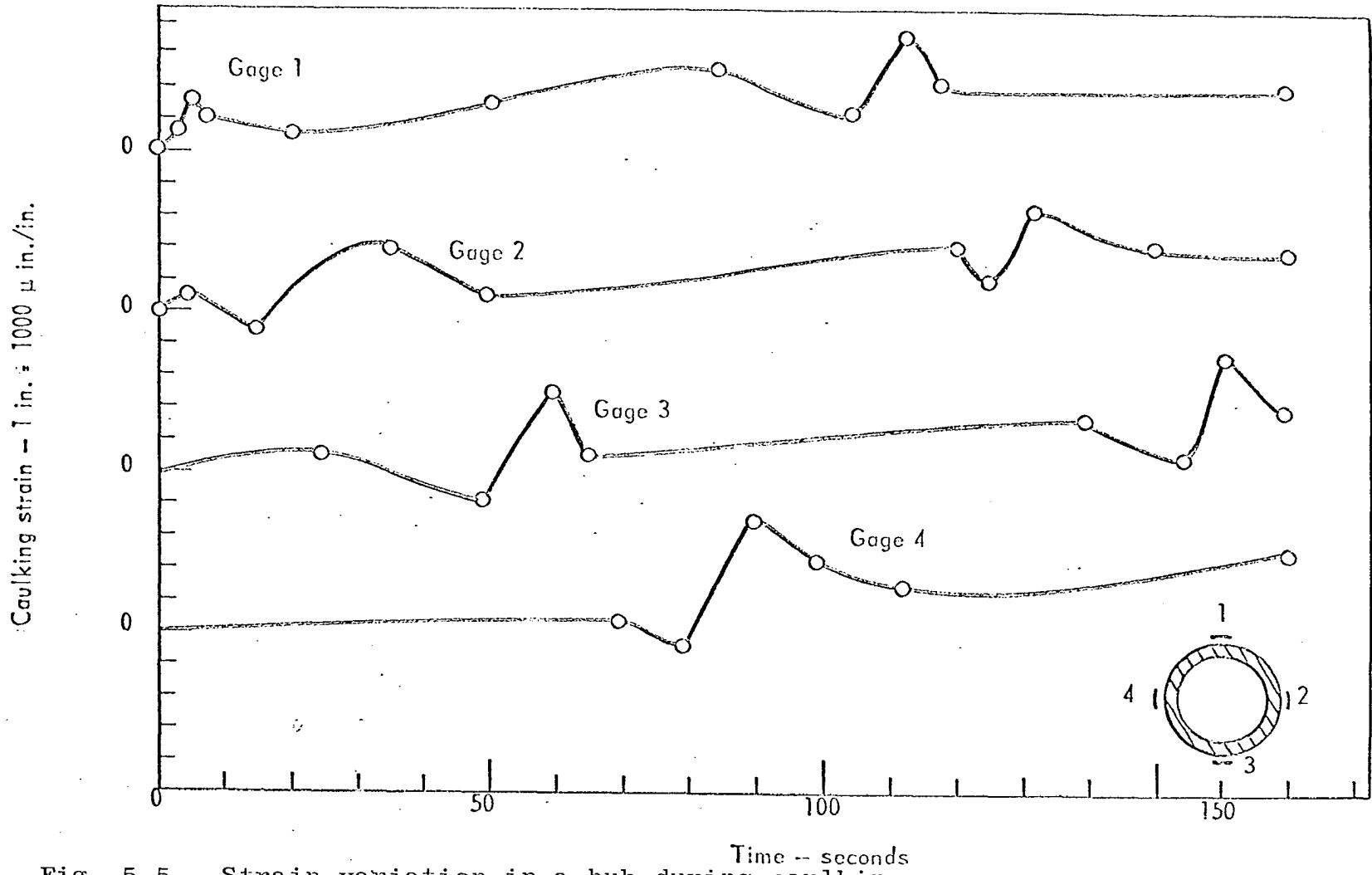


Fig. 5.5. Strain variation in a hub during caulking

2) the force is assumed static rather than dynamic. By assuming the equivalent caulking force as static, no increase in metal strength was taken into consideration. Thus, the ultimate strength of the metal was assumed 21,000 psi in tension and 45,000 psi in bending even though in actual caulking, these ultimates could be higher.

5.6 Effect of Lead Depth on the Maximum Strains

The depths of the lead ring surface below the rim of the hub varied slightly from one test to another. This variation was mainly due to the amount of the lead poured. To investigate the change of strain in the hub due to the variation of lead height, hub of pipe 4F7 was used. Three circumferential gages were bonded on the hub bead. Gage #1 was at the edge of the bead, gage #2 was at the middle of the bead area, and gage #3 was at the other end of the bead next to the hub wall. Two tests were conducted. In the first, lead was poured 0.2 inches from the hub edge. In the second, lead was poured flush with the hub edge.

Strains due to ordinary caulking in the first test were 150, 250, and 200 μ in./in. in gages 1, 2, and 3, respectively. The corresponding strains in the second test were 450, 550, and 450 μ in./in., or twice those of the first test. In both tests, joints were caulked with the same austerity. Thus, the above strains indicate that the depth of the lead surface in the joint is a very important factor in determining the maximum strains. Codes, however, specify

that this depth should not extend more than 1/8 inch after the joint is caulked.

Due to severe caulking, strains in the first test mentioned above were 250, 400, 450 μ in./in. in gages 1, 2, and 3, respectively. This corresponds to about 75 % increase in the strain from normal to severe caulking. Hence, the austerity of caulking as well as the depth of the lead surface from the edge of the hub affect the joint strains.

5.7 Relaxation Test

The maximum caulking strains occurred during the caulking operation. However, strains induced in the joints after the caulking operation were of appreciable amount. These strains diminished with time as lead crept. The speed with which these strains diminished was of importance. Thus, the remaining amount of strain after caulking in the hub and spigot at any time should be superimposed on any additional strains on the pipe system after installation. To obtain the relaxation pattern of strains, gages were bonded on the hub of pipe 4F11 and spigot of 4A7. Gages employed are shown in the headings of Table 5.6. The location of the gages is shown in Fig. 4.4. The magnitude of the strains was measured by a Baldwin-Lima-Hamilton strain indicator type N.

Table 5.6. Relaxation of strain (μ in/in) in caulked joints

Time Days	Gages on Spigot ^a				Gages on Hub ^a	
	2	3	4	9	9	10
0	+250	+720	+240	-470	+320	+210
1	+240	+460	+160	-300	+240	+190
2	+220	+400	+130	-280	+220	+170
3	+180	+360	+110	-270	+190	+160
7	+200	+340	+110	-240	+190	+150
16	+180	+330	+110	-180	+190	+140
22	+170	+300	+100	-180	+170	+130
38	+150	+230	-	-180	+170	+110
43	+140	+250	-	-140	+180	+110

^a Gage locations are shown in Fig. 4.4.

The strains reduced to one-half their original value within the first three days after caulking (Table 5.6). The percentage of strain reduction was a function of the original value of strain. The higher the initial strain, the faster the reduction. The strains in gage #4 of the spigot and gage #9 of the hub were plotted as shown in Fig. 5.6. The figure shows that the creep of lead continuous even after 30 days. However, the rate of decrease is much less significant.

Since the pipe system has to be tested for leakage before being used, and since this test takes at least one day, it can be concluded that by the time the pipe system is ready for domestic use, most of the caulking forces had diminished to a certain value. This value is about 180 lbs./in. and is much smaller than the caulking force immediately after caulking (720 μ in./in. in the spigot and 320 μ in./in. in the hub).

5.8 Caulking at Low Temperatures

Three tests were conducted to determine the effect of low temperatures, if any, on the ultimate strength of caulked hubs. Dry ice was used to cool the pipe down to -50° F. Joints were then severely caulked at this low temperature. However, no hub failure occurred in the tests conducted. Thus, based on these three tests, it was concluded that the hub strength is not affected by a drop of 130° F from normal room temperature.

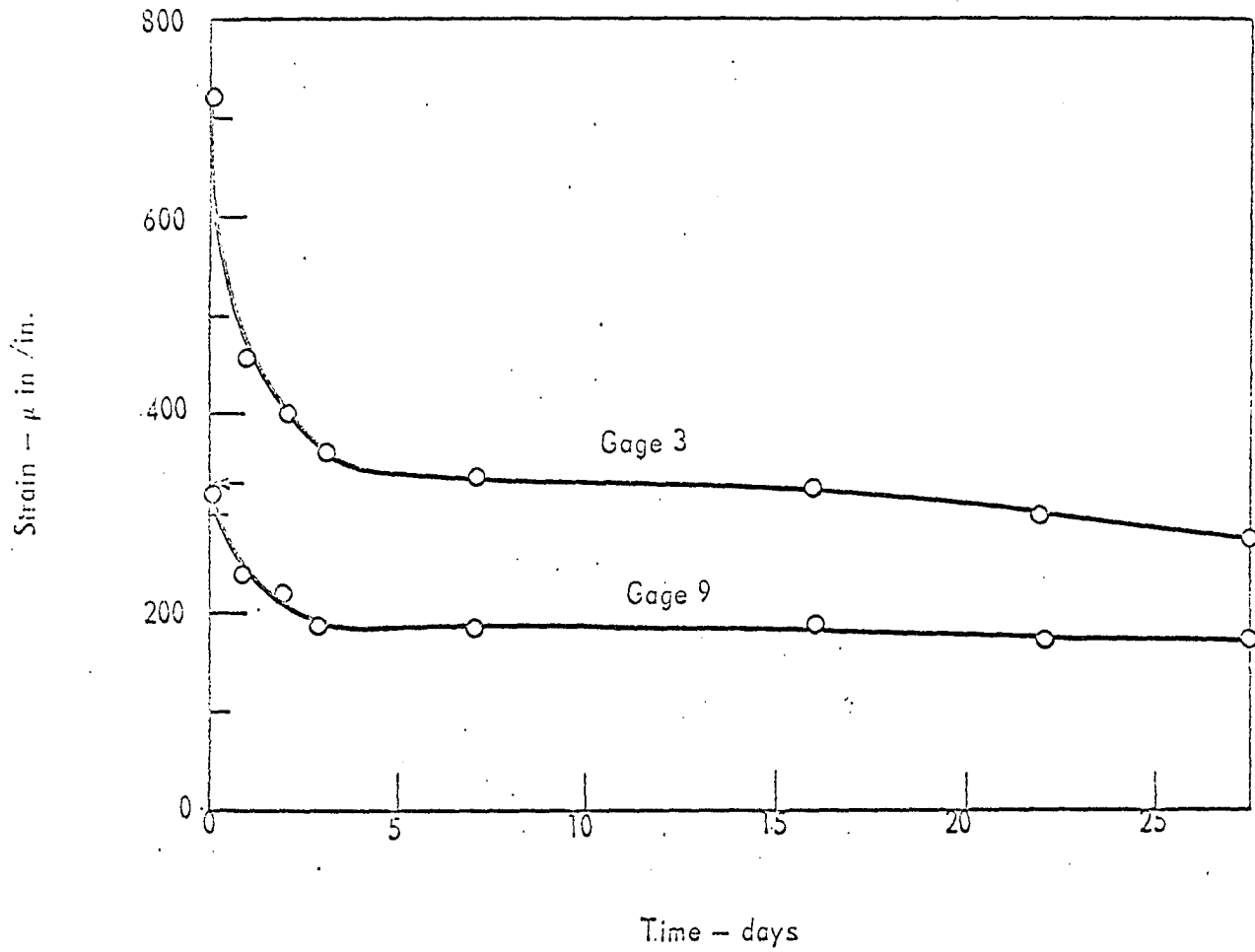


Fig. 5.6. Strain relaxation of gage No. 3 of spigot 4A7 and gage No. 9 of hub 4F11

5.9 Summary of Strain Due to the Joining Operation

The maximum strains obtained from joining two pipes are now compared. From Chapter 4, the maximum yarning tensile strain was 100μ in./in. in the hub and 275μ in./in. in the spigot. Thermal strains were 95μ in./in. in the hub and 310μ in./in. in the spigot. From this chapter and Chapters 8 and 9, the maximum tensile caulking strain varied from 260 to 900μ in./in. in the hub and 300 to 500μ in./in. in the spigot.

Thus, in the joining process, caulking strains are the most critical. Hubs and spigots that can withstand the caulking strains can perform adequately under the influence of yarning and thermal strains. Hence, in the design criteria for hubs and spigots, only caulking strains will be considered.

The maximum caulking strain in the hubs and spigots does not vary significantly around the joint as shown in Section 5.5. Measuring the strain at one point will be sufficient to indicate the maximum strain.

The depth of the lead ring surface below the hub end, as discussed in Section 5.6, effects significantly the maximum caulking strains. Thus, the lead ring was poured to about the same level in every test conducted so as to reduce any variation.

Normal caulking mentioned above is not to be thought of as a fixed operation or a specified procedure. Caulking strains are effected by many factors. The most important

factors are the amount of severity of caulking, size of the caulking tools, and the level of the lead ring surface in the joint. If the caulking tool is too thick, it may act as a wedge between the hub and spigot causing unnecessary hub failure. Also, if the cross sectional area of the end of the caulking tool is too large, the amount of energy per unit area of lead will be less than that required to make a good sound joint. It has been observed in the laboratory that plumbers generally use larger tools on larger pipes. If the blow by the hammer to the tool is not increased in proportion to the size of the tool, the joints caulked with the larger tools will not be as good as those with smaller tools.

6. ELASTOMERIC GASKET JOINTS

6.1 Introduction

A new method of joining pipes is by inserting an elastomeric gasket between the hub and spigot. The procedure consists of inserting the gasket into the hub and lubricating the inside face that will hold the spigot. A special jack is then used to force the spigot end into the gasket forming a sealed joint. The strains induced in the hub and spigot by the jack vary from one point to another around the joint. The strains also vary from test to test. This variation is caused mainly by the position of the jack, the speed of jacking, tolerance of the hub and spigot dimensions, and the amount of lubricant in the gasket.

6.2 Strains in the Hubs and Spigots

Hub 4D15 and spigot 4D16 were used for the strain investigation. The maximum strains obtained during the joining process are shown in Table 6.1. The gages listed in the table have the locations shown in Fig. 4.4. The maximum tensile strains were 65μ in./in. in the hub and 460μ in./in. in the spigot. Both strains were circumferential. The maximum compressive strains were 60μ in./in. longitudinally in the hub and 640μ in./in. circumferentially in the spigot. All other gages had lower strains as indicated by Table 6.1. Since the joining tensile strains

Table 6.1. Strains^a in elastomeric gasket joints

Gage No.	HUB		Gage No.	SPIGOT	
	Max. Tension	Max. Comp.		Max. Tension	Max. Comp.
1	0	15	1	130	120
2	0	20	2	100	25
3	15	20	3	80	30
4	5	25	4	180	40
5	0	60	5	210	-
6	10	10	6	10	0
7	5	40	7	115	520
8	15	20	8	420	640
10	60	-	9	100	640
12	65	-	10	460	-
13	45	10	11	290	-
14	35	-	12	220	-
15	50	0			
16	5	10			
17	5	20			

^aGiven in μ in/in.

were as high as the compressive strains, and since the ultimate strength of cast iron in tension is about 1/4 that of compression, the tensile strains govern the design of the hubs and spigots. However, the maximum tensile strains in a lead-oakum joint discussed in Chapters 5, 8, and 9, varied from 260 - 900 μ in./in. in the hub and 300 - 500 μ in./in. in the spigot. These strains are higher than the governing strains in the elastomeric joints. Therefore, hubs and spigots designed to withstand strains in lead-oakum joints will be very adequate for elastomeric gasket joints.

7. EFFECTS OF BUILDING MOVEMENTS AND SOIL SETTLEMENTS ON STRENGTH REQUIREMENTS FOR PIPE SYSTEM

7.1 Introduction

The effect of building movements and soil settlement on the behavior of cast iron soil pipe is investigated in this chapter. The amount of strains induced depends on the magnitude of deformation in the pipe system. This deformation is limited by a certain range so that the joint does not leak and the pipe system remains functional.

A series of beam tests were conducted in order to investigate the effects of imposed deformations. These tests included the studies of:

1. Behavior of individual pipes, and lead-oakum joints subjected to bending
2. Ultimate strength of lead-oakum joints subjected to bending
3. Leakage of lead-oakum and elastomeric gasket joints.

Except for a few 8-inch pipe tests, most of the tests were for 4-inch pipes.

7.2 Behavior of Individual Pipes and Lead-Oakum Joints Subjected to Bending

Two single pipe tests were conducted using the test setup shown in Fig. 7.1. The test results, shown in Fig. 7.2, indicates that the elementary beam theory

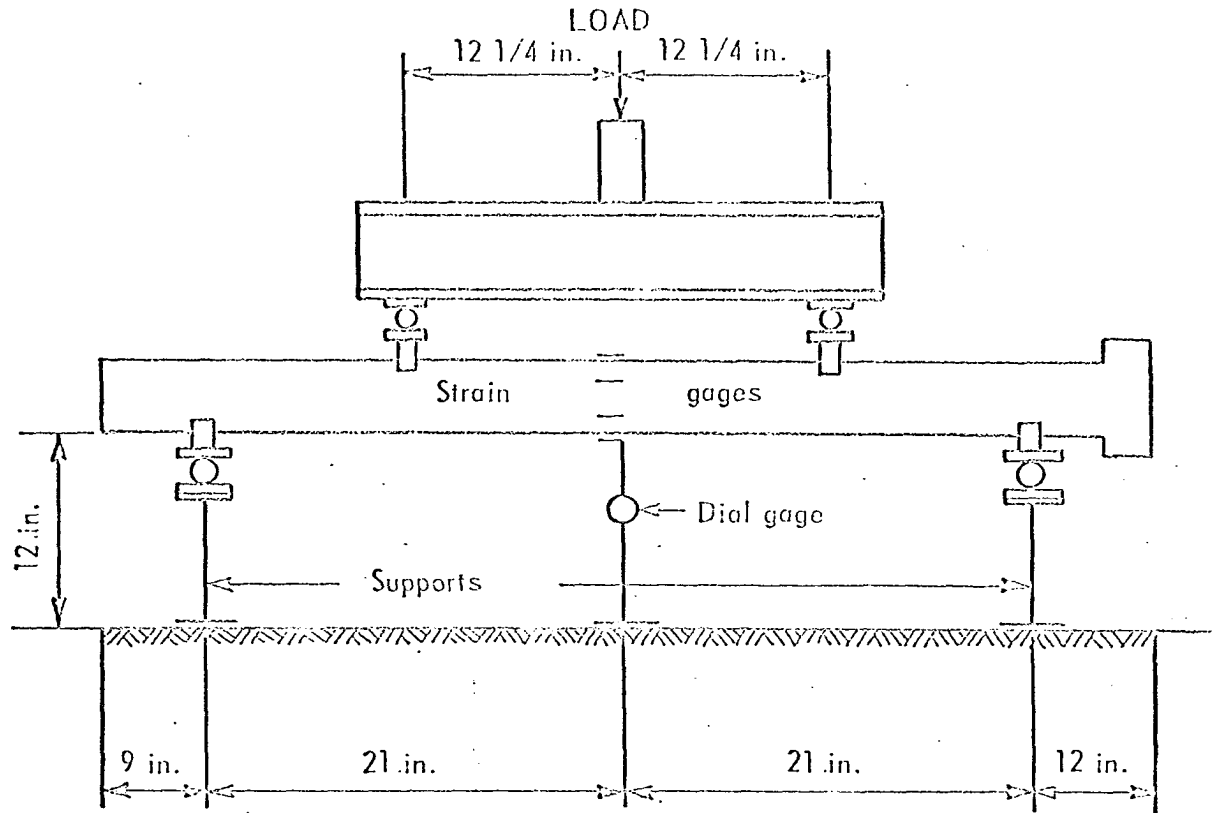


Fig. 7.1. Setup for single pipe test

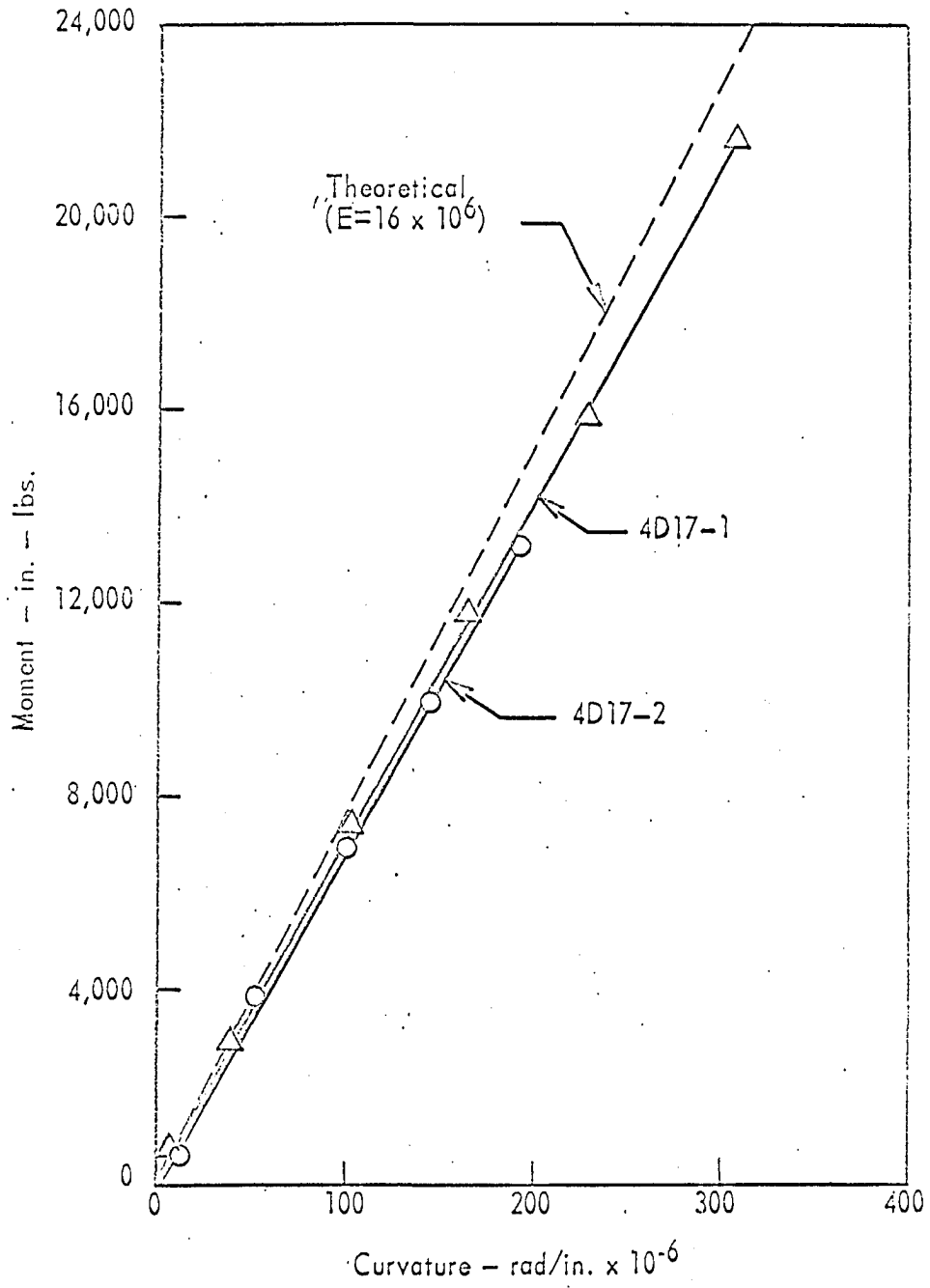


Fig. 7.2. Moment curvature relations for single pipe tests

discussed in Section A.1.5 can be used to predict accurately the behavior of single pipes. It is to be noted that these tests were conducted in the working load range and that the behavior of pipes near ultimate may be somewhat different.

Seven two-pipe beam tests were conducted to study the behavior of lead-oakum joints under bending using 4-inch pipes. The general test setup for the two-pipe beam tests is shown in Fig. 7.3. All tests showed moment-rotation curves and strain distribution curves similar to those shown in Figs. 7.4 and 7.5.

Figure 7.4 indicates that at any given bending moment, the amount of joint rotation is fairly close from one test to another. Some variation, however, is expected. This variation is mainly due to the severity with which the lead ring in the joint is caulked, the amount of lead in the joint, and the speed with which the test was conducted.

The stress distribution in the spigot shown in Fig. 7.5 is not linear. This is mainly due to the fact that the spigot end tends to bear against the wall of the hub and as a result the ends of the pipes are subjected to a combination of bending moment, axial force and/or horizontal frictional force. The magnitude of strains, which might effect the hub and spigot design, will be discussed in connection with the occurrence of leakage in Section 7.4.

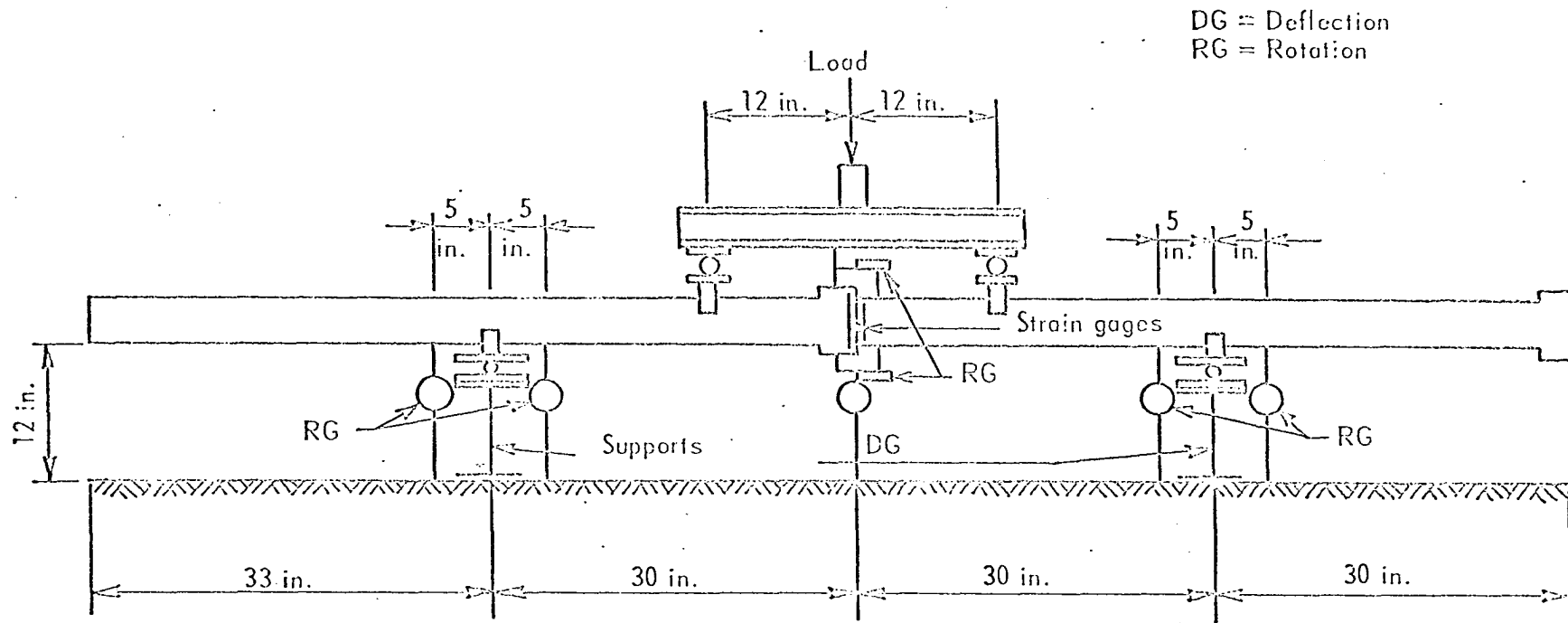


Fig. 7.3. Setup for two-pipe test

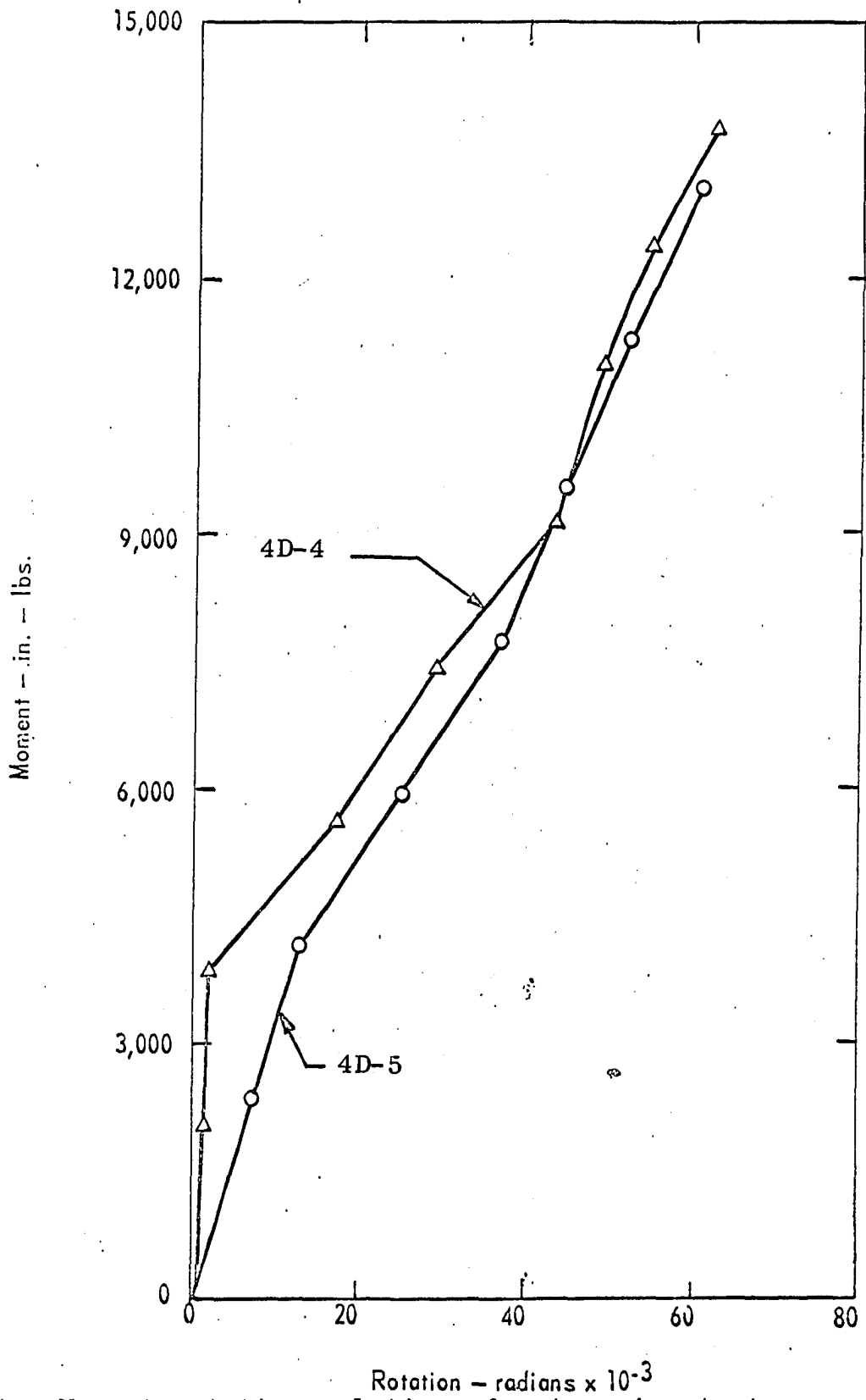


Fig. 7.4. Moment rotation relations for two-pipe tests

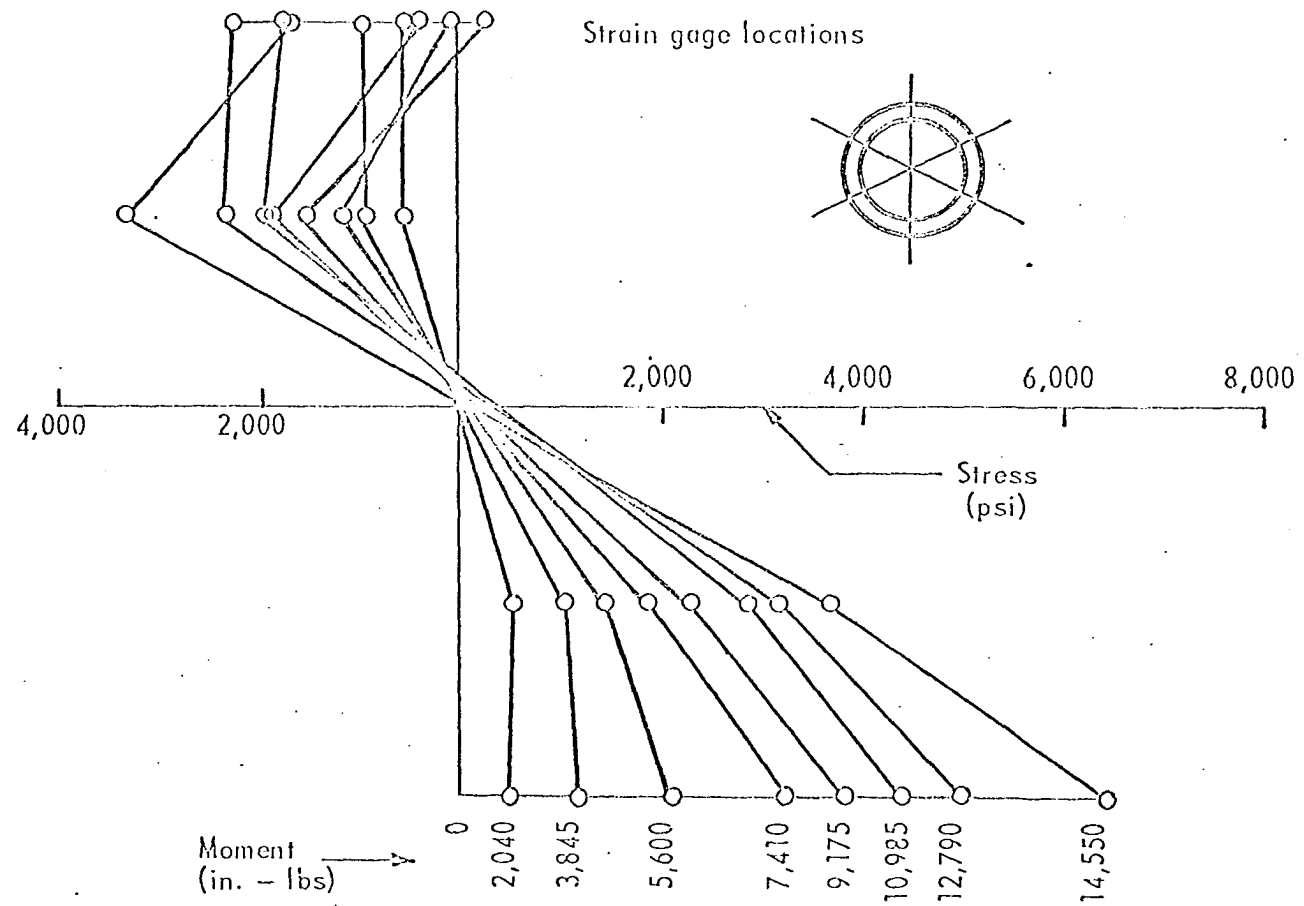


Fig. 7.5. Stress distribution in the spigot of a test joint

The most important information desired in the bending tests of joints is the capacity of the joint to resist relative rotation of the two pipe ends meeting at the joint, namely, the rotational restraint of the joint. The slope of the moment-rotation curve gives this information. The values of rotational restraints for 7 tests range from 129,000 to 200,000 in-lbs. per radian with an average value of 154,000 in-lbs. per radian. The significance of the rotational restraint of a joint is illustrated in Fig. 7.6. In this figure, the load-deflection relation for a beam consisting of two 5 foot pipes joined by a lead-oakum joint (case B is compared to the load-deflection curves for two ideal beams, one with a 10 foot pipe (case A) and the other with two 5 foot pipes joined by a frictionless pin (case C). All pipes are of identical size and material and all beams are assumed to be fixed at both ends. The center deflection for these cases can be expressed as:

$$\text{Case A, } \frac{w\ell^4}{384EI}$$

$$\text{Case B, } \frac{w\ell^4}{142EI}$$

$$\text{Case C, } \frac{w\ell^4}{128EI}$$

where,

w = intensity of the uniform load, lbs./in.

ℓ = span length of the beam, inches

E = modulus of elasticity for the pipe material, psi

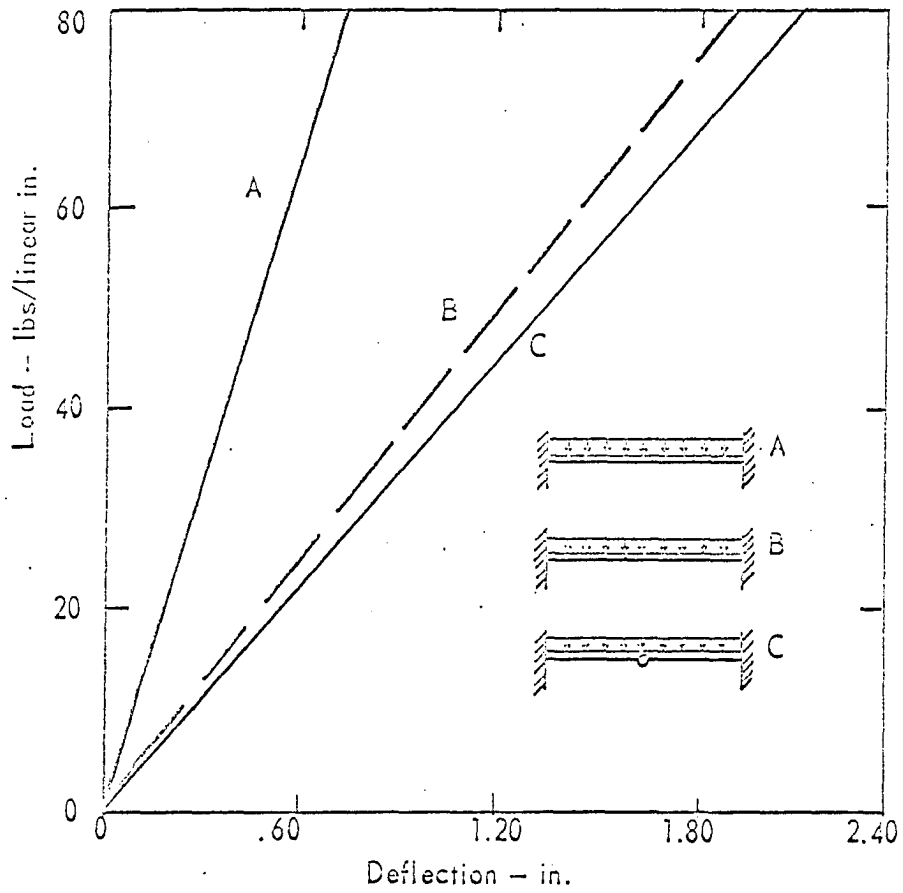


Fig. 7.6. Load deflection relations for a two-pipe continuous beam compared with idealized cases

I = moment of inertia of the pipe section, inch^4 .

The value of 200,000 in-lbs. per radian, which was the highest obtained in the test, was used as the rotational restraint of the joint in deriving the expression for center deflection for case B. Figure 7.6 indicates that the load-deflection curve for the actual pipe system tested, case B, is very close to that of case C. Thus, for practical purposes, the rotational restraint of a lead-oakum joint can be neglected.

In addition to the 4-inch pipes, two tests were conducted using 8-inch pipes. The average rotational restraint of the joint was found to be 355,000 in-lbs. per radian. This value is about 1.8 times greater than the rotational restraint for the 4-inch pipes (200,000 in-lbs. per radian). However, the rigidity of an 8-inch pipe, which depends on the moment of inertia, is more than 9 times greater than that of the 4-inch pipes. Hence, compared to the rigidity of the pipes, the rotational restraint of the 8-inch joints is much less than the 4-inch joints. This makes the assumption of using a frictionless pin for a joint well justified.

It can be concluded that pipe systems need not be analysed as a structural system (as discussed in Sections A.1.5 and A.1.7) since joints may be considered as pins. It is also concluded that a pipe system must be supported

at all joints since otherwise it will act as an unstable structure.

It is assumed that the torsional restraint of the joint is in the same order as the rotational restraint of the joint under bending and thus can also be neglected in practice.

7.3 Ultimate Strength of Lead-Oakum Joints Subjected to Bending

A total of ten two-pipe beam tests were conducted using 4-inch pipes in order to observe the behavior of lead-oakum joints under bending when the beams were loaded to failure. Time of testing varied from one to ten minutes. The average result of these tests is shown in the first row of Table 7.1. The result of these ultimate load tests indicates that a two-pipe system with a lead-oakum joint can sustain a considerable amount of loading and a considerable amount of deformation before failure occurs.

The rotational angle at the joint of the 8-inch pipe is shown in the second row of Table 7.1. The ultimate joint moment for the 8-inch pipe (88,000 in-lbs.) is about 2.4 times greater than the moment for the 4-inch pipe (36,300 in-lbs.).

7.4 Leakage Tests for Elastomeric and Lead-Oakum Joints

Nine leakage tests were conducted for 4-inch pipes with lead-oakum joints. In each test, the pipes were filled with water and sealed after the joint was made. This condition was kept for 24 hours so that the oakum had a chance to be completely soaked with water. The pipes were

Table 7.1. Summary of ultimate and leakage test results

Test	Load lbs.	Joint Displacement Inches	Joint Moment lbs.-in.	Joint Rotation Degrees	Location of Failure
1. Ultimate strength test for 4-inch pipe ^a	4040	3.80	36300	14.6	Hub ^b
2. Ultimate strength test for 8-inch pipe ^c	9775	4.10	88000	15.7	-
3. Leakage test for lead-oakum joint, 4-inch pipe ^d	700 ^e	0.47	6270	0.9	-

^aAverage of ten tests.

^bOut of ten tests conducted, seven had hub failures. One broke at the barrel, one at the spigot, and one did not break.

^cFor one test only.

^dAverage of nine tests.

^eAll values in this row are for pressurized pipes (water pressure of 5 psi).

Table 7.1. (Continued)

Test	Load lbs.	Joint Displacement Inches	Joint Moment lbs.-in.	Joint Rotation Degrees	Location of Failure
4.	2650 ^f	5.07	23850	9.6	-
5. Leakage test for lead-oakum joint, 8-inch pipe	985 ^e	3.05	8880	5.8	-
6.	3440 ^f	4.06	31000	7.7	-
7. Leakage test for elastomeric gasket joint, 4-inch pipe ^g	470 ^e	4.06	4200	7.7	-

^fAll values in this row are for unpressurized pipes (pipes were only filled with water).

^gAverage of six tests.

then subjected to 5 psi pressure, induced by compressed air, for at least 2 hours. A two-pipe beam test was then conducted with water and 5 psi pressure inside the pipes. Continuous visual inspection was used to detect the leakage.

The averaged results of the leakage test for the lead-oakum joint of the 4-inch and 8-inch pipes are shown in Table 7.1. The ratios between the joint rotations at ultimate and the occurrence of leakage for the 4-inch pipes were 16.3 for pressurized pipes and 1.52 for non-pressurized pipes. In the case of 8-inch pipes, the ratios were 2.70 for pressurized pipes and 2.05 for non-pressurized pipes.

The 5 psi pressure for leakage tests was initially selected as adequate for easy detection of the leakage. It also corresponds to the magnitude of the pressure in the water test (10 feet of water) and the air test (5 psi) commonly used in the inspection of plumbing systems. The results of leakage tests as summarized in Table 7.1 indicate that the joint rotations at which leakage occurs is a function of the internal pressure. Furthermore, the non-pressurized pipes apparently represent the pipes under actual service condition more realistically. It should be realized, however, that the pipe system may cease to be functional before leakage occurs, if the leakage is caused by rotation of the joint. Pipes are usually installed with a minimum slope of 1/8 inch per foot for pipe 4-inches or

larger. Assuming a pipe system was installed with this minimum slope, then a joint rotation of twice $(1/8)/12$ radians, or 1.2 degrees will reverse the slope of the connecting pipe and stop the flow of the contents in the pipes. Thus, a pipe system can no longer be considered functional when the joint rotation becomes large enough to either cause leakage or inhibit the free flow of the content. It is interesting to note that for 4-inch pipes, one degree joint rotation is about the maximum permissible from both leakage and flow considerations. For 8-inch pipes, the joint rotation of one degree is also about maximum permissible from flow consideration. In view of the fact that these rotations are well below the ultimate joint rotations at which breakage of hub and/or spigot occurs, it can be concluded that joint rotation caused by building movements and earth settlements have no effect on pipe thickness requirements.

The results of bending tests on the elastomeric gasket joints are also shown in Table 7.1. The table indicates that under the same 5 psi pressure, an elastomeric gasket joint can undergo a considerably larger amount of rotation (7.7 degrees) before leakage occurs compared to a lead-oakum joint (0.9 degrees). The average bending moment at leakage (4,200 in-lbs.) is smaller than that of lead-oakum joints (6,270 in-lbs.). It may be concluded, therefore, that the

strains near the elastomeric gasket joint due to joint rotation will not be a problem in the design of pipe thickness. In other words, any pipe with sufficient strength for lead-oakum joints will have more than ample strength for gasket type joints.

In view of the low magnitude of bending strains in the pipes at the permissible joint rotation, it can be assumed that strains will also be small in bends and fittings. Even with an intensification factor (A.1.7) of 2 due to bending, strains will still be below those of ordinary caulking. Thus, again, joint rotation will not be a governing factor in the thickness design.

7.5 Conclusion

Based on the above experiments and results, the following conclusions can be stated:

1. The elementary beam theory can be used to predict the behavior of a single pipe under bending in the working range
2. Lead-oakum joints possess very little rotational restraint
3. A pipe system becomes non-functional because of leakage or flow obstruction with a relatively small joint rotation under a bending moment considerably smaller than the ultimate bending moment. Thus, imposed deformations due to building movements or inadequate pipe supports

will make the system non-functional long before stresses near the joint become high enough to warrant special consideration in the design of pipe thickness.

The above conclusions reached were primarily based on studies of test results from 4-inch and 8-inch pipes. Similar results are expected for other sizes of pipes.

8. DESIGN RECOMMENDATIONS FOR THE HUBS

8.1 Preliminary Design Charts

It was shown in Section 5.3 that the maximum caulking strain in the hub is given by Eqs. 5.1 and 5.38 as:

$$\epsilon_{\Phi} = w/a$$

and at $x = -F$, the strain is given by

$$\begin{aligned} \epsilon_{\Phi} = \frac{1}{a} & (c_1 \sin BF \sinh BF - c_2 \sin BF \cosh BF \\ & - c_3 \cos BF \sinh BF + c_4 \cos BF \cosh BF) \end{aligned}$$

where c_1 , c_2 , c_3 , and c_4 are given by Eqs. 5.2, 5.17, 5.18, and 5.19 in terms of M , Q , and P . For any specified cross section, the values of M and Q can be evaluated in terms of P as discussed in Section 5.3. Thus, constants c_1 to c_4 are linear functions of the force P . The corresponding maximum caulking stress is:

$$\begin{aligned} \frac{\sigma_{\Phi}}{P} = \frac{E\epsilon_{\Phi}}{P} = \frac{E}{a} & (c_5 \sin BF \sinh BF - c_6 \sin BF \cosh BF \\ & - c_7 \cos BF \sinh BF + c_8 \cos BF \cosh BF) \quad (8.1) \end{aligned}$$

where c_5 , c_6 , c_7 , and c_8 are equal to c_1/P , c_2/P , c_3/P and c_4/P , respectively.

Using Eq. 8.1, numerical values of σ_{Φ}/P were obtained for various values of the variables, A , S , F , and R . Note that constants c_5 , c_6 , c_7 , and c_8 in Eq. 8.1 are functions of these variables. The value of A is constant for each pipe size and is given in Table 8.1.

Table 8.1. Values of A for various pipe diameters

pipe diameter	values of A inches
2	3.00
3	4.03
4	5.03
5	6.03
6	7.03
8	9.38
10	11.52
12	13.63
15	16.88

Curves were then plotted relating σ_{Φ}/P to R (Appendix D) for given values of pipe size, S, and F. These form the preliminary design charts. The computer program for the computation of σ_{Φ}/P is shown in Fig. D.1 of Appendix D.

In a given pipe size, for any specific value of σ_{Φ}/P shown in the charts, fixed relations can be obtained between R and F for various S values. Thus, the ratio σ_{Φ}/P must be established before these preliminary charts can be used to develop the final design charts. For σ_{Φ} , the minimum tensile strength of 21,000 psi as specified by the cast iron soil pipe industry was used. The values of P were determined for each pipe diameter as explained in the following section.

8.2 Evaluation of the Caulking Pressure P

The equivalent caulking force P was determined experimentally for 4, 8, and 12-inch pipes of brands A to F. Each joint was caulked, and the maximum circumferential strain at the edge of the hub bead during caulking was recorded (second column of Table 8.2). These strains were measured by means of FAE gages. A total of 28 tests were conducted. Eight of these tests were in the 4-inch pipes, 11 in the 8-inch pipes, and 9 in the 12-inch pipes. Unless otherwise indicated, the caulking strains shown in the table are for adequately caulked joints. In this study, an adequately caulked joint is one that does not leak after being filled with water for 24 hours and then pressurized at 5 psi for one hour. For the 8 and 12-inch pipes, it was usually difficult to obtain joints that could hold the 5 psi pressure without leaking after the first caulking. When this happened, the joints were recaulked until leakage stopped. The maximum caulking strains recorded from the start of the caulking until the joint passed the specified test are shown in Table 8.2 as "caulking strains".

The dimensions of the pipes are such that the thickness of the lead ring increased with the pipe size. The thickness of the lead ring was 0.32 inch for the SV weight of the 2, 3, 4, 5, and 6-inch pipes. This thickness increased to 0.67 inch for the 15-inch pipe. This increase in thickness exposed more surface area of the lead ring that

Table 8.2. Strains and forces in pipe hubs

Test No.	Caulking Strain μ in./in.	P	Comments
4A4-14	500	431	caulked by plumber #1
4A17-15	500	445	caulked by plumber #1
4A18-16	400	358	caulked by plumber #1
4C6-17	350	309	caulked by plumber #1
4E5-18	300	278	caulked by plumber #1
4E14-19	550	399	caulked by plumber #1
4F5-20	400	412	caulked by plumber #1
4F8-21	450	368	caulked by plumber #1
8A8-22	850	760	caulked by plumber #2
8B1-23	500	522	caulked severely by plumber #2
8B7-24	950	860	caulked severely ^a
8C2-25	500	568	caulked severely by plumber #2
8C7-26	900	566	caulked severely by plumber #2

^aAccording to the plumber.

Table 8.2. (Continued)

Test No.	Caulking Strain μ in./in.	P	Comments
SD2-27	400	466	caulked by plumber #2
SD9-28	500	406	" " " "
SE2-29	500	722	" " " "
SE8-30	950	696	" " " "
SF1-31	350	460	" " " "
SF8-32	850	447	" " " "
12A8-33	500	499	cracked while caulked by plumber #2
12B1-34	450	432	cracked while caulked by plumber #2
12C1-35	700	638	caulked by plumber #2
12C8-36	550	353	" " " "
12D1-37	700	818	" " " "
12E2-38	450	610	" " " "
12E9-39	800	540	cracked while caulked by plumber #2
12F1-40	400	453	caulked by plumber #2
12F7-41	650	412	" " " "

had to be caulked. Thus, while the 4-inch hubs were caulked once around the outside and once around the inside of the lead ring, the 8 and 12-inch hubs were caulked once around the outside, once around the inside, and a final round on the outside again. This caulking process was considered as normal.

Table 8.2 indicates some variation in the measured strains. This variation is expected for the various pipe sizes. The variation is mainly due to the dimensions of the hubs, properties of the metal, and the austerity of caulking, which is affected by the condition of the plumber. It is impossible even for one plumber to be consistent in his performance. The plumber's performance is affected by the atmosphere in which he has to work, the time of the day, his mental attitude, and his physical condition. It is very likely that the last joint a plumber makes in the day will be caulked considerably less than the first joint of the day.

The measured maximum caulking strain and the values of A, S, F, and R (listed in Table B.1, Appendix B) for each pipe were substituted into Eq. 8.1 to obtain the corresponding equivalent caulking force. The modulus of elasticity of cast iron was assumed to be 16,000,000 psi. This modulus may be on the high side. However, the higher the modulus of elasticity assumed, the higher the resulting caulking force will be. Therefore, the equivalent computed caulking

forces may be slightly above the true values. The P forces for all pipes tested are shown in the third column of Table 8.2. The computer program for solving Eq. 8.1 is shown in Fig. D.38 of Appendix D.

Because of the variation in measured caulking strains, the values of P indicated in Table 8.2 also vary with different pipes of the same size. Variation occurs also with different sizes. The variation in equivalent caulking forces is summarized in Table 8.3 for the different sizes used.

It is interesting to note that the size and shape of the key in the hub bead seems to have some important bearing on the value of P. Appendix B shows that there is quite a variation in the shapes and sizes of the keys in beads of the 4, 8, and 12-inch hubs. The largest key was in the 8-inch hubs and the smallest in the 4-inch hubs. The equivalent caulking force was also largest in the 8-inch hubs and smallest in the 4-inch hubs as shown in Table 8.3.

To establish design values of equivalent caulking forces, a factor of safety of two was selected and applied to the mean caulking force values in Table 8.3. It must be kept in mind that the stress formula is based upon a linear stress-strain relationship for cast iron. Any ductility that the cast iron may possess will result in a hub with more strength than the linear formula predicts. Since the stress-strain relationship of cast iron is non-linear, it

Table S.3. Equivalent caulking forces, lbs./in.

	4-inch	8-inch	12-inch
Minimum value	278	406	353
Mean value	374	588	530
Maximum value	445	862	820

may appear that the factor of safety selected is on the high side. However, the ultimate strength that any cast iron product possesses is dependent upon the amount and type of physical defects present in the casting. Blow-holes, cracks, segregation of the impurities, and coarse-grain structure are the most common type of defects. It has been observed in the laboratory that the hub is more likely to possess defects than the barrel or spigot portion of the pipe. Based upon the above, the factor of safety selected will allow joints to be properly caulked without failure. Using a factor of safety of 2, the design values of the equivalent caulking forces P for the 4, 8, and 12-inch hubs become 748, 1176, and 1060, respectively. The factor of safety selected and applied to the mean equivalent caulking force values was sufficiently large to give design values that are larger than the maximum values. The caulking force acting on the hub for pipe size less than 4-inch was assumed to be the same as for the 4-inch size. For pipes larger than 8-inch, the caulking forces were assumed to be the same as for the

8-inch size. A linear interpolation between the caulking pressures for the 4-inch and 8-inch size was used for the 5-inch and 6-inch sizes. This resulted in the following equivalent caulking forces shown in Table 8.4.

Table 8.4. Equivalent caulking forces with a safety factor of 2

Size, Inches	Caulking force, lbs./in.
2, 3, 4	748
5	855
6	962
8, 10, 12, 15	1176

Knowing the design caulking forces listed in Table 8.4 for all pipe sizes, and taking $\sigma_{\phi} = 21,000$ psi, the design ratios σ_{ϕ}/P were determined. These ratios were used to obtain design charts for all pipe sizes as explained in the next section.

8.3 Design Charts

The ratio σ_{ϕ}/P was determined for each pipe size as discussed above. Knowing this ratio, specific values of S, R, and F were obtained from the charts in Appendix D.

The relationship between these values is shown in Figs. 8.1 to 8.9 for the various pipe sizes. From these figures, any design combination for the hub dimensions could be obtained. For example, for the 4-inch hubs, if R is chosen as 0.36 inches and F as 0.80 inches, then from Fig. 8.3, S should be 0.12 inches.

8.4 Observations on Presently Manufactured Hubs

Hub configurations of presently manufactured pipes vary significantly from one size to another and from one manufacturer to the next. Most of the variation occurs in the 4-inch hubs as shown in Appendix B. Theoretical and experimental results indicate that the strains at the base of the hub are almost negligible compared to the strains in the lip area. Therefore, reinforcing the base of the hub is unnecessary unless for purposes other than for strength during joint construction. In the 4-inch hubs shown in Appendix B, brands A, D, and E have reinforcements that are more than is needed in resisting the joint construction strains.

Also, since the caulking strains are relatively small at the base of the hub, no extra metal is needed. In the 8 and 12-inch hubs, brands E and F seem to have adequate metal in the hub base. For the same size pipes, other brands appear to have extra metal at the base of the hub that is more than ample to resist the joint construction strains.

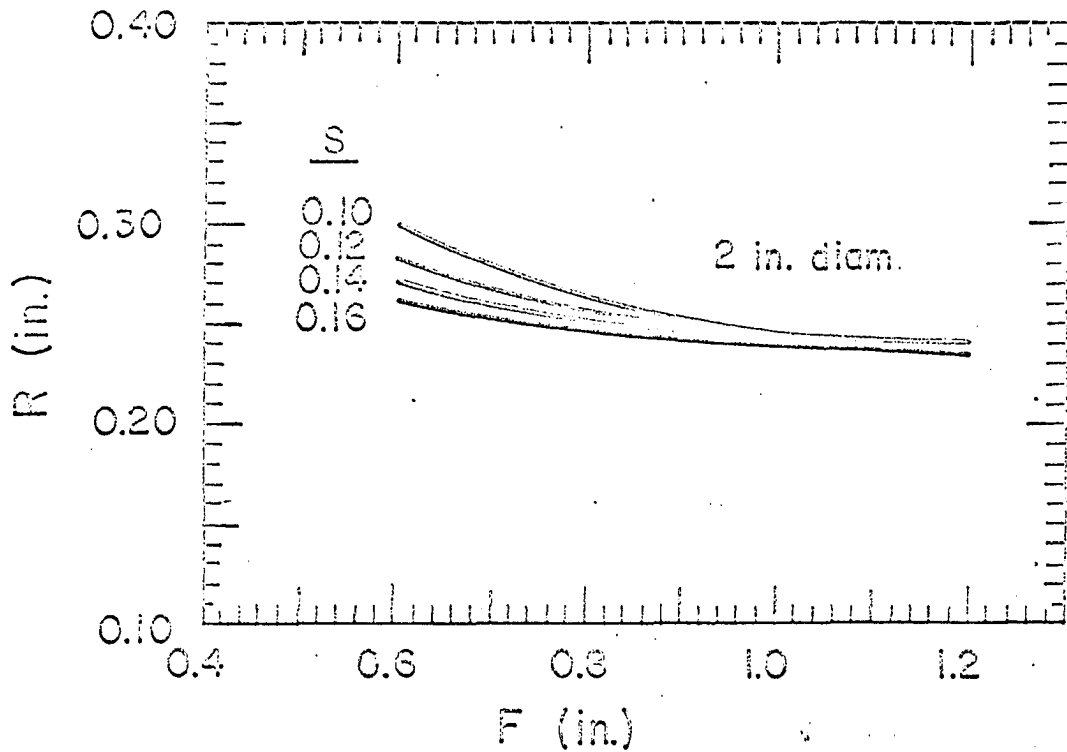


Fig. 8.1. Relationship between hub dimensions F , R , and S for 2-inch pipes

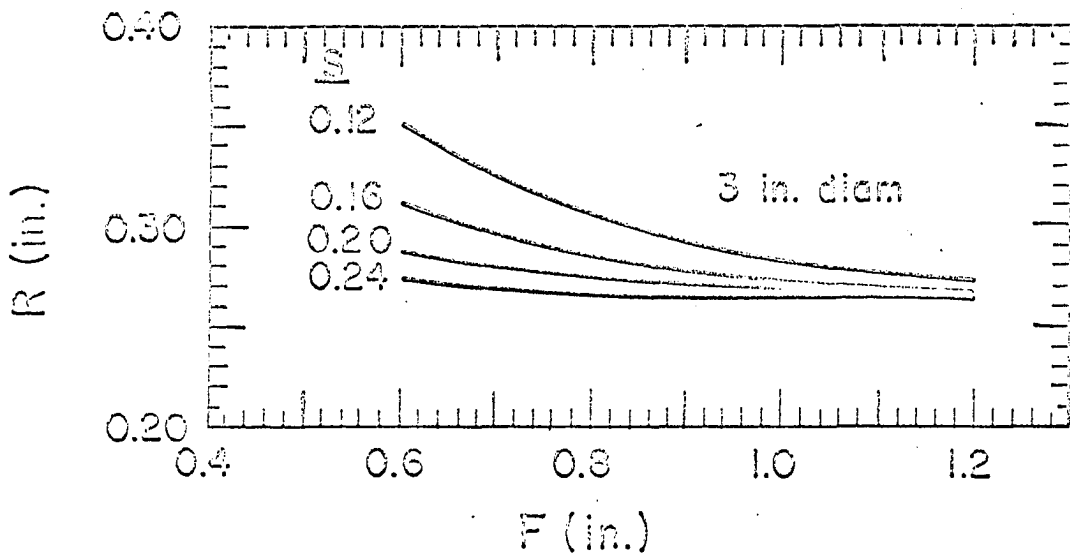


Fig. 8.2. Relationship between hub dimensions F , R , and S for 3-inch pipes

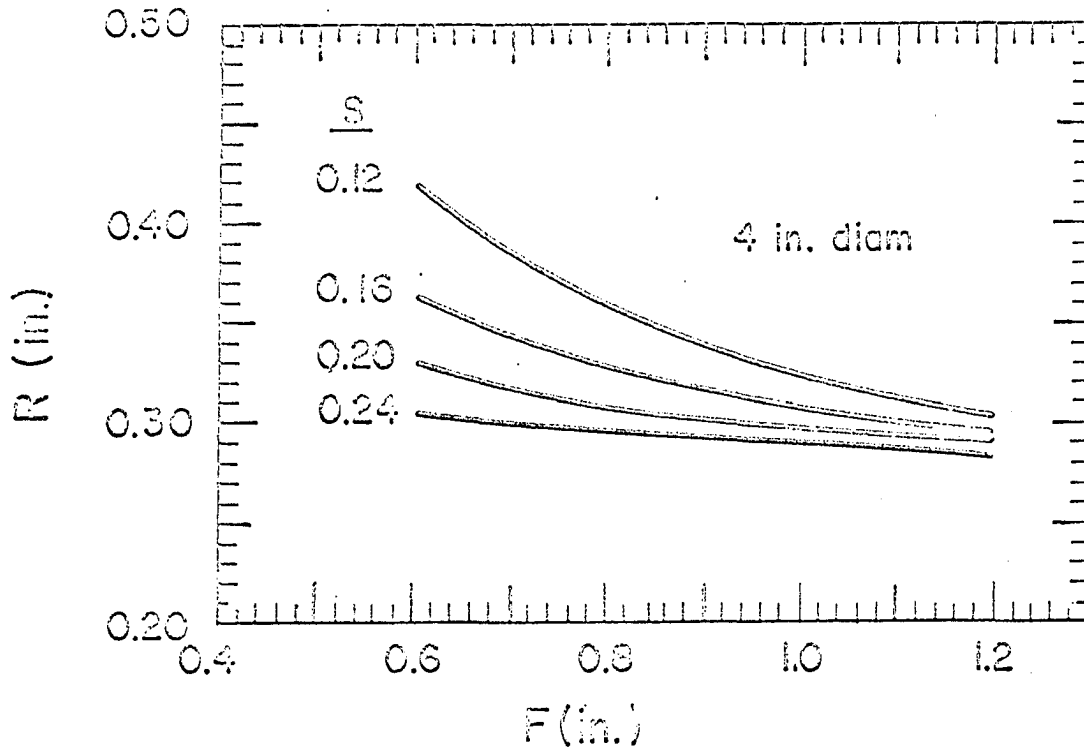


Fig. 8.3. Relationship between hub dimensions F , R , and S for 4-inch pipes

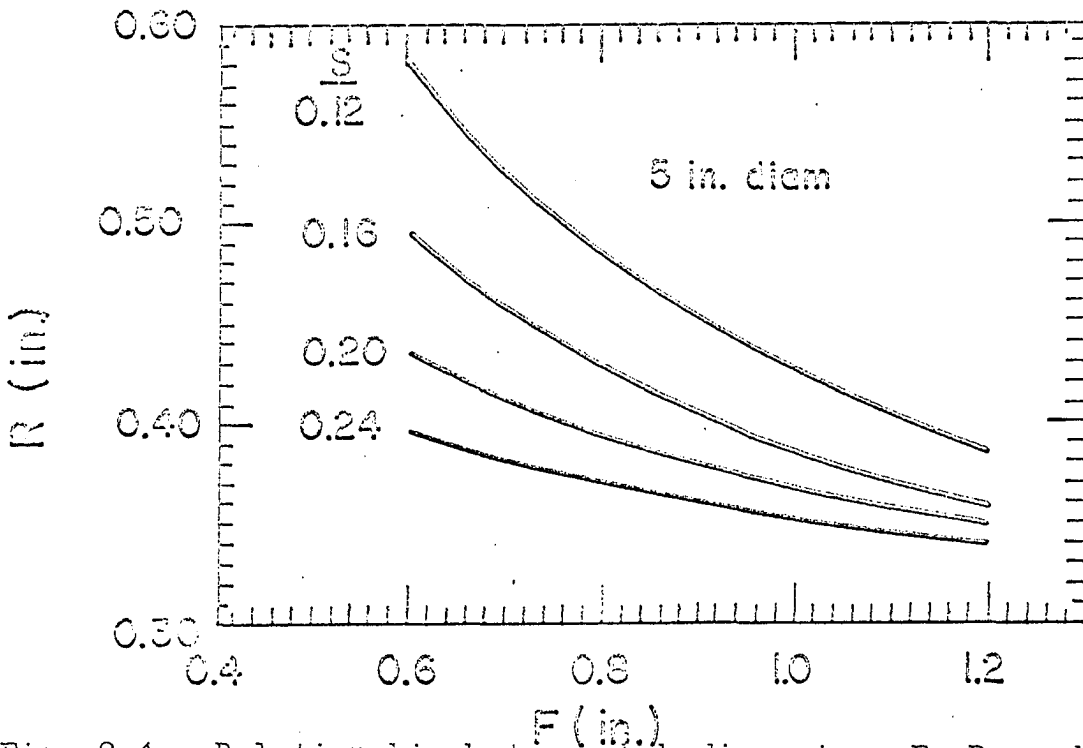


Fig. 8.4. Relationship between hub dimensions F , R , and S for 5-inch pipes

Fig. 8.5. (top) Relationship between hub dimensions F, R,
and S for 6-inch pipes

Fig. 8.6. (bottom) Relationship between hub dimensions F, R,
and S for 8-inch pipes

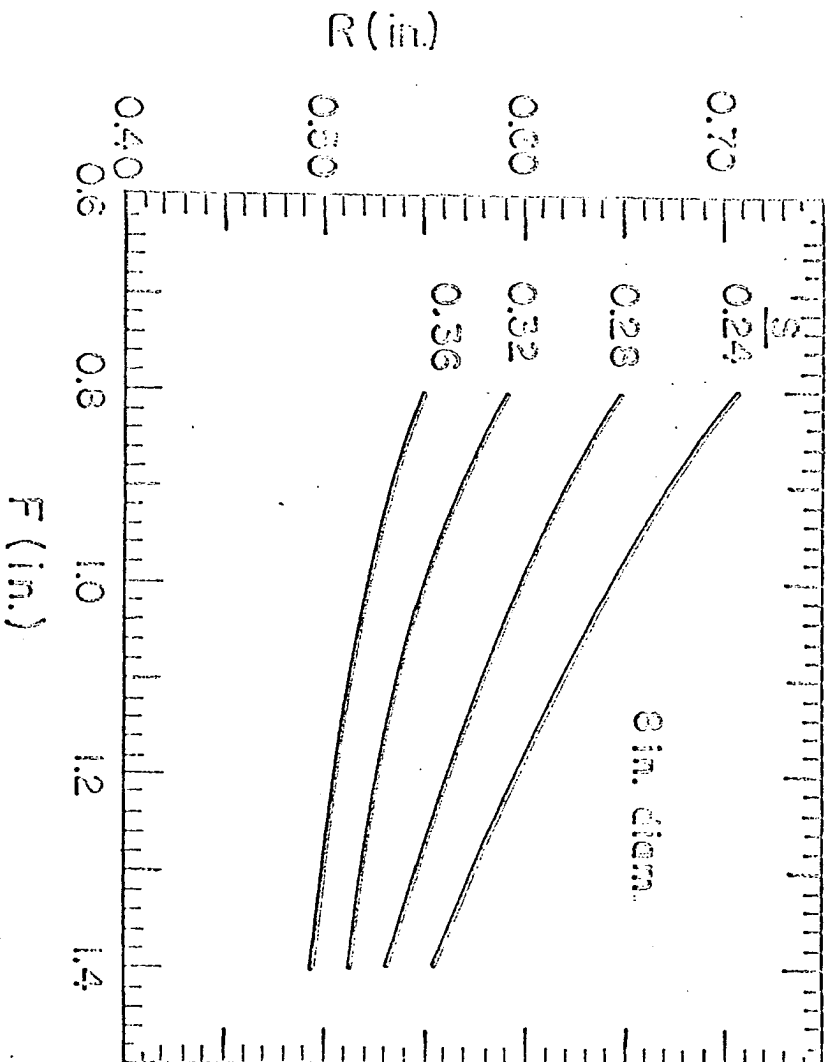
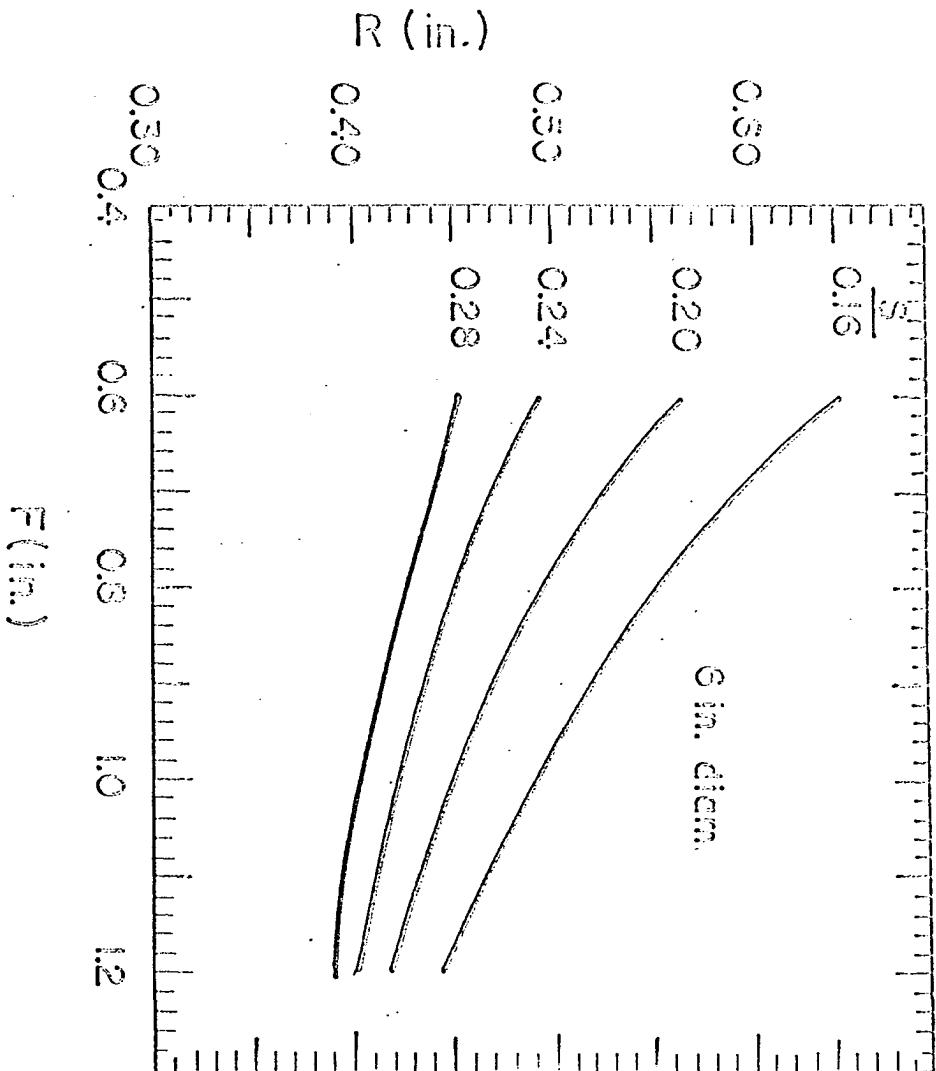
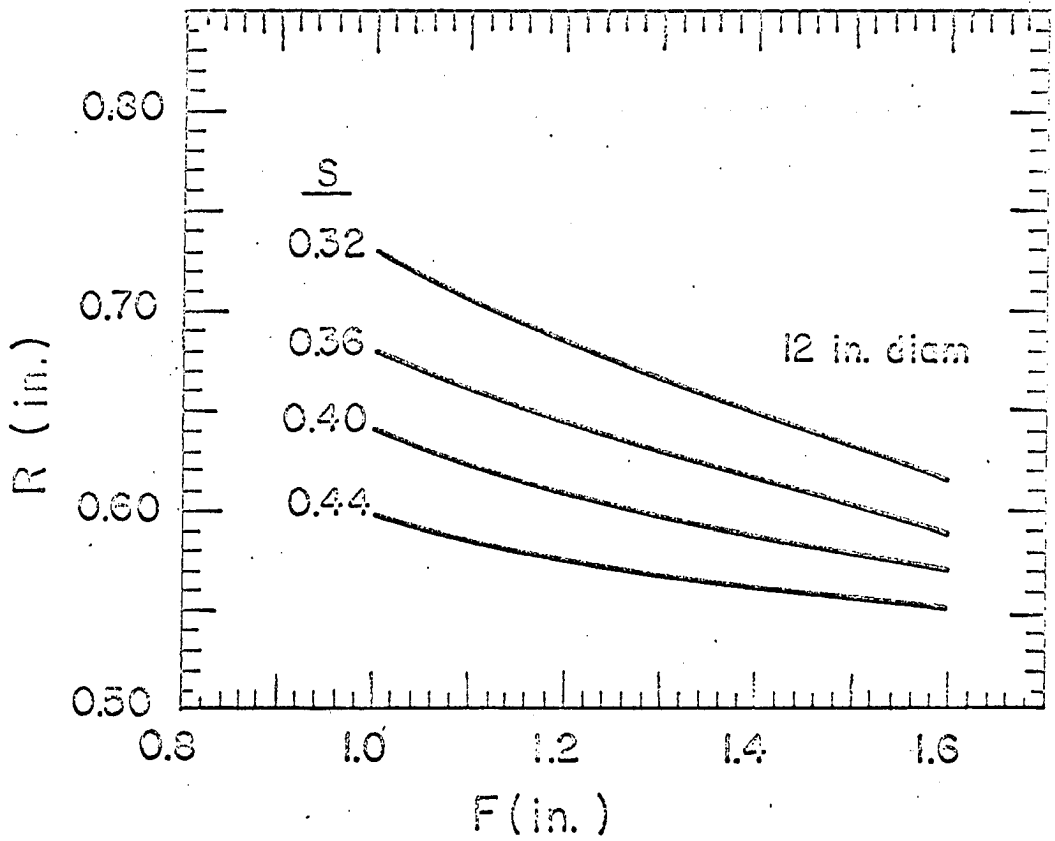
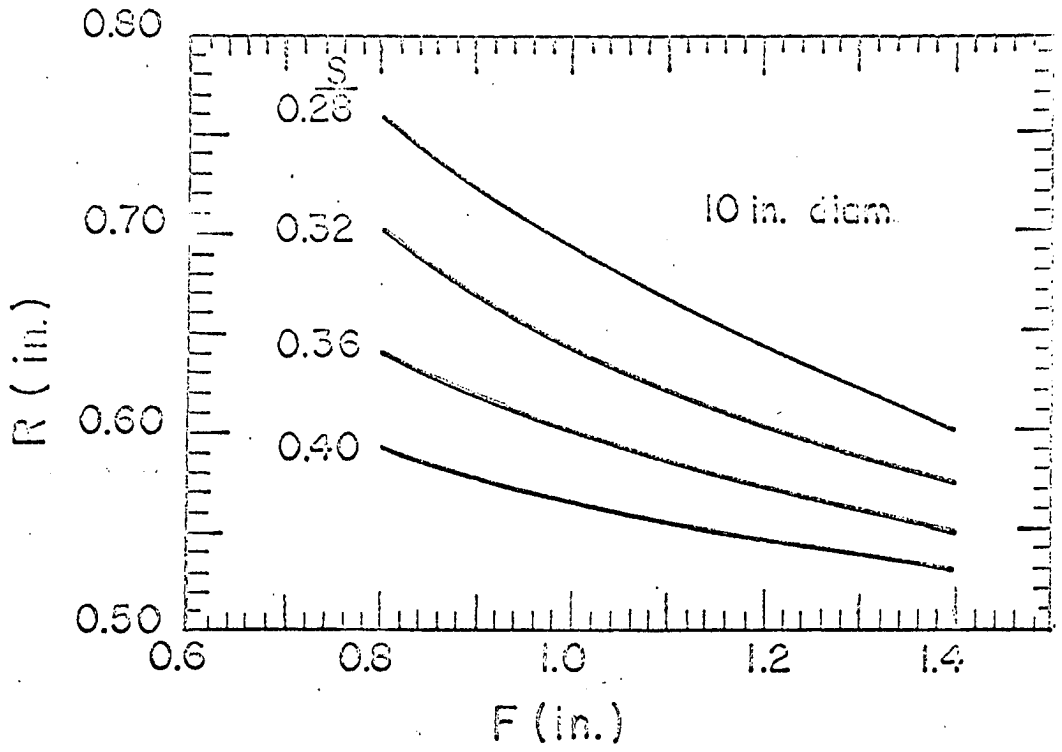


Fig. 8.7. (top) Relationship between hub dimensions F, R, and S for 10-inch pipes

Fig. 8.8. (bottom) Relationship between hub dimensions F, R, and S for 12-inch pipes



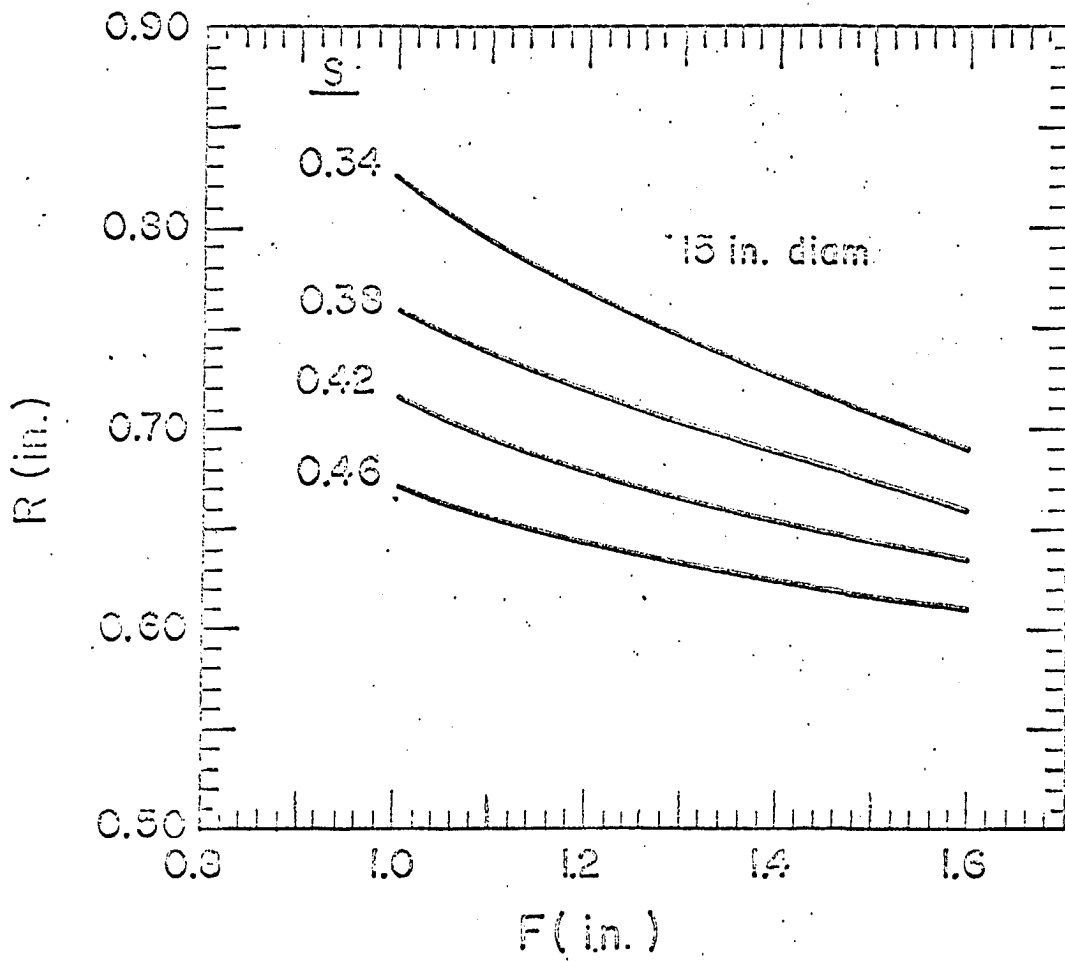


Fig. 8.9. Relationship between hub dimensions F, R, and S for 15-inch pipes.

9. DESIGN RECOMMENDATIONS FOR THE SPIGOTS

9.1 Design Chart

It was shown in Section 5.4 that Eq. 5.49 is given by

$$\sigma_{\ell} = \frac{1.16 r^{0.5} P_1}{t^{1.5}} \quad (5.49)$$

would be used in plotting a design chart. This chart is plotted in Fig. 9.1. Once the design value of σ_{ℓ}/P_1 for each particular pipe size is established, the thickness can be determined from this chart.

9.2 Determination of the Stress σ_{ℓ} and the Caulking Force P_1

Because the maximum tensile stresses in the spigot is due to bending moments, the design value of σ_{ℓ} is taken as 45,000 psi, the minimum specified modulus of rupture.

The caulking force P_1 was determined from Eq. 5.46 of Section 5.4. This equation is given by

$$\epsilon_{\ell} = \frac{1.25 r^{0.5} P_1}{Et^{1.5}} \quad (5.46)$$

In using this equation, a modulus of elasticity of 16,000,000 psi was used. The longitudinal caulking strains were obtained through experiments for the 4, 8, and 12-inch spigots. In obtaining these strains, four tests were conducted on the 4-inch pipes, one test on the 8-inch, and one test on the 12-inch pipe. Substituting these strains into Eq. 5.46, the

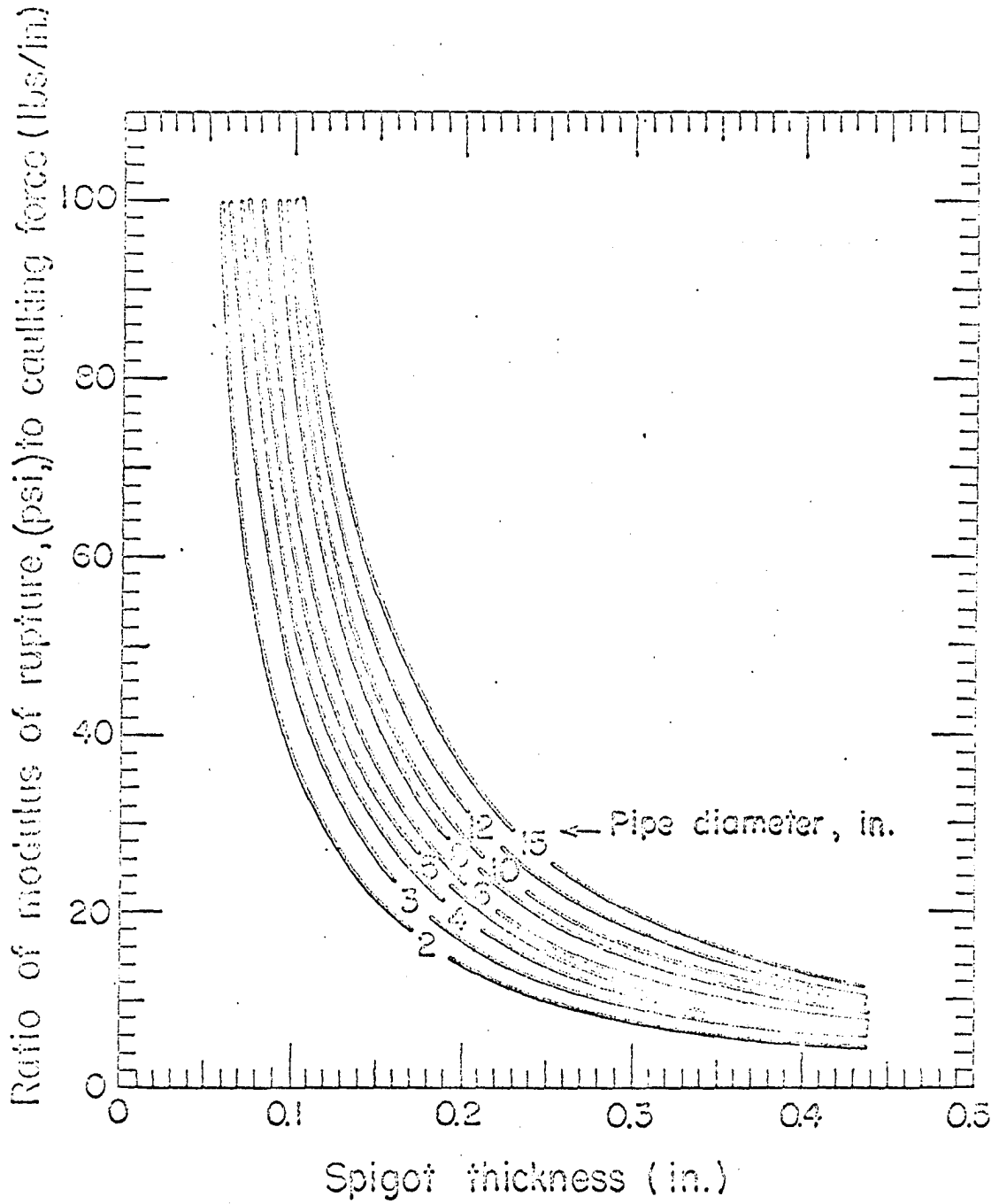


Fig. 9.1. Relationship between ratio of modulus of rupture to caulking force and spigot thickness

caulking forces are obtained. These forces are shown in Table 9.1.

Table 9.1. Caulking forces in pipe spigots

Dimater of pipe inches	Caulking force, P_1 lbs./in.
4	221, 234, 312, 376
8	509
12	430

The number of tests conducted might seem to be on the low side. However, it was felt that extensive testing was not needed based on the following reason. The survey of the performance of cast iron pipes (Appendix A) indicated that in practice, very few spigots fail due to the joint construction operation. Thus, it was anticipated that presently manufactured spigots have an ample factor of safety. A few tests were conducted, so that the equivalent caulking forces can be determined, and the thickness requirement can be established analytically.

Since only one test was conducted on the 8-inch pipe (Table 9.1), the joint of this pipe was severely recaulked to determine if the normal caulked joint values were indicative of a normally caulked joint and to establish an appropriate factor of safety for design. The caulking force due to the

second severe caulking increased to 940 lbs./in. This established that if a factor of safety of 2 is used in design, even a severely caulked joint would not fail when the pipes are designed for the caulking forces established from "normally" caulked joints.

In order to determine the required spigot thickness, it was necessary to establish design caulking forces for all sizes of pipes. The average caulking force (4 tests) for the 4-inch pipes was 285 lbs./in. It is recommended that this force be also used for the 2-inch and 3-inch diameter pipes. Since the caulking force for the 8-inch diameter pipes was larger than that determined for the 12-inch pipe, it is recommended that a caulking force of 510 lbs./in. be used for the 8, 12, and 15-inch diameter pipes. For the 5 and 6-inch diameter pipes, a linear variation between the forces for the 4-inch pipe and the 8-inch pipe is recommended. Using a factor of safety of 2, the design caulking forces shown in Table 9.2 were determined.

Using $\sigma_{\ell} = 45,000$ psi, and the caulking forces P_1 shown in Table 9.2, the required spigot thicknesses can be obtained from the design chart of Fig. 9.1. The required spigot thicknesses for different pipe sizes are listed in Table 9.3.

The thicknesses shown in Table 9.3 were obtained by considering the strains due to the joint construction operation. These thicknesses (with a factor of safety of 2 against failure) were about 1/2 those of the presently manufactured

Table 9.2. Caulking forces in various pipe diameters

Spigot diameter inches	Caulking forces lbs./in.
2, 3, 4	570
5	685
6	795
8, 10, 12, 15	1020

Table 9.3. Recommended spigot thicknesses

Spigot diameter inches	Required spigot thicknesses, inches
2	0.062
3	0.073
4	0.082
5	0.092
6	0.110
8	0.145
10	0.153
12	0.162
15	0.177

thicknesses. Hence, presently manufactured spigot thicknesses are very safe with respect to the joint construction operation. However, the minimum spigot thicknesses might be governed by other factors such as the manufacturing process. The determination of such factors is beyond the scope of this research.

10. DESIGN RECOMMENDATIONS FOR THE BARRELS

10.1 Design Chart

Chapter 3 showed the method of evaluating earth and surface live loads and then conversion to 3-edge bearing loads for various bedding installations of the 8-inch pipe. The method used can be extended for all pipe diameters. Following the same procedure discussed in Sections 3.3, 3.4, and 3.5, 3-edge bearing loads were obtained for all pipe diameters used in this research. These loads are shown in Table 10.1. By knowing the pipe diameter, height of fill, and the bedding condition, a 3-edge load can be obtained from the table.

The loads given in Table 10.1 are the maximum that can generally be expected. Thus, pipes with thicknesses based on these loads are on the verge of breaking if placed under the considered working conditions. However, in order for the calculated earth load to occur, all the extreme conditions assumed must occur simultaneously. Since it is possible for these extreme conditions to occur simultaneously, but not likely, a relatively low factor of safety against failure can be used. It is suggested that a minimum factor of safety of 1.25 be employed in the determination of the wall thicknesses. Therefore, a desired factor of safety

Table 10.1. Equivalent 3-edge bearing loads^a for various pipe installations

Pipe Diameter inches	Max. Ht. of Fill feet	Bedding and Backfill Condition				
		A	B	D	E	F
2	8	400	370	400	300	260
	12	560	510	550	430	370
	16	740	680	770	560	490
	20	-	-	-	-	-
3	8	540	490	540	410	360
	12	810	730	770	620	540
	16	1080	980	1040	830	720
	20	1350	1230	1320	1040	900
4	8	680	610	690	520	450
	12	1040	920	1020	790	680
	16	1420	1260	1330	1090	930
	20	1780	1580	1710	1360	1170
5	8	830	740	890	640	540
	12	1290	1140	1250	990	840
	16	1750	1550	1660	1340	1140
	20	2170	1920	2070	1660	1420
6	8	980	850	1060	750	630
	12	1480	1290	1470	1130	960
	16	2010	1750	1930	1540	1300
	20	2530	2210	2410	1940	1640
8	8	1260	1080	1520	960	800
	12	1870	1610	2190	1430	1200
	16	2570	2210	2980	1970	1640
	20	3290	2830	3710	2520	2100
10	8	1610	1360	1760	1230	1010
	12	2320	1960	2570	1780	1460
	16	3090	2620	3430	2370	1940
	20	4010	3390	4350	3070	2520

^a Load given in pounds per ft. for most critical installation considered.

Table 10.1. (Continued)

Pipe Diameter inches	Max. Ht. of Fill feet	Bedding and Backfill Condition				
		A	B	D	E	F
12	8	1870	1560	2060	1430	1160
	12	2670	2220	2930	2040	1660
	16	3580	2990	3920	2750	2230
	20	4590	3820	4940	3520	2850
15	8	2330	1890	2520	1780	1420
	12	3320	2690	3740	2550	2020
	16	4420	3580	5010	3390	2690
	20	5550	4490	6280	4250	3380

(say 1.25) should be applied to the 3-edge bearing loads in Table 10.1.

By knowing the final 3-edge bearing load (including the factor of safety), the thickness can be determined from Fig. 10.1. This figure was obtained by plotting Eq. 2.1 for the various pipe diameters using a modulus of rupture of 45,000 psi.

The use of Table 10.1 and Fig. 10.1 is illustrated below. It is desired to determine the wall thickness required for an 8-inch pipe with bedding and backfill condition B and with a maximum height of fill of 12 feet. A factor of safety of 1.25 against failure is specified.

From Table 10.1,

for a factor of safety of 1.00; $W = 1610$ lbs./ft.

for a factor of safety of 1.25; $W = 1.25 \times$
 $1610 = 2010$ lbs./ft.

From Fig. 10.,

required net thickness, $t = 0.17$ inches.

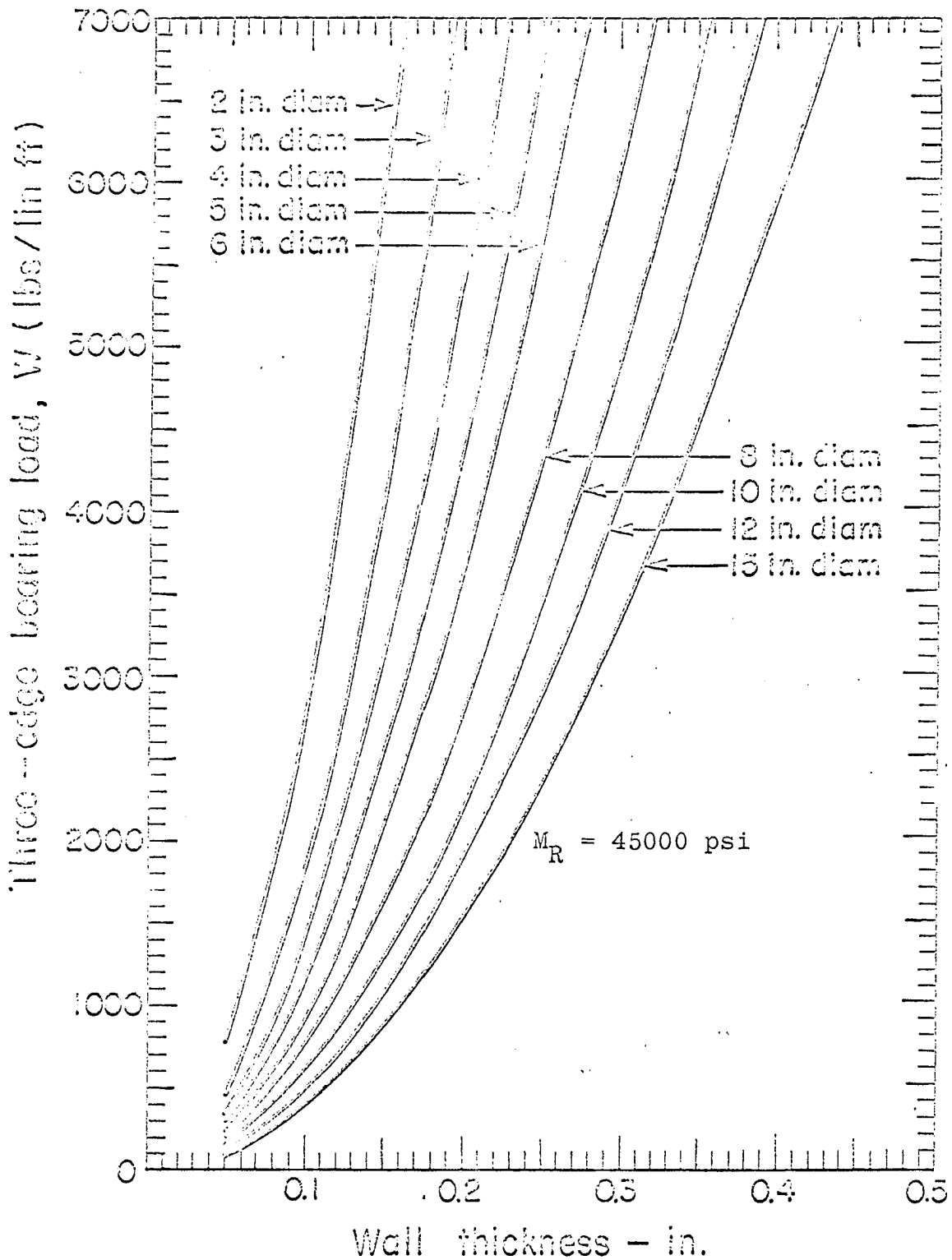


Fig. 10.1. Relationship between three-edge bearing load and pipe wall thickness for various pipe diameters

11a. SUMMARY

In order to determine the required thicknesses of the pipe components, it was necessary first to consider the types of forces acting on pipe and fitting systems. In general, these factors can be categorized according to the following stages of the pipe life:

1. Manufacturing
2. Transportation
3. Installation
4. Service Life.

In the manufacturing stage, stresses were caused by the differential cooling of pipe. Residual stresses, caused by such cooling, were measured on the outside surface of pipes and fittings. Their magnitude was too small to control the thickness (Tables 2.1 and 2.2). Also, the effect of residual stresses on the ultimate strength of cast iron was negligible (Table 2.3).

Stresses during the transportation stage were caused mainly by the impact forces that occur during loading, hauling, and unloading. These forces were not considered in this research since a product such as cast iron soil pipe should be handled with the degree of care necessary to insure delivery on the job in a good condition.

Stresses induced during the installation stage resulted from the joining of pipes together. The two joints of concern were the gasket and lead-oakum joints. Stresses in the gasket joints did not govern the thickness requirements since they were lower than those of the lead-oakum joints. In lead-oakum joints, stresses were due to yarning the oakum, pouring lead on top of the oakum, and caulking the lead to form a sealed joint. Strain gages were bonded on critical areas of the hub and spigot. Measured yarning strains were very little in magnitude (Table 4.1) and were neglected. Maximum critical thermal strains were lower than maximum critical caulking strains (Figs. 4.7, 4.8, 5.1 and 5.2). Also, they dissipated to a negligible amount by the time caulking strains reached their maximum value. Hence, thermal strains were not considered in the design criteria for thicknesses. Maximum caulking critical strains were obtained in the hubs and spigots of 4, 8, and 12-inch pipes. These strains were substituted into equations, derived from theory of shells, relating strains to forces and dimensions of hubs and spigots. An average of these forces, with a safety factor of 2, in each of the 4, 8, and 12-inch pipes was calculated. The average forces of the 2 and 3-inch pipes were assumed to be the same as the 4-inch pipes and the average forces of the 12 and 15-inch pipes were assumed to be the same as the 8-inch pipes. A linear interpolation of forces between the 4 and

8-inch pipes was assumed in calculating forces acting on the 5 and 6-inch pipes (Tables 8.4 and 9.2). In hubs, these forces were substituted into the appropriate equations and charts were then plotted relating the various parameters, i.e., hub bead thickness, hub bead length, and hub wall thickness, to each other (Figs. 8.1 and 8.9). In spigots, thicknesses were obtained directly by substituting the forces into the governing equation (Table 9.3).

Stresses induced in pipe during its service life were due to building movements and earth loading. Stresses due to movements that rendered the pipe system non-functional were too small to govern the design. In earth loading, variables considered were ditch width and depth, size and thickness of pipes, surface live loads, and bedding conditions. Taking the most critical combination of these variables, loads were obtained on the various pipe sizes. These loads were then converted to equivalent 3-edge bearing loads (Table 10.1). By knowing the 3-edge bearing loads, including a factor of safety, thicknesses can be determined from Eq. 2.1 (which was plotted in Fig. 10.1 for convenience) for the various pipe diameters using a modulus of rupture of 45,000 psi.

In a buried pipe system, the maximum height of fill and bedding condition are known. Thus, thicknesses of barrels to adequately withstand these conditions can be determined from Table 10.1 and Fig. 10.1. The theoretical spigot thicknesses

are determined from Table 9.3. In hubs, variables are the bead thickness, bead length, and hub wall thickness. By choosing any two suitable variables, the third is obtained from one of Figs. 8.1 to 8.9. Thus, the barrel, spigot, and hub dimensions can be evaluated to adequately withstand forces acting on pipe during its life span.

For a pipe system in buildings, the same criteria holds for evaluating the hub and spigot dimensions. The barrel thickness may be made the same as above. Otherwise it is made enough to withstand handling and transportation forces.

11b. ACKNOWLEDGMENTS

The author would like to thank Dr. R. E. Untrauer, Head of the Structural Research Laboratory, for his assistance and advice throughout the research program. His suggestions and ideas were invaluable to the progress of the research and his encouragement and guidance were of great appreciation.

The author would also like to thank Dr. W. W. Sanders, Jr. for his assistance in the earth-loading phase of the research, and to Dr. Ti-ta Lee for his help with the computer programs and the research phase concerning the bending of the pipe systems.

Acknowledgment is due to the Cast Iron Soil Pipe Institute for sponsoring the project and furnishing test specimens and equipment.

Acknowledgment is also due to the Mechanical and Electronics shops of the Engineering Research Institute for fabricating and furnishing all needed equipment, and to the plumbing shop of Iowa State University for their cooperation with the Research Staff and for providing the plumbers.

12. LITERATURE CITED

1. Papamichalopoulos, G. A study of design requirements for buried cast iron soil pipe. Unpublished M.S. thesis. Ames, Iowa, Library, Iowa State University. 1966.
2. Spangler, M. G. Soil engineering. 2nd edition. Scranton, Pa., International Textbook Co. 1960.
3. Wiggin, T. H., Enger, M. L., Schlick, W. J. A proposed new method of determining barrel thickness of cast iron pipe. American Water Works Association Journal 31: 841-909. 1939.
4. Spangler, M. G. Negative projecting conduits. Iowa State College Engineering Experiment Station Report 14. 1952-53.
5. Timoshenko, S. and Woinowsky-Krieger, S. Theory of plates and shells. New York, N.Y., McGraw-Hill Book Co., Inc. 1959.
6. Cast Iron Soil Pipe Institute. Cast iron soil pipe and fittings: Specification Data Standard HS-65. Washington, D.C., author. 1965.
7. American Society for Testing and Materials. 1967 book of A.S.T.M. standards. Part 2. Ferrous castings. A.S.T.M. designation A48-64. Philadelphia, Pa., author. 1967.
8. American Water Works Association. American standard for cast iron pipe centrifugally cast in metal molds for water or other liquids. American Water Works Association Journal 54: 307-333. 1962.
9. American Water Works Association. American standard for cast iron pipe in sand lined molds for water or other liquids. American Water Works Association Journal 54: 335-367. 1962.
10. Garrity, L. V. Detroit experience with sulphur compound joining material. American Water Works Association Journal 47: 455-464. 1955.
11. Murphy, G. Advanced mechanics of materials. New York, N.Y., McGraw-Hill Book Co., Inc. 1946.

12. Michel, R. Elastic constants and coefficients of thermal expansion of piping materials proposed for 1954 Code for pressure piping. American Society of Mechanical Engineers Transactions 77: 151-159. 1955.
13. Crocker, S. Piping handbook. 4th edition. New York, N.Y., McGraw-Hill Book Co., Inc. 1945.
14. Blair, J. S. Stresses in tubes due to internal pressure. Engineering 170: 218-221. 1950.
15. Buston, W. J. and Burrows, W. R. Formulas for pipe thickness. American Society of Mechanical Engineers Transactions 73: 575-581. 1951.
16. M. W. Kellogg. Mechanical Engineers Co. Design of piping systems. New York, N.Y., John Wiley and Sons, Inc. 1964.
17. Parkus, H. Thermal stress in pipes. Journal of Applied Mech. 20: 485-488. 1953.
18. Mendelson, A. and Manson, S. S. Approximate solution to thermal shock problems in plates, hollow spheres and cylinders with heat transfer at surfaces. American Society of Mechanical Engineers Paper 54A-264. 1954.
19. Marston, A. and Anderson, A. O. The theory of loads on pipes in ditches, and tests of cement and clay drain tile and sewer pipe. Iowa State College of Engineering Experiment Station Bulletin 31. 1913.
20. Marston, A. The theory of external loads on closed conduits in light of the latest experiments. Iowa State College Engineering Experiment Station Bulletin 96. 1930.
21. Spangler, M. G. Investigation of loads on three cast iron pipe culverts under rock fills. Iowa State College Engineering Experiment Station Bulletin 104. 1931.
22. Schlick, W. J. Loads on pipe in wide ditches. Iowa State College Engineering Experiment Station Bulletin 108. 1932.
23. Clayton, W. C. Design charts for tubes subjected to bending. Aviation 41: 41, No. 2: 80-82, 205. 1942.
24. Allison, G. E. and Niles, A. S. Designing tubes for bending loads. Machine Design 22: 163-165. 1950.

25. Fevre, W. L., Jr. Torsional strength of steel tubing as affected by length. *Product Engineering* 20: 133-136. 1949.
26. Markl, A. R. C. Piping flexibility analysis. *American Society of Mechanical Engineers Transactions* 77: 127-149. 1955.
27. Abraham, E. D. and McGlure, G. M. How Stresses affect branch connection. *Petroleum Refiner* 34: 117-120. 1955.
28. Fessler, H. and Lewin, B. H. Stress distribution in Tee-junction of thick pipes. *British Journal of Applied Physics* 7: 76-79. 1956.
29. Prior, J. C. Investigation of bell and spigot joints in cast iron water pipes. *Ohio State University Engineering Experiment Station Bulletin*. 87: 1-57. 1935.
30. Vinieratos, S. D. and Zeno, D. R. Piping flexibility and stresses. New York, N.Y., Cornell Maritime Press. 1941.
31. Porter, H. Chart method for pipe stress calculation. *Engineer* 212: 1074-1078. 1961.
32. Hsiao, K. H. Calculating pipe stresses efficiently: further simplification. *Heating, Piping and Air Conditioning* 34: 194-200. 1962.
33. DeHarte, R. C. Determination by moment distribution of reactions and moments arising from expansion of piping systems. *Montana State College Engineering Experiment Station Bulletin* 3. 1948.
34. Picardi, E. A. How to apply method of slope deflection to thermal stress analysis of piping. *Petroleum Processing* 8: 368-372. 1953.
35. Wolosemick, F. E. Methods of making piping flexibility analysis. *Heating, Piping and Air Conditioning* 19: 69-74. 1947.
36. American Water Works Association. Manual for computation of strength and thickness of cast iron pipe. New York, N.Y., author. 1957.
37. Clay Products Association. Clay pipe engineering manual. Barrington, Illinois, author. 1965.

38. Denton, A. A. and Alexander, J. M. New method for measurement of local residual stresses in tubes. *Journal of Mechanical Engineering Science* 5: 89-90. 1963.
39. Gascoyne, J. W. Analysis of pipe structures for flexibility. New York, N.Y., John Wiley and Sons, Inc. 1959.
40. Brock, J. E. How to determine free expansions of piping due to pressurization and nonuniform heating. *Heating, Piping and Air Conditioning* 36: 152-155. 1964.

13. APPENDIX A.

A.1 Literature Survey

A.1.1 Material properties of cast iron Material properties most needed for the analysis of stresses and deflections of structural members and systems are the ultimate strength and modulus of elasticity. The coefficient of thermal expansion is also needed when the temperature effect is involved.

The current Commercial Standard for Cast Iron Soil Pipes and Fittings (6) require either a tension bar test or a transverse (flexural) strength test for the determination of the strength and modulus of elasticity. The maximum stresses determined from tensile tests vary between 20,000 psi and 60,000 psi (7). The tensile strength is specified to be not less than 21,000 psi (6).

The specified minimum modulus of rupture as given by the American Water Works Association varies between 31,000 psi for pit cast iron to 40,000 psi for centrifugally cast pipe (8, 9). The modulus of elasticity for pipes centrifugally cast in metal molds is specified as 12,000,000 psi while the modulus of elasticity for pipes centrifugally cast in sand lined molds is specified as 10,000,000 psi. If any of the two moduli is increased by a certain percentage, the modulus of rupture is to be increased by the same percentage.

The coefficient of thermal expansion for cast iron as given by various investigators vary to some extent. Garrity gave a modulus (α) of 5.8×10^{-6} in/in $^{\circ}$ F (10) and Murphy gave $\alpha = 5.5 \times 10^{-6}$ in/in $^{\circ}$ F (11). Michel stated that α is equal to 6.10×10^{-6} in/in $^{\circ}$ F at 400 $^{\circ}$ F and increases to approximately 7.19×10^{-6} in/in $^{\circ}$ F at 1,000 $^{\circ}$ F (12).

A.1.2 Stresses in pipes due to internal pressure

Internal pressures in pipes produce stresses in three directions: longitudinal, transverse, and radial at a given point in the pipe wall. For thin pipes with closed ends, these stresses are (13):

$$\sigma_{\ell} = \frac{pd}{4t} \quad \sigma_t = \frac{pd}{2t} \quad \sigma_r = -p \quad (\text{A.1})$$

where:

σ_{ℓ} , σ_t , σ_r = longitudinal, transverse, and radial stresses, respectively, with tensile stress considered as positive, psi
 p = intensity of internal pressure, psi
 d = inside diameter of the pipe, inches
 t = thickness of the pipe, inches.

Another set of expressions for maximum stresses due to internal pressure is given by Blair (14) as:

$$\sigma_{\ell} = \frac{pd^2}{D^2 - d^2} \quad \sigma_t = \frac{p(D^2 + d^2)}{D^2 - d^2} \quad \sigma_r = -p \quad (\text{A.2})$$

where D is the outside diameter. All other terms are the same as in Eq. A.1.

Various expressions for failure criteria under combined stresses have been proposed based on different theories of failures (15, 16, 17). Murphy stated that, according to available test data, Rankine's maximum normal stress theory is satisfactory for brittle cast iron (11).

The maximum normal stress in a pipe subjected to internal pressure is the transverse stress. The magnitude of this stress can be computed using Eqs. A.1 and A.2 or a widely used simplified formula given by Buston and Burrows (15):

$$\sigma_t = p (0.5 D/t - 0.4) \quad (\text{A.3})$$

This last equation gives the stress within one percent of that calculated by Eqs. A.2 for $D/t \geq 5$ which is considered as the entire useful range.

A.1.3 Thermal stresses in individual pipes The longitudinal stress in a straight pipe of uniform thickness due to uniform temperature change of the entire pipe is:

$$\sigma_l = \alpha E \Delta T$$

where:

α = coefficient of thermal expansion

Δt = temperature change

E = modulus of elasticity.

For the same pipe, the stress due to linear radial variation of temperature from the inside face to the outside face is given by Timoshenko (5) as

$$\sigma_t = \frac{\pm E\alpha(t_1 - t_2)}{2(1 - \nu)}$$

where ν is Poisson's ratio and t_1 and t_2 are the temperatures at the inside and outside surfaces of the pipe. For the above equation $\sigma_t = \sigma_l$ since no bending is involved. At the spigot end, $\sigma_l = 0$ and the transverse stress becomes:

$$\sigma_l = \frac{E\alpha(t_1 - t_2)}{2(1 - \nu)} \left(1 - \nu + \sqrt{\frac{1 - \nu^2}{3}} \right)$$

where,

E = modulus of elasticity, psi

α = coefficient of thermal expansion, in./in./°F

$t_1 - t_2$ = temperature difference.

Parkus considered the case of hot liquid flowing steadily through a pipe and transferring heat to the surrounding walls (17). By equating the amount of heat lost by the liquid to the amount of heat conducted from the wall into the pipes, he derived expressions for thermal stresses in the pipe for this case.

Mendelson and Manson (18) presented a method of computing thermal stresses in hollow cylinders due to sudden and rapid changes in temperature. This method makes use of polynomial approximations to find the temperature distributions.

A.1.4 Earth loading of buried pipes Extensive series of theoretical and experimental investigations of the loads imposed on buried pipes under various field installations was conducted by Professor A. Marston of Iowa State University (19, 20). This work was continued by M. G. Spangler,

W. J. Schlick, and others (2-4, 21, 22). The three main classes of conduits were classified as (2): 1) ditch conduit, 2) positive projecting conduit, and 3) negative projecting conduit. A ditch conduit is defined as one which is installed in a relatively narrow ditch dug in undisturbed soil and which is then covered with earth backfill. A positive projecting conduit is one which is installed in a shallow bedding with its top projecting above the surface of the natural ground and which is then covered with an embankment. A negative projecting conduit is one which is installed in a narrow and shallow ditch with its top at an elevation below the natural ground surface and which is then covered with an embankment.

The maximum loads on ditch conduits is given by:

$$W_c = C_d \gamma B_d^2 \quad (\text{A.4})$$

where:

W_c = load on conduit, pounds per linear foot

γ = unit weight (wet density) of filling material,
pounds per cubic foot

B_d = horizontal width of ditch at top of conduit, feet

C_d = load coefficient for ditch conduits. This coefficient can be evaluated from Fig. 24-3 of Reference 2.

The maximum load on a positive projecting conduit is given by 2:

$$W_c = C_c \gamma B_c^2 \quad (\text{A.5})$$

where:

W_c and γ are as given above

B_c = outside width of conduit, feet

C_c = load coefficient for positive projecting conduits. This coefficient is obtained from Fig. 24-8 of Reference 2.

For a negative projecting conduit, the maximum load is given by (2):

$$W_c = C_n \gamma B_c^2 \quad (\text{A.6})$$

where:

W_c , γ , and B_d are as given above

C_n = load coefficient for negative projecting conduits.

This coefficient is obtained from Figs. 24-10 to 24-13 of Reference 2.

Equation A.4 indicates that the load on a ditch conduit is a function of the width of the ditch in which the conduit is placed; that is, the wider the ditch, the greater is the load on a conduit in it. However, there is a limiting width called the transition width beyond which this principle does not apply. In a ditch which is very wide relative to the conduit, the sides of the ditch will be far enough away from the conduit that they have no affect on the magnitude of the load on the conduit. The load on the conduit is considered constant for all width equal or greater than the transition width.

Studies by Schlick (18) on the effect of the width of ditch on the load transmitted to a rigid conduit indicates that

it is safe to calculate the load by means of the ditch-conduit formula for all widths of ditch below that which gives a load equal to the load indicated by Eq. A.5 for a positive projecting conduit. In other words, as the width of the ditch increases, other factors remaining constant, the load on a rigid conduit increase in accordance with the theory for a ditch conduit until it equals the load determined by the theory for a projecting conduit. For greater widths, the load remains constant regardless of the width of the ditch.

Figure 24-15 of Reference 2 gives values of the ratio of width of ditch to width of conduit, at which the loads on a rigid conduit are equal by both the ditch conduit theory and the projecting conduit theory. For values of this ratio less than those given in the figure, the load on a conduit may be determined by the ditch conduit theory. For greater values of this ratio, use the projecting conduit theory.

A.1.5 Bending and torsional stresses Bending stresses
in pipes can be calculated from

$$\sigma = Mc/I$$

and the torsional stresses can be calculated from

$$r = \Gamma r/2I$$

where:

M = moment in the pipe, in-lbs.

Γ = torque in the pipe, in-lbs.

c = one half the depth of the pipes, inches

r = radius of the pipe, inches

I = moment of inertia of the pipe, inch^4 .

Based on the above equations, charts have been developed to facilitate the design of pipes (23, 24). However, no consideration was given to buckling failure of such pipes nor the effect of the length of such pipes on the torsional strength. Fevre (25) summarized the theory of failure in torsion and presented formulas derived by other authors for the maximum shearing stress due to torsion. His comparison of test results with the theories showed that presently available theories do not agree with test results. Conclusions from the test data were:

1. Torsional strength of tubes with low D/t ratios is unaffected by the change in length; where D is the diameter, and t is the thickness.
2. Torsional strength of tubes with relatively high D/t ratio is dependent on the L/D ratio of the tube where L is the length of tube.
3. The value of D/t at which the length becomes a factor of torsional strength varies with the material properties. That is, length becomes a parameter at decreasing value of D/t with increasing ultimate tensile stress of the tube material.

A.1.6 Stresses in joints and fittings Fittings in a general pipe system can be classified into three categories, namely: 1) bends-- for directional changes, 2) branches--

for gathering and distributing the material inside the piping system, and 3) special fittings-- such as reducers, increasers, traps, etc.

The general beam theory cannot be used directly to determine stresses in bends since they act as curved beams. Two methods have been used to analyze these bends. The first is called the flexibility method and the second is called the intensification method. By solving for the deflection or stresses by the ordinary beam theory and modifying the result by either of the above two methods, a good approximation of the stress can be obtained (16, 26).

The branch is inherently a point of weakness in pipe systems and gives rise to severe stress intensification because of the abrupt changes in geometry. To formulate a theoretical solution for the stresses in a branch is a very difficult if not an impossible task. Based on test results in unreinforced branches, Abraham and McGlure (27) concluded that the region of high stress is a very narrow one near the intersection, and that the ratio of the high stress to nominal stress vary from two to five for internal pressure and one to twelve for bending. The stress distribution in a Tee junction of thick pipes was studied by Fessler and Lewin (28).

Hub and spigot joints, screwed joints, and flanged joints, are some of the common joints used in a general pipe system. In cast iron soil pipe systems, hub and spigot joints are used almost exclusively with the spigot either beaded or

plain. Much work has been done on stresses in joints exclusive of hub and spigot types. However, the work of Prior (29) does deal with stresses at a hub and spigot joint caulked with soft lead. Based on test results, Prior suggested the formula:

$$P = \frac{3800}{D + 6} - 40$$

where:

P = maximum internal pressure in psi causing incipient failure

D = nominal diameter of the pipe in inches.

A.1.7 Structural analysis of pipe systems The piping system constitutes a structural system which is usually highly statically indeterminate. In order to determine stresses in various parts of a piping system accurately, it is necessary to carry out the statically indeterminate analysis of the individual components. Such an analysis assumes that the material is linearly elastic, deformations are small, and effects of axial and shearing forces are negligible. Most of the analysis procedures written so far are for stresses due to thermal expansion.

One method of analysis is the moment-area approach (16, 30). This method used the flexibility and stress intensification methods to determine the stresses. However, it gives greater moments and forces than those obtained experimentally. Another approach is the elastic center

method (31). This approach can also be modified by the flexibility and intensification methods in it (32). Other approaches used in the analysis of the piping system are moment distribution (33), slope deflection (34), and column analogy (35).

A highly accurate method using Castigliano's Energy approach was developed by the Kellogg Company (16) with supplementary charts to simplify the calculations.

A.1.8 Thicknesses, residual stresses, and supports

Most of the literature available on thickness requirements take into consideration pressurized or nonpressurized pipes with external soil loadings. Forces include (36): water hammer, internal static pressure, load from the backfill, and load and impact from passing vehicles. A similar procedure is applied for clay pipes (37).

Residual stresses in pipes are due to differential cooling of different areas of the pipes. These residual stresses can be best measured by bonding electric-resistance strain gages then taking the difference between the initial and the stress relieved states. Another method of measuring residual stresses is by using an optical-interferometer device (38).

The locations and types of pipeline supports must be considered when an analysis is made of a piping system. The most comprehensive coverage of piping hangers is that given by Gascoyne (39). The use of pipe supports is covered in

detail with tables given for the determination of support spacing. Diagrams and photographs of various types of pipe supports are presented.

Rigid hanger problems were treated by Brock (40). In this discussion, the author assumes that at the points of support, the following conditions prevail:

1. The hangers exert no axial force on the pipe.
2. The hangers exert no moment on the pipe.
3. Deflection of the pipe support is completely prevented.

A.2 Survey of Performance of Cast Iron Soil Pipe and Fittings

A questionnaire concerning breakage of cast iron soil pipes and fittings was mailed to inspectors, contractors and wholesalers throughout the United States to obtain information on the behavior of SV and XH weight pipes and fittings. The information desired was in the following areas: 1) Handling, which includes transit, storage, loading and unloading, 2) Construction of joints which includes yarning, leading, caulking, aligning and cutting, and 3) Performance during the service life such as freezing, heating, inadequate pipe supports, building movements, corrosion, improper bedding, etc. The format of the questionnaire is shown in Fig. A.1.

The turnout was 29%. The percent of those observing breakage for the various areas indicated above is shown in Fig. A.2. This figure shows that more than 50% of those questioned observed breakage in the following five areas: transit, loading and unloading, caulking, cutting, and improper

Fig. A.1. Questionnaire

IOWA STATE UNIVERSITY
OF SCIENCE AND TECHNOLOGY
Ames, Iowa 50010

ENGINEERING RESEARCH INSTITUTE

October 25, 1965

Dear Sir:

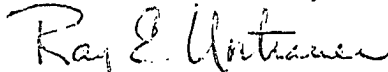
The Structural Research Laboratory of the Iowa Engineering Experiment Station is presently engaged in an extensive research project sponsored by the Cast Iron Soil Pipe Institute. The objective is to determine the structural requirements for the pipe and fittings to perform satisfactorily in both home and commercial installations. In particular, the object is to determine a single weight of pipe (one thickness for each size) that will perform satisfactorily under all conditions.

It is expected that this research effort will result in pipe with more uniform and realistic factors of safety with regard to the handling, construction, and operational stresses in the pipe and fittings. Furthermore, it is anticipated that this research will result in a more economical sanitary plumbing system to both home and commercial users.

One of the topics in our Research Plan is to make a survey of selected agencies concerning cast iron soil pipe and fitting performance. The results of this survey will help us in our planning of the tests and undoubtedly will benefit the general public. Therefore, please have your field superintendent fill out the enclosed questionnaires and return one copy in the enclosed self-addressed stamped envelope. The second copy you may wish to keep in order to compare your observations with the results of the survey. At the completion of this survey, we will send the results to all those requesting them by marking the appropriate box on the questionnaire.

I wish to thank you in advance for helping us in a research project that will undoubtedly benefit both the public and industry.

Sincerely yours,



Ray E. Untrauer
Professor in Charge
Structural Engineering

REU:lm

SURVEY OF CAST IRON SOIL PIPE PERFORMANCE

Instructions: Mark an X in squares at right according to your answer. Please note that markings are asked for both weights of cast iron pipe (SV and XH) for each item. For example, suppose that you have observed cracks in the spigot end of a pipe caused by handling, in transit, and that these were observed seldom in SV pipe and often in XH pipe. You would then place an X in the SV row under yes, seldom and spigot. In the XH row, you would place an X under yes, often and spigot.

1. Have you observed breakage or cracking in pipe and fittings due to the following causes:	If yes, check appropriate boxes below					
	Frequency			Location		
	Yes	No	Seldom	Often	Hub	Spigot Barrel
a) Handling						
1) In transit	SV					
	XH					
2) Storage	SV					
	XH					
3) Loading and unloading	SV					
	XH					
b) Making lead-oakum joint						
1) At time of yarning	SV					
	XH					
2) Pouring of lead	SV					
	XH					
3) Adjustment of alignments	SV					
	XH					
4) Caulking	SV					
	XH					
5) Cutting	SV					
	XH					

Fig. A.1. (Continued)

Yes No Seldom Often Hub Spigot Barrel

2. Have you observed breakage during life of pipe after construction due to following reasons:

- a) Freezing SV
XH
- b) Hot temperature of contents SV
XH
- c) Inadequate pipe supports SV
XH
- d) Building movements SV
XH
- e) Corrosion SV
XH
- f) Improper bedding, laying or backfilling SV
XH

3. Have you observed breakage during assembly of gasket type joints?

Yes No
SV
XH

4. Do you use the following cast

Frequency of
Total CISP Joints
Less Between Over
than 30% and 70%
Yes No 30% 70%

- a) Lead-oakum joint, extra heavy pipe & fitting
- b) Lead-oakum joint, service wt. pipe & fitting
- c) Gasket type joint, extra heavy pipe & fitting
- d) Gasket type joint, service wt. pipe & fitting
- e) no hub joint

Fig. A.1. (Continued)

5. If you wish to add additional information on your observations as to the performances and failures of cast iron soil pipe and fittings with either lead-oakum joints, facet type joints, or other type joints, please write your comments below. This will make the survey even more complete. Thank you.

(Use back of sheet if more space is needed.)

6. (OPTIONAL) Name and address of firm, city or agency that filled out this questionnaire.

7. Please check in box at right and fill in above address if you wish to receive the results of this survey.

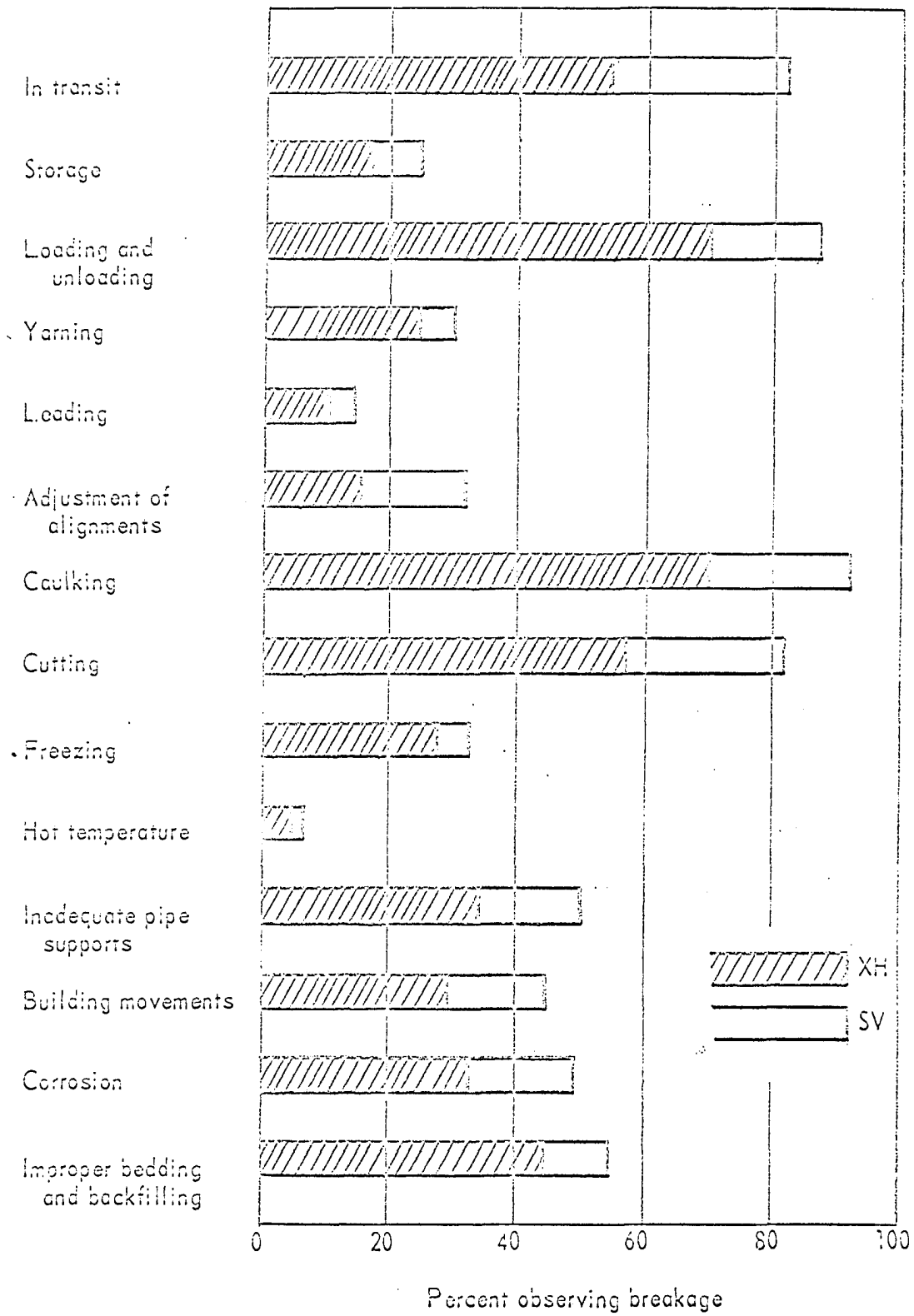


Fig. A.2. Percent observing breakage

bedding and backfilling. In the other areas 50% did not observe any breakage or if they did it did not affect the performance of the system.

More important in determining the performance of a system is the frequent breakage observed rather than breakage observed. Figure A.3 shows the percentage of those observed frequent breakage. Only four areas had more than 10% observed breakage and these are: transit, loading and unloading, caulking and cutting. 15% observed frequent breaking in transit, 24% observed frequent breaking in loading and unloading, 29% in caulking and 24% in cutting. These 4 areas are tabulated in Table A.1. This table shows that about 55% observed breakage in the hub while in transfer. The spigot had 35% observance and 11% observed breakage in the barrel. The percent of observed breakage in the loading and unloading process is very close to that of the transit process. In caulking, however, 29% of the observed frequent breakage was in the hub and only 1% in the spigot. In cutting, most of the breakage occurs in the barrel which is expected since cutting involves mostly the barrel. The table shows that most of the breakage occurs in the hub of the pipes and fittings. Apparently, performance of the barrel has been satisfactory in all usage except for cutting. A more detailed expansion of Table A.1 is shown in Table A.2 where the four areas of breakage are tabulated with respect of inspectors, contractors, and wholesalers.

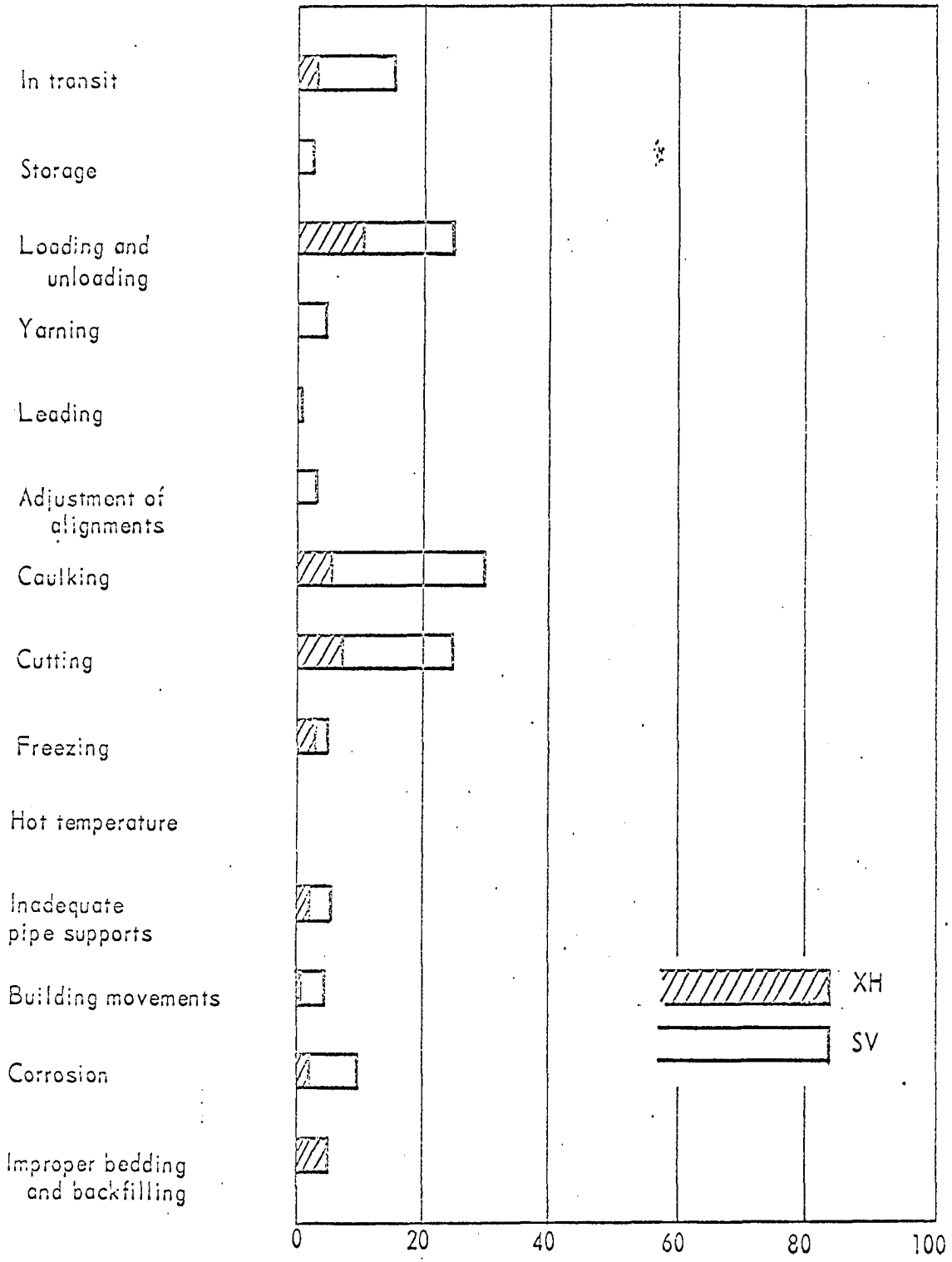


Fig. A.3. Percent observing frequent breakage

Table A.1. Areas in which frequent breakage was observed by more than 10%

Item		Percent Observing Frequent Breakage	Location of Breakage, %		
			Hub	Spigot	Barrel
In Transit	SV	15	51	35	14
	XH	3	57	34	9
Loading and Unloading	SV	24	55	30	15
	XH	10	60	30	10
Caulking	SV	29	99	1	0
	XH	6	99	1	0
Cutting	SV	24	6	22	72
	XH	7	6	24	70

Most of the comments from inspectors, contractors and wholesalers are shown in Section A.2.1. Some of the most interesting ones are:

1. It is desirable to have one weight.
2. Performance has been satisfactory for spun cast pipe of both SV and XH weights.
3. Most of the damage to pipe is done during shipping and handling.
4. More failures can be attributed to improper installation or poor workmanship than to quality of material.
5. Pipe which cracks during cutting is generally not uniform in thickness around its circumference.
6. Some manufacturers are not properly marking their pipe and fittings as to tell what grade or weight it is.

Table A.2. Comparison of observations made by inspectors, contractors and wholesalers

	Breakage Observed	Percent Making Observation				
		<u>Frequency</u>		<u>Location</u>		
		Seldom	Often	Hub	Spigot	Barrel
<u>In Transit, SV Weight</u>						
Inspectors	82	27	15	40	18	11
Contractors	78	60	15	52	36	12
Wholesalers	96	75	18	39	61	14
<u>In Transit, XH Weight</u>						
Inspectors	43	36	1	31	15	5
Contractors	58	51	5	39	24	7
Wholesalers	68	64	0	32	28	4
<u>Loading & Unloading, SV Weight</u>						
Inspectors	90	55	28	80	30	20
Contractors	85	54	20	60	32	15
Wholesalers	90	52	28	38	59	17
<u>Loading & Unloading, XH Weight</u>						
Inspectors	70	56	6	50	20	11
Contractors	71	51	13	54	24	7
Wholesalers	72	60	8	28	44	4
<u>Caulking, SV Weight</u>						
Inspectors	98	54	36	81	0	0
Contractors	93	57	25	72	1	0
Wholesalers	62	48	14	52	5	0

Table A.2. (Continued)

	Breakage Observed	Percent Making Observation				
		<u>Frequency</u>		<u>Location</u>		
		Seldom	Often	Hub	Spigot	Barrel
		<u>Caulking, XH Weight</u>				
Inspectors	74	59	6	59	0	0
Contractors	71	57	7	55	2	0
Wholesalers	52	52	0	48	0	0
		<u>Cutting, SV Weight</u>				
Inspectors	83	45	27	4	15	62
Contractors	82	49	22	5	17	46
Wholesalers	77	50	27	9	14	50
		<u>Cutting, XH Weight</u>				
Inspectors	55	44	6	1	16	38
Contractors	57	42	7	3	10	34
Wholesalers	63	53	11	16	11	37

7. A noticeable increase of breakage is occurring on the spigot and during transit due to increased demand for plain end, ten ft. lengths.
8. In bakeries, bars, and grills, the bottom of the horizontal pipe is corroded away.
9. Since the use of detergents, there has been an increase in corrosion in the barrel which in some cases required replacement of the line.

A.2.1 Comments from inspectors, contractors and wholesalers

A.2.1.1 Comments from City Plumbing Inspectors

1. Our city plumbing code allows only extra heavy pipe and fittings and lead-oakum joints.
2. Performance and longevity of cast iron pipe and fittings have been excellent in this city (Lawrence, Mass.). The few cases of failure (corrosion) were due to improper venting or no vent at all, or its use where waste effluent was highly corrosive.
3. I found in personal use of XH soil pipe that it cannot be cut with a hammer and chisel. A soil pipe cutter has to be used.
4. We allow the use of SV pipe for pipe and fittings for vent lines only.
5. Industry should stress more on proper laying, bedding and backfilling. Gasket type--closer tolerances of hub to gasket to spigot of pipe and fittings. Mark spigot end for insertion depth. Standardization of dimensions for all manufacturers (Ty Seal, Duo Tite).
6. It is my belief that cast iron drainage is the most desirable and permanent pipe of today. Do not use gasket type joints or no hub joints.
7. The following answers are from the Plumbing Inspection Departments' observations and may not reflect a true analysis, since many of the causes contained in your questionnaire may, in fact, be problems but usually corrected prior to an inspection of this department.

Our department has found the performance of CISP to be quite adequate. This is especially true of the new spun pipe with its uniform wall thickness.

Workmanship, as in any type of installation, is of great importance.

8. SV not allowed to be used in any construction whatsoever here (Portland, Maine).
9. The increased demand for plain end, ten foot length of gasket type cast iron pipe, a noticeable increase of breakage is occurring on the plain end in transit.
10. At this time, the state Exam's of Plumbers are formulating a uniform code gasket type pipe, has not been included in the Code.
11. Gasket type joints not permitted.
12. No trouble with lead-oakum XH pipe and fittings. We do not use SV cast iron pipe, only XH cast iron pipe.
13. We do not use SV pipe.
14. Have observed occasional breakage of barrel of SV pipe when using gaskets, especially 6" size on up.
15. Cast iron failures have been very noticeable on bar waste drainage lines.
16. I have observed that cast iron pipe, lead-oakum joints, when installed in a horizontal position when used for hot water wastes from commercial dishwashers and the like will invariably leak at the joints.
17. The Plumbing Code of the city of St. Louis permits the use of gasket type joints. However, only a very few installations have been made using this product. I would like to state that, in my opinion, I feel that the proposition of all foundaries making only one weight of cast iron pipe would certainly be a great advantage to the plumbing industry as a whole and would be in the best interest of public health and safety.
18. Even during our recent earthquake, there was not, to my knowledge, any breakage of cast iron pipe, except where the ground gave way causing the pipe to break from shear weight above (Alaska).

19. Gasket type joints were allowed this past year on written request for each installation of building drains and stacks. Permitted by Plumbing Code for house sewers and storm drains. Would like to see a standardized gasket and one weight of cast iron soil pipe.
20. The city of Peoria Plumbing Code requires XH soil pipe. With the modern manufacturing methods, the wall thickness is more uniform. I believe there is a need to manufacture a one wall thickness soil pipe. Your project is very worthwhile.

I have not experienced any problems with soil pipe, those that do arise are a result of handling from the factory to the job. Another contributing cause is the untrained mechanic. I have observed many mechanics liking to make two pours on a lead-oakum joint. This is for alignment of fittings, etc. by driving the first pour before pouring and caulking the last results in more broken hubs. Compare this with the joint made with the joint runner.

We also use the gasket type joint, (Ty Seal, Dualite). This gasket is not standardized and some plumbers have problems assembling this type of joint; they cut off the rear compression ring. With the proper assembled joint, we have had joints separate during a water test when the pipe is not restrained.

No hub soil pipe is used in Peoria. This would add many problems for the plumbing inspector.

21. Gaskets are not practical for closet bends because they do not provide a sufficiently rigid joint. Gaskets in 8" and larger sizes give problems in assembly.
22. I think it is a good idea to study the possibility of standardizing of one weight of cast iron soil pipe.
23. Gasket type joints permitted only on building sewers. Less than 1% used in Omaha.
24. All drain or soil pipes beneath or above basement floor must be XH cast iron pipe with leaded and caulked joints.
25. Inadequate pipe supports tend to make caulked joints pull apart.

26. Now that both XH and SV cast iron pipe are super spun, we seldom have breakage unless it's just plain carelessness in loading and unloading. Gasket type joints are used in house sewers only and roof drains. Most of the contractors use white oakum and only yarn it in, therefore, there is less breakage by caulking. XH cast iron is required for buildings of over 3 stories in height and under streets and sewers.
27. SV pipe that cracked while cutting was found not to be uniform in thickness around its circumference.
28. We use only XH cast iron soil and waste pipe in the city of Bethlehem; population approximately 76,000, 54 master plumbers registered. This survey includes the findings of 36 of the 54.
29. City Code specifies XH soil pipe with caulked joints--can use type L copper up to 2" only.
30. In the city of Allentown, Pa., we do not use any hub joint cast iron pipe. Approximately 90% of the installations are lead-oakum; 10% gasket type joints.
31. I observed little trouble with cast iron soil pipe and fittings in use of lead-oakum joints. Many gasket type joints used outside of the building do not test tight because of difference in tolerances of pipe diameter and gasket material. Lead-oakum is used to replace the gasket if it does not fit, making extra work and some breakage. SV cast iron pipe is not approved in our ordinance.
32. We are changing our ordinance to permit the use of SV pipe on both waste and vent piping.
33. Some manufacturers are not properly marking their pipe and fittings as to tell what grade or weight it is.
34. There is a marked carelessness on the part of the journeymen in the supporting of gasket type joints and no hub joint systems.
35. In my opinion, the biggest percentage of defects in cast iron pipe is caused in shipping and handling.

36. Gasket type joints used mostly on water service here--not too much on the sanitary. Our code calls for the use of XH soil pipe underground; hardly any trouble with this.
37. Our plumbing code only permits XH soil pipe and fittings with oakum and 1" minimum lead poured joints caulked inside and out. You may use either regular tarred oakum or white oakum.
38. Gentlemen--I am in complete agreement on one weight soil pipe and fittings. XH cast iron soil pipe and fittings would greatly benefit the owners and contractors - gasket joints are not permitted or allowed.
39. We have had some trouble with thick and thin spun pipe. I am very much in favor of one weight soil pipe.
40. Code does not permit gasket type or other type joints, only lead-oakum XH cast iron inside building, SV on outside sewer lines.
41. These new gasket type joints and no hub joints have recently been approved and consequently have had little experience with this type of joint. For this reason it is difficult to make a comparison.
42. We get a good grade of cast iron pipe in this area. We seldom find any trouble with the breakage or cracking of the pipe.
- 43 and
44. Inasmuch as we are a plumbing installation inspection department, we have little opportunity to observe breakage in transit, storage, loading and unloading. However, we have noted appreciable amounts of breaking during installation. We find that both SV and XH are satisfactory for use as drainage and vent on plumbing installations.
45. It is my opinion that SV pipe used with lead-oakum and caulked has proved itself to be the best joint to be used in any plumbing installation. Gasket type joints make a good installation on outside building sewers. XH pipe should be used underground or in any building 3 stories or more.

46. Gasket type joints are permitted underground only.
47. Our problem areas are caused by unstable bay bottom fill-some of high organic and others of high clay content. Where certain soil conditions exist, graphitic corrosion is often found.
48. In the city of Wilmington we use only XH soil pipe. Very good success.
49. Gasket joint is not allowed by city code.
50. I have had no opportunity to observe gasket type joints or the no hub joint.
51. No gasket type joints for cast iron soil pipe has been installed in this city.
52. Gasket type joint has not been used in Montgomery.
53. When soil pipe freezes, it has not been installed in accordance with our code.
54. Gasket type joint is not approved.
55. Caulked joints bleed. No hub joint bands strip before maximum torque is applied. No hub must be supported at each joint and fitting when in a horizontal position.
56. Cast iron pipe and fittings have been used in Durham in the house sewer and drain for about thirty years. We have found some to be satisfactory and above par to other materials.
57. In my 20 years experience, the amount of cast iron breakage has been relatively small, especially immediately following WW II.
58. We have no failure of cast iron pipe.
59. City code pg. 84, P11.133 Underground Piping Within Buildings. All drains within buildings, when underground, shall be of cast iron soil pipe, either SV, centrifugally spun, or XH.
60. Information submitted is limited to our knowledge gained from our inspection of plumbing installations as the local code enforcement agency.

61. Gasket and no hub not approved for use in our area.
62. Frequency of breakage in transit is hard to determine. Contractor usually returns pipe and we know nothing of it.
63. (e) of Part 2: only on discharge side of septic tanks.
64. More failures can be laid to improper installation or poor workmanship than to quality of material.
65. It is our observation that gasket type joints are presenting less problems and allow more flexibility in installation.
66. Lack of rigidness in vertical pipes causes pipe to be out of walls with the gasket type joint and not as self-supporting as lead-oakum. Less amount of leaks with gasket than with lead.
67. Hanging is big problem with no hub.
68. We have found cracked hubs and barrels occasionally have hairline cracks filled with tar which shows up in testing and caulking of the joints. Also sand hoes in fittings which were filled with tar.
69. SV cast iron pipe and fittings are permitted in any type of building in the waste and vent system regardless of size, either under or above ground. For this reason, the vast majority of cast iron pipe and fittings used in Seattle and King county are SV. This would obviously have a definite reflection on the above answers.

A.2.1.2 Comments from contractors

1. In our 52 years experience, we find the XH cast iron soil pipe is most durable (with lead-oakum joints) for use underground or inside work.
2. We have experienced much failure in the top of horizontal soil pipe after approximately 40 years of service. This refers to pipe in basement above floor.
3. We have found as much as 15% of our soil pipe poorly cast. The inside wall was not concentric with the outside wall and when cutting with a chisel and hammer, it splits on the thin wall badly.

4. We do not use SV pipe, and as of this date, never used gasket type joints.
5. Our work is controlled by codes and specifications and limits pipe to XH cast iron and joints to about 95% lead-oakum.
6. The "new" gasket type joint has just been introduced in this area and approved by our local code, but we have not used it yet.
7. Fittings are shipped with pin holes in them. Quality of both pipe and fittings is getting poorer.
8. Very few gasket type joints have been used in the Delaware area. In Wilmington and New Castle county, standard cast iron pipe is not permitted.
9. Sand holes and irregular castings, mainly in fittings, cause us the most trouble.
10. In above ground installations, except for New York City, which is behind times, cast iron pipe and fittings are being replaced by copper tubing and fittings which are much more manageable and easier to install.
11. We use primarily gaskets on runs and branches are lead-oakum for stability. We use mostly XH cast iron pipe, but have seen SV and used small amounts. It does not have the feel of security when working with it that XH does.
12. We use cast iron soil pipe (XH) with lead-oakum exclusively from 3" diameter up, as we have found no corrosive effect after 40 years on most installations.
13. We have used XH cast iron pipe for many years and have had little or no trouble with it.
14. We find that in bakeries and bar and grills that the bottom of the horizontal pipe is eaten away.
15. I wish to say that we have always used lead-oakum joints, and over my 43 years in business, have found it extremely satisfactory. You will note I signed seldom on most questions asked because I have had very, very little trouble with either medium or XH cast iron soil pipe. As you probably

know, we are also using a lot of DWV copper tubing on our soil waste lines above ground.

16. Would suggest that numbers and letters be kept off face of hub.
17. With spun soil pipe, there are fewer burrs and honey-combing of the pipe.
18. I have found SV weight pipe to vary in inside diameter and weight, especially 2" and 3" pipe. 3" x 10 singles are crooked, and 3" x 10 doubles are very heavy and undersize in inside diameter.
19. Maintain a single standard?
20. We have never used either "no hub" or "gasket type" soil pipe, however, some of it is now coming into area. We use almost all XH pipe and have had excellent results. In 25 years of business, no failures.
21. We have used the lead-oakum joints only and have had satisfactory service from these.
22. Believe we should have one weight of cast iron soil pipe only. Between SV and XH, a little heavier than SV.
23. We have always used lead-oakum joints on all types of work but the gasket type joint appears to be a satisfactory method of joining soil pipe and fittings.
24. Gasket joints are very good.
25. I am for one standard soil pipe to be used in all construction for use with lead or gaskets at the option of the installer. Today the quality is very good.
26. Most breakage is caused by the variance in wall thickness when cutting. Casting is not even. Sand holes in the last 5 or 6 years are frequent.
27. We have found the gasket joint pipe very good for underground work. Above ground or stacking no good where the joint will twist. It tests very good. Our local code calls for XH only.

28. Uneven thickness of pipe, thick on one side and thin on the other, will crack at times even when using a wheeler cutter. Uneven diameter of pipe, when using gasket type joints, sometimes will almost fall together and other times can hardly be forced together.
29. All in all, we have very little trouble with soil pipe and fittings.
30. We think the gasket type joint is a good improvement. We have not had occasion to use no hub, but will not hesitate when it is specified or when we can change the owner's mind.
31. I feel that the most of our breakage is due to rough handling while in transit. Also, we have at times received such inferior pipe that would have extremely thin walls in spots. These would break while attempting to cut the pipe.
32. Outside of handling roughly and poor workmanship, we have very little breakage; sometimes in remelting used lead, the plumber will get too much tin in the lead. This is hard and will crack hub when caulking.
33. Some soil pipe has sand holes in the pipe and fittings. SV soil pipe is not allowed in Minnesota.
34. My observation as to the performance or failure of the above has been that either lead-oakum or gasket type joints are very good if properly done. However, more joints can be made in a given time with the gasket type, so there is a labor saving element.
35. During the last 5 years, since the use of detergents, we have found much more corrosion on the barrel of soil pipe which in some cases requires replacement of the line.
36. Our experience with gasket type joints has not been too good. Had considerable leak trouble due to poor uniformity of hub casting. The groves inside of the hub were not cast clean.
37. Failures due to hot temperature occurred where steam power boilers, in which the boiler water had been treated, was introduced into the lines. Failures due to corrosion were noted where pipe received

waste from areas where oranges and lemons were processed.

38. I think this is the best idea that has come up in a long time. Keep up the good work.
39. The gasket type joint has just recently been approved in our vicinity, so we do not have too much experience with it but believe it has many advantages. Believe the greatest amount of breakage is caused by poor handling by shop workmen.
40. Gasket joint is usually more flexible.
41. We have experienced no trouble in approximately 30 years of use.
42. Standardize the industry to a good no lead-oakum joint. Make only XH pipe and fittings.
43. They should keep the bead on the spigot end, for pipe with cauling joints, the oakum gets through.
44. From some foundries, the soil pipe and fittings are still not uniform. Therefore, on gasket pipe and fittings, some gaskets work better than on others. Some of the hubs have little or no space for making the joints. The above is true of some foundries in our locality, but not all.
45. Too often there is not enough space between hub and spigot of XH pipe and fittings to make a good joint. Also, XH spigots will not fit in SV hubs.
46. Most of the problems I have indicated have been with cast pipe. On spun pipe, the only breakage that I have seen was in shipping.
47. Our experience has shown that 50% or more of breakage is due to uneven casting.
48. With all the new processes of making pipe, we still notice non-uniform walls in both XH and SV pipe. It was our understanding that the spinning process would eliminate this problem, however, we still feel it exists.
49. Cast iron pipe, both SV and XH, is too hard. Breaks or splits sometimes when cutting.

50. SV pipe is fine now that it is spun. The old cast pipe was too thin on one side.
51. With the use of a gasket type joint, we have found it to be a fast and non-leaking joint. It also will allow give and movement (limited) for building movement, etc.
52. We use lead-oakum joints above ground and gasket type below ground.
53. I think a one weight soil pipe for the entire industry would be good.
54. Breaks in barrel during cutting is caused by irregular thickness. Have noted on several occasions pin holes in fittings. Much labor is lost if this is noted after installation. We are primarily engaged in commercial and institutional work which is engineered and this is the reason why we use lead-oakum joints.
55. There is no substitute for cast iron pipe and fittings.
56. Most cast iron soil pipe comes cracked from rough handling by freight companies or wholesalers. This is probably caused by throwing fittings. We seldom ever have cracked joints when caulking unless it has been cracked before.
57. We strongly believe that today's SV pipe and fittings with caulked or gasket type joints is, due to manufacturing improvements in the past few years, a very satisfactory material for all uses where soil pipe is required.
58. I have replaced cast iron soil stocks in buildings that you could push your thumb through. Whether it was caused by sewer gas or rust I couldn't say.
59. Most failures on barrel due to cutting is caused by imperfect molding (thin and thick sides or walls). Also, some with hubs broken in transit and unloading or handling.
60. Have just started using gasket type joints. Seems to be okay and men like it except when wet and muddy.

61. Hubs and spigots are not uniform in size for easy installation. 95% of our work is with the Navy who specifies XH soil, lead joints only.
62. I believe we should continue to use cast iron soil pipe, a little better grade than SV perhaps.
63. Sand holes. Poor casting.
64. We prefer the spun pipe as the wall thickness is more uniform. We don't like gasket type. In our residential work, we use no hub practically exclusively.
65. Some brands of soil pipes are uneven in wall thickness and alignment.
66. I have observed big cracks and breaks on cast iron SV pipe which is probably caused by sewer gas and not by corrosion or water.
67. Would like to see code changed to use SV for all usage with gasket type joint allowed inside building. Present code requires use of gasket joints on sewers only. Your work should be with city departments to get code changed to allow gasket type joining on all plumbing work.

A.2.1.3 Comments from wholesalers

1. We have only handled the lead-oakum type. From ads we believe the gasket type is okay.
2. We have much less problems with spun pipe.
3. We use an equal amount of SV and XH pipe depending on boro codes, but find that either weight will outlast the normal life of the building.
4. If all our materials gave us as little trouble as our cast iron soil pipes, we would be very fortunate.
5. We are a supply house where plumbers buy soil pipe. All items listed are negligible with but one exception - that is the cutting of soil pipe. Plumbers are having untold problems when cutting pipe. Both SV and XH. An even cut is impossible.

6. Have sold little gasket type pipe. However, we have experienced no difficulty with the product. Have never sold, nor stocked, no hub pipe or fittings.
7. More uniform sizing in the wall of the soil pipe when spinning or casting.
8. Don't think plastic insert gasket should be ruled out of specifications. Most have been successful.
9. I believe a better inspection problem on the pipe and fitting would help cut cost of installation due to sand holes and other material defects. A lot of pipe is not uniform all the way around.
10. Gasket joint should be uniformly sized to all to make acceptable for stocking and use by trades.
11. Cannot give true report on gasket type joint as it has not been approved generally in Montana.
12. We are still of the opinion that SV pipe and fittings should have beaded ends for lead-oakum joint. Plain end pipe and fittings create more breakage in handling.
13. In our opinion, the no hub joint is a distinct improvement over either the lead-oakum or gasket types on above ground piping. Experience with gasket type and SV lead-oakum types is not conclusive at this time.

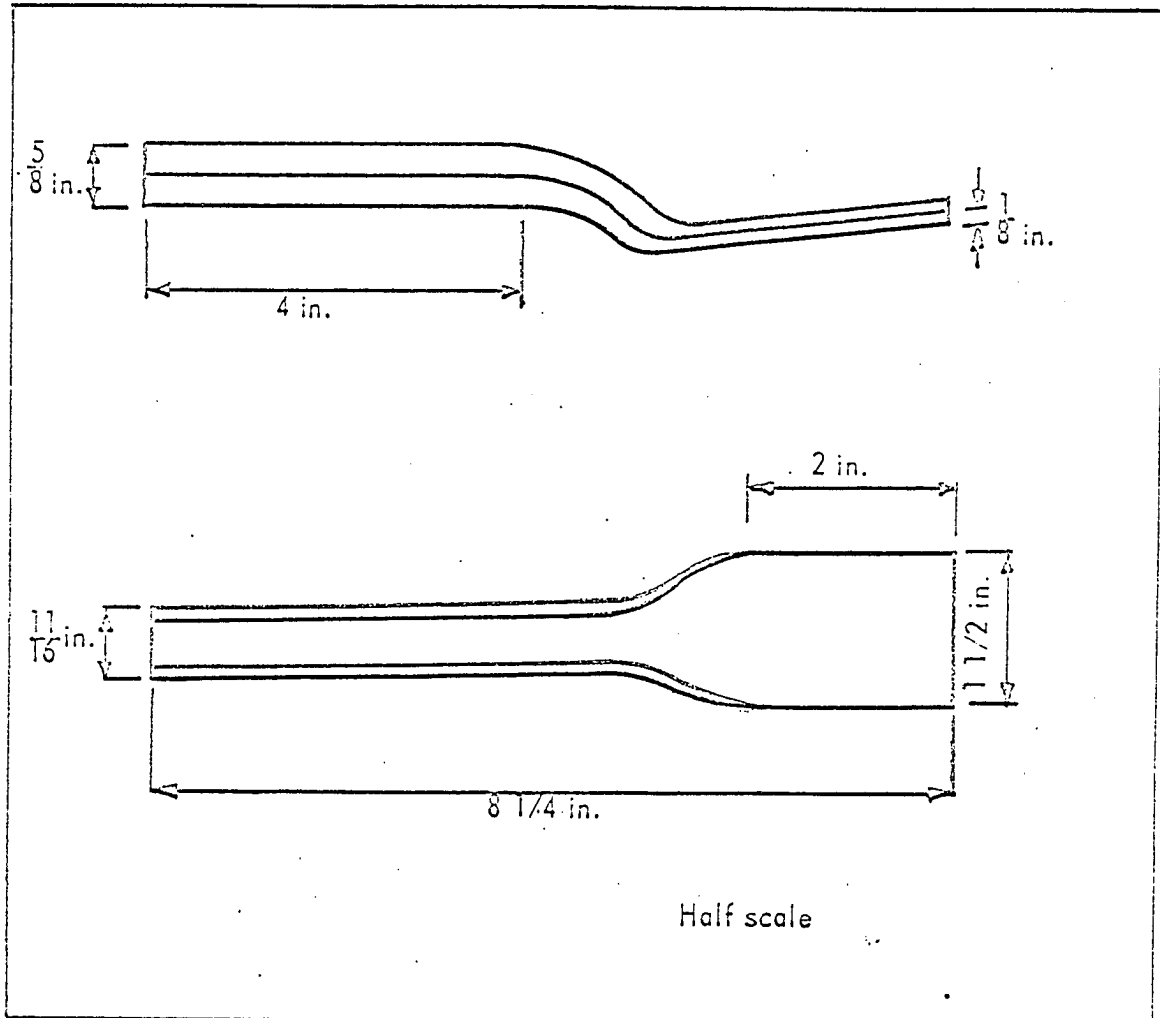


Fig. A.4. Ordinary yarning iron

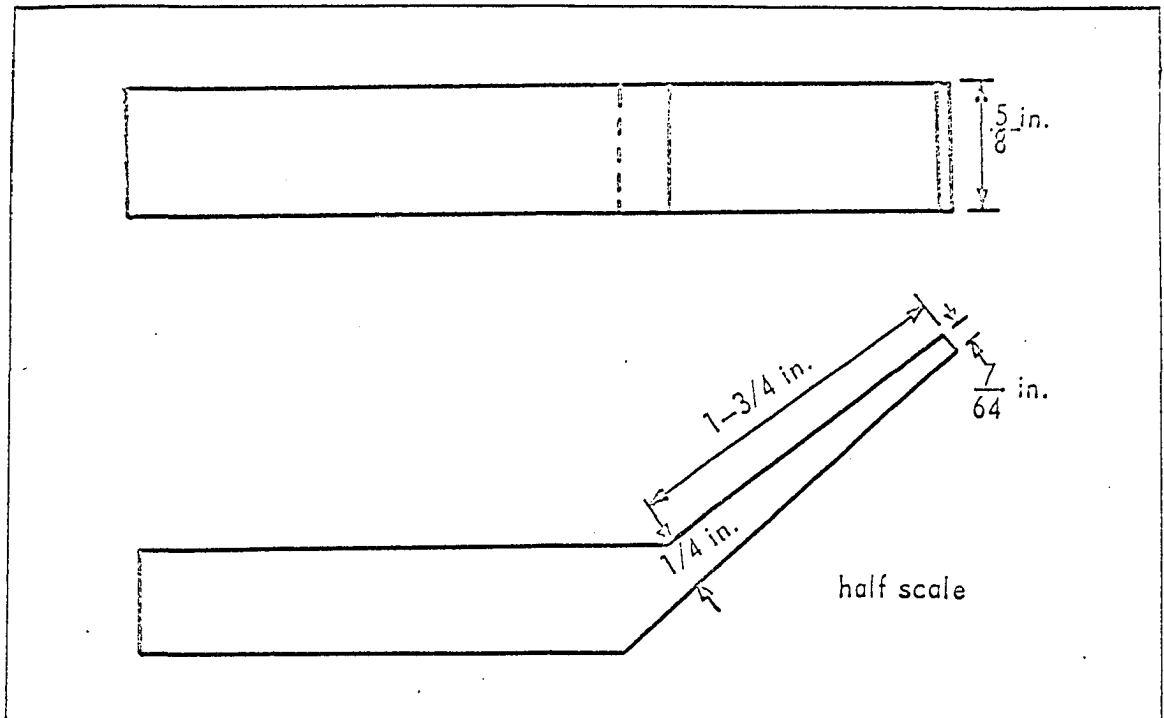


Fig. A.5. Small yarning iron

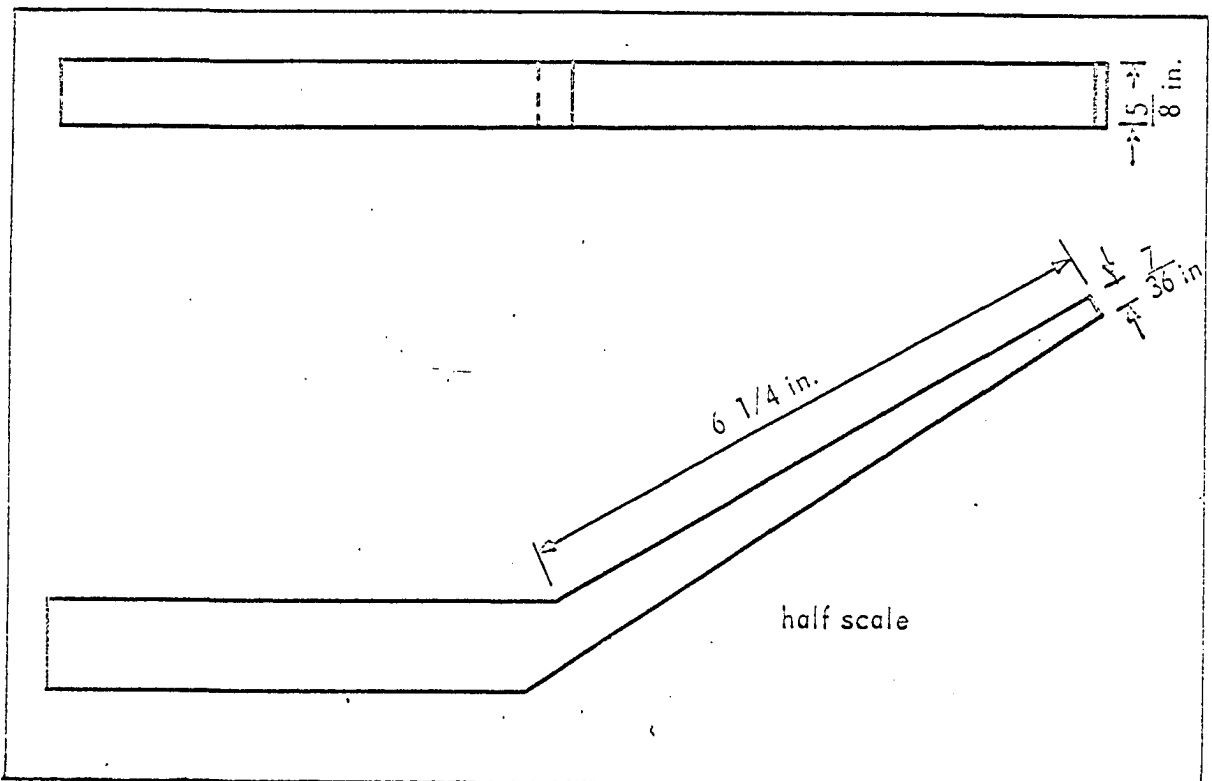


Fig. A.6. Long yarning iron

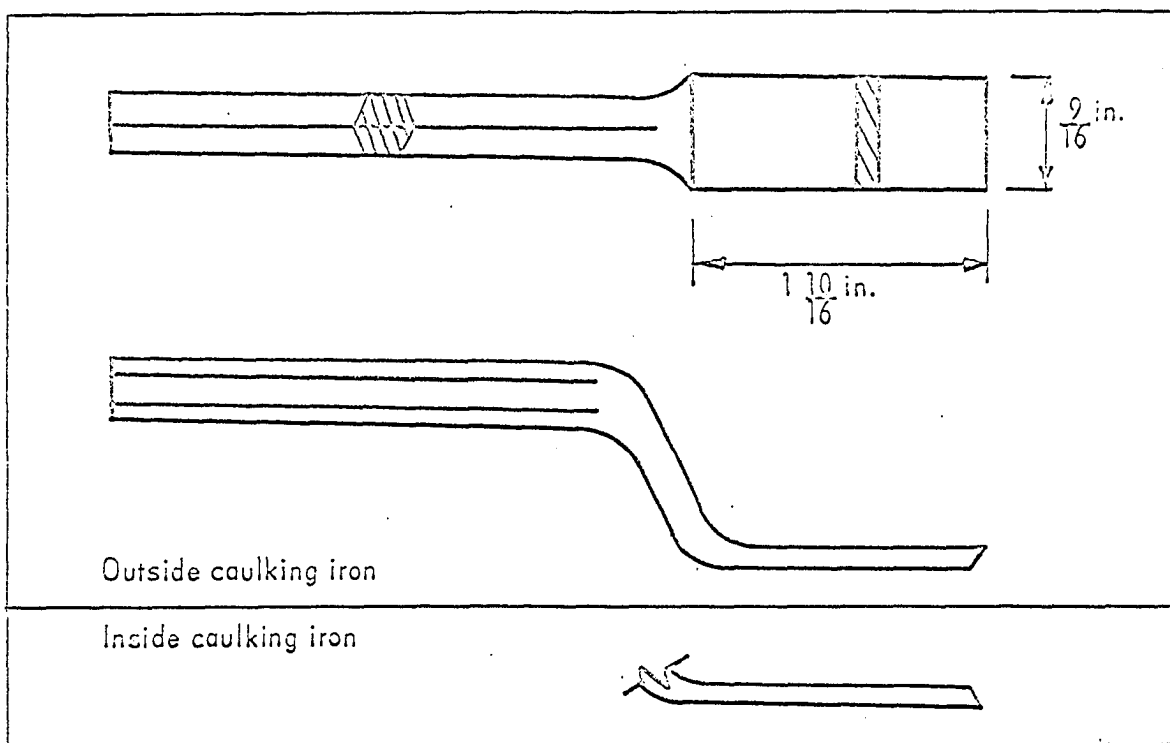


Fig. A. 7. Ordinary caulking iron

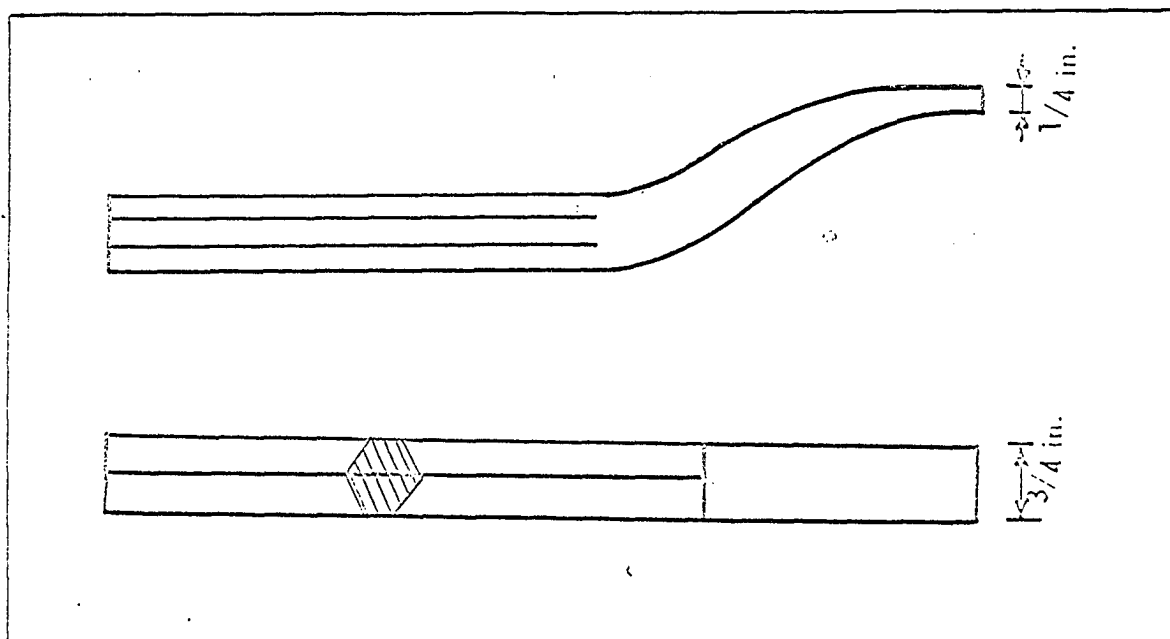


Fig. A.8. Heavy caulking iron

14. APPENDIX B. MAIN DIMENSIONS OF THE PIPES USED AND
HUB CONFIGURATIONS OF VARIOUS BRANDS

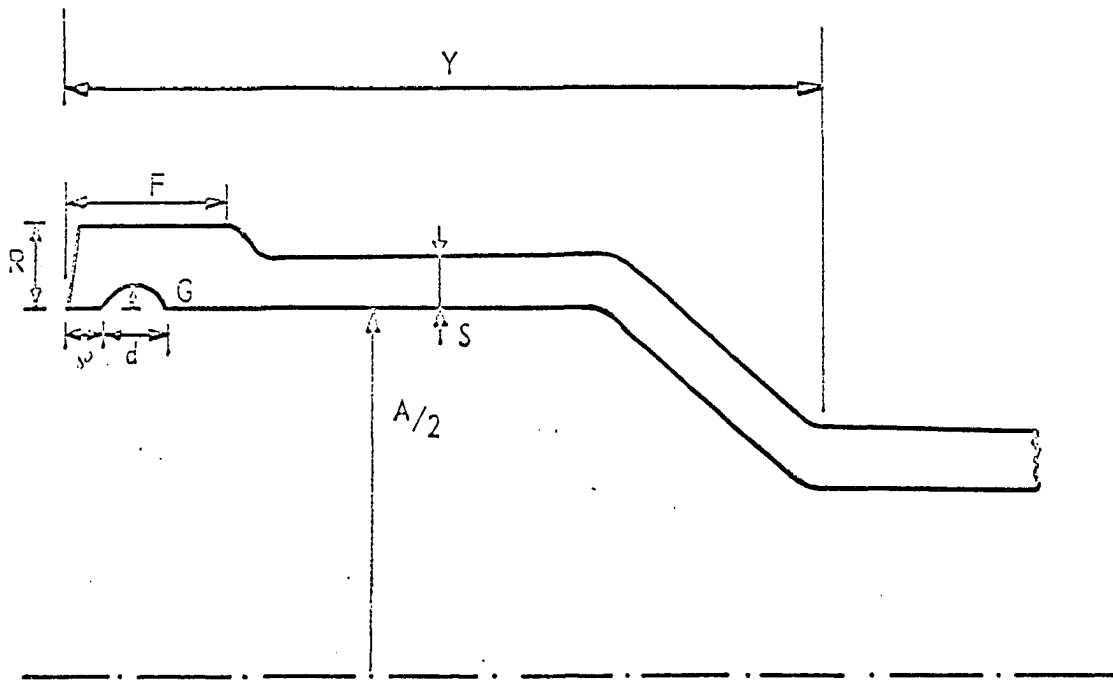


Fig. B.1. Main dimensions of pipes

Table B.1. Main dimensions of test specimens, inches

Specimen Number	F	Y	R	p	d	S	G	A
4A4*	1.00	3.44	0.44	0.31	0.31	0.28	0.14	5.44
4A17	1.06	3.31	0.48	0.34	0.47	0.22	0.16	5.22
4A18	1.00	3.25	0.47	0.31	0.38	0.31	0.11	5.08
4B2*	1.00	3.50	0.45	0.25	0.41	0.32	0.13	5.20
4B14	0.75	3.50	0.41	0.16	0.50	0.27	0.11	4.99
4C6*	0.44	3.81	0.47	0.13	0.53	0.40	0.12	5.26
4C18	0.53	3.44	0.40	0.16	0.53	0.34	0.15	4.91
4D2*	0.94	3.38	0.49	0.16	0.50	0.32	0.11	5.27
4D5*	0.94	3.38	0.52	0.19	0.47	0.36	0.11	5.25
4D11*	0.88	3.22	0.54	0.19	0.44	0.35	0.10	4.99
4E5*	1.00	3.44	0.46	0.31	0.50	0.29	0.10	5.23
4E14*	0.94	3.25	0.41	0.28	0.44	0.18	0.10	5.02
4F1	0.78	3.41	0.55	0.19	0.50	0.42	0.15	5.22
4F8*	0.88	3.44	0.46	0.31	0.63	0.22	0.10	5.00
4F12	0.94	3.38	0.43	0.25	0.63	0.24	0.10	4.93
8A8	0.91	4.28	0.58	0.28	0.44	0.37	0.14	9.39
8B1*	0.81	4.28	0.63	0.41	0.41	0.44	0.10	9.41
8C2	0.56	5.16	0.69	0.34	0.53	0.52	0.13	9.52
8C7	0.38	4.88	0.53	0.38	0.50	0.34	0.13	9.30
8D2	1.09	4.16	0.69	0.34	0.44	0.42	0.14	9.54
8D9	1.19	4.38	0.53	0.38	0.47	0.30	0.14	9.38
8E2	1.22	4.00	0.78	0.38	0.50	0.48	0.13	9.38
8E8	1.15	3.73	0.50	0.38	0.62	0.30	0.14	9.32
8F1	1.19	4.91	0.75	0.38	0.94	0.48	0.13	9.47
8F8	1.17	4.72	0.42	0.33	0.77	0.22	0.14	9.34
12A8	1.34	4.94	0.69	0.34	0.38	0.41	0.12	13.64
12B1*	1.22	5.41	0.66	0.34	0.44	0.44	0.12	13.83
12B7	1.19	5.22	0.59	0.31	0.38	0.37	0.12	13.56
12C1	0.78	6.16	0.69	0.41	0.47	0.45	0.10	13.83
12C8	0.75	5.75	0.59	0.27	0.53	0.33	0.14	13.63
12D1	1.44	5.19	0.78	0.38	0.50	0.45	0.14	13.84
12E2	1.38	4.63	0.81	0.63	0.59	0.57	0.11	13.75
12E9	1.47	4.59	0.50	0.66	0.67	0.37	0.15	13.44
12F1	1.47	5.31	0.76	0.47	0.81	0.47	0.16	13.75
12F7	1.38	5.00	0.51	0.50	0.84	0.32	0.14	13.47

*Tarred pipe.

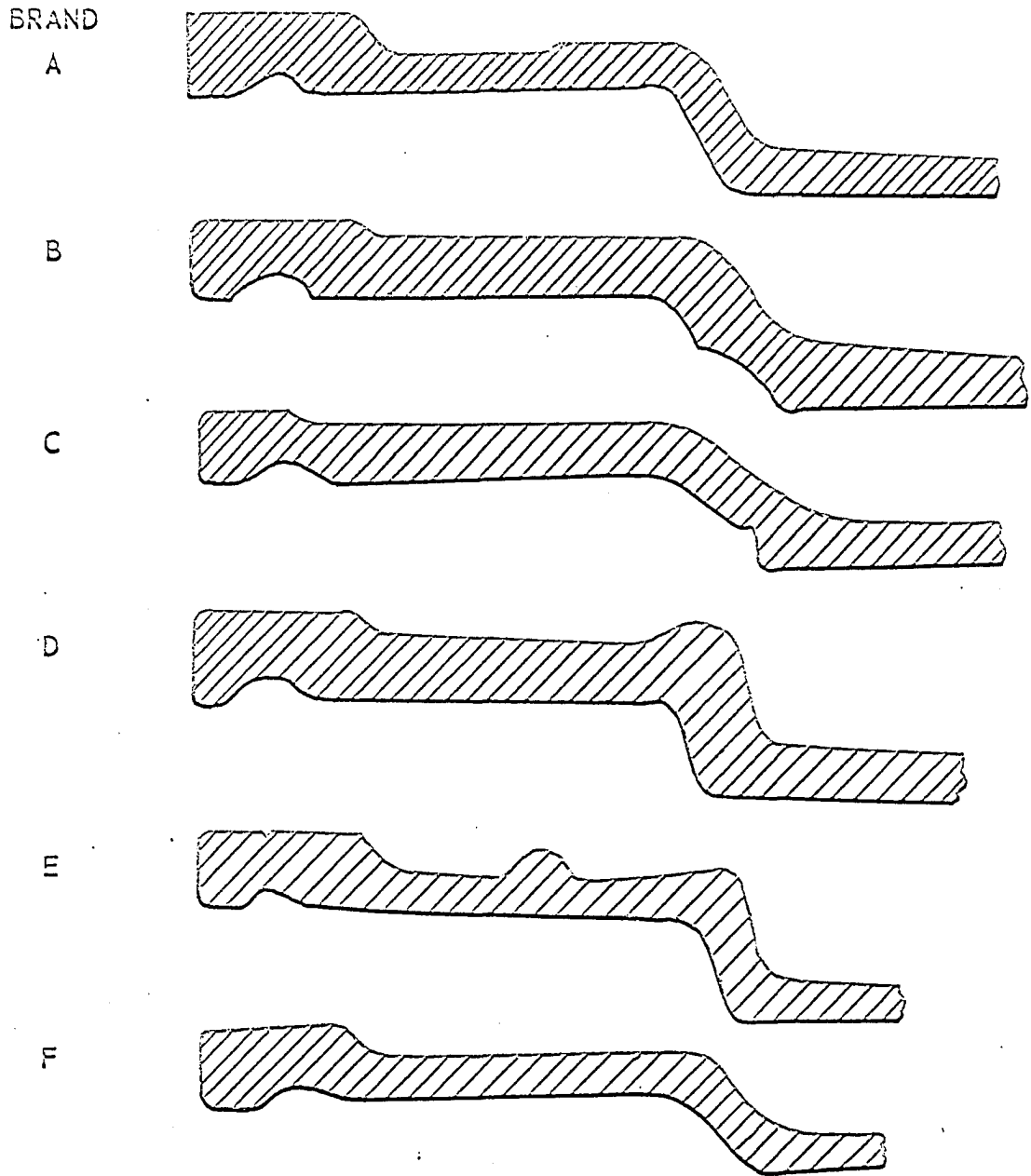
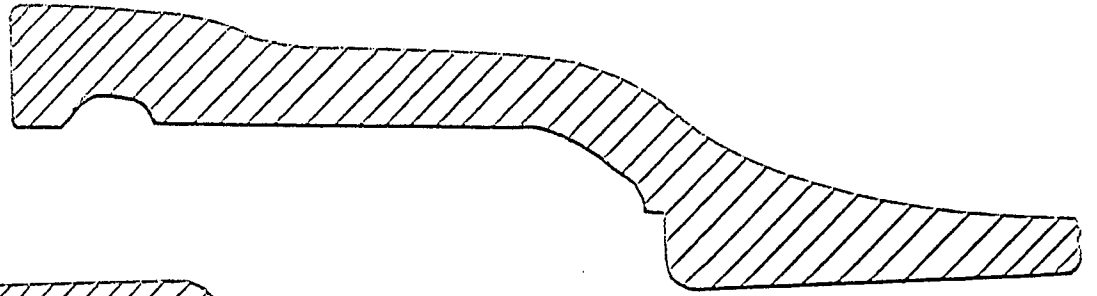


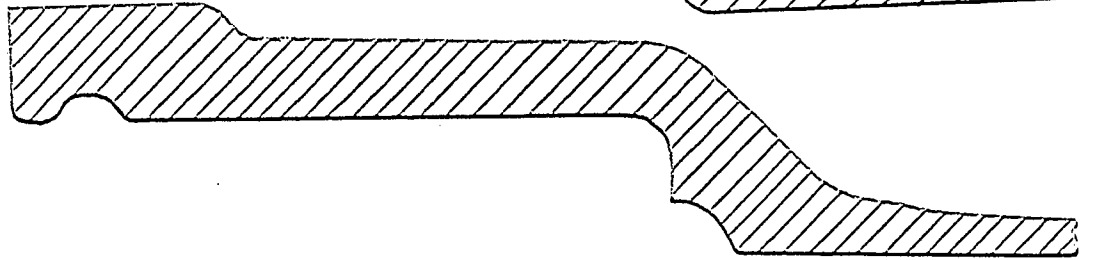
Fig. B.2. Hub configurations of 4-inch pipes

BRAND

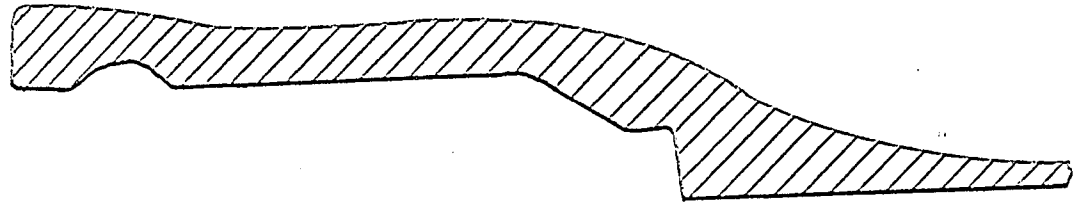
A



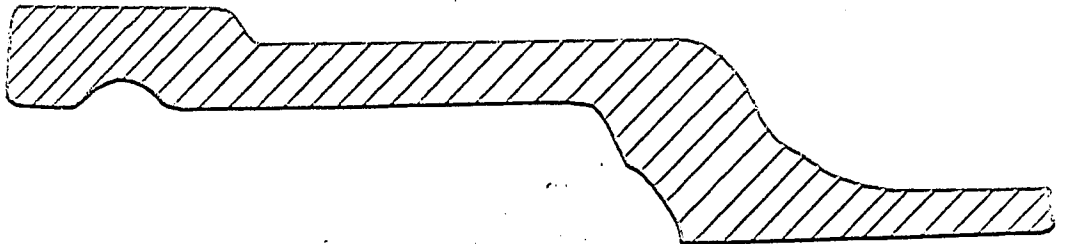
B



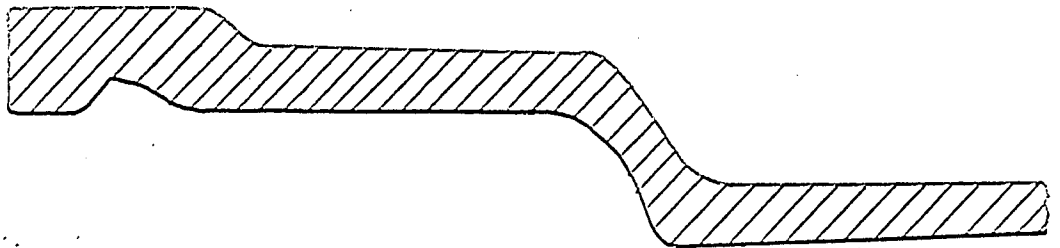
C



D



E



F

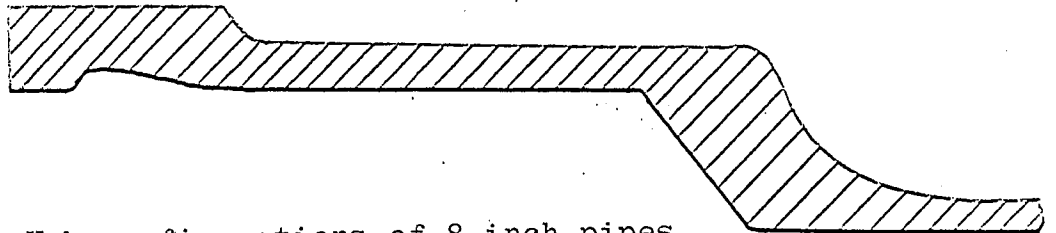
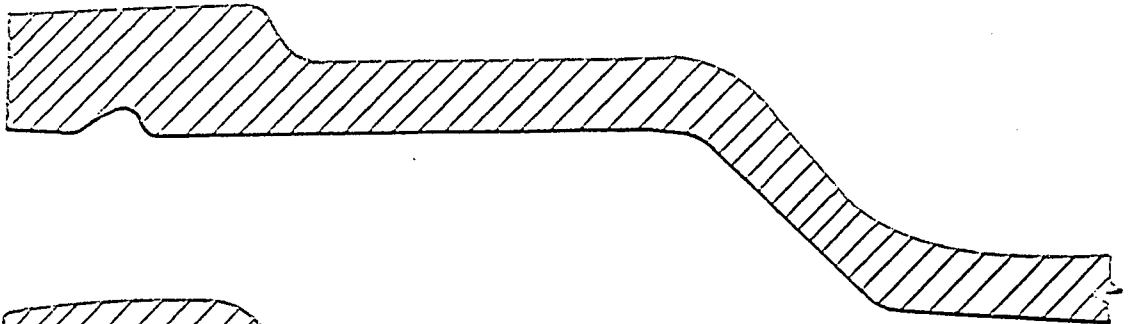


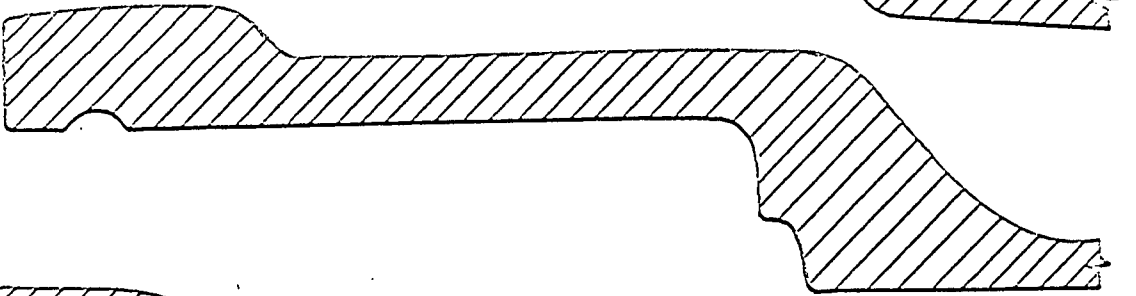
Fig. B.3. Hub configurations of 8-inch pipes

BRAND

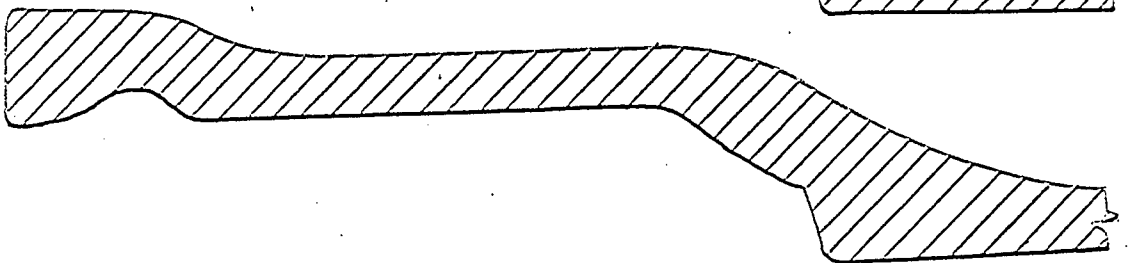
A



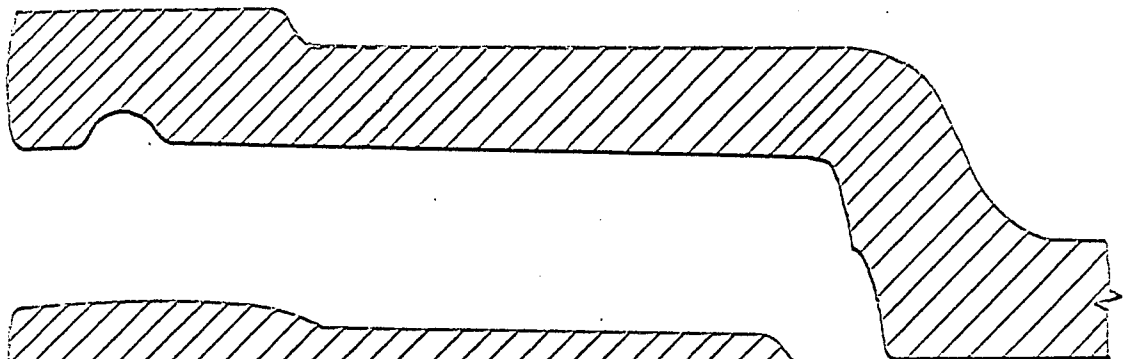
B



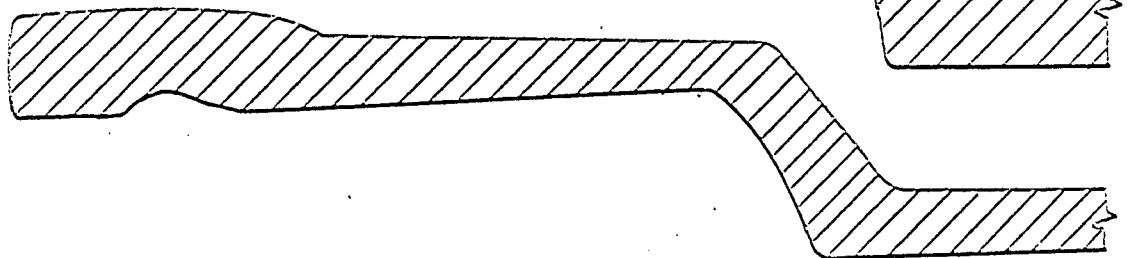
C



D



E



F

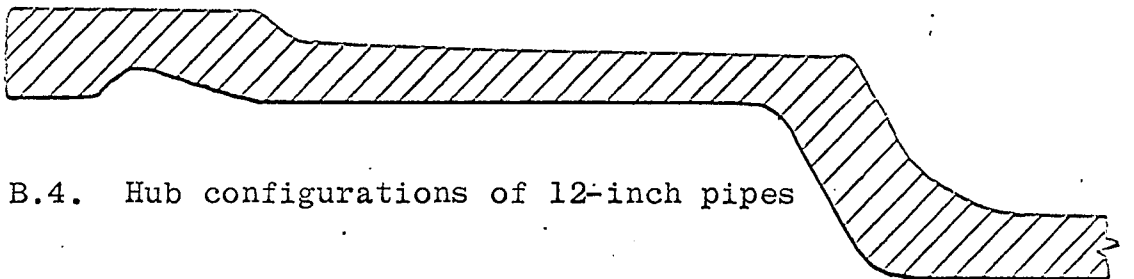


Fig. B.4. Hub configurations of 12-inch pipes

15. APPENDIX C.

C.1 Comparison Between Strains Obtained by means of Oscilloscopes and Brush Amplifiers

The dynamic and static strain components of a typical yarning operation is shown in Fig. C.1. The strains were measured by means of an oscilloscope. The figure indicates that the strains were very small. The maximum dynamic component shown is 60μ in./in. (each cm. corresponds to 100μ in./in.). The maximum total strain in this yarning operation is also 60μ in./in.

Instead of using the oscilloscopes for strain measurement (4 strain channels for each test setup), the Brush Amplifiers were used (8 strain channels for each test setup). These amplifiers were easier to balance and calibrate. A sample strain record taken by the amplifiers for the same gage, but of a different test, is shown in Fig. C.2. The figure indicates that although the amplifiers are not as sensitive as the oscilloscopes, the measured strains are in the same order as those measured by the oscilloscopes. The maximum strain was 40μ in./in. (each division corresponds to 10μ in./in.). The difference in strain is partly due to the fact that Fig. C.1 and C.2 are for different tests.

By comparing the two figures, it can be concluded that the Brush Amplifiers give a close indication of measured

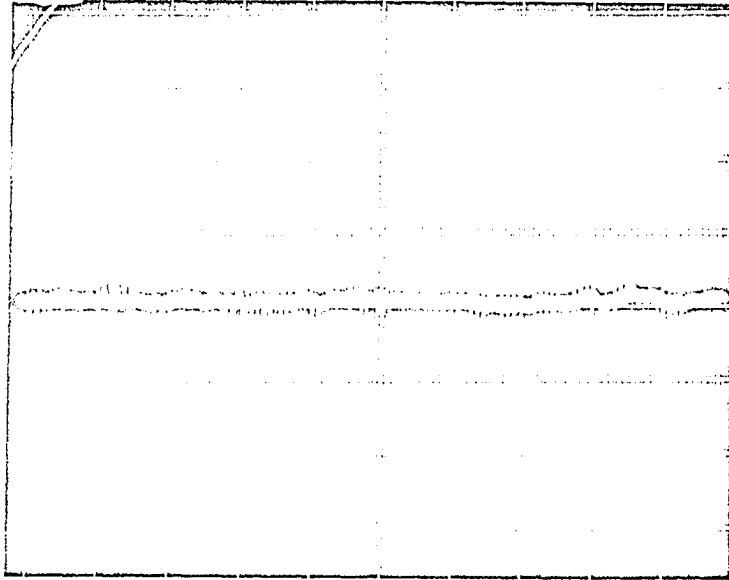


Fig. C.1. Yarning strain in the hub as recorded by oscilloscopes

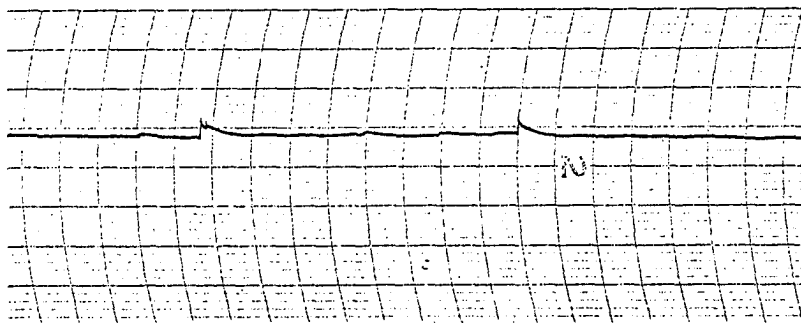


Fig. C.2. Yarning strains in the hubs as recorded by Brush Amplifiers

strains. Thus they were used in measuring all yawning strains to reduce the amount of testing.

C.2 Caulking Strains

Caulking strains consist of dynamic and static components as shown in Fig. C.3. This figure shows only an initial small portion of caulking circumferential strain wave in a SV hub. The figure indicates that the major dynamic strain occurs within the first 0.001 seconds after hammering the caulking iron against the joint (horizontal scale of the figure is 0.0005 sec./cm.). The rest of the wave (part of which is shown in the figure) can be considered as static component. The maximum dynamic strain is about 200μ in./in. (vertical scale of the figure is 100μ in./in.). The maximum static strain is about 100μ in./in.

Figure C.3 shows the initial portion of a strain wave due to one hammer blow. In the next blow, a dynamic and static strain is superimposed on the remaining static component of the blow shown in Fig. C.3. The new dynamic component will also be around 200μ in./in. However, the total static strain is the sum of the static strain and the remaining static strain of the previous blow. The total sum of this static strain due to caulking a joint is larger than the dynamic strain component of separate blows as shown in Fig. C.4. In this figure, the horizontal sweep is 5 sec./cm. (the vertical is 500μ in./in.). Due to this slow sweep, the

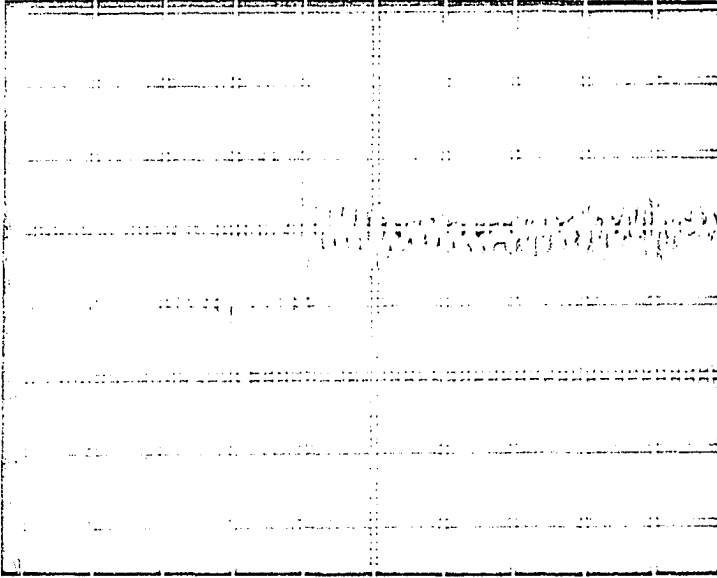


Fig. C.3. Fast sweep trace of a caulking strain wave (single blow)

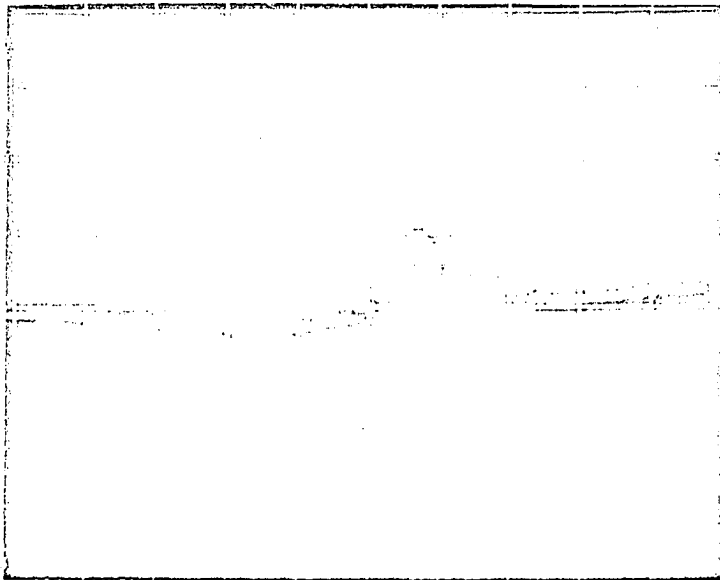


Fig. C.4. Slow sweep trace of caulking strain waves (several blows)

dynamic component looks like a bleb and the change in the static components of strains govern. However, the maximum strain considered in design was taken as static plus dynamic. All caulking record was taken in slow sweep of the CRO beam. This procedure saved time, expenses, and more data was obtained in any one test setup.

16. APPENDIX D. COMPUTER PROGRAM FOR THE DETERMINATION OF DESIGN CHARTS; DESIGN CHARTS FOR THE VARIOUS PIPE DIAMETERS USED; AND COMPUTER PROGRAM DETERMINING THE FORCE P FOR SPECIFIC DIMENSIONS

```

S.0001      DIMENSION SN(10) ,FN(10),RN(10)
S.0002      SINH(X)=TANH(X)/SQRT(1.-TANH(X)*TANH(X))
S.0003      COSH(X)=1./SQRT(1.-TANH(X)*TANH(X))
S.0004      READ (1,101) E, POISON
S.0005      101 FORMAT (E10.3,F10.4)
S.0006      READ (1,200) NSIZE,NS,NF,NR
S.0007      200 FORMAT (4110)
S.0008      WRITE (3,300)
S.0009      300 FORMAT (1H1,10X,'MAXIMUM STRESS GIVEN IS IN PSI',5X,'UNIT LOAD IS
              1IN POUND PER LINEAR INCH CIRCUMFERENTIALLY')
S.0010      RAT=1.0-POISON*POISON
S.0011      WRITE (3,301) E,POISON,RAT
S.0012      301 FORMAT (6F20.8)
C
S.0013      START COMPUTATION FOR EACH CASE
S.0014      DO 99 JSIZE=1,NSIZE
S.0015      WRITE (3,203)
              203 FORMAT (1H1,'STRESS FACTORS FOR GIVEN SETS OF S,F,R'///
              1'ALL IN INCH - POUND UNIT')
S.0016      READ (1,201) ISIZE, A, Y
S.0017      201 FORMAT (I10,2F10.4)
S.0018      WRITE (3,204) ISIZE,A,Y
S.0019      204 FORMAT (1H0,5X,'SIZE = ',I5,10X,'A = ',F6.2,10X,'Y = ',F6.2)
S.0020      WRITE (3,205)
S.0021      205 FORMAT (1H0,14X,'S',14X,'F',14X,'R',2X,'STRESS FACTOR')
S.0022      READ (1,202) (SN(IS),IS=1,NS)
S.0023      READ (1,202) (FN(IFN),IFN=1,NF)
S.0024      READ (1,202) (RUN(IRN),IRN=1,NR)
S.0025      202 FORMAT (8F10.4)
S.0026      DO 99 JS=1,NS
S.0027      S=SN(JS)
S.0028      WRITE (3,207)
S.0029      207 FORMAT (1H )
S.0030      DO 99 JF=1,NF
S.0031      F=FN(JF)
S.0032      WRITE (3,207)

```

Fig. D.1. Computer program used in preparing Figs. D.2 - D.37

```

S.0033 DO 99 JR=1,NR
S.0034 R=RN(JR)
S.0035 RL=(A+R)/2.
S.0036 RS=(A+S)/2.
S.0037 R2=R*R
S.0038 S2=S*S
S.0039 DL=E*R*R2/(12.*RAT)
S.0040 DS=E*S*S2/(12.*RAT)
S.0041 DELTA4=3*RAT/(R2*RL*RL)
S.0042 ALPHA4=3*RAT/S2*RS*RS)
S.0043 BETA2=SQRT(BETA4)
S.0044 BETA1=SQRT(BETA2)
S.0045 BETA3=BETA1*BETA2
S.0046 ALPH2=SQRT(ALPH4)
S.0047 ALPH1=SQRT(ALPH2)
S.0048 ALPH3=ALPH1*ALPH2
C
PREPARATORY CALCULATIONS
BF=BETA1*F
DLB2=DL*BETA2
DLB3=DL*BETA3
DSA2=DS*ALPH3
DSA3=DS*ALPH3
SBF=SIN(BF)
CBF=COS(BF)
SHBF=SINH(BF)
CHBF=COSH(BF)
SBF2=SBR*SBF
CBF2=CBF*CBF
SHBF2=SHBF*SHBF
CHBF2=CHBF*CHBF
COTLTM=2.*DLB3*SBF2-SHBF2)
SC=SBF*CRF
SSH=SBF*SHBF
SCH=SBF*CHBF
CSH=CBF*SHBF

```

Fig. D.1. (Continued)


```

S.0067      CCH=CBF*CHBF
S.0068      SHCH=SHBF*CHBF
C           UNIT LOAD AT END - P=1 PLI  OUTWARD POSITIVE
S.0069      WLP=(SCH-CSH)/BOTTOM
S.0070      THETLP=2.*BETA1*SSH/BOTTOM
C           UNIT Q AT JUNCTION, POSITIVE Q CAUSES CLOCKWISE END ROTATION
S.0071      WLQ=(SHCH-SC)/BOTTOM
S.0072      THETLQ=BETA1*(SBF2+SHBF2)/BOTTOM
S.0073      WRQ=0.5/DSA3
S.0074      THETRQ=-0.5/DSA2
C           UNIT M AT JUNCTION , POSITIVE IF CLOCKWISE AT INSIDE END OF LIP
S.0075      WLM=BETA1*(SBF2*CHBF2+CBF2*SHBF2)/BOTTOM
S.0076      THETLM=2.*BETA2*(SC+SHCH)/BOTTOM
S.0077      WRM=-0.5/DSA2
S.0078      THETRM=ALPH1/DSA2
C           SOLUTION OF Q AND EM
S.0079      WRLQ=WRQ-WLQ
S.0080      WRLM=WRM-WLM
S.0081      TRLQ=THETRQ-THETLQ
S.0082      TRLM=THETRM-THETLM
S.0083      DET=WRLQ*TRLM-TRLQ*WRLM
S.0084      QTOP=WLP*TRLM-THETLP*WRLM
S.0085      EMTOP=WRLQ*THETLP-TRLQ*WLP
S.0086      Q=QTOP/DET
S.0087      EM=EMTOP/DET
C           COMPUTE CONSTANTS IN THE DEFLECTION EXPRESSION - FOR UNIT P.
S.0088      C1=-0.5*EM/DLB2
S.0089      C2=(BETA1*EM*(SC+SHCH)+Q*SBF2+SSH)/BOTTOM
S.0090      C3=(BETA1*EM*(SC+SHCH)+Q*SHBF2*SSH)/BOTTOM
S.0091      C4=(BETA1*EM*(SBF2*CHB2+CBF2*SHBF2)+Q*(SHCH-SC)-(CSH SCH))/BOTTOM
S.0092      WFREE=C1*SSH-C2*SCH-C3*CSH+C4*CCH
S.0093      STRESS=E*WFREE/RL
S.0094      WRITE (3,206 S,F,R,STRESS
S.0095      206 FORMAT (4F15.4)
S.0096      99 CONTINUE
S.0097      STOP
S.0098      END

```

Fig. D.1. (Continued)

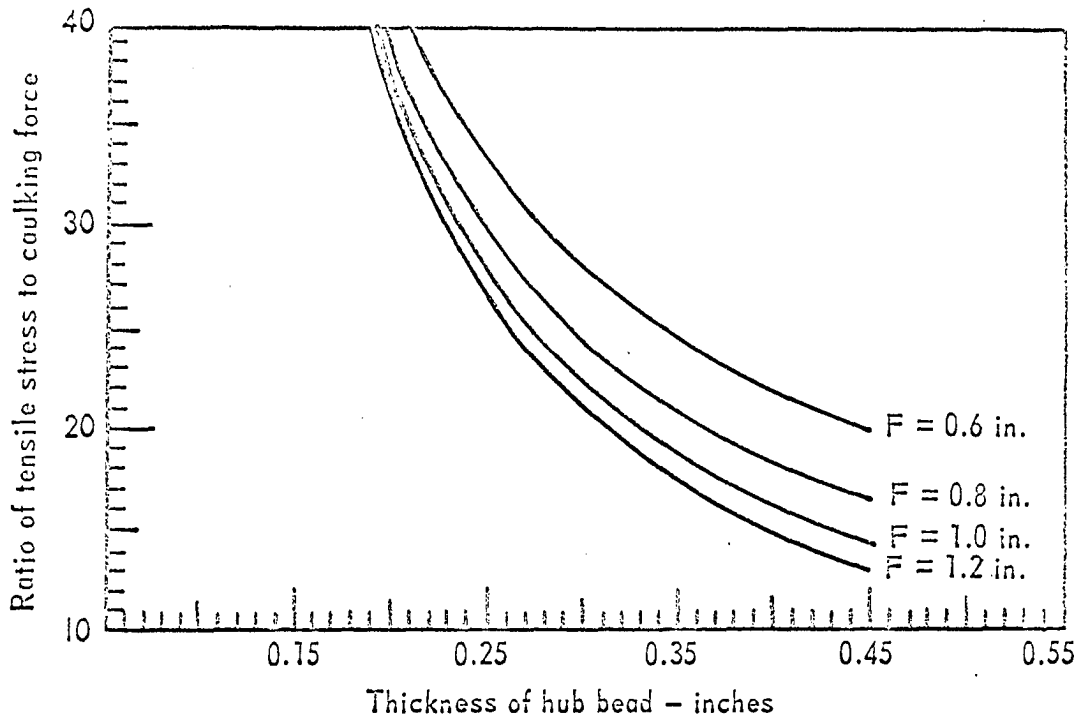


Fig. D.2. Design parameters for 2-inch hubs with hub wall thickness of 0.10 inch.

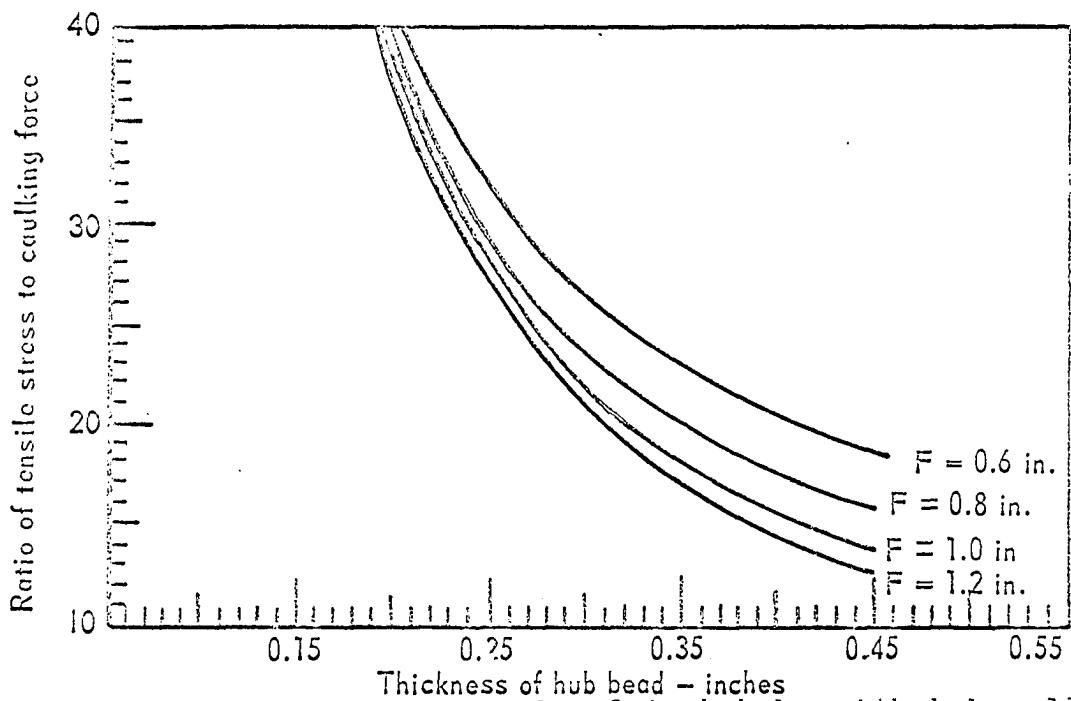


Fig. D.3. Design parameters for 2-inch hubs with hub wall thickness of 0.12 inch.

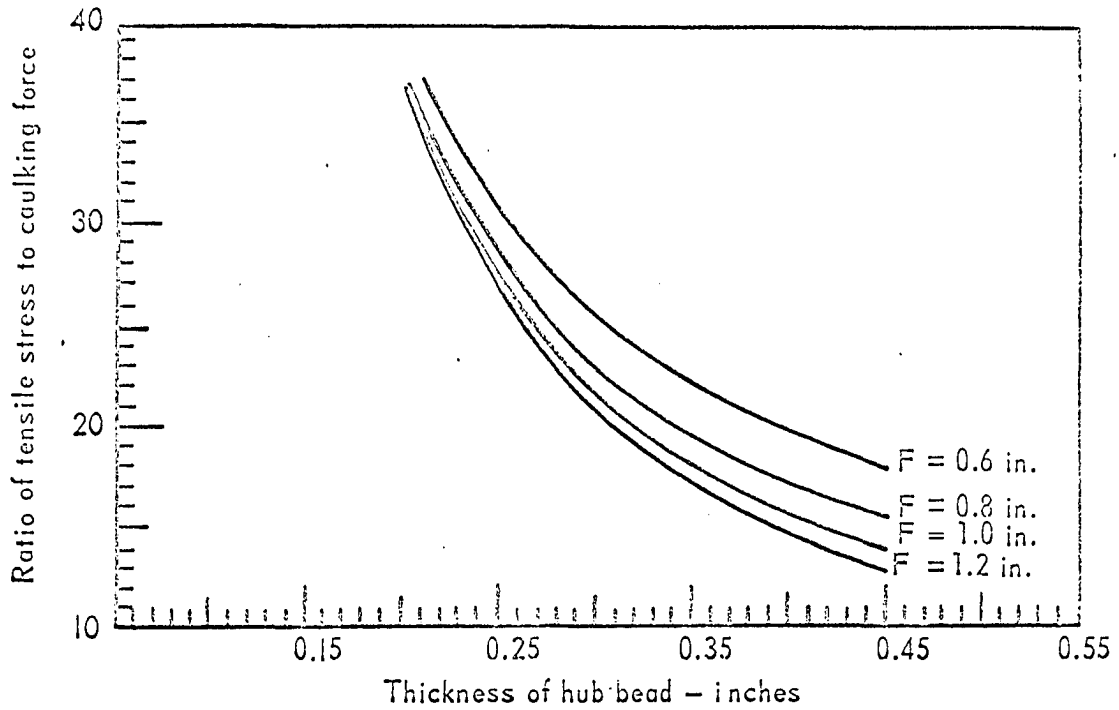


Fig. D.4. Design parameters for 2-inch hubs with hub wall thickness of 0.14 inch

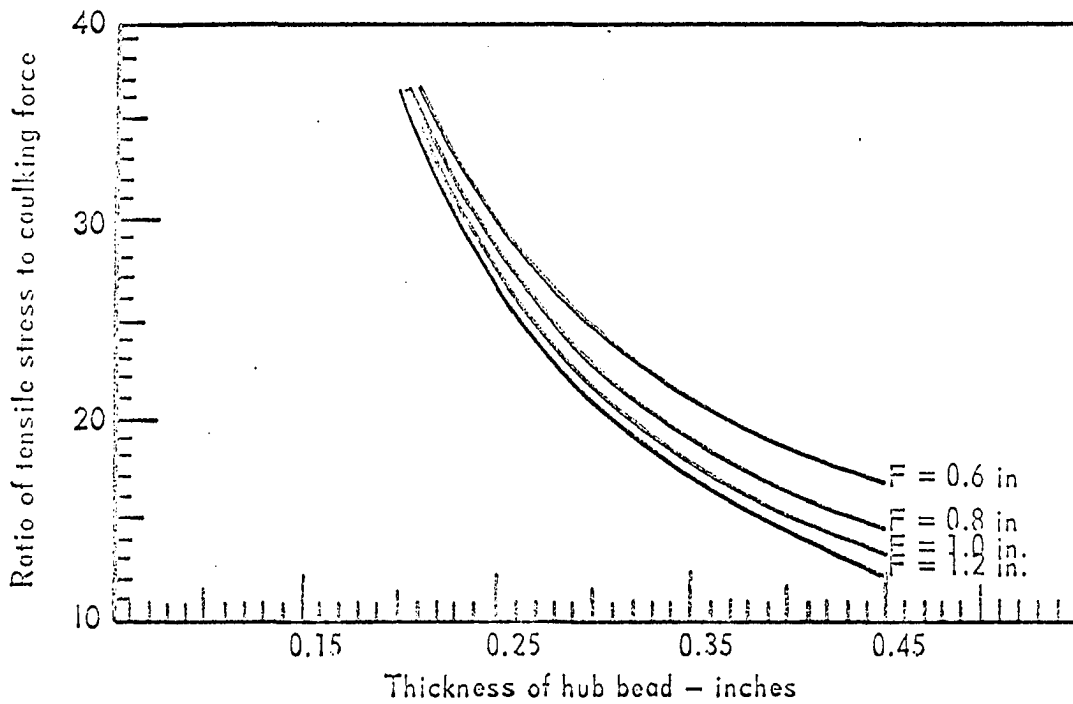


Fig. D.5. Design parameters for 2-inch hubs with hub wall thickness of 0.16 inch

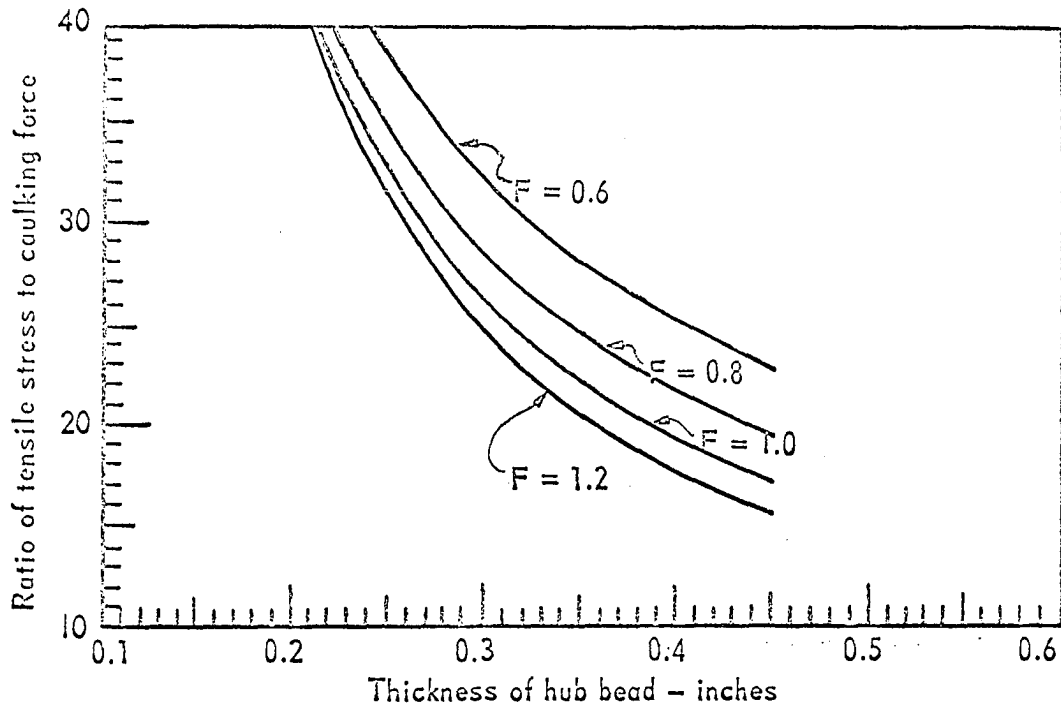


Fig. D.6. Design parameters for 3-inch hubs with hub wall thickness of 0.12 inch

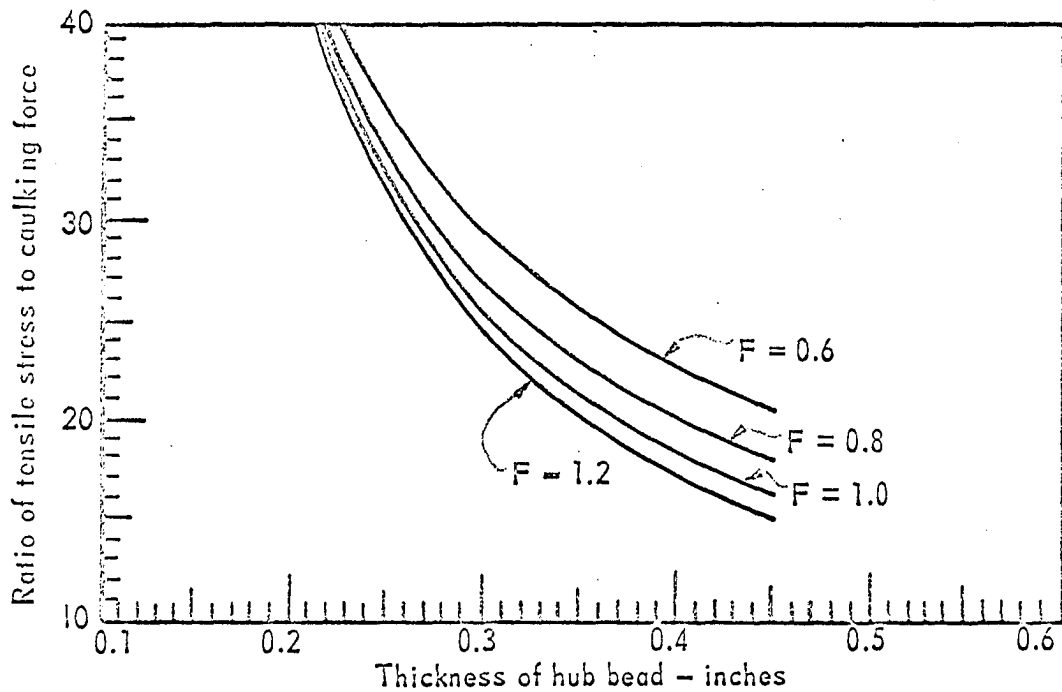


Fig. D.7. Design parameters for 3-inch hubs with hub wall thickness of 0.16 inch

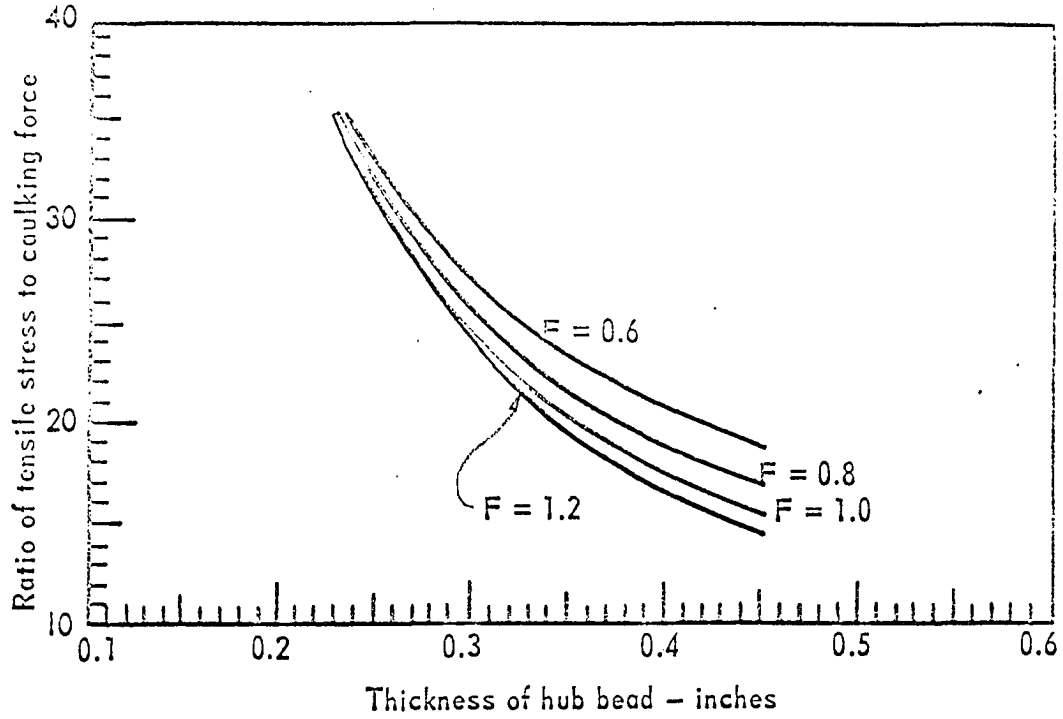


Fig. D.8. Design parameters for 3-inch hubs with hub wall thickness of 0.20 inch

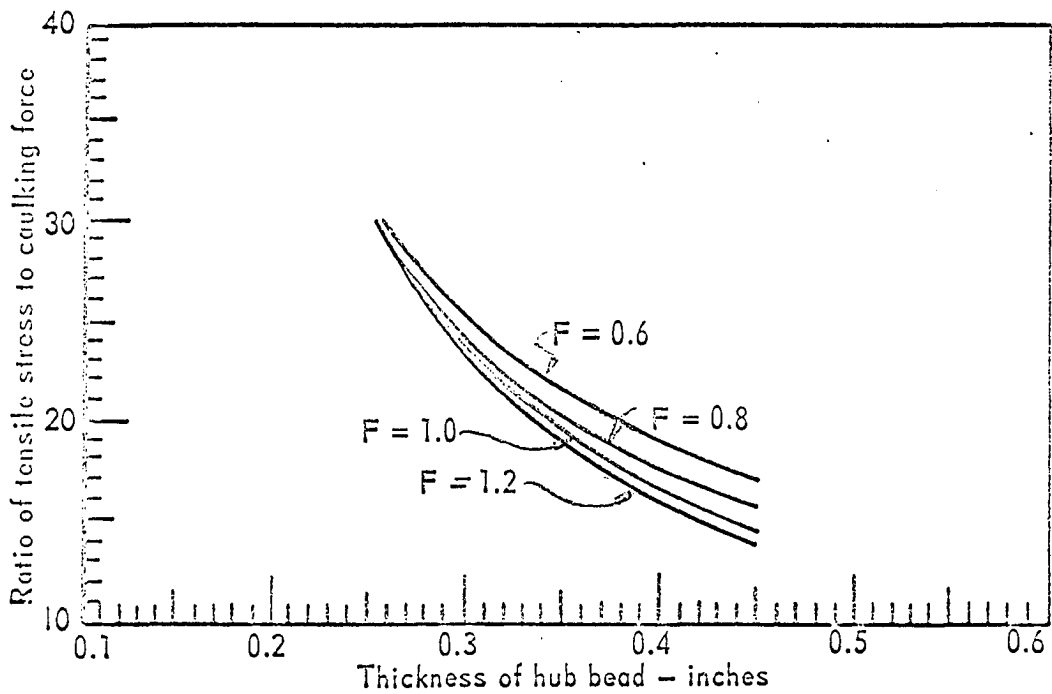


Fig. D.9. Design parameters for 3-inch hubs with hub wall thickness of 0.24 inch

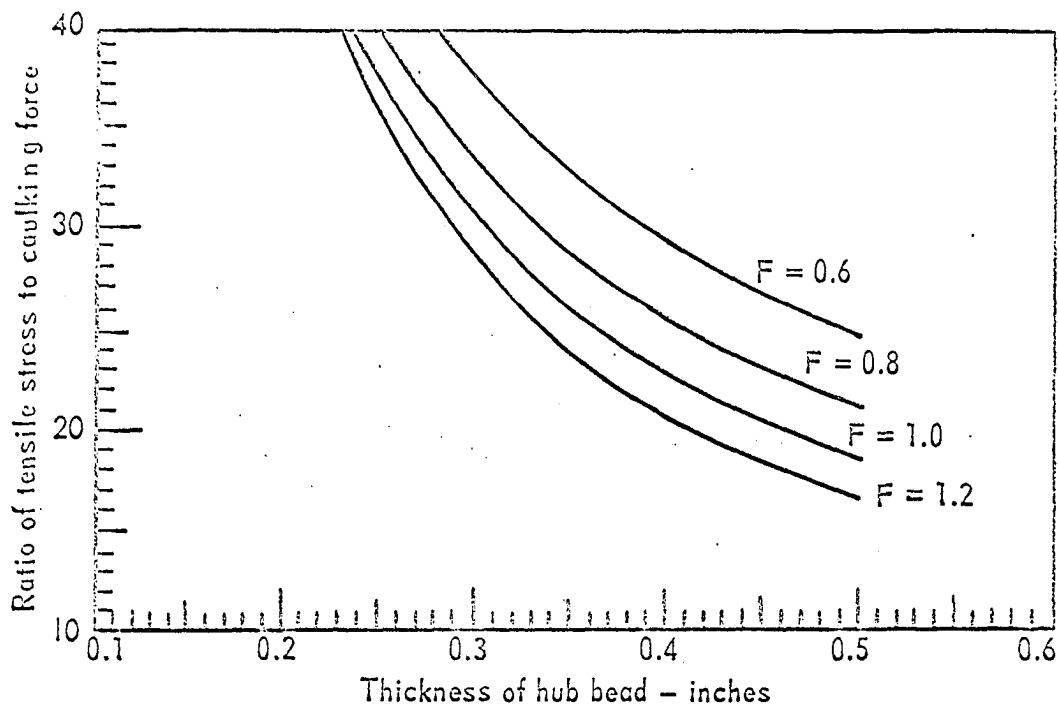


Fig D.10. Design parameters for 4-inch hubs with hub wall thickness of 0.12 inch

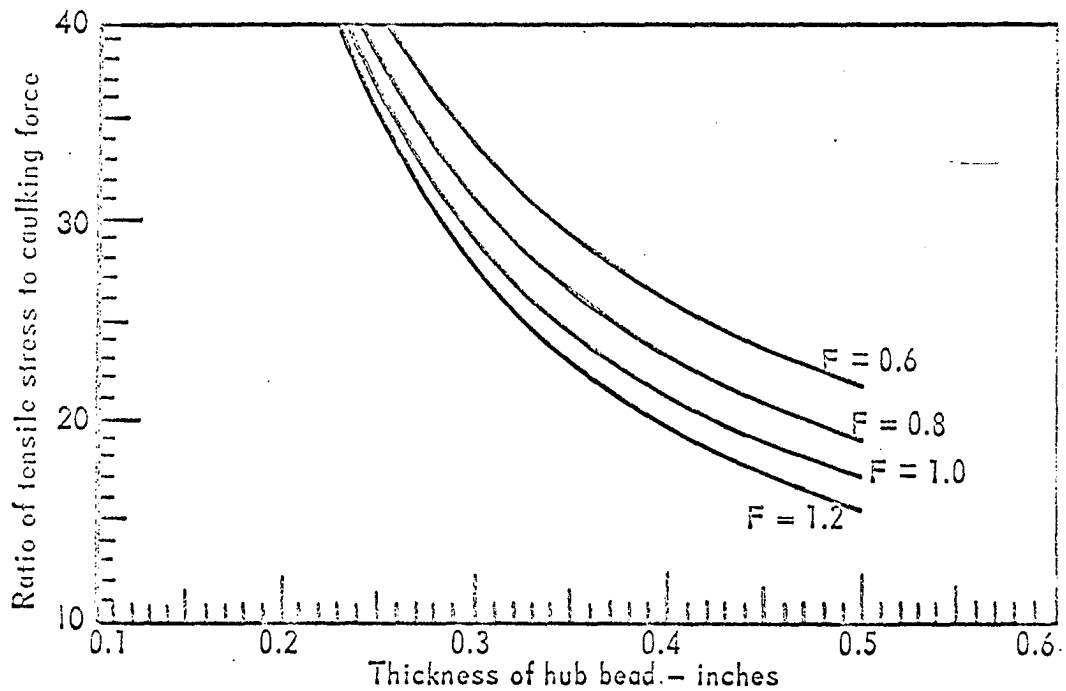


Fig. D.11. Design parameters for 4-inch hubs with hub wall thickness of 0.16 inch

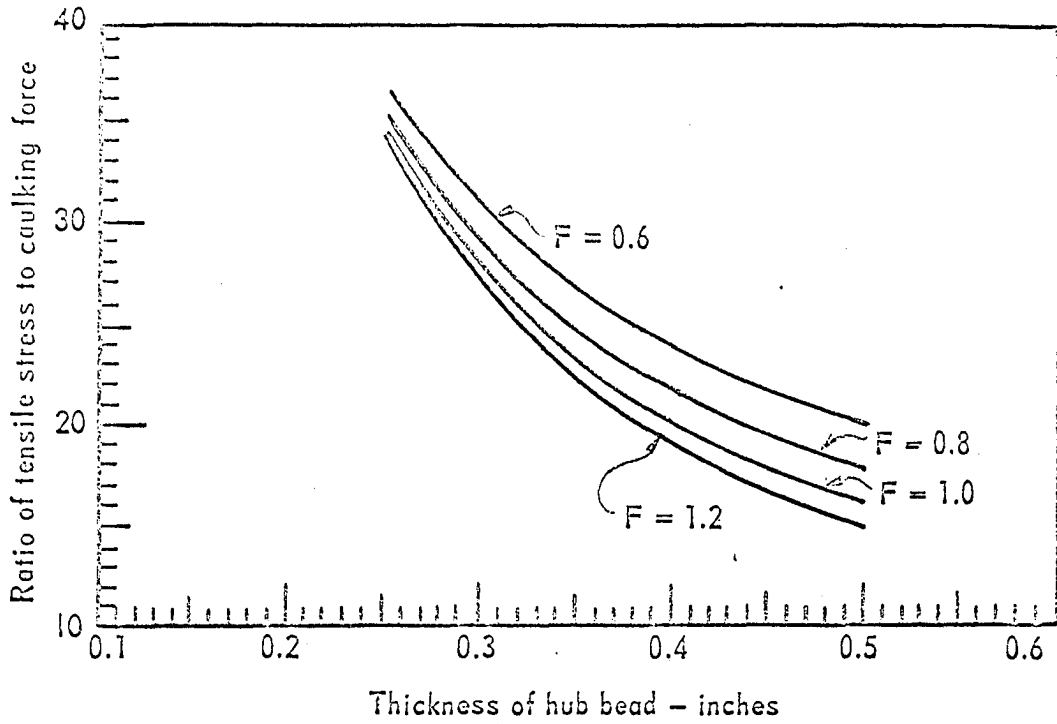


Fig. D.12. Design parameters for 4-inch hubs with hub wall thickness of 0.20 inch

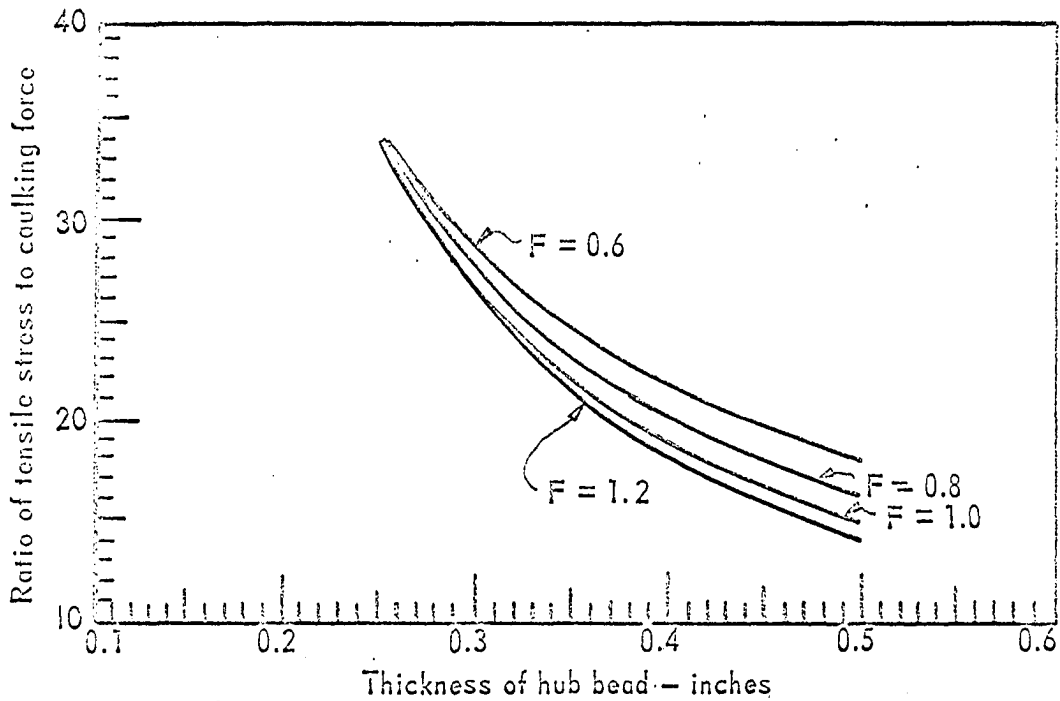


Fig. D.13. Design parameters for 4-inch hubs with hub wall thickness of 0.24 inch

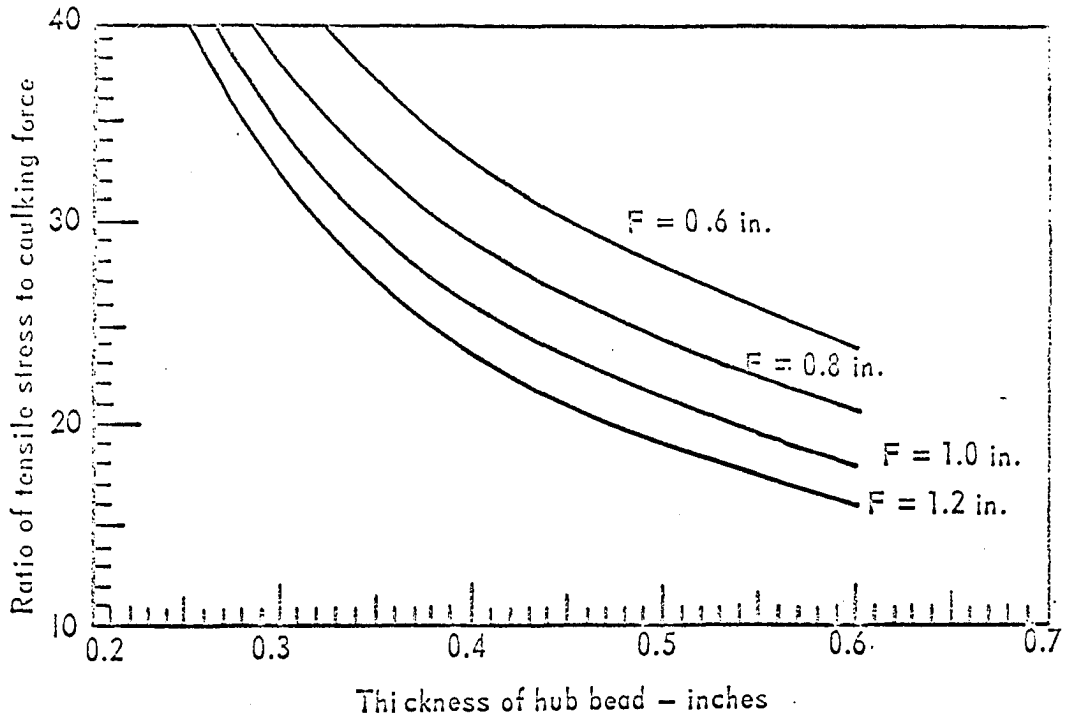


Fig. D.14. Design parameters for 5-inch hubs with hub wall thickness of 0.12 inch

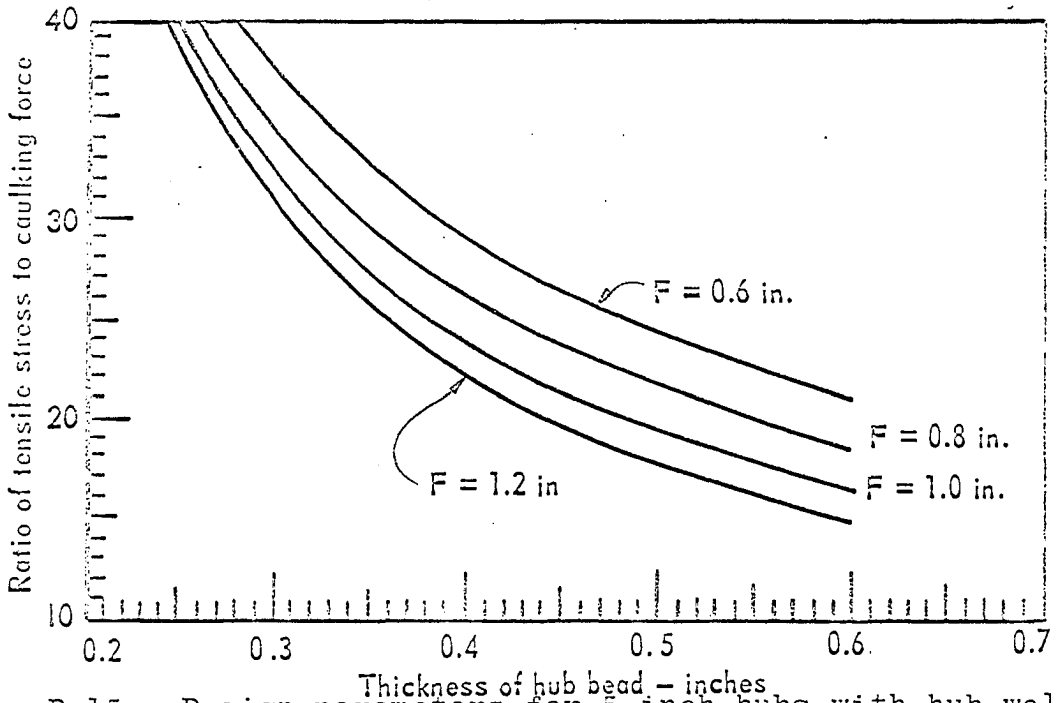


Fig. D.15. Design parameters for 5-inch hubs with hub wall thickness of 0.16 inch

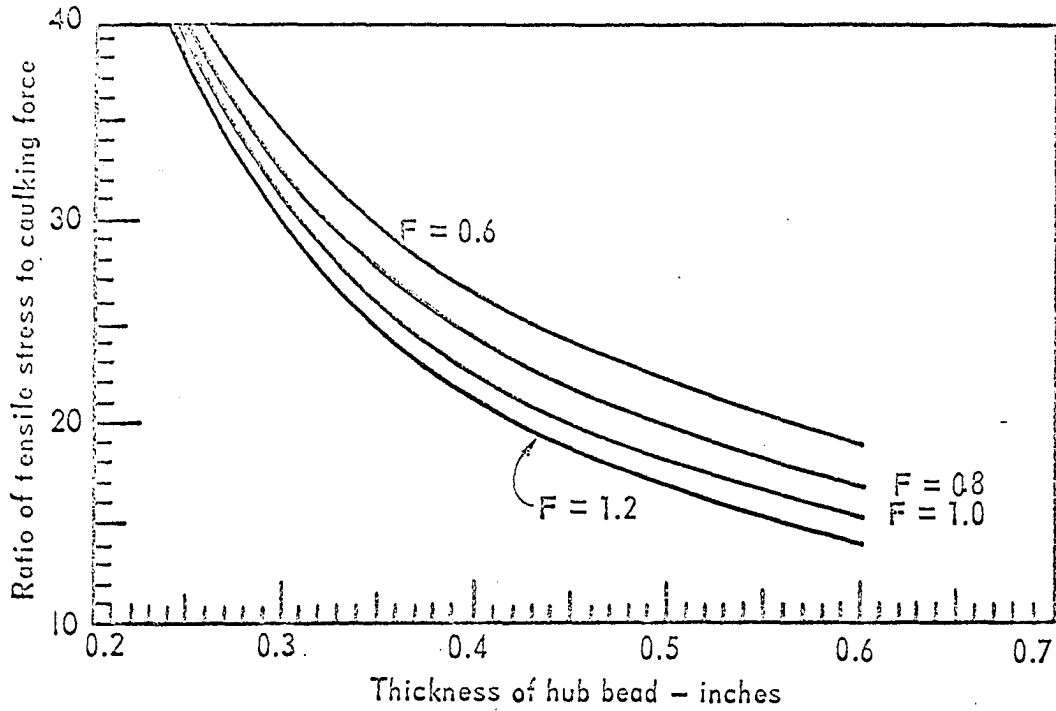


Fig. D.16. Design parameters for 5-inch hubs with hub wall thickness of 0.20 inch

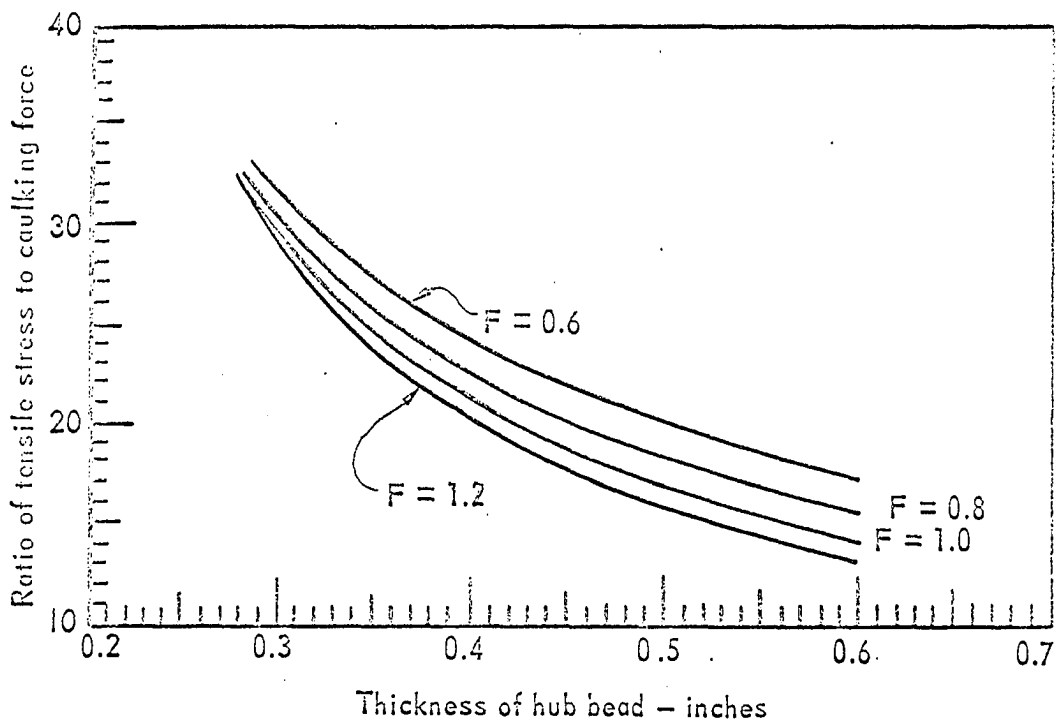


Fig. D.17. Design parameters for 5-inch hubs with hub wall thickness of 0.24 inch

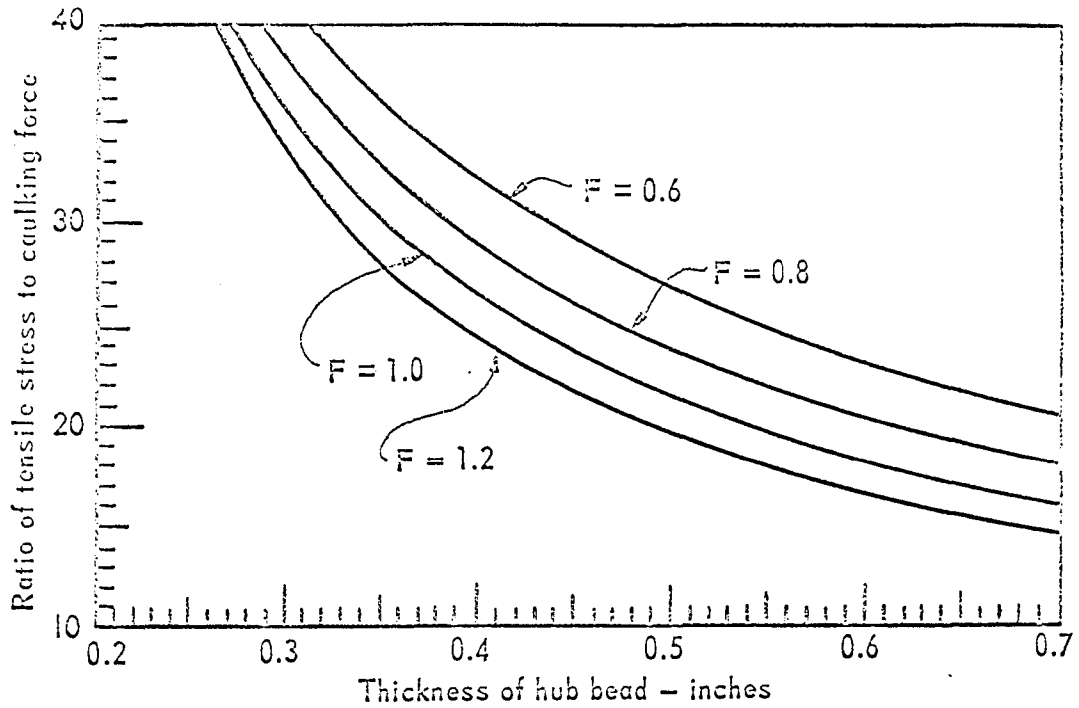


Fig. D.18. Design parameters for 6-inch hubs with hub wall thickness of 0.16 inch

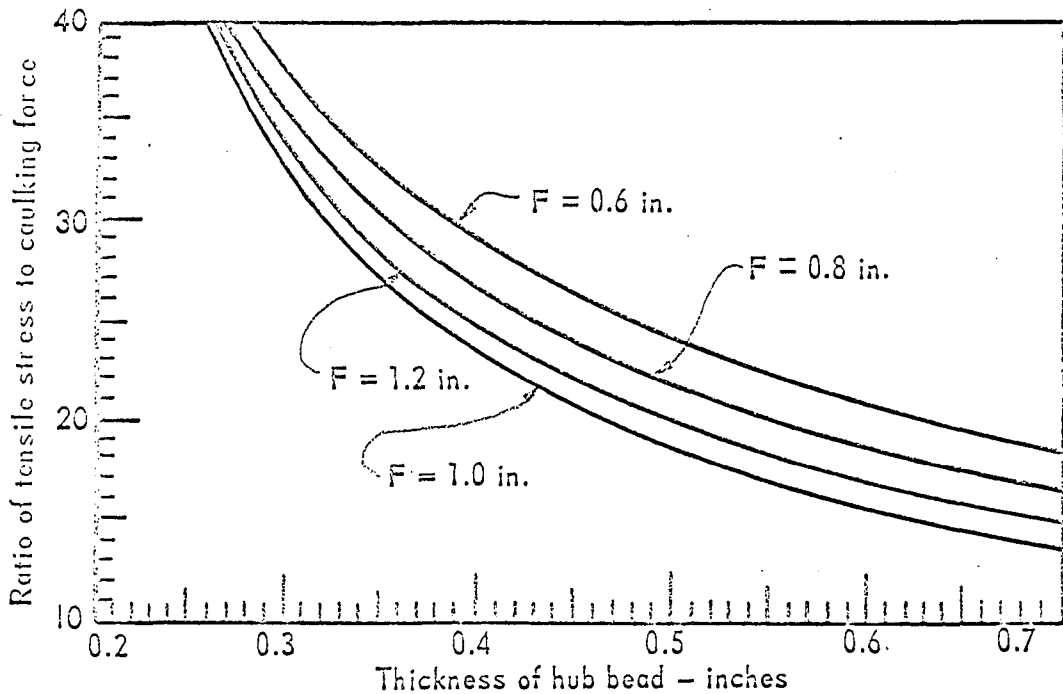


Fig. D.19. Design parameters for 6-inch hubs with hub wall thickness of 0.20 inch

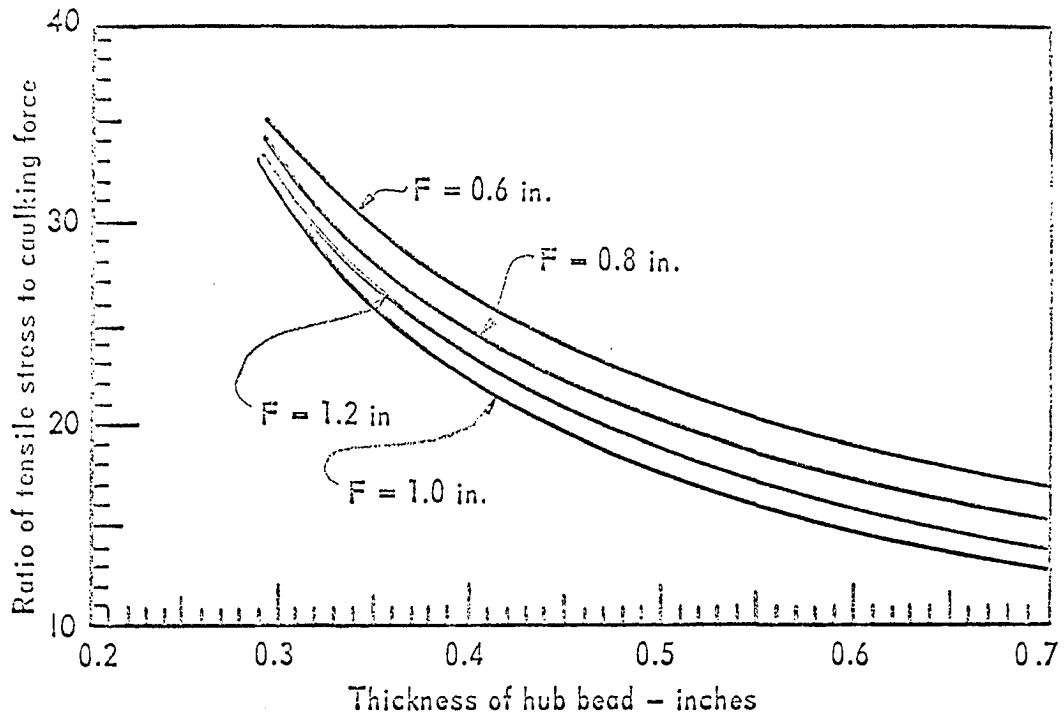


Fig. D.20. Design parameters for 6-inch hubs with hub wall thickness of 0.24 inch

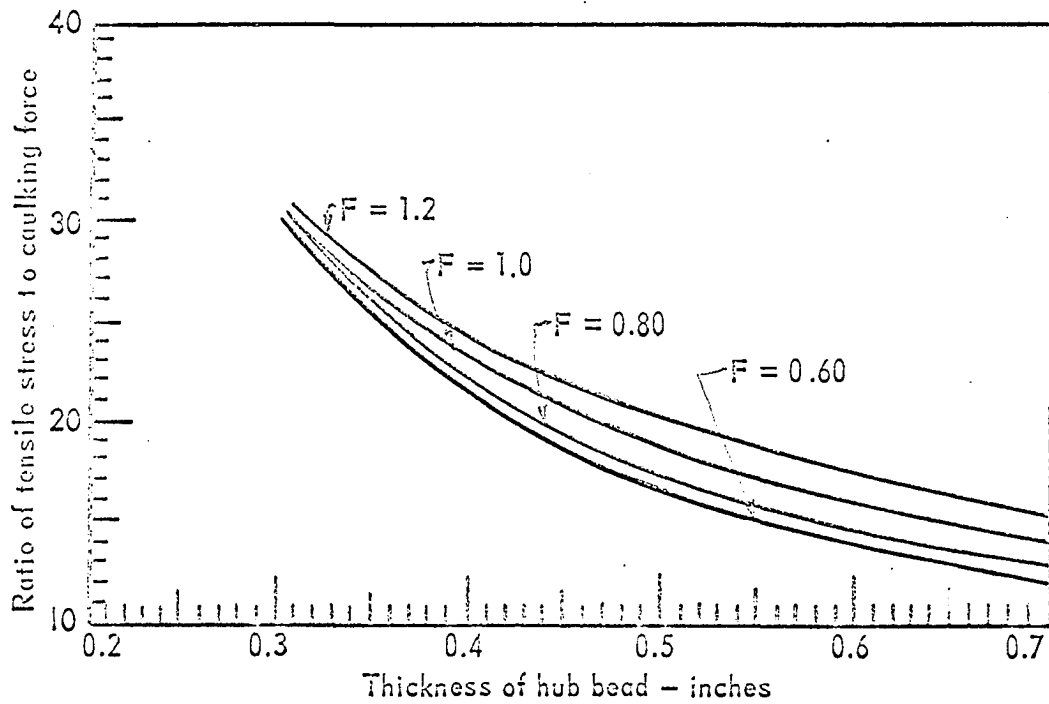


Fig. D.21. Design parameters for 6-inch hubs with hub wall thickness of 0.28 inch

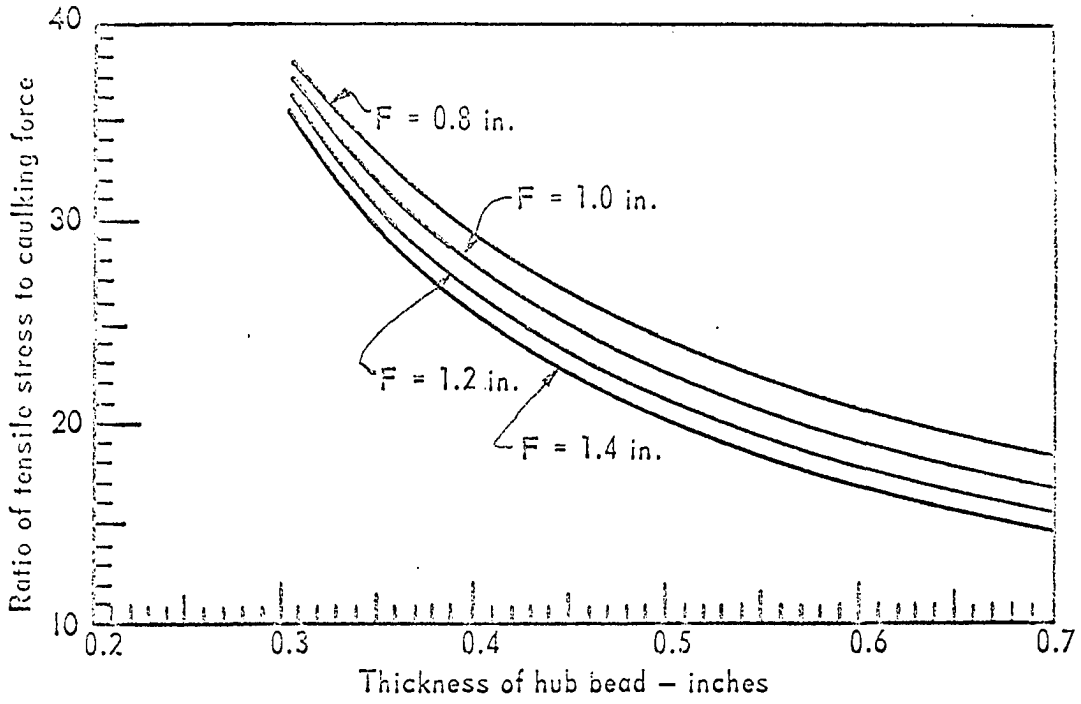


Fig. D.22. Design parameters for 8-inch hubs with hub wall thickness of 0.24 inch

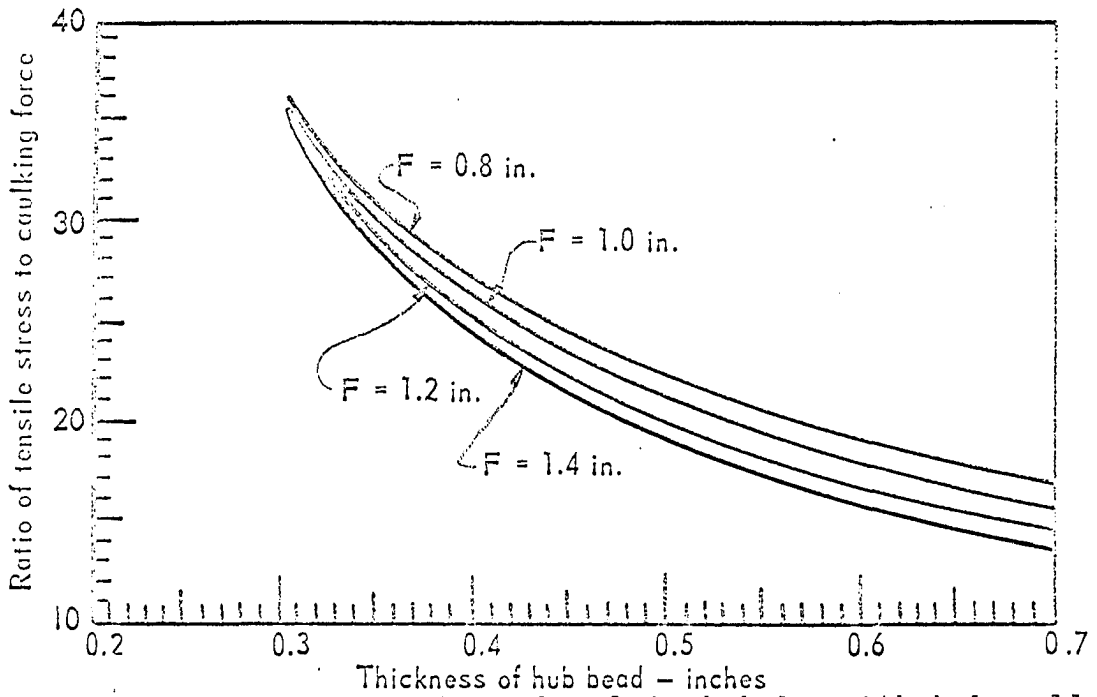


Fig. D.23. Design parameters for 8-inch hubs with hub wall thickness of 0.28 inch

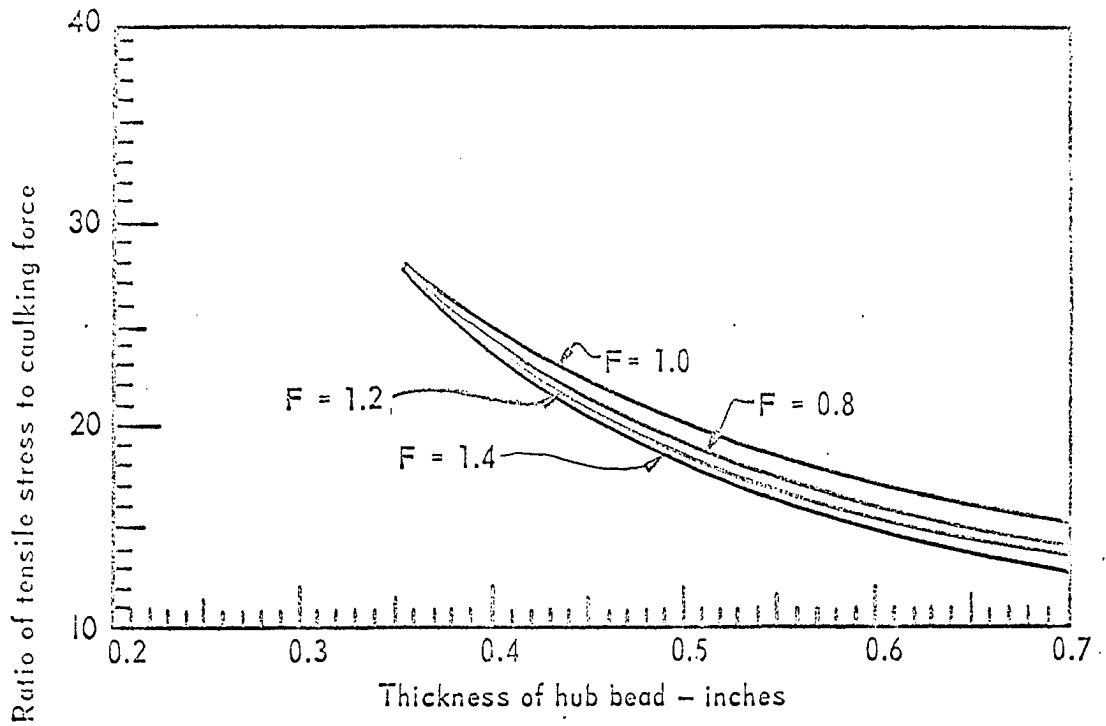


Fig. D.24. Design parameters for 8-inch hubs with hub wall thickness of 0.34 inch

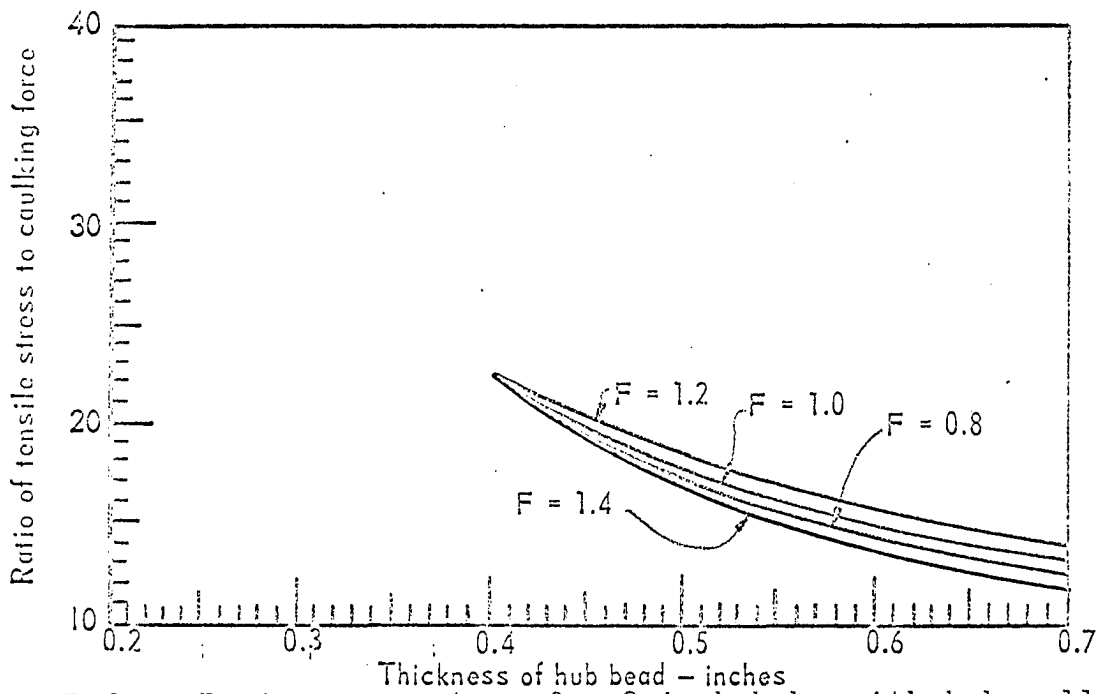


Fig. D.25. Design parameters for 8-inch hubs with hub wall thickness of 0.40 inch

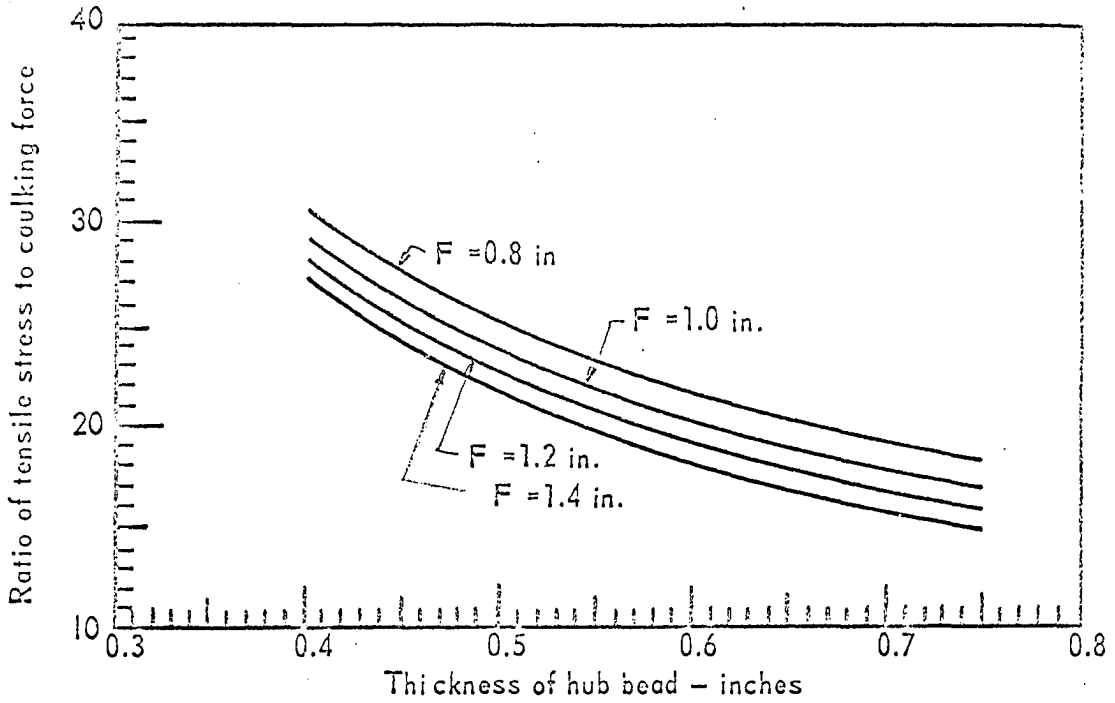


Fig. D.26. Design parameters for 10-inch hubs with hub wall thickness of 0.28 inch

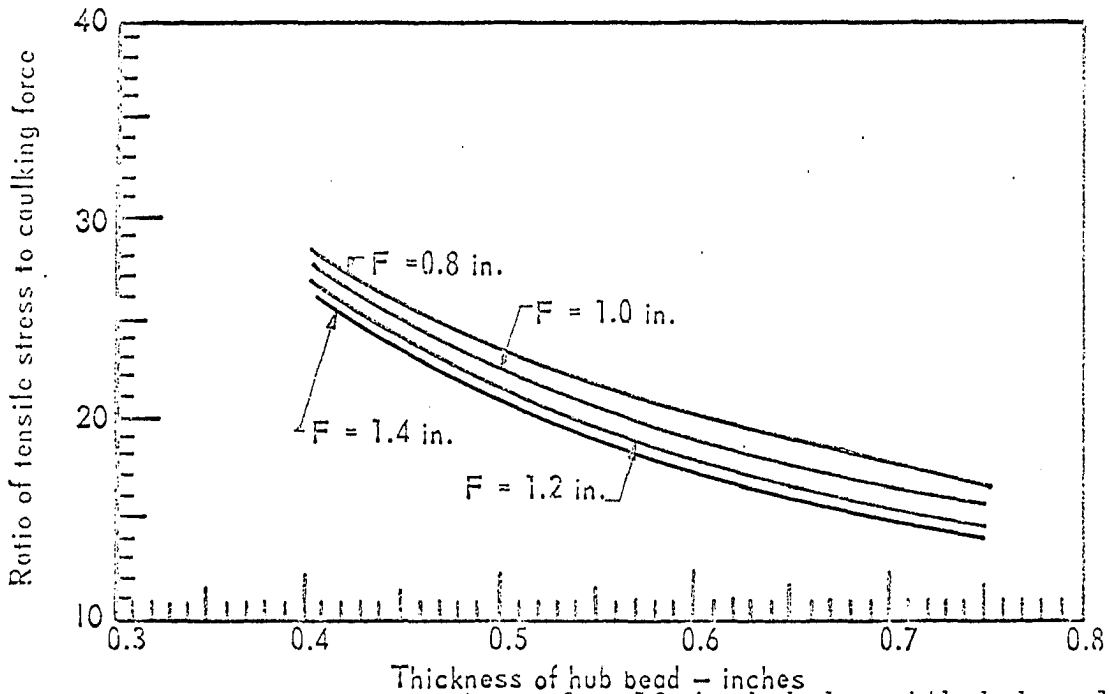


Fig. D.27. Design parameters for 10-inch hubs with hub wall thickness of 0.32 inch

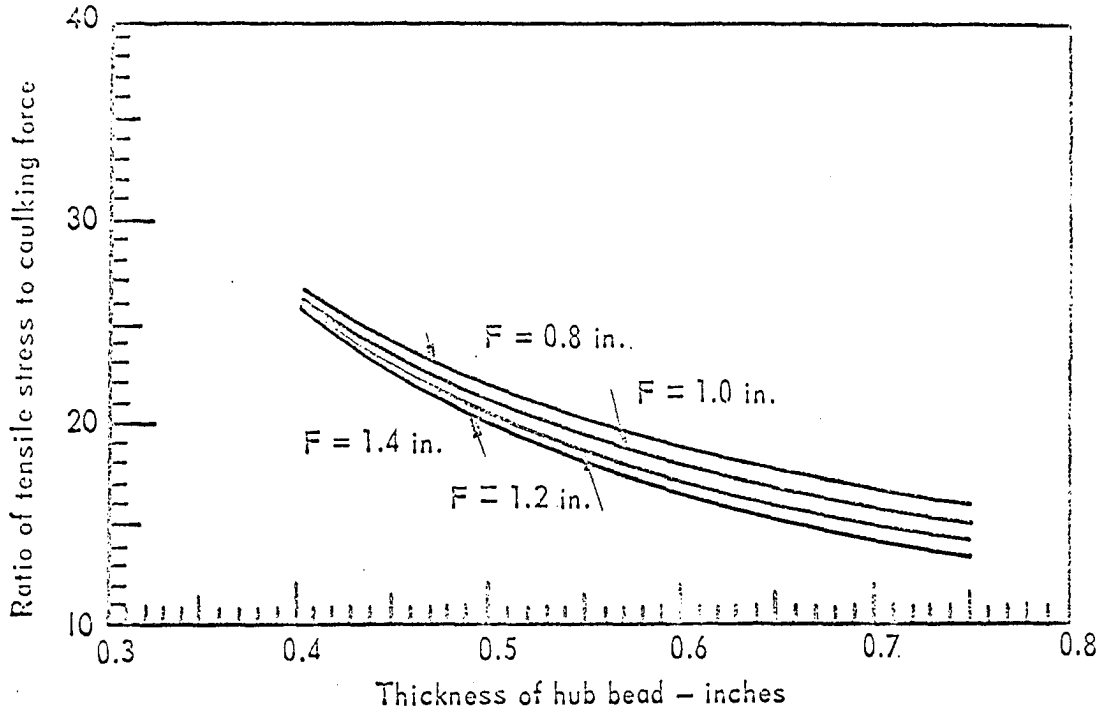


Fig. D.28. Design parameters for 10-inch hubs with hub wall thickness of 0.36 inch

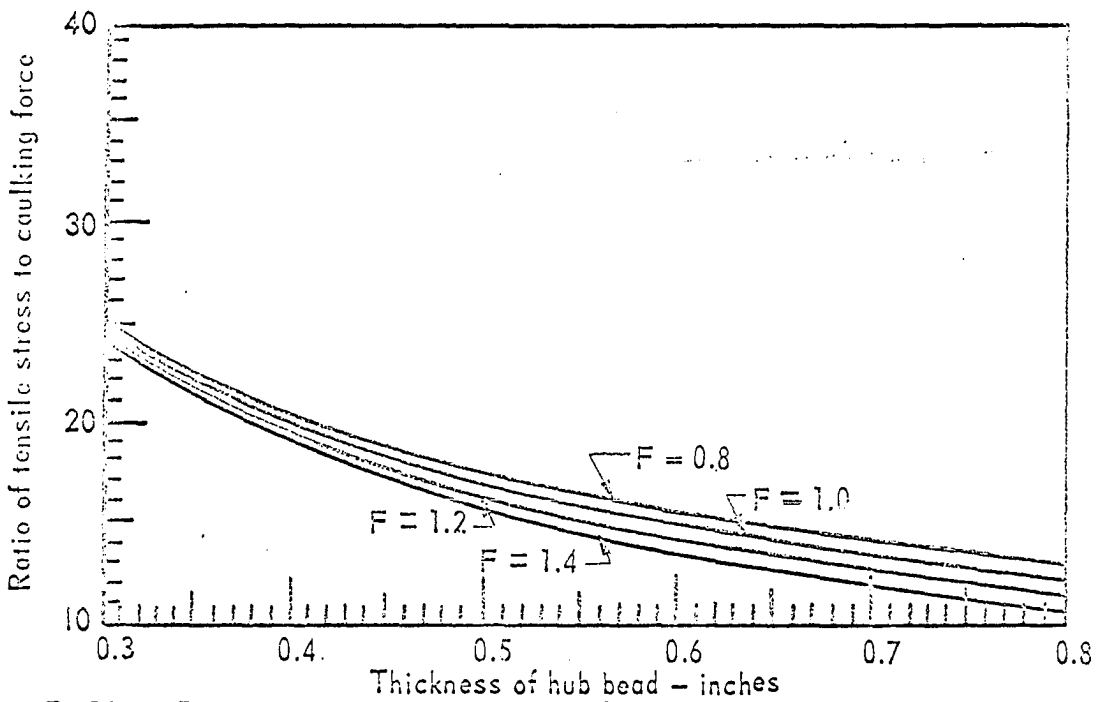


Fig. D.29. Design parameters for 10-inch hubs with hub wall thickness of 0.40 inch

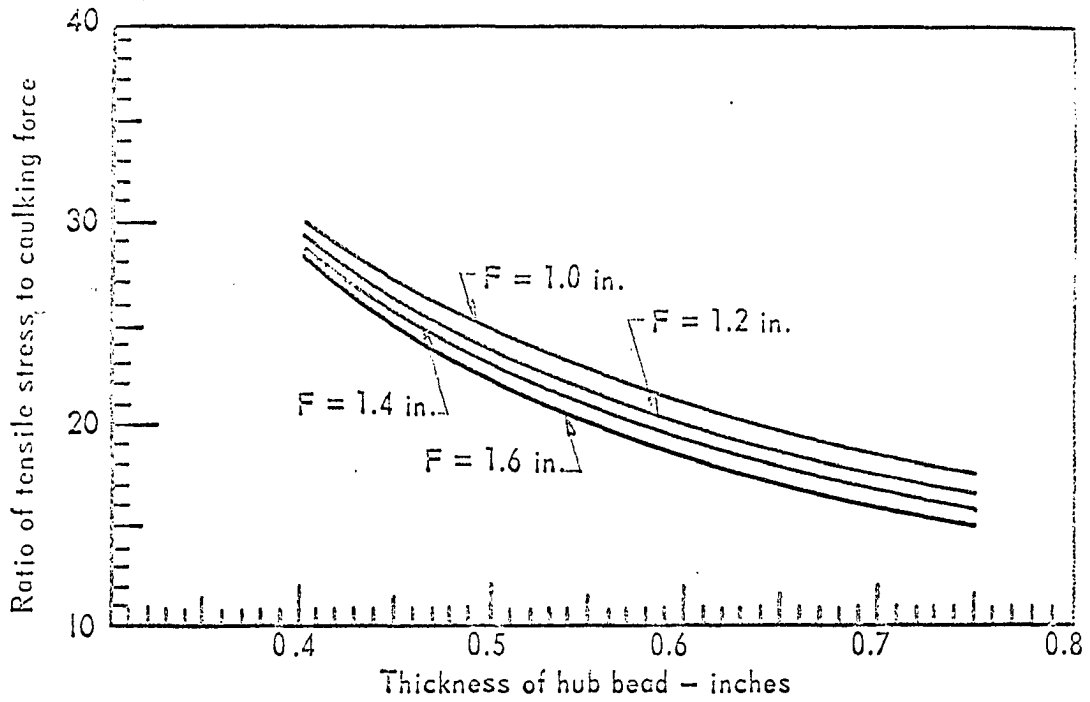


Fig. D.30. Design parameters for 12-inch hubs with hub wall thickness of 0.32 inch

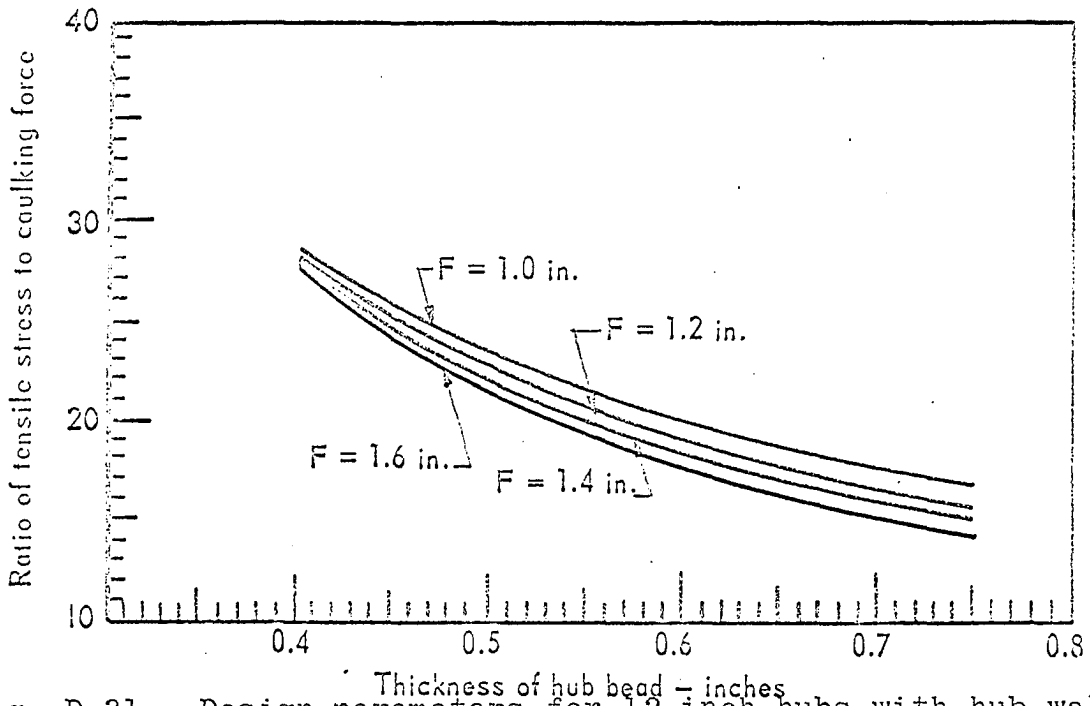


Fig. D.31. Design parameters for 12-inch hubs with hub wall thickness of 0.36 inch

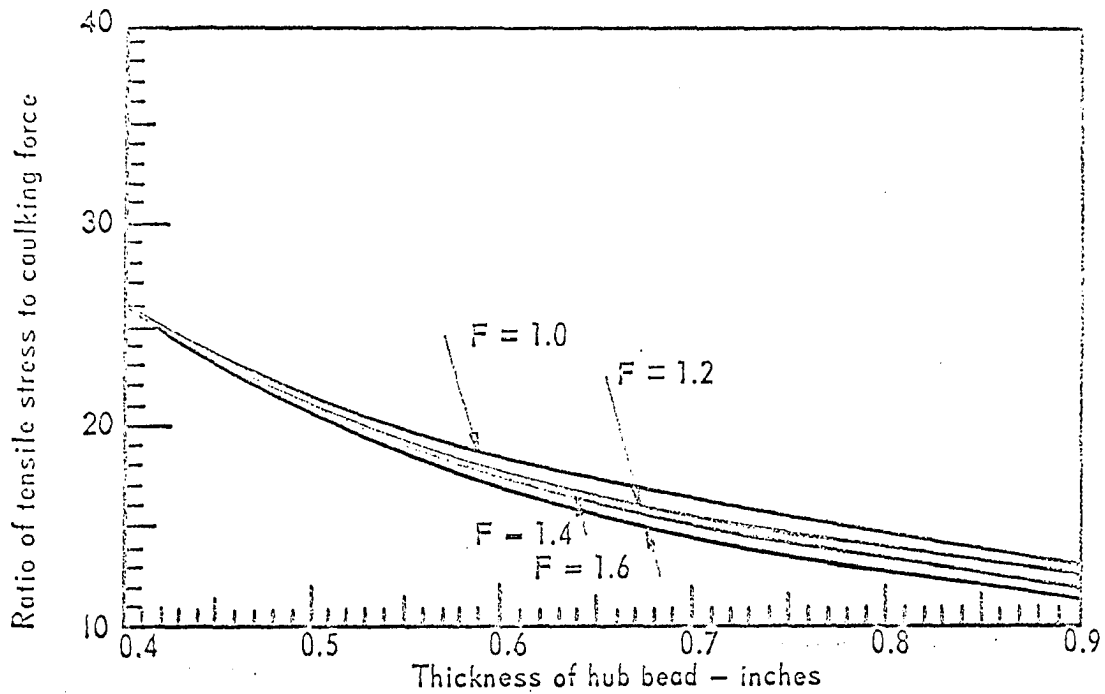


Fig. D.32. Design parameters for 12-inch hubs with hub wall thickness of 0.42 inch

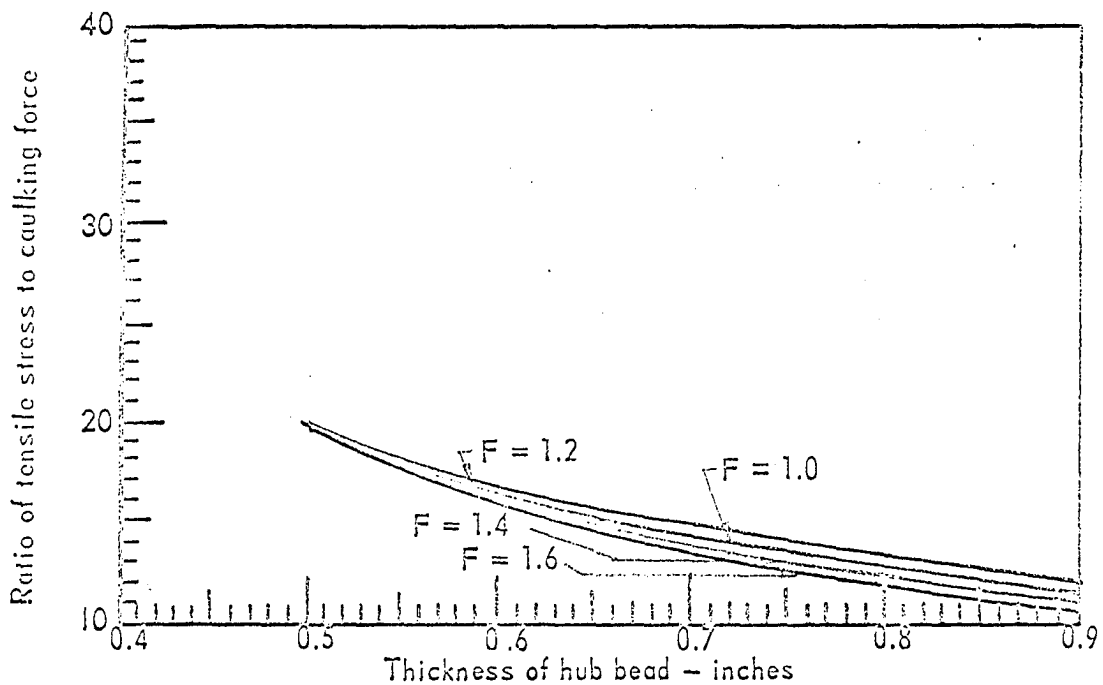


Fig. D.33. Design parameters for 12-inch hubs with hub wall thickness of 0.48 inch

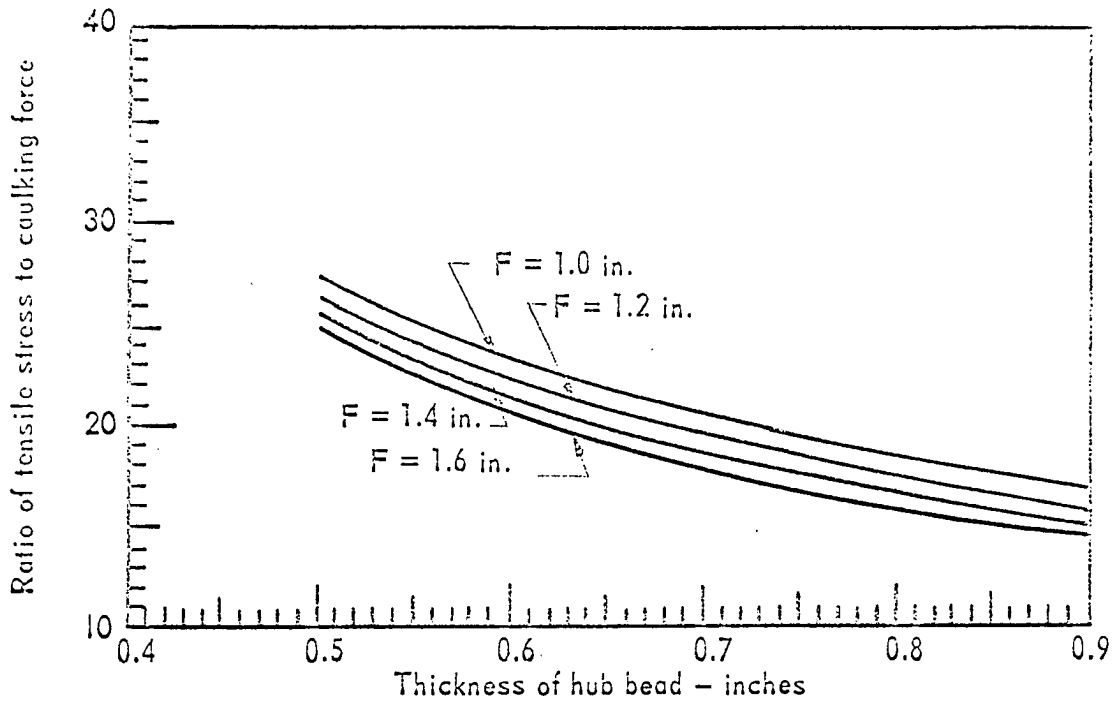


Fig. D.34. Design parameters for 15-inch hubs with hub wall thickness of 0.34 inch

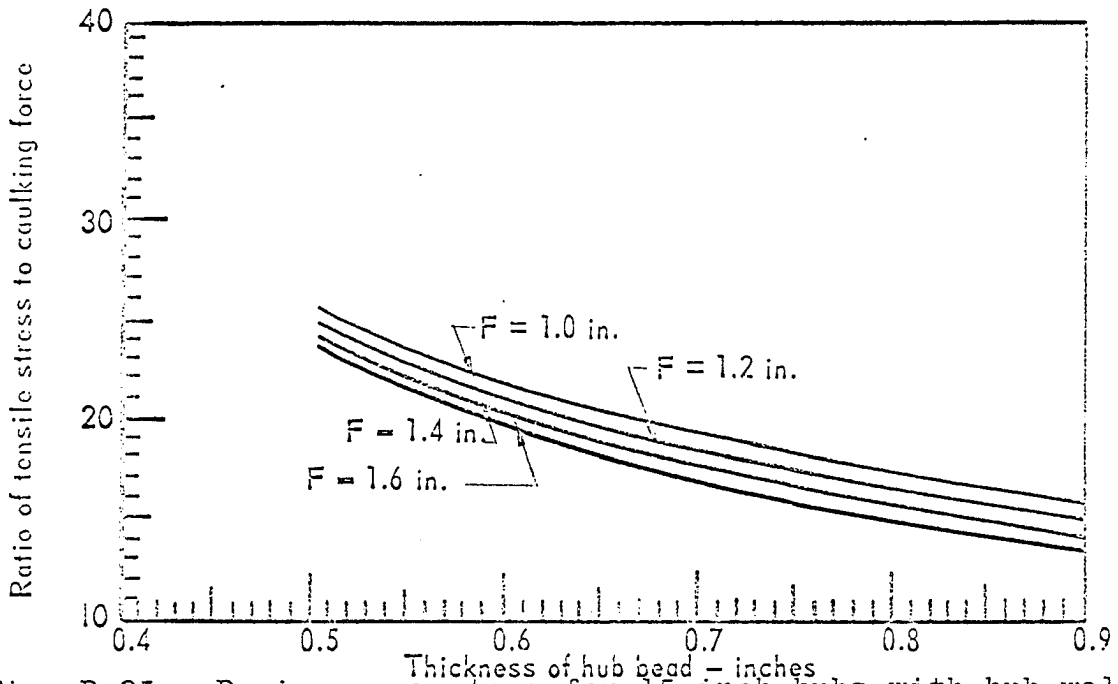


Fig. D.35. Design parameters for 15-inch hubs with hub wall thickness of 0.38 inches

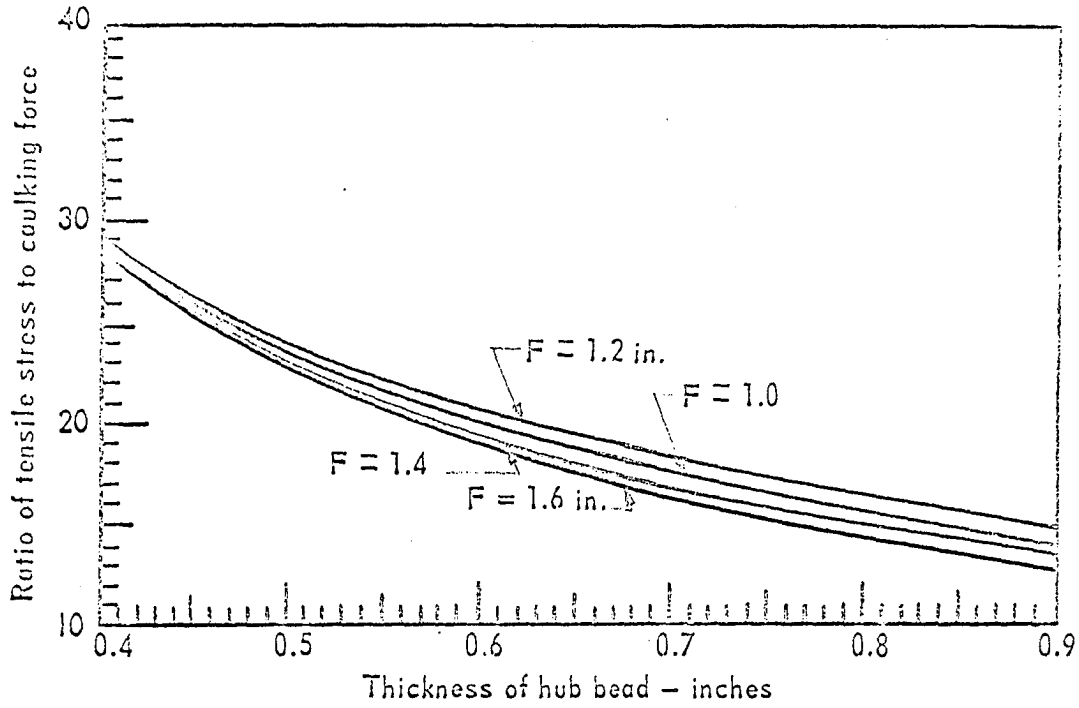


Fig. D.36. Design parameters for 15-inch hubs with hub wall thickness of 0.42 inch

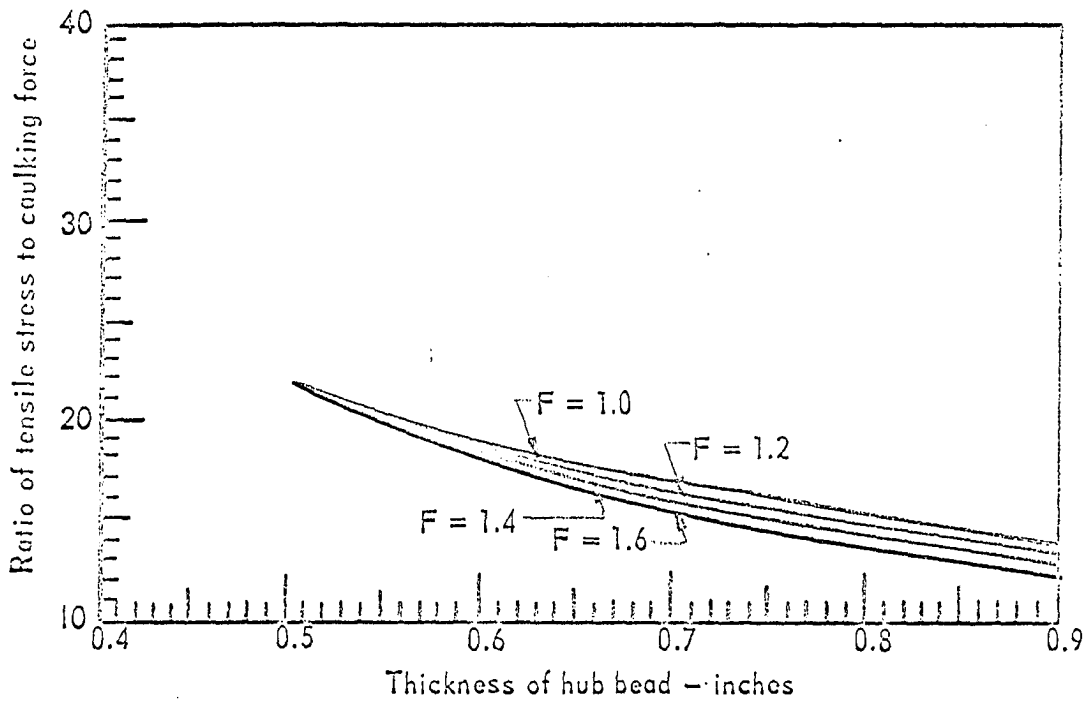


Fig. D.37. Design parameters for 15-inch hubs with hub wall thickness of 0.48 inch

```

S.0001          SINH(X)=TANH(X)/SQRT(1.-TANH(X)*(TANH(X))
S.0002          COSH(X)=1./SQRT(1.-TANH(X)*TANH(X)
S.0003          READ (1,100) KASE
S.0004          100 FORMAT (I10)
S.0005          READ (1,101) E, POISON
S.0006          101 FORMAT (E10.3,F10.4)
S.0007          WRITE (3,300)
S.0008          300 FORMAT (1H1,10X,'MAXIMUM STRESS GIVEN IS IN PSI',5X,'UNIT LOAD IS
                1 IN POUND PER LINEAR INCH CIRCUMFERENTIALLY')
S.0009          RAT=1.0-POISON*POISON
S.0010          WRITE (3,100) KASE
S.0011          WRITE (3,301) E,POISON,RAT
S.0012          301 FORMAT (6F20.8)
S.0013          WRITE (3,401)
S.0014          401 FORMAT (1H0,1X,'I',9X,'A',9X,'G',9X,'D',8X,'RT',9X,'R',9X,'F',9X,
                1 'S',5X,'SHEAR',4X,'MOMENT',6X,'W FREE',6X,'STRESS')
C
S.0015          DO 99 I=1,KASE
S.0016          READ (1,102) RT,F,S,A,G,D
S.0017          102 FORMAT (6F10.4)
S.0018          R=(F*RT-.667*G*D)/F
S.0019          RL=(A+R)/2.
S.0020          RS=(A+S)/2.
S.0021          R2=R*R
S.0022          S2=S*S
S.0023          DL=E*R*R2/(12.*RAT)
S.0024          DS=E*S*S2/(12.*RAT)
S.0025          BETA4=3*RAT/(R2*RL*RL)
S.0026          ALPHA4=3*RAT/(S2*RS*RS)
S.0027          BETA2=SQRT(BETA4)
S.0028          BETA1=SQRT(BETA2)
S.0029          BETA3=BETA1*BETA2
S.0030          ALPH2=SQRT(ALPH4)
S.0031          ALPH1=SQRT(ALPH2)
S.0032          SLPH3=ALPH1*ALPH2

```

Fig. D.38. Computer program used in determining appropriate factors of safety of various pipe hubs tested

```

C
S.0033      BF=BETA1*F
S.0034      DLB2=DL*BETA2
S.0035      DLB3=DL*ALPH3
S.0036      DSA2=DS*ALPH2
S.0037      DSA3=DS*ALPH3
S.0038      SBF=SIN(BF)
S.0039      CBF=COS(BF)
S.0040      SHBF=SINH(BF)
S.0041      CHBF(COSH(BF)
S.0042      SBF2=SBF*SBF
S.0043      CBF2=CBF*CBF
S.0044      SHBF2*SHBF*SHBF
S.0045      CHBF2*CHBF*CHBF
S.0046      BOTTOM=2.*DLB3*(SBF2+SHBF2)
S.0047      SC=SBF*CBF
S.0048      SSH=SBF*SHBF
S.0049      SCH=SBF*CHBF
S.0050      CSH=CBF*SHBF
S.0051      CCH=CBF*CHBF
S.0052      SHCH=SHBF*CHBF
C
S.0053      UNIT LOAD AT END - P=1 PLI  OUTWARD POSITIVE
S.0054      WLP=(SCH-CSH)/BOTTOM
            THETLP=2.*BETA1*SSH/BOTTOM
C
S.0055      UNIT Q AT JUNCTION, POSITIVE Q CAUSES CLOCKWISE END ROTATION
S.0056      WLQ=(SHCH-SC)/BOTTOM
            T ET Q=BETA:*(SBF2+SHBF2)/BOTTOM
S.0057      WRQ=0.5/DSA3
S.0058      THETRQ=-0.5/DSA2
C
S.0059      UNIT M AT JUNCTION , POSITIVE IF CLOCKWISE AT INSIDE END OF LIP
S.0059      WLM=BETA1*(SBF2*CHBF2+CBF2*SHBF2)/BOTTOM
S.0060      THETLM=2.*BETA2*(SC+SHCH/BOTTOM
S.0061      WRM=-0.5/DSA2
S.0062      THETRM=ALPH1/DSA2
C
            SOLUTION OF Q AND EM
            WRLQ=WRQ-WLQ

```

Fig. D. 38. (Continued)

```

S.0063      WRLQ=WRQ&WLQ
S.0064      WRLM=WRM&WLM
S.0065      TRLQ=THETRQ-THETLQ
S.0066      TRLM=THETRM-THETLM
S.0067      DET=WRLQ*TRLM-TRLQ*WRLM
S.0068      QTOP=WLP*TRLM-THETLP*WRLM
S.0069      EMTOP=WRLQ*THETLP-TRLQ*WLP
S.0070      Q=QTOP/DET
S.0071      EM=EMTOP/DET
C           COMPUTE CONSTANTS IN THE DEFLECTION EXPRESSION - FOR UNIT P.
S.0072      C1=-0.5*EM/DLB2
S.0073      C2=(BETA1*EM*(SC+SHCH+Q*SBF2+SSH)/BOTTOM
S.0074      C3=(BETA1*EM*(SC+SHCH+Q*SHBF2+SSH)/BOTTOM
S.0075      C4=(BETA1*EM*(SBF2*CHBF2+CBF2*SHBF2)+Q*(SHCH-SC)-(CSH-SCH))/BOTTOM
S.0076      WFREE=C1*SSH-C2*SCH-C3*CSH+C4*CCH
S.0077      STRESS=E*WFREE/RL
S.0078      WRITE (3,400) I,A,G,D,RT,R,F,S,Q,EM,WFREE,STRESS
S.0079      400 FORMAT (1H0,I2,9F10.4,E12.4,F12.4)
S.0080      99 CONTINUE
S.0081      STOP
S.0082      END

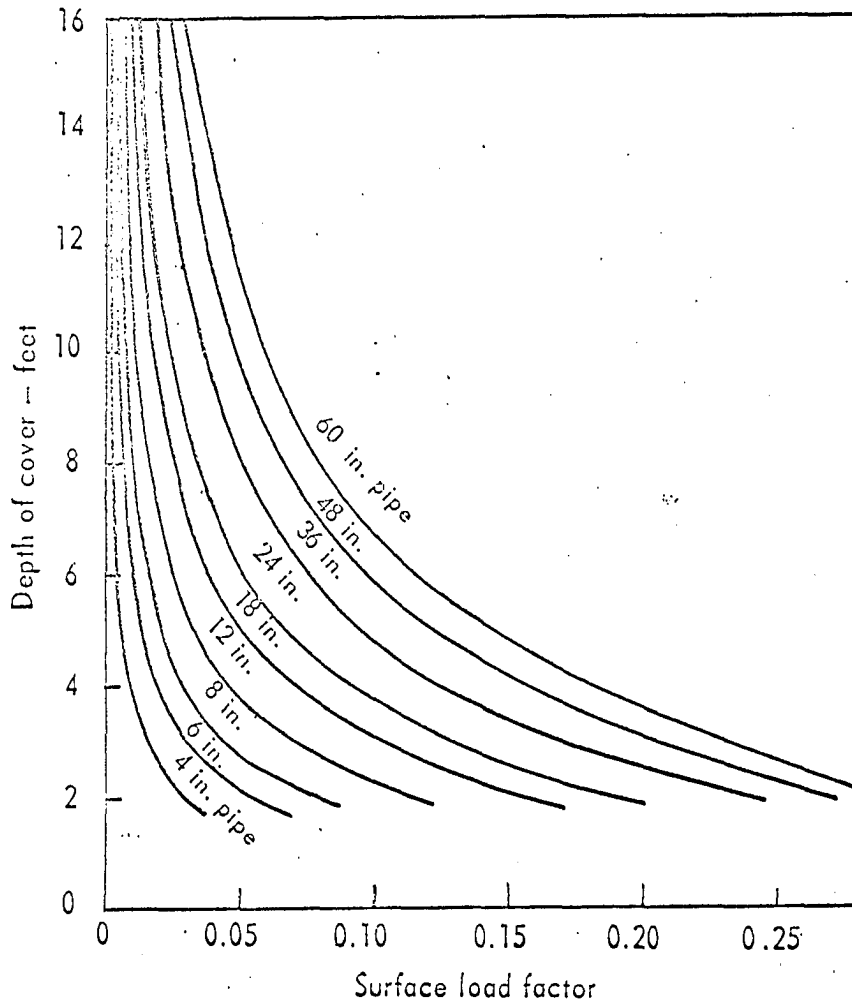
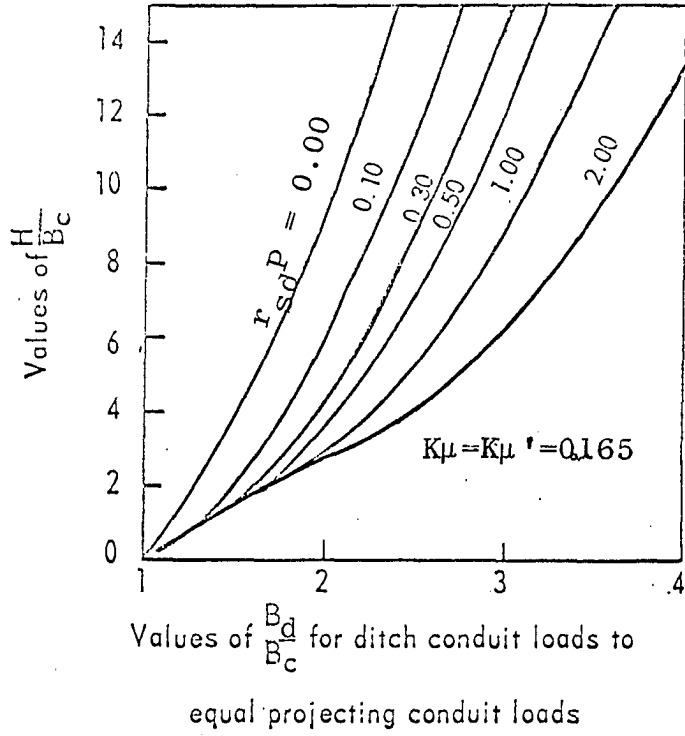
```

Fig. D.38. (Continued)

17. APPENDIX E. DESIGN CHARTS FOR EARTH AND SURFACE LIVE
LOADING ON PIPES

Fig. E.1. (top) Curves for transition-width ratio (2)

Fig. E.2. (bottom) Surface load factors for two passing trucks (3)



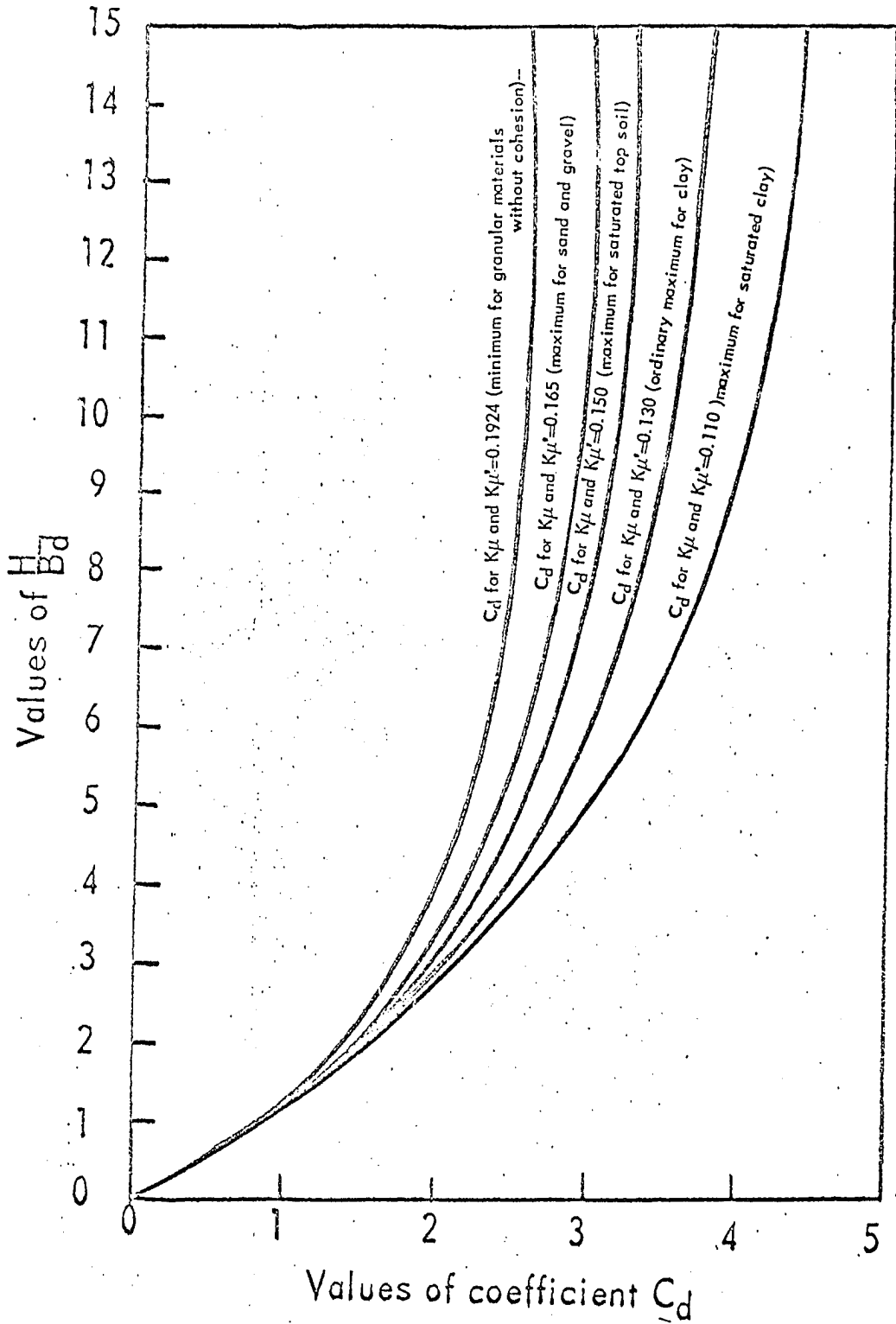


Fig. E.3. Diagram for coefficient C_d for ditch conduits(2)

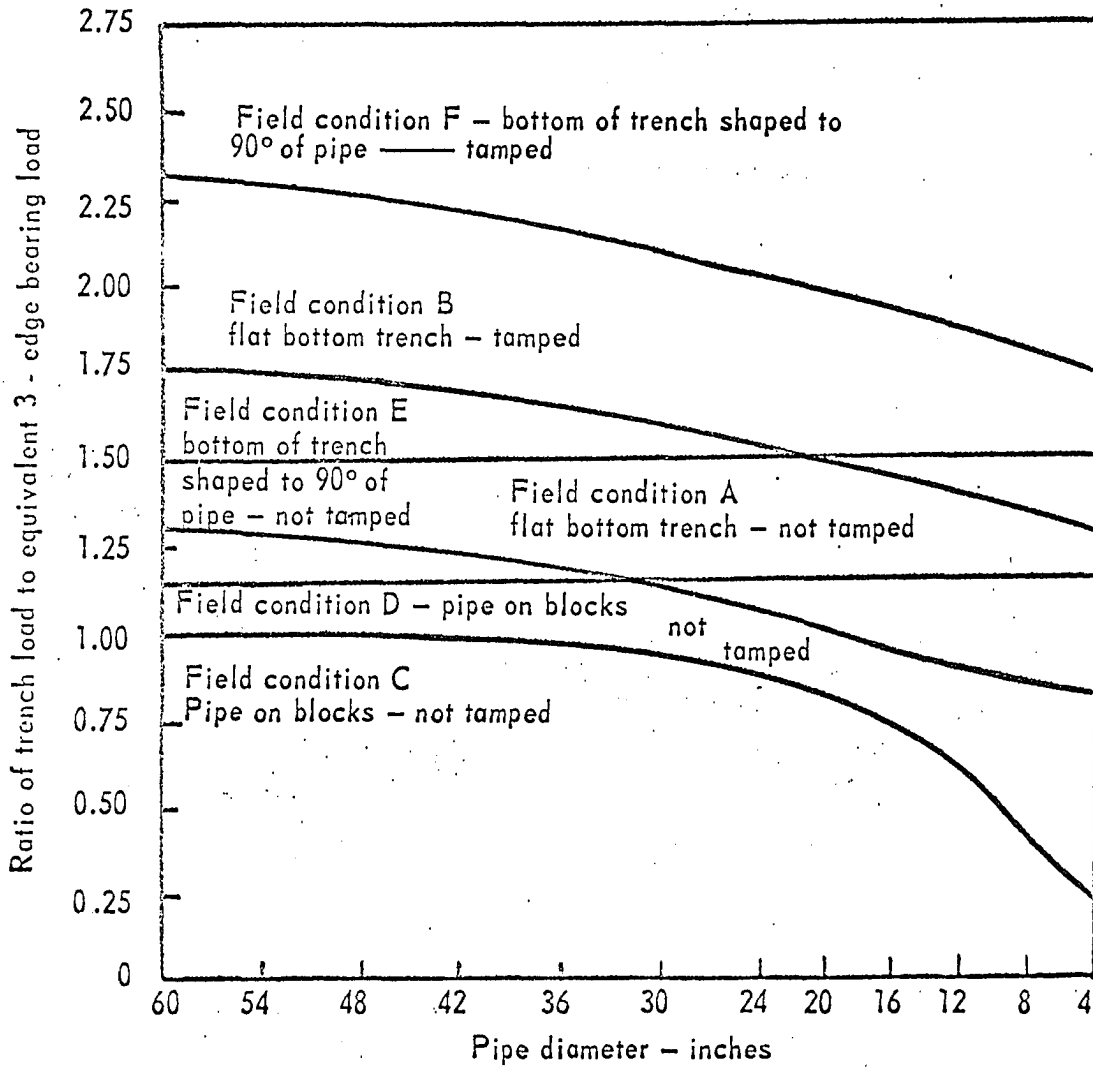


Fig. E.4. Relationship between pipe diameter and ratio of trench load to equivalent 3-edge bearing load (2)

Table E.1. Percentage of trench load on pipes (3)

Pipe Size in.	Percentage of Truck Load Used							
	2 1/2-3 1/2 ft. Cover		4-7 ft. Cover		8-10 ft. Cover		Over 10 ft. Cover	
	Field Conditions							
	A, B, E, F	C, D	A, B, E, F	C, D	A, B, E, F	C, D	A, B, E, F	C, D
4-12	100	78	100	84	100	90	100	95
14	92	78	100	84	100	90	100	95
16	88	78	95	84	100	90	100	95
18	85	78	90	84	100	90	100	95
20	83	78	90	84	95	90	100	95
24-30	81	78	85	84	95	90	100	95
36-60	80	78	85	84	90	90	100	95